19951078 37
324377
35 0036
8p

NASA Conference Publication 10143, Volume 3

Fourth High Alpha Conference
NASA Dryden Flight Research Center
July 12–14, 1994

(NASA-CP-10143-Vol-3) FOURTH HIGH ALPHA CONFERENCE, VOLUME 3 (NASA. Dryden Flight Research Center) 191 p

N95-14251
--THRU--
N95-14259
Unclas

G3/02 0016100

NASA Conference Publication 10143, Volume 3

Fourth High Alpha Conference
NASA Dryden Flight Research Center
Edwards, California
July 12–14, 1994

National Aeronautics and
Space Administration

Office of Management

Scientific and Technical
Information Program

1994

Foreword

High-angle-of-attack flight research and development has matured in the past 5 years. We have seen four different aircraft investigate the different methods of stability, control, and effectiveness of high-angle-of-attack flight. Of these four vehicles, three use thrust vectoring to achieve their goals. Production aircraft, such as the F-22, are now using thrust vectoring. The use of forebody vortex control has been and is being investigated in flight, as well as in ground facilities. Considerable research, development, and validation of ground predictive tools, including computational fluid dynamics, wind tunnels, and simulations, have taken place to enable better, faster, cheaper development of new aircraft and modification of current aircraft.

The goal of the Fourth High Alpha Conference, held at the NASA Dryden Flight Research Center on July 12–14, 1994, was to focus on the flight validation of high-angle-of-attack technologies and provide an in-depth review of the latest high-angle-of-attack activities. Areas that were covered include high-angle-of-attack aerodynamics, propulsion and inlet dynamics, thrust vectoring, control laws and handling qualities, tactical utility, and forebody controls.

This document is a compilation of presentations given at the Fourth High Alpha Conference. The presentations included in this document are included as supplied by the presenters with no modifications. This conference, along with its predecessors, was sponsored by the NASA High Alpha Technology Program Steering Committee.

Fourth NASA High Alpha Conference
NASA Dryden Flight Research Center
July 12–14, 1994

Table of Contents—Volume 3

Forebody Controls (cont'd.)

Integration of a Mechanical Forebody Vortex Control System into the F-15, Richard E. Boalbey, Kevin D. Citurs, Wayne L. Ely, Stephen P. Harbaugh, William B. Hollingsworth, and Ronald L. Phillips, McDonnell Douglas Corporation, St. Louis, MO

Flight Evaluation of Pneumatic Forebody Vortex Control in Post-Stall Flight, Dr. Lawrence A. Walchli, Wright Laboratory, Wright Patterson AFB, OH

Tactical Utility

19950107838
350063
209

N95-14252

1610
P-19

INTRODUCTION

The U.S. Navy has conducted a limited flight test evaluation of the F/A-18 HARV, the purpose of which was to provide in-flight validation of extensive ground-based simulation, assessment of overall handling qualities at high angle of attack (AOA), and determination of tactical utility benefits generated from the aircraft's thrust vectoring system. This evaluation was part of a joint NASA/Navy study which was initiated to quantify high AOA control power requirements under the NASA High Angle of Attack Technology Program (HATP). Currently, flying qualities specifications define control power requirements qualitatively. As tactical aircraft continue to push the envelope in terms of high AOA maneuverability, control power becomes an increasingly important design driver.

This presentation will highlight results from the latest Navy evaluation of the HARV (March 1994) and focus primarily on the impressions from a piloting standpoint of the tactical utility of thrust vectoring. Issues to be addressed will be mission suitability of high AOA flight, visual and motion feedback cues associated with operating at high AOA, and the adaptability of a pilot to effectively use the increased control power provided by the thrust vectoring system.

Navy And The HARV: High Angle Of Attack Tactical Utility Issues

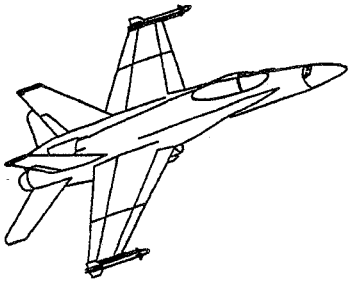

LT C. A. Sternberg, USN
Capt Ricardo Traven, CAF
Mr. James Lackey

Naval Air Warfare Center
Patuxent River, Maryland

BACKGROUND

This was the second of two evaluations conducted by the U.S. Navy, the first being in November of 1992. Unique to these evaluations was the operational F/A-18 background of the three test pilots. All three test pilots had over 1,000 flight hours each in the F/A-18. The first evaluation on the F/A-18 HARV consisted of two flights flown by LT Dave Prater (USN) and focused primarily on flying qualities, pitch control margin/nose down pitch recovery capability and a limited look at tactical utility.

The second evaluation was completed in March of 1994 and focused on validating extensive ground based simulation on lateral directional control power requirements, high AOA flying qualities and tactical utility.

LT C. A. Sternberg (USN) and Capt Ricardo Traven (CAF) piloted the F/A-18 HARV for a total of eight test missions (7.1 flight hours) in one week (21 to 25 March, 1994) which was a new NASA F/A-18 HARV record. LT Sternberg became the fifth pilot to ever fly the HARV and Capt Traven was the sixth.

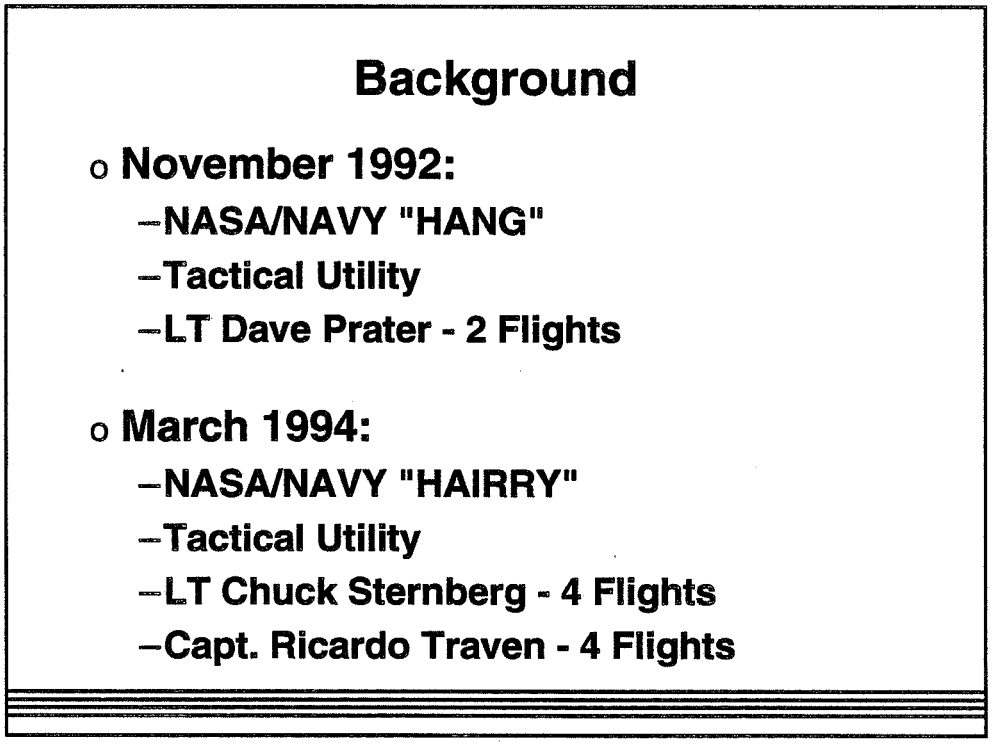

TEST OBJECTIVES

The objectives of the flight test were:

(1) Provide in-flight validation of extensive ground-based simulation studies, including specific maneuver setup and execution, rating methodology and limited data comparison between flight test and simulator research.

(2) Assess overall handling qualities at high angle of attack (AOA) including motion effects on pilot orientation and spatial awareness , pilot cueing and pilot workload.

(3) Determine tactical utility benefits generated from the aircraft's thrust vectoring system.

Although the majority of flight test concentrated on simulation validation and test methodology verification, the pilots were able to take a limited look at the "tactical utility" of the HARV with thrust vectoring. The implementation of thrust vectoring on the HARV allowed the Navy to assess the implications of increased control power at high AOA on a current operational platform. Tactical utility testing consisted of conducting "canned" basic fighter maneuvers against a NASA F/A-18 target airplane. Both offensive and defensive maneuvers were evaluated.

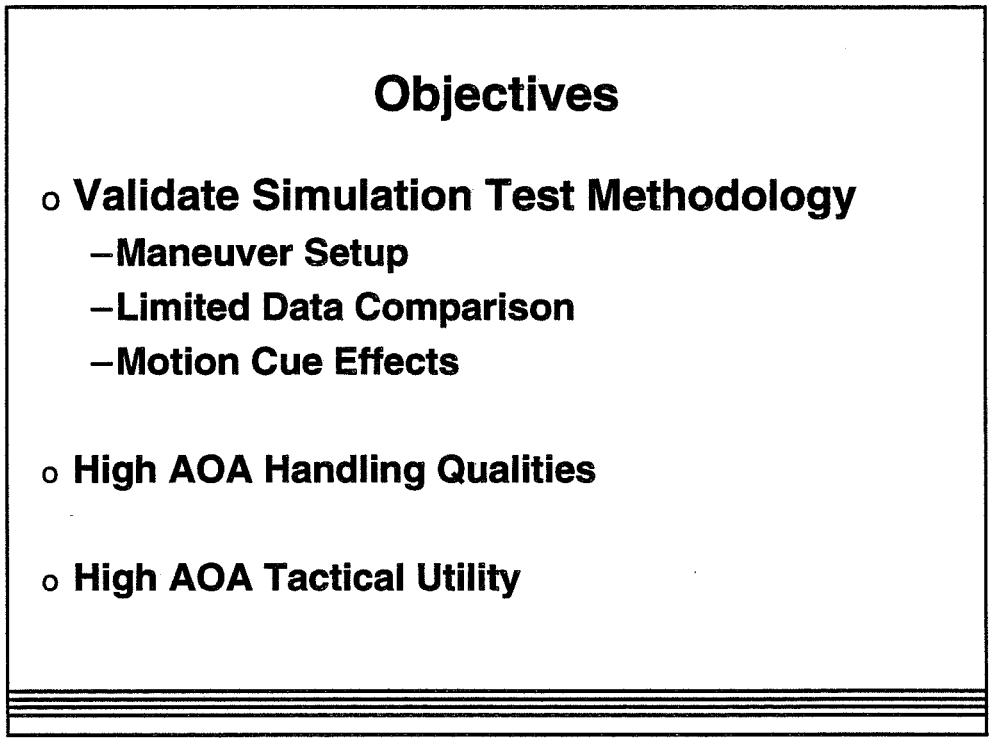

FLIGHT PROFILES

This evaluation was planned in four phases. The first flights, Phase I, concentrated on introducing the pilots to the HARV's handling qualities up to 70 deg AOA. Phase I maneuvers contained more quantitative closed loop maneuvers in order to expand the Navy's High AOA data base and provide the pilots with an introduction to flight at High AOA. These maneuvers consisted of bank angle and heading captures, loaded rolls and constant thrust stabilized pushovers.

Phase II consisted of maneuvers that highlighted the lateral directional axes and evaluated roll performance and handling qualities during gross acquisition tasks. These maneuvers were developed by the test team during extensive simulation under the HAIRRY program and are commonly referred to as HAIRRY maneuvers. HAIRRY is an acronym for "High AOA Investigation of Requirements for Roll and Yaw" and is a joint U.S. Navy/NASA project which is part of NASA's High AOA Technology Program. The purpose of the HAIRRY program is to quantitatively identify/define lateral directional control power requirements at high AOA for incorporation into next generation aircraft design specifications. Data gathered included pilot comments, maneuver ratings, and dynamic response characteristics.

Phase III consisted of tactical/mission representative tasks to evaluate the overall tactical utility of thrust vectoring. These maneuvers were tactically oriented and were designed to minimize "pure" performance differences between the HARV and the target aircraft and provide repeatable engagements so that engagements flown with thrust vectoring on and off could be compared. For direct comparisons, the variations between setups needed to be minimized and the maneuvers were designed with that in mind. Tactically oriented maneuvers included: 1 v 1 canned setups against a predictable target, J Turns (Post-Stall Reversals), and Flat Scissors. The focus of these maneuvers was to assess how the pilots effectively used thrust vectoring in an "operational environment".

Profiles

- **Phase I - HARV Fam**
  - **Bank / Heading Captures**
- **Phase II - HAIRRY**
  - **Lateral Gross Acquisition**
  - **Offensive Loaded Reversals**
  - **Defensive Rolls**
- **Phase III - Tactical Utility**
  - **Flat Scissors**
  - **J Turn**
  - **1v1**

HAIRRY

Although the HAIRRY maneuvers were designed primarily for evaluating open loop roll performance and handling qualities during target capture, they provided some insight as to the tactical utility benefits of such a maneuver. The maneuvers were designed to gather quantitative data but were intentionally designed to be mission oriented. These maneuvers were designed to eliminate the longitudinal axis from the equation. The team wanted to focus specifically on the lateral directional axes. The maneuvers were also designed in such a way that they could be executed in flight the same way they were executed in the simulator. This allowed for a direct comparison of flight test and simulation data.

The three maneuvers used were the Lateral Gross Acquisition , Offensive Loaded Reversal and Defensive Roll. The Lateral Gross Acquisition and the Offensive Loaded Reversal maneuvers were initiated using a full lateral stick, step input (feet on the floor) followed by at least 130 to 180 deg of bank angle change, and ended with a capture of the target between vertical bars on HUD. This allowed the pilot to evaluate open loop roll performance as well as Handling Qualities during the capture portion of the task. The Defensive roll was basically on open loop roll performance task with no capture, but the pilot used an attacking aircraft to evaluate his ability to maintain situational awareness during the maneuver. During the simulation the maximum steady state roll rate and roll mode time constant were varied and each maneuver was performed over the full range of AOA's from 15 to 60 deg. In flight, the parametrics were not varied per se, but these maneuvers were flown first with the baseline flight controls (no thrust vectoring) and then flown with the thrust vectoring on (Research Flight Control Systems - RFCS, engaged). This allowed the pilots to evaluate the effects of a substantial increase in control power provided by the RFCS.

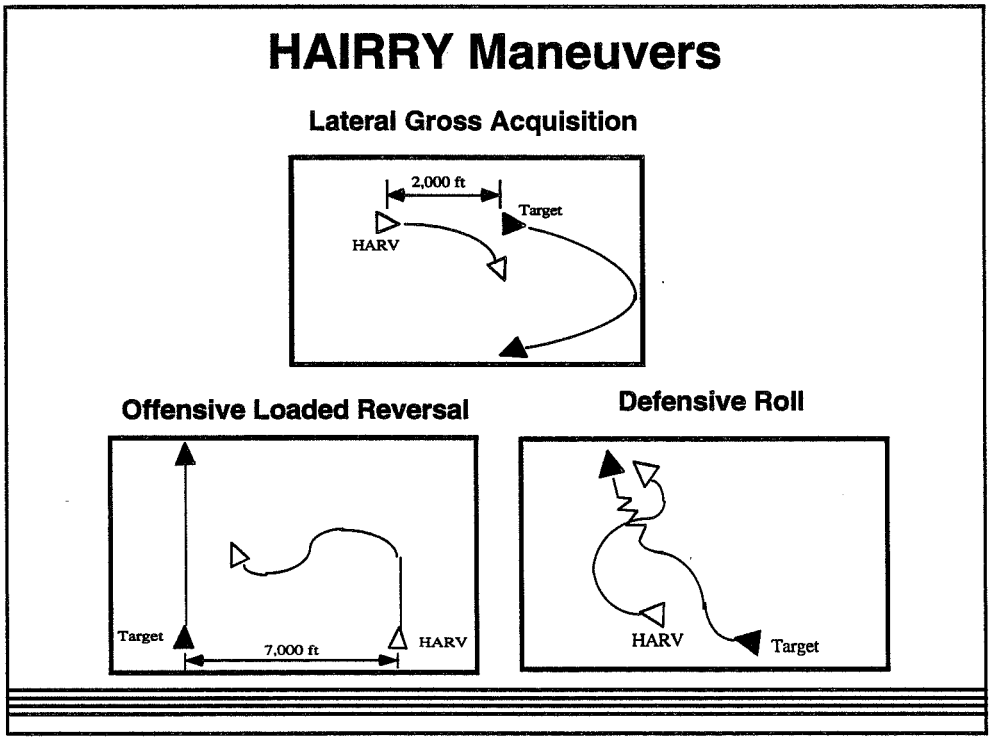

OPERATING IN THE HIGH AOA ENVIRONMENT

Tactical Maneuvering in the High AOA environment differs significantly between conventional aircraft (F/A-18/F-14) and Thrust vectoring/augmented aircraft (HARV).

In addition to the limited AOA achievable, "conventional" platforms are severely limited in the lateral directional axes at high AOA due to reduced control power and increased departure susceptibility. As a result, to utilize the lateral directional axis, the AOA must first be reduced to achieve acceptable performance. Once the AOA is reduced, the aircraft is rolled to reposition the lift vector, and then the AOA is increased as required for the tactical situation. In this manner, the axes are decoupled intentionally by the pilot to compensate for a control system that provides unsuitable lateral directional performance at High AOA.

It is in this manner the the HARV has an advantage over the conventional design in that the augmented control system provides the pilot with enhanced lateral directional performance at High AOA and the pilot is not required to decouple the axes manually. This opens up a whole new way of thinking and provides the pilot with an enhanced set of tools to prosecute the tactical situation..

In the past, it seems the general mindset about thrust vectoring was the ability to fly to 70 AOA, to pitch to 70 deg AOA. Much of the emphasis was all pitch and very little about rolling/yawing at those AOA's. During the HARV evaluation, the test pilots made a conscious and concerted effort to investigate the lateral directional axes from a tactical perspective.

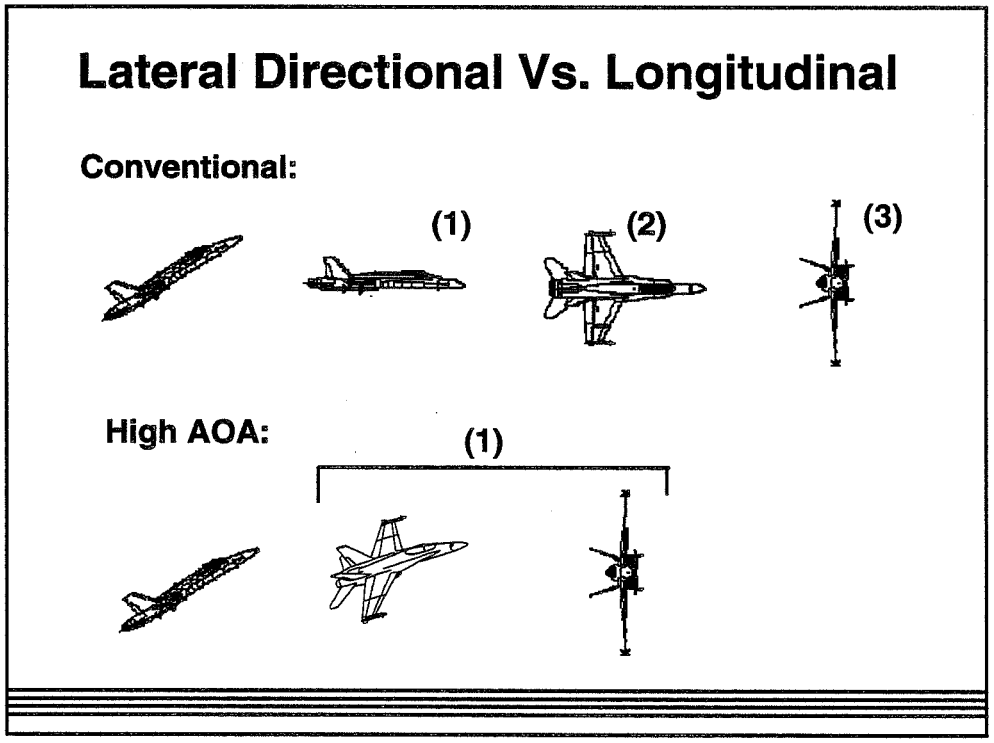

ROLL PERFORMANCE CLASSIFICATION

When a pilot executes a capture task designed to evaluate the lateral directional axes, the resulting comments are based on two aspects of the aircraft response - the roll performance during the bank angle change to get to the target and the handling qualities during the capture. The pilot bases his comments on roll performance on the initial roll response, perceived linearity of the roll response and roll rates, as well as time required to perform a given task. Handling qualities aspects deal with the ability to roll the airplane and then capture a target as in the gross acquisition task. The pilot's handling qualities comments deal not so much with roll performance, but on the predictability and controllability of the lateral directional axes in accomplishing the task. Looking at either issue separately can be misleading. The handling qualities might be superb, but the roll performance may be so poor as to be tactically useless.

Therefore, the test team decided it was imperative to separate roll performance issues form handling qualities issues. In order to "quantify" the pilots' comments on mission suitability/roll performance and separate handling qualities issues, the Roll Performance Classification (RPC) scale was developed by the Navy/NASA HAIRRY team. The RPC scale isolated maneuvering aspects only and thus could more directly correlate pilot ratings/comments with control power-related characteristics .

The RPC scale relates roll performance/lateral directional maneuverability to mission effectiveness. It is very task dependent and relies on the pilot's tactical experience to evaluate the roll performance. It was intentionally designed to be simple - The "Good, bad, ugly" scale. The beauty of this scale is in its simplicity. Roll performance which is evaluated as "Enhancing, tactically superior" is rated as a 1. Unacceptable roll performance is rated as a 4. Tasks which exhibit roll performance between these two levels are broken out in the figure below.

Connecting The Pilot w/ The Engineer

Roll Performance Classification

Roll Performance for Mission Effectiveness	Improvements in Roll Performance	Numerical
Enhancing - Tactically Superior	None Warranted	1
Satisfactory - Mission Requirements Met	May be warranted, but not required	2
Unsatisfactory - Mission Requirements Not Met	Required	3
Inadequate - Could Not Perform Maneuver	Mandatory	4

ROLLING ABOUT THE VELOCITY VECTOR

An important issue to consider when discussing tactical utility is whether the pilot is able to interpret and predict his flight path and or position his lift vector to capture a target, especially at very high AOA's. Will disorientation be a factor?

During flight test, one of the pilots came up with a "method" for describing how he was able to adapt to the high AOA environment and helps to describe the "AOA cone" for the folks on the ground.. It's called"Sterno's Lampshade on a Dog" high AOA visualization technique. The alpha cone to a HARV pilot is like a lampshade on a dog.

It is quite common for a dog to wear a "lampshade" or plastic cone on his head to keep from chewing stitches or whatever. In a very short period of time, the dog learns how to perform his daily routine with this lampshade on his head and he adapts quite quickly.

When a pilot straps on the HARV or any other high AOA vehicle, he is, in a sense, strapping on a lampshade, which is defined by his AOA. The pilot can visualize his "Lampshade" or ALPHA cone by sampling the aircraft's lateral directional response at a given AOA. The small perturbations describe a small arc and the pilot can extrapolate the dimensions of his cone based on that small cone segment. The pilot can visualize where this "Lampshade" is and can superimpose it on the outside world. The pilot may use his "lampshade" in the following manner. In a tactical scenario, the pilot knows where the target is, predicts his flight path and determines the best way to get the target to fly into his "lampshade" for the capture. Once the target has intersected the "lampshade" surface, the pilot can can use the lateral directional axes for the capture. Of course, there are some instances where this is not practical and a more conventional capture would be more efficient, but we'll show some examples where this kind of technique can be useful.

Utilizing the "lampshade" in the high AOA environment allows the pilot to modify his way of thinking about air-to-air engagements

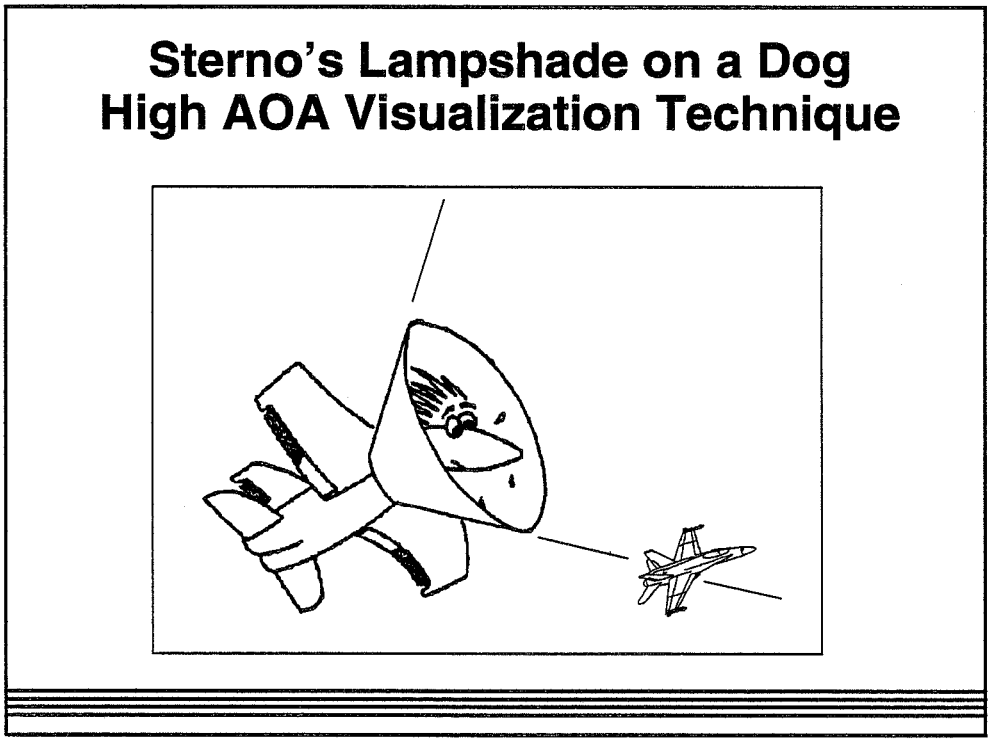

TACTICAL UTILITY MANEUVERS

Three maneuvers were used to look at tactical utility. These maneuvers were designed to eliminate a direct performance comparison and factor out thrust to weight effects. The HARV suffers dramatically from a thrust to weight standpoint and our purpose was not to evaluate the HARV's tactical utility, but evaluate the tactical utility of the thrust vectoring system. To accomplish this purpose, all maneuvers were flown first with the thrust vectoring disengaged, i.e. the baseline HARV airframe. The maneuvers were then repeated with the thrust vectoring system engaged.

The flat scissors maneuver emphasized the slow speed knife fight.

The J-turn was the test pilot's first look at a classic post stall reversal. It emphasized larger magnitude, more aggressive maneuvering using the entire alpha range of the aircraft. It was imperative that the test pilots learned and understood the post stall reversal prior to moving on the the 1v1 maneuver.

The 1v1 maneuver was more of a free form exercise which was initiated from fixed initial conditions. This maneuver allowed the pilot the freedom to maneuver the aircraft as he saw fit to prosecute and capture the target in the shortest amount of time. It was basically an open forum where the pilot could experiment with the added capability provided by the HARV and discover/exploit those regions. After the 1v1 was flown with the RFCS on and off, the HARV was given a 2,000 ft altitude advantage at the merge, which was increased by 2,000 ft for subsequent maneuvers with a maximum split of 6,000 ft.

During the J-turn and 1v1 Maneuvers, the targets flew a prebriefed flight path so that a direct comparison could be made between maneuvers flown with thrust vectoring on and off.

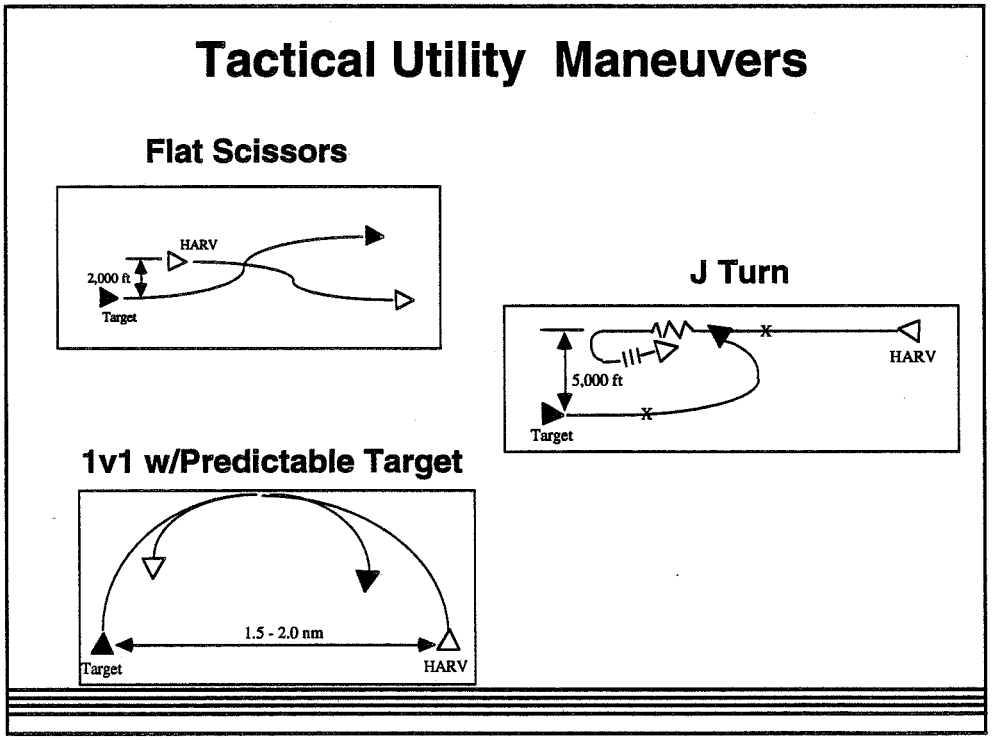

FLAT SCISSORS

The Flat Scissors forced a slow speed knife fight at close quarters from a neutral setup. In this type of fight, lateral directional maneuverability and the ability to fly slower than one's opponent is critical.

When flown with the baseline HARV, the HARV was unable to achieve any tactical advantage over the chase Hornet. The flying qualities and lateral directional maneuverability of the HARV were very poor and evaluated as "unsuitable" for the mission, RPC 3.

With the thrust vectoring engaged, the HARV had a clear and distinct advantage over the target aircraft. It was a night and day difference. The HARV was able to achieve a tactical advantage almost immediately by exploiting the ability of the HARV to fly much slower/higher AOA than the target aircraft and maneuver at will while maintaining that high AOA. Another advantage enjoyed by the HARV was to ability to maneuver much more effectively in the lateral directional axes at Clmax and below. By being able to maneuver aggressively in the lateral directional axes at 35 AOA, where the target aircraft was flying, the HARV was able to quickly obtain an offensive advantage by early turning and maneuvering aggressively to reposition behind the target aircraft without using extremely high AOA range.

The thrust vectoring capability of the HARV provided it with a clear and distinct advantage over the baseline F/A-18 with similar thrust to weight. The superior lateral directional maneuverability at Clmax and below, and the ability to fly and maneuver at extreme AOA's is a distinct tactical advantage in the slow speed arena.

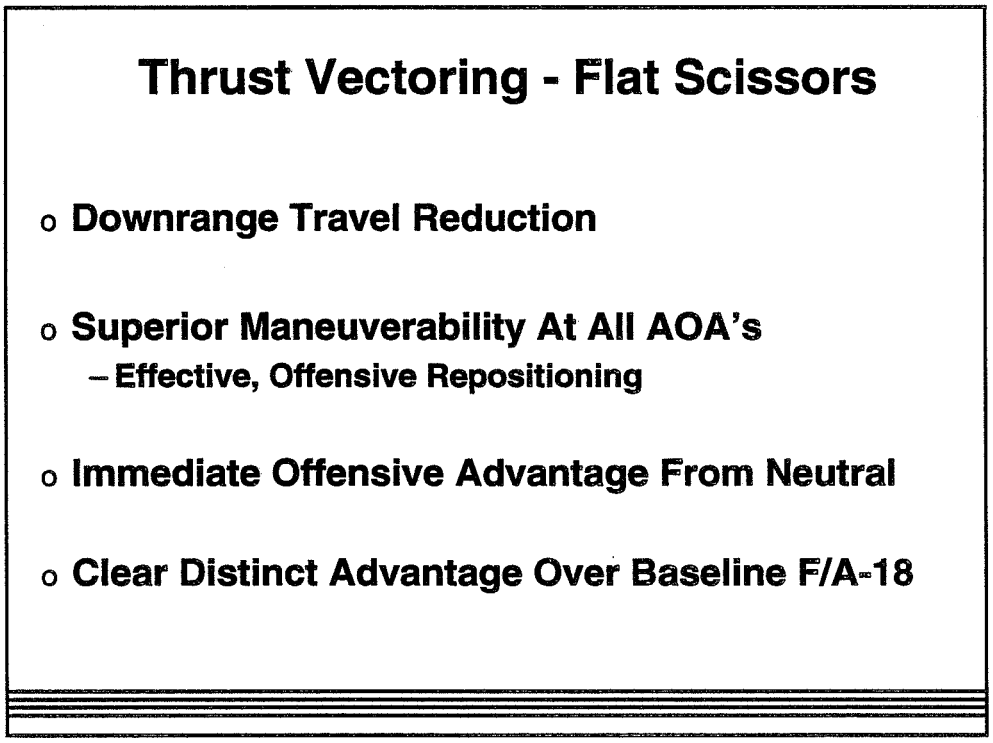

J TURN / POST STALL REVERSAL

The J-turn/Post Stall Reversal was used both as a training maneuver and a tactical maneuver. It was used initially to introduce the pilots to the techniques required to execute this unique maneuver. Once this was accomplished, the pilots evaluated the tactical utility of the maneuver in acquiring a target. Both pilots found it particularly advantageous in prosecuting a target provided that a large altitude advantage was enjoyed.

The setups worked out such that the pilot pitched to 50 to 60 deg AOA, then when the target had "entered the lampshade", 4,000 ft below and offset laterally, a pure lateral directional capture was performed using full lateral stick. The HARV ended up directly overhead the target 60 to 90 deg nose down. It was flown as a high to low, vertical capture. The pilot had to time the lateral input depending on the lateral separation and slant range of the target. Even with all those variables, the pilots were able to perform successful captures after only a couple of attempts. This was in indication that the pilots were able to adapt rather quickly to this new environment.

Both pilots agreed that this maneuver was very dependent on the initial setup and that it could only be used in very specific instances during a fight when the pilot had the required separation and altitude advantage. This maneuver was very dependent on a high to low capture for tactical usefulness .

One situation the pilot must be careful to avoid is the blind lead turn. There were many cases where it would have been advantageous to begin the maneuver, but it had to be delayed in order to ensure clear view of the target throughout the maneuver. This is an issue that will become more critical as more aircraft are capable of high AOA flight.

Being able to perform this maneuver is a distinct tactical advantage when used properly. It was evident from this maneuver that if used incorrectly or at the wrong time it could be particularly disadvantageous due to the predictability and large altitude/ energy losses involved.

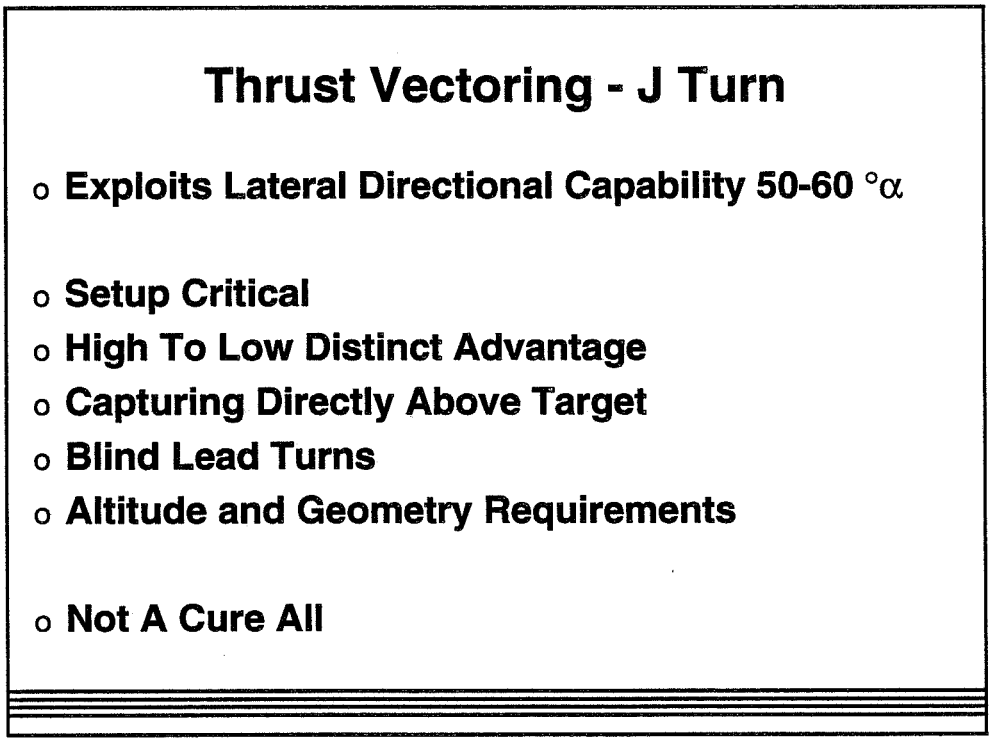

1v1

The 1v1 was an effective maneuver for evaluating not just the capabilities of the HARV but evaluating the "capability of the pilot" to use the increased control power to his advantage. Because the pilot was able to prosecute and capture the target in any way he saw fit, the test team was able to evaluate the capability of the pilot to use the added capabilities of the HARV.

The HARV was allowed to maneuver at will after a 180 out pass with the target. The target performed a 300 kt, 3 g level turn until the HARV made the capture. With thrust vectoring off, the HARV executed a max power, energy sustaining, nose low, slice turn back towards the target at corner speed using 4 to 4.5 g. The target was captured from low to high using an aggressive, energy dissipating pull to 35 AOA. During this maneuver, very little roll rate was commanded, and time to capture was based primarily on maximum turn performance at corner speed, with a maximum pitch rate command to capture. The initial plan for the thrust vectoring on capture was to fly the first part of the capture the same, but initiate the pitch capture much earlier by exploiting the capability of the HARV to pitch to 70 deg AOA. During the simulation this did not decrease the time to capture dramatically. There had to be a better way. Instead of trying to exploit the longitudinal axis, why not exploit the lateral directional axes? It was decided to utilize the superior lateral directional capability of the HARV and the "lampshade" technique for the capture.

At the merge, instead of digging nose low back towards the target, the velocity vector was "cast" up at the merge, like the beginning of the J-turn and eased back toward the target in one circle flow. The HARV then delayed "on the perch" at mid range AOA (35-45 degrees) to conserve energy and predicted the targets flight path. At this point an altitude advantage had been gained and lateral separation had been achieved.. When the target flew into the HARV's lampshade, a pure lateral directional capture was executed, high to low.

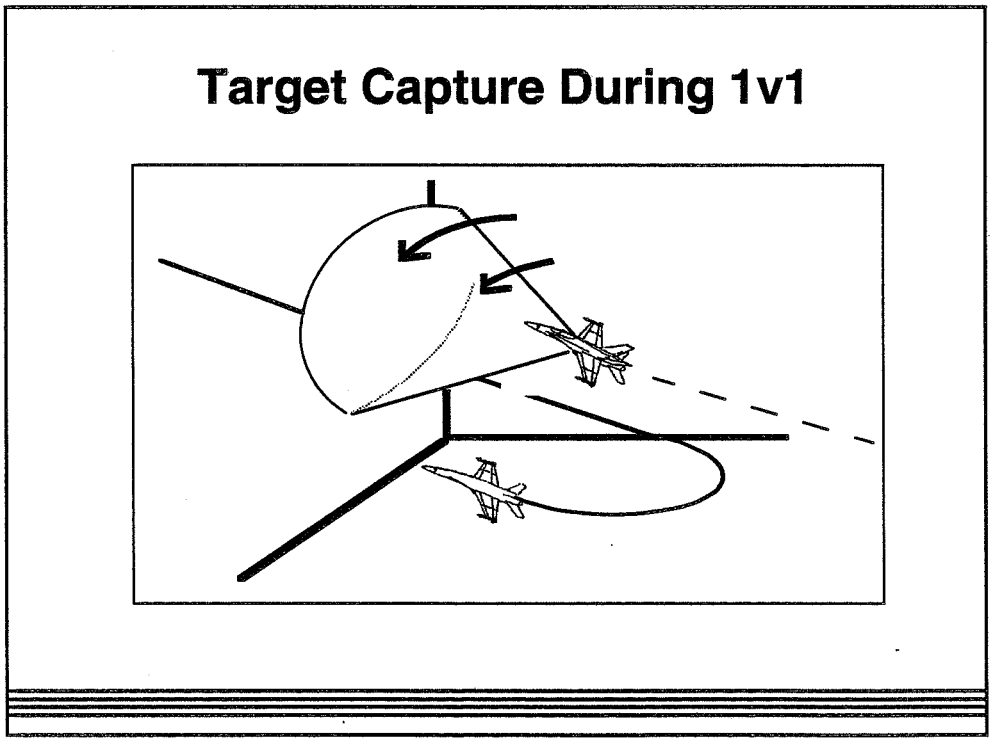

1v1 CONCLUSIONS

The 1v1 was flown multiple times by both pilots, and different techniques were utilized as described earlier. Not all 1v1's worked out as the pilots had planned, but some useful conclusions were drawn from even the less than successful captures.

1. Using the capability of the HARV to roll at high AOA's is just as tactically advantageous as being able to pitch to 70 deg AOA. In some cases, it was even more unpredictable from a target's perspective and should not be discounted. An increased emphasis on utilizing the lateral directional axes is warranted.

2. An altitude/energy advantage is even more critical when maneuvering beyond Clmax than it is in conventional aircraft due to the high energy losses experienced at high AOA. The post stall capability must be used judiciously and carefully for it to be effective.

3. Both pilots adapted quickly to this new environment and were able to use the increased capabilities of the HARV to a tactical advantage. It's not too hard.

4. After using the post stall capabilities of the HARV, energy addition is critical and emphasizes the need for bigger motors and lighter systems.

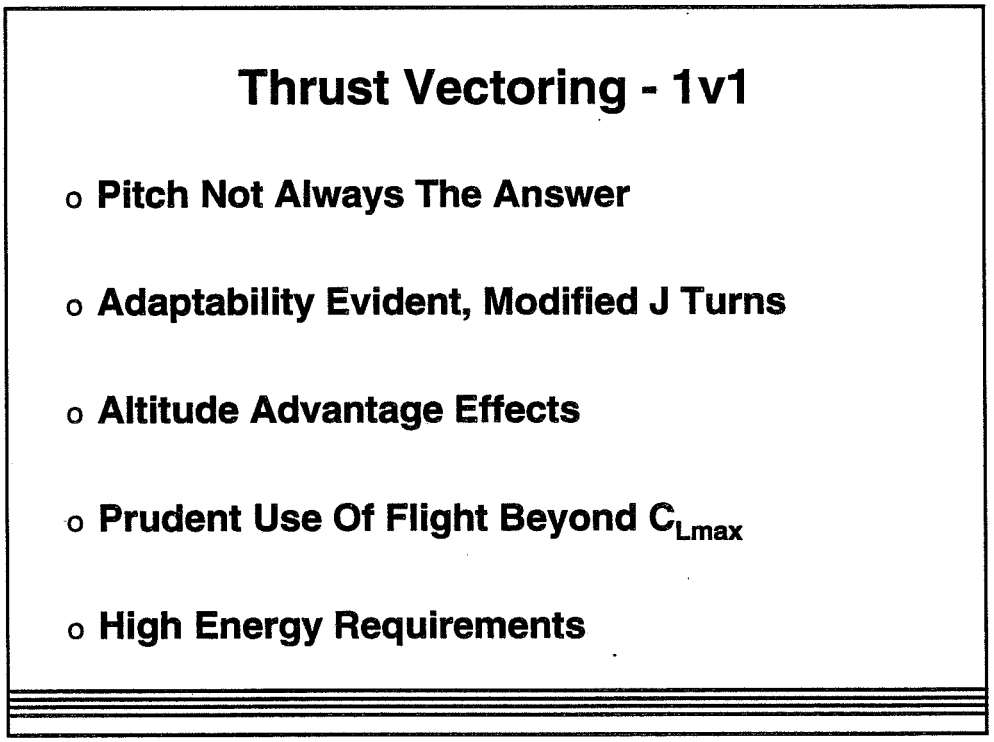

ROLL PERFORMANCE CLASSIFICATION

The Roll Performance Classification proved to be simple and useful during flight test. The simplicity was a benefit, especially since between maneuvers the pilot also had to provide comments and HQR's on the capture. The RPC's given for the maneuvers were consistent between pilots and correlated nicely with pilot comments. It was evident that the RPC was very maneuver specific and one must be careful not to correlate RPC's will roll performance data without identifying the maneuver. For instance, during a flat scissors, where very little roll rate was commanded, for that task, 10 deg/sec might have been tactically superior but that same roll rate during a guns defense would have been unacceptable. Interpilot data was consistent for the same maneuver.

The pilots emphasize that although simple, the RPC scale does help to quantify pilot comments and tactical utility. The scale can be used in a general sense for any maneuver, since specific performance criteria is not identified. It is good method to help to evaluate tactical utility when no other quantitative data is available.

The RPC provided consistent results and correlated fairly consistently with simulator data.

When RPC ratings are used in conjunction with HQR's, regions of acceptable handling qualities and performance can be identified. This scale also allowed the pilot to interpret the tactical situation and rate lateral directional performance based on his own background, knowledge and tactical experience.

RPC Scale

- **Simple, Effective, Easy To Use**
- **Maneuver Specific**
- **Consistent Results**
- **Allows Pilot Interpretation Of Tactical Situation**

RPC AND TACTICAL UTILITY

The RPC was also useful as a another measure of tactical utility. RPC ratings for maneuvers flown with the baseline HARV were all 3's and 4's. This was in the unsuitable, unacceptable range for roll performance. Flying identical maneuvers with the thrust vectoring engaged, resulted in RPC ratings in the 1 to 2 range which is the "suitable" and "tactically superior" range. It was clear from the pilot comments during both the HAIRRY maneuvers and the tactical maneuvers that the thrust vectoring provided the pilot with increased tactical utility. These pilot comments backed up and correlated nicely with the RPC ratings. Again, the beauty of the RPC scale is that it has the flexibility to be used for almost any task and gives the pilot the ability to rate the maneuver based on his perception of the tactical utility.

Maneuver Summary

Maneuver	AOA	RPC TV Off	RPC TV On
Lateral Gross Acquisition	15	---	1
	30	3	2
	40	---	2
	60	---	2
Offensive Loaded Reversal	15	---	1
	30	4	2
	45	---	2
	60	---	2
Defensive Roll	30	3	2
	45	---	1
	60	---	2
Flat Scissors	30	3	1
J Turn	A/R	---	2
1v1 Level	A/R	---	1
1v1 6K' Split	A/R	---	2

PILOT ADAPTABILITY / SPATIAL AWARENESS

One of the key components of the tactical utility equation and one that must not be left out is the pilot. The pilot interprets the tactical situation and decides what actions must be taken to achieve the desired outcome. Regardless of what capability the engineers have given his airplane, his knowledge and more importantly his perception of his own capabilities will affect his actions. Is the pilot's perception of what is happening close to reality? When a pilot commands roll and perceives the aircraft yawing, will that create a spatial awareness problem? Are his perceptions influenced by the dynamics of the task and the problem of prosecuting a bogey?

One of the purposes of this flight test was to find out what the pilot actually perceives and how he interprets the situation, specifically at high AOA. Both pilots had extensive simulator time at high AOA, but how would actual flight test affect his comments on tactical utility and spatial orientation.

After eight flights, numerous closed loop, open loop and tactical tasks, both pilots were of the same opinion - "This is great, it's just like any other kind of flying." "Easy to use, feels good." "It's intuitive, even at extreme AOA's, the coning effect was not disorienting in any respect." "No surprises". Keeping in mind, that this was both pilot's first experience with flight at those extreme angles of attack, up to 70 degrees, these comments are poignant. Neither pilot ever felt disoriented. Neither pilot felt any significant sideforces and each pilot adapted very quickly to high AOA flight. Both pilots were very surprised that it felt so natural. They had expected some disorientation or at least some confusion, especially when "coning" around at 70 deg AOA.

Both pilots learned how to use the high AOA capability of the HARV very quickly. After only a few tactical maneuvers, pilots were flying the HARV very efficiently and minimizing time to kill during the 1v1's. Both pilots were able to factor the capabilities of the HARV into their tactical plan real time and successfully maneuver the aircraft. It was evident that flight at extreme angles of attack will pose no more of a training problem in the fleet than normal ACM training. It's just another tool that the fleet pilot needs to learn how to use.

Pilot Adaptability

- **High AOA Flight Regime Adaptability**
- **Good Simulator Fidelity**
- **No Disorientation**
- **Intuitive, Felt Natural**
- **No Extensive Training Required**
  (If Ricardo could figure it out . . .)

DEPARTURE RESISTANCE

A tremendous tactical benefit from the thrust vectoring system on the HARV is the superb departure resistance that it enjoys. For many years, departures, subsequent out-of-control flight and even aircraft and aircrew losses have been a somewhat regular occurrence in the ACM business. Some solutions have been limitations to the aircraft in terms of AOA but in the HARV we have increased departure resistance by expanding the aircraft envelope.

Throughout all eight flights, there were no departures and at no time did the pilot even approach the departure boundaries. This is a significant point given that these maneuvers were targeting the edge of the current HARV envelope using abrupt, full stick, long duration inputs.

A departure during an ACM engagement is usually followed by the departing aircraft getting gunned. Departure resistance is a **significant** tactical advantage. This is an aside that is often overlooked. This allows the pilot to spend less time worrying about dancing around the edge of the envelope and more time flying right on the edge if required.

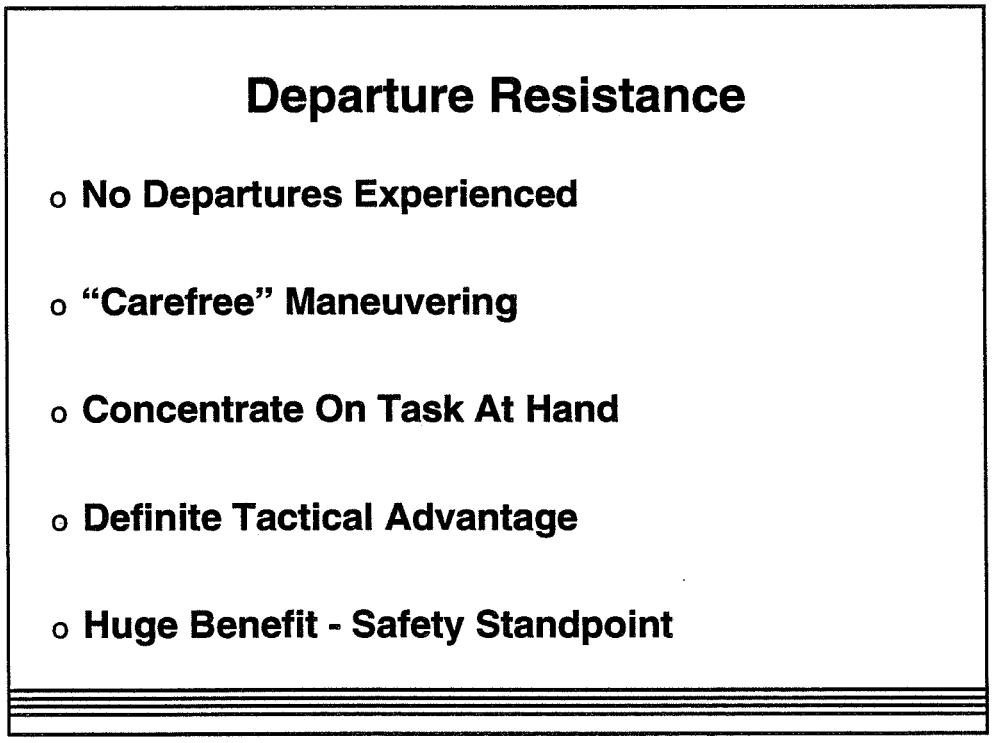

LATERAL STICK VERSUS RUDDER PEDALS AT HIGH AOA

There are two basic schools of thought on how the lateral-directional axes should be controlled at high AOA. One school of thought espouses the "Classical" theory that flight control laws should be written with pilot perceived motion as the driver. i.e. Yawing motion at high AOA should be controlled by rudder pedals and roll should be controlled by lateral stick. The proponents of this theory argue that it would be disorienting to the pilot to input lateral stick at 60 deg AOA and perceive almost a pure yawing motion, the coning effect.

The other side of the argument we'll call the "Feet on the floor" guys. This school of thought believes in simplicity such that at high AOA's, lateral stick controls all lateral directional motion with the flight controls coordinating sufficiently not to warrant use of rudder pedals.

Most high AOA simulation efforts utilize feet on the floor control laws for interpilot and intrapilot data consistency Both Navy pilots have been involved in many feet on the floor simulations and one was a proponent of the classical method and one was a feet on the floor guy.

After having flown the HARV both pilots are firm in their belief that flying "feet on the floor" at high AOA is quite natural, easily adaptable and poses no spatial awareness or disorientation problems. Other than providing consistent results for test missions, it is very simple, and simplicity when flying at high AOA's is key.

A compromise for both parties would have the rudder pedals and lateral stick command the same control system response at high AOA. In this way, a pilot would be able to use what feels comfortable to him. The only difficulty would be that at lower AOA's, it is desired to have rudder pedals command yaw and lateral stick command roll. There needs to be a crossover AOA below which rudder pedals and lateral stick behave in a "conventional" sense. Currently in the F/A-18, the crossover AOA where the rudder pedal to rolling surface interconnect comes into play is 13 deg AOA.

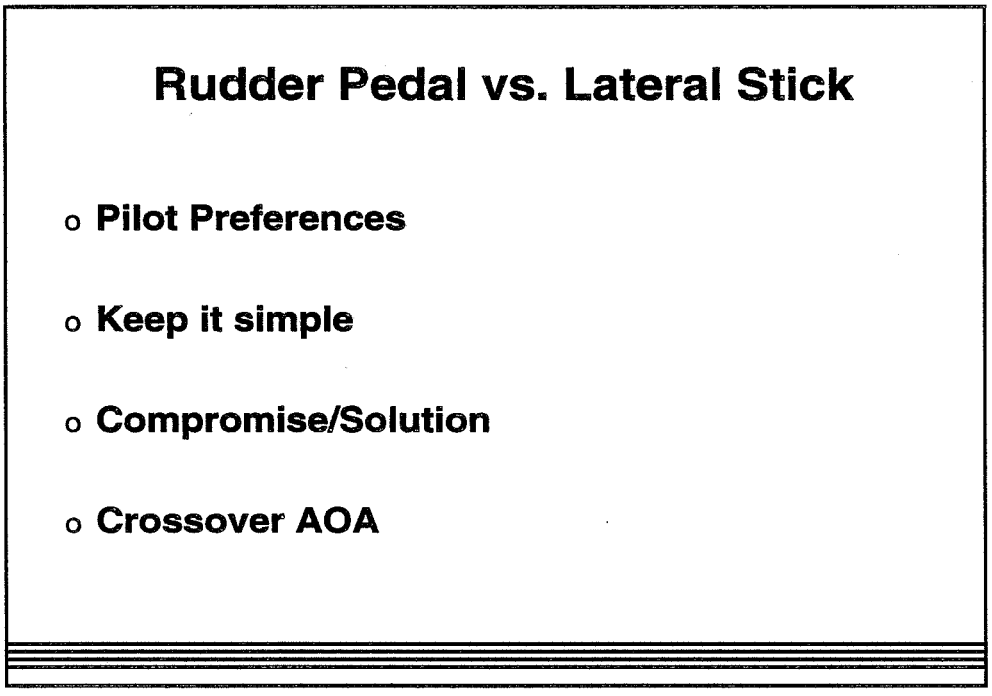

CONCLUSIONS

The test team is convinced that the additional control power provided to the HARV by the thrust vectoring system is tactically advantageous to the fighters of the future in terms of providing the pilot with an "enhanced" set of tools to enter the fight with.

Both pilots were able to experience the tactical benefits that thrust vectoring provided them on the HARV. The increased control power was quite impressive at the extreme angles of attack (45 deg and above) and the ability to fly and maneuver at the extreme AOA's proved superior in a slow speed flight. The thrust vectoring also provided a significant capability when operating at or just below CLmax, (35 deg AOA in the F/A-18). In some cases this added capability at moderate AOA's was more tactically useful that the ability to fly at 70 deg AOA. The pilots found that only momentary excursions to 60 to 70 deg AOA were practical due to the large energy losses experienced at these AOA's.

The increased control power allowed the HARV pilot to maneuver much more effectively within the current Hornet envelope and maneuver at will outside the envelope, resulting in a clear and distinct tactical advantage.

The pilots were pleasantly surprised at the tactical utility of the lateral directional maneuverability at all AOA's. They realized that although the ability to pitch to extreme AOA's, it is also a significant capability to command significant roll/yaw rates at those AOA's.

Both pilots concluded that the full potential of the thrust vectoring system would not be realized until a much higher thrust to weight ratio is achievable on the test platform. The large energy losses experienced during high AOA maneuvering requires more thrust, quicker energy addition - We need bigger motors and lighter, integrated systems.

Finally, thrust vectoring is not a cure all in the tactical environment, but it adds some tremendous benefits to the fighter pilot's bag of tricks and it is essential to have this capability in fighters of the future.

Conclusions

- **Benefits At Extreme AOA's**
  - **Lateral Directional Maneuverability/Repositioning**
  - **Pitch Pointing/Intimidation**
- **Judicious Use**
  - **Large Energy Dissipation Post Stall**
  - **Altitude/Energy Advantage Critical**
  - **Emphasizes Need For Bigger Motors/Lighter Systems**
- **Benefits Inside Current Envelope**
  - **$\leq C_{Lmax}$**
- **Not A Cure All**
  - **Powertool For Your Toolbox**

Forebody Controls

19950707839
35004
N95-14253
16102
p. 12

An overview of the computational effort to analyze forebody tangential slot blowing is presented. Tangential slot blowing generates side force and yawing moment which may be used to control an aircraft flying at high angle of attack. Two different geometries are used in the analysis--the High Alpha Research Vehicle, which is a highly instrumented F/A-18, and a generic chined forebody. Computations using the isolated F/A-18 forebody are obtained at full-scale wind tunnel test conditions for direct comparison with available experimental data. Additional non-time-accurate solutions using the isolated forebody are used to predict the effect of slot blowing at transonic flight conditions. The effects of over- and under-blowing on force and moment production are analyzed. Time-accurate solutions using the isolated forebody are obtained to study the force onset time lag of tangential slot blowing. The effect of blowing on the burst point location are analyzed by obtaining computations using the aircraft geometry, which includes the wing, empennage, and faired-over inlets. The effect of blowing on the aerodynamic loads on the vertical tails are analyzed using time-accurate computations. Comparison with available experimental data from full-scale wind tunnel and sub-scale wind tunnel tests are made. Computations using the generic chined forebody are obtained at experimental wind tunnel conditions, and the results compared with available experimental data. The effect of jet parameters and slot location are studied. This computational analysis compliments the experimental results and provides a detailed understanding of the effects of tangential slot blowing on the flow field about simple and complex geometries.

COMPUTATIONAL ANALYSIS OF FOREBODY TANGENTIAL SLOT BLOWING

KEN GEE
MCAT INSTITUTE

ROXANA M. AGOSTA-GREENMAN
YEHIA M. RIZK
LEWIS B. SCHIFF
AMES RESEARCH CENTER

RUSSELL M. CUMMINGS
CALIFORNIA POLYTECHNIC STATE UNIVERSITY,
SAN LUIS OBISPO

4th NASA High Alpha Conference/Workshop
Dryden Flight Research Center
Edwards, CA
July 12-14, 1994

MCAT Institute

HIGH ALPHA NASA AMES

Aircraft flying at high incidence may experience a large, unintended side force and yawing moment which can lead to departure of the aircraft from the desired flight path. Forebody tangential slot blowing can be used to provide the pilot with a means to control the side force and yawing moment and use them to control the aircraft. The numerical investigation focuses on the implementation of forebody tangential slot blowing on the NASA High Alpha Research Vehicle (HARV). The HARV is a highly instrumented F/A-18 used in flight tests to obtain a database on the behavior of the flow field about aircraft flying at high angles of attack. Since future aircraft designs, such as the YF-22, differs from the F/A-18 in the use of a chined forebody instead of a smooth, rounded forebody, forebody tangential slot blowing is also applied to a generic chined forebody to investigate the effectiveness of such a combination.

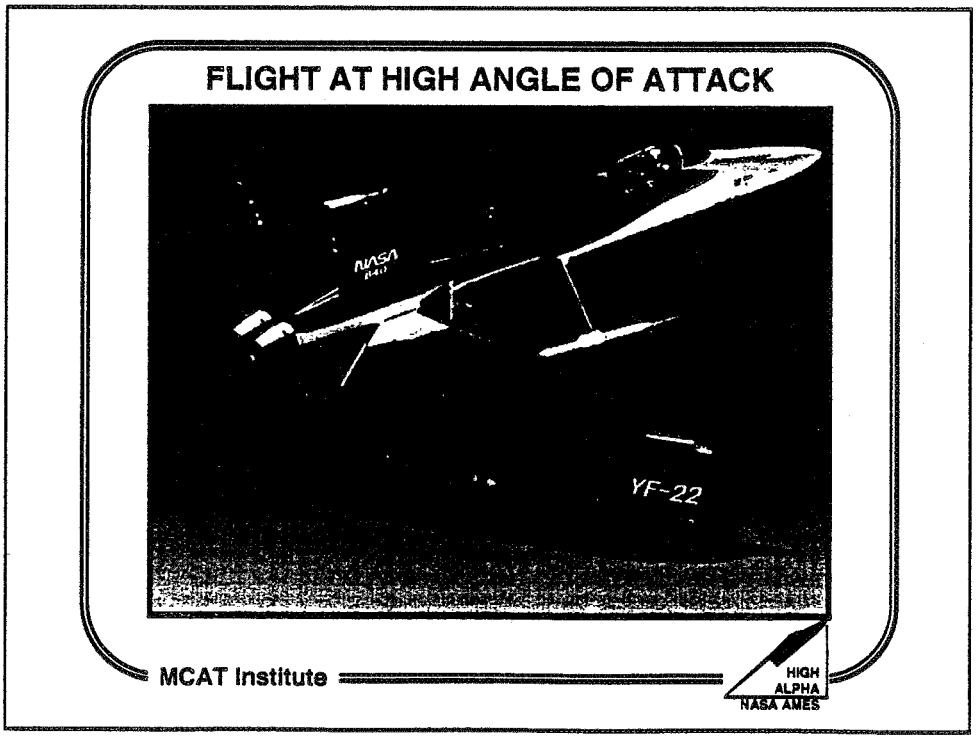

An overview of the presentation is shown in this slide. The objectives of the numerical study will be outlined. The numerical method used to solve the governing equations is briefly discussed, including the flow solver used, the grid system employed, and the boundary conditions applied. The results are presented in two parts. The first part covers the effectiveness of forebody tangential slot blowing on the HARV geometry, using both isolated forebody and wing/body/tail geometries. The second part presents results of applying forebody tangential slot blowing on an isolated chined forebody. Finally, conclusions drawn from the results obtained during from this investigation is presented.

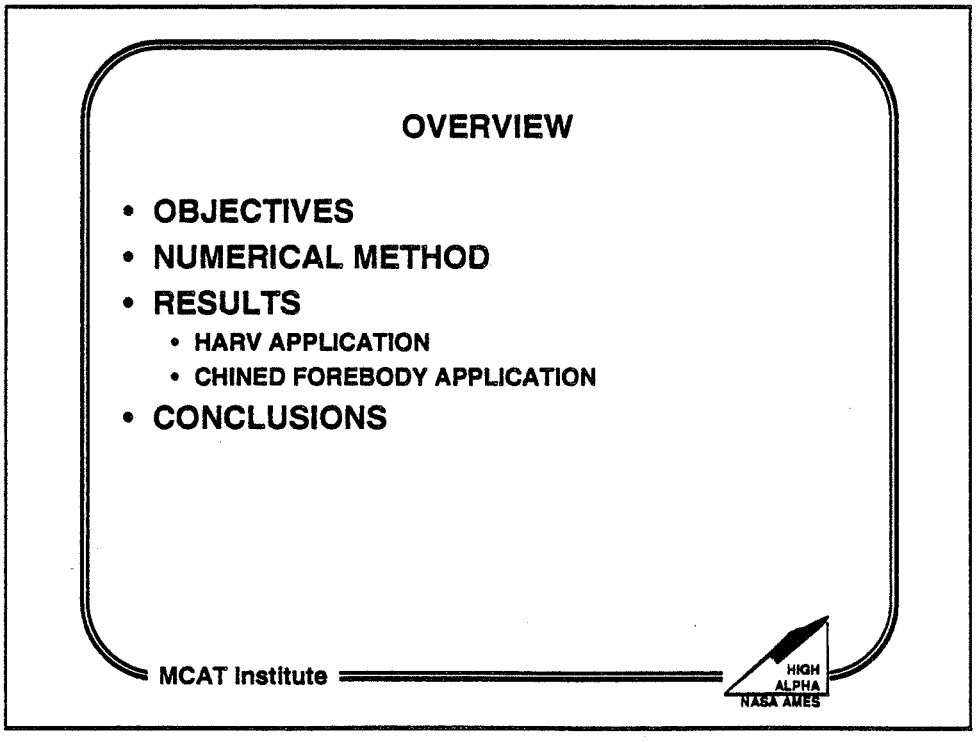

The investigation involving the HARV configuration is divided into four parts. A solution using the isolated HARV forebody is obtained at full-scale wind tunnel test conditions and compared with experimental data to determine the accuracy of the numerical method and the ability of the method to resolve the surface pressure coefficients. Solutions using a more complete geometric representation of the HARV, including wing, deflected leading-edge flap, empennage, and faired-over engine inlet, show the effect of blowing on the flow field about the aircraft. These solutions provide clues about how the side force and yawing moment are generated. Time-accurate solutions using the aircraft geometry provide data on the changes in the aerodynamic loads on the vertical tails due to blowing. This can have an effect on tail buffet. Finally, the effect of freestream Mach number on blowing over the isolated HARV forebody is investigated. The use of the isolated forebody allows for a number of solutions to be made, so that a range of Mach numbers and jet mass flow rates can be investigated. The analysis of blowing on the chined forebody also includes comparison of computed results with experimental data, along with an investigation of the effect of jet parameters and slot location on force and moment generation at various angles of attack.

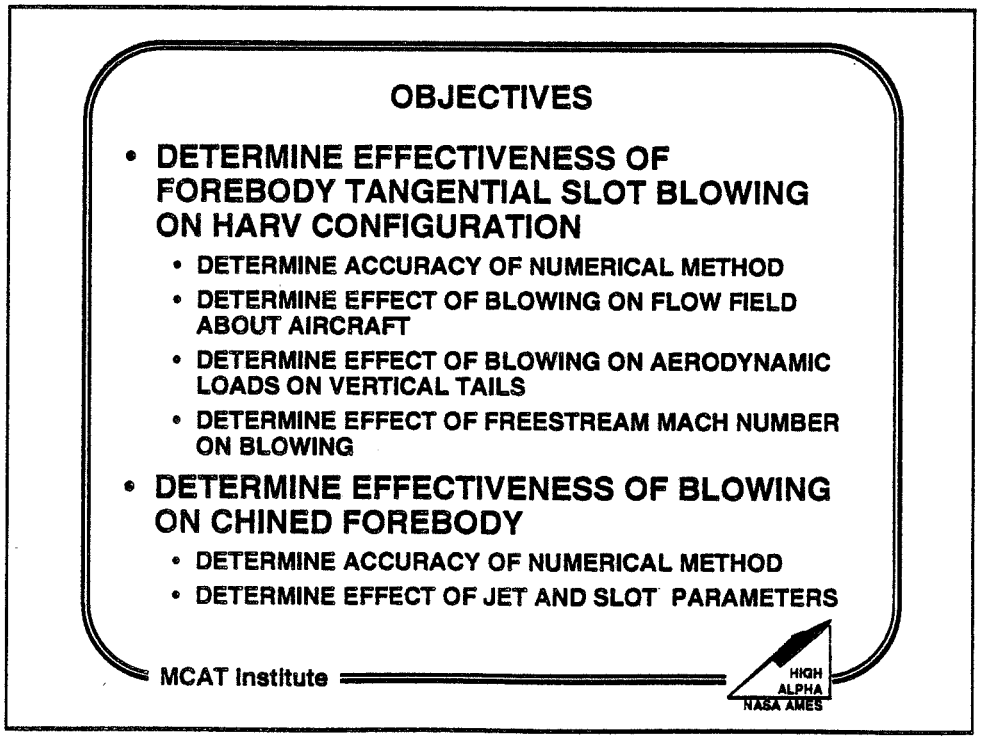

To simplify the process of generating grids about a complex geometry such as the HARV, the overset grid method[1] is used. In this method, the HARV geometry is divided into parts, and separate grids are generated about each part using a hyperbolic grid generator. The grids are then combined and a communication scheme is generated to pass boundary information among overlapping grids. The communication scheme does not require the grid boundaries to match faces.

Since the flow about an aircraft flying at high angle of attack is three-dimensional and separated, solution of the three-dimensional, thin-layer Navier-Stokes equations is required to accurately model the flow. The flow solver used to solve the Navier-Stokes equations is F3D.[2] F3D uses approximate factorization and partial flux splitting to obtain upwind differencing in the streamwise direction and central differencing in the other two directions. F3D is second-order accurate in space, and can be first- or second-order accurate in time. The time-accurate computations use first-order time accuracy. The solutions are obtained assuming fully turbulent flow. For closure, the Baldwin-Lomax algebraic turbulence model[3] is used. In the fuselage and forebody grids, the Degani-Schiff modifications[4] to the Baldwin-Lomax model is implemented.

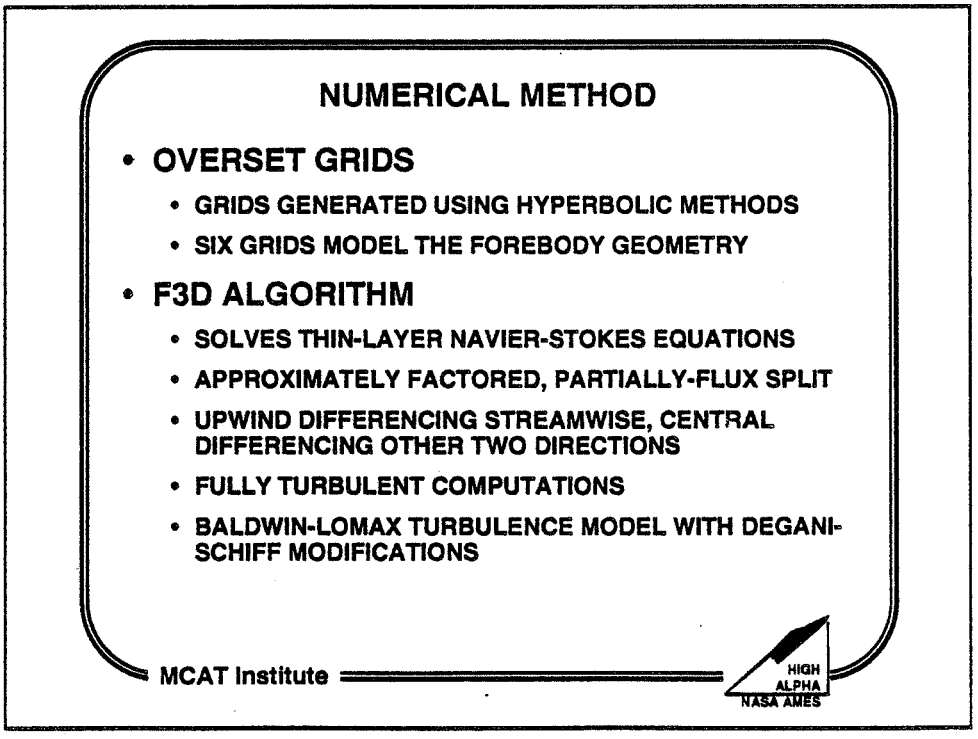

Full-scale wind tunnel experiments were carried out in the NASA Ames 80 by 120 ft. wind tunnel using an F/A-18 model.[5] The model was fitted with a forebody tangential slot blowing system. The system consisted of a 48 in. slot, beginning 3 in. from the nose. The slot was divided into six 8 in. sections. Each section was connected to a valve, which in turn led to a plenum. Thus, the active slot length can be controlled. Blowing occurred on the port side. A dummy slot was located on the starboard side to maintain symmetry in the model.

The computational grid system modeled this slot geometry, including the backward-facing step of the slot itself. The active slot length is controlled through the use of boundary conditions that model the jet parameters. A solution is obtained using the isolated forebody geometry at wind tunnel test conditions.[6] The results are then compared with the experimental data to determine the accuracy of the numerical method, especially in the jet region.

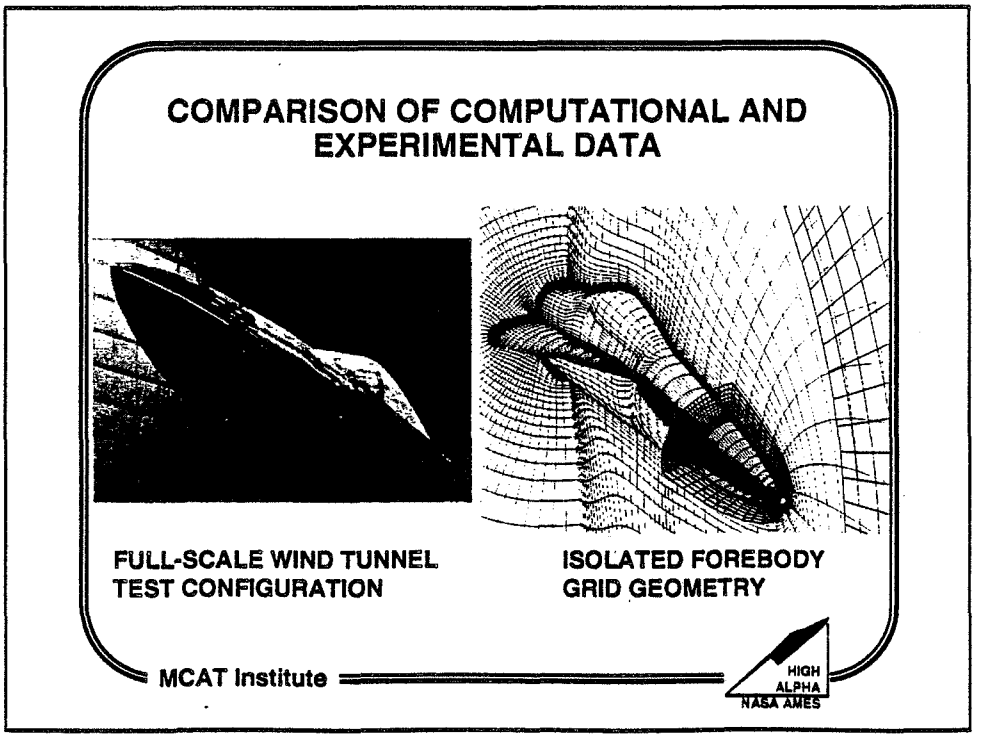

The computed surface pressure coefficient is compared with full-scale wind tunnel test data at the five pressure stations located on the forebody barrel. The computed results compare quite well with the experimental data. The computed results resolve the suction peak due to the attached jet quite accurately in the first two pressure ring locations. There is a suction peak associated with the separation of the jet in the computational result, located near $\phi = 200°$, which does not occur in the experimental data. This may be due to the use of the Baldwin-Lomax turbulence model in the attached jet region. At the aft two pressure rings, the asymmetry in the pressure distribution is resolved, with the blowing-side surface pressure slightly lower than the non-blowing-side surface pressure. This contributes to the side force and yawing moment obtained from blowing. These results provides confidence in the numerical method to accurately predict the effects of forebody tangential slot blowing on the flow field about the F/A-18.

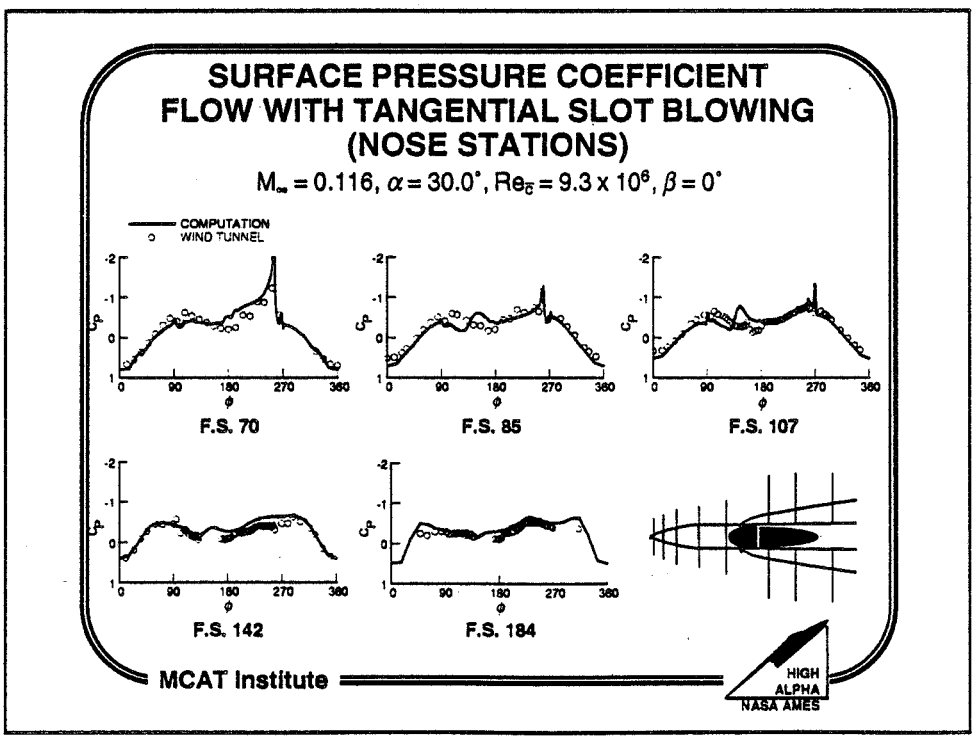

Since blowing has an effect on the entire flow field about an aircraft flying at high angle of attack, solutions are obtained using the aircraft geometry model at a typical flight condition.[7] The solutions show the effect of blowing on the flow field and the ability of the blowing system to operate at a flight condition. The grid system consists of 22 grids, totalling 1.8 million grid points. The computational grid model contains the major features of the HARV, including the wing, deflected leading-edge flap, and vertical and horizontal tails. Simplifications are introduced to facilitate the modeling. The engine inlets are faired-over and the boundary layer diverter vent is highly simplified. However, these simplifications should have minimal impact on the major flow characteristics.

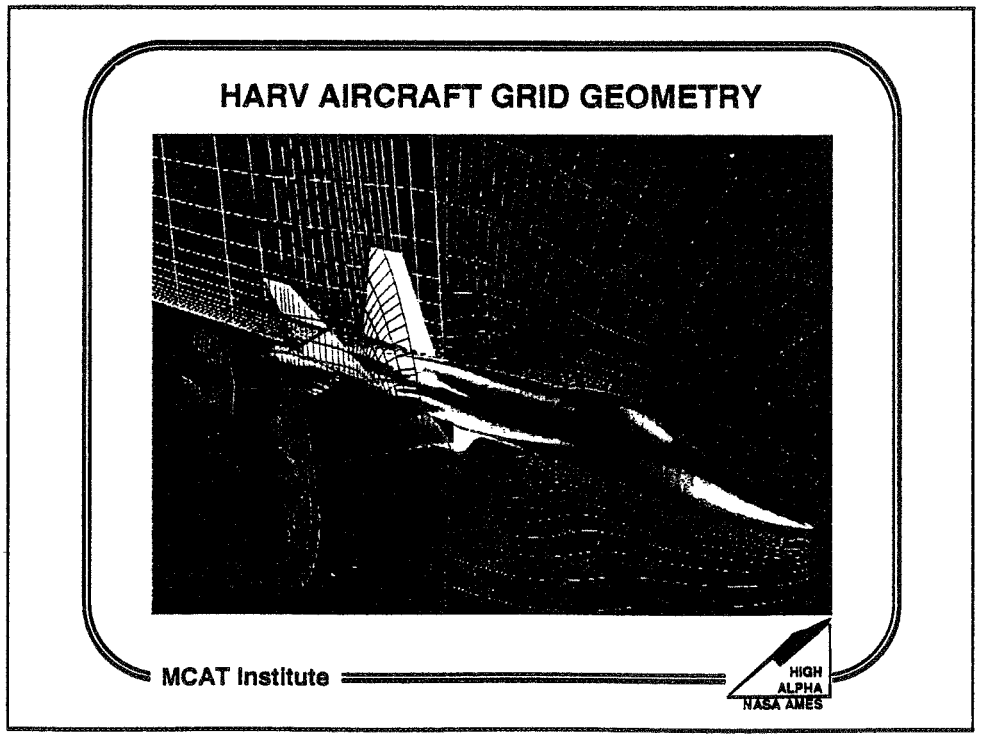

The effect of forebody tangential slot blowing is not limited to the flow field about the nose. The most noticeable effect on the flow field about the aircraft is the asymmetric LEX vortex burst caused by blowing. The blowing-side LEX vortex bursts sooner than the non-blowing-side LEX vortex, as shown in the above figure. This has been confirmed by flow visualization taken in the full-scale wind tunnel tests. However, the computed burst point position of both LEX vortices are aft of the burst points observed in the experiment. This is due to using a coarse grid system. The blowing-side LEX vortex becomes stronger than the non-blowing-side LEX vortex, which leads to the asymmetric burst points. This difference in vortex strength also creates a side force and yawing moment in the direction of the blowing side. The yawing moment obtained from the computations compare quite well with the experimental data from the full-scale wind tunnel test. Since the flow aft of the vortex burst is unsteady, the averaged time-accurate yawing moment agrees better with the experimental values than does the averaged steady-state yawing moments. However, the averaged steady-state yawing moments do provide a good approximation without the computational expense of the time-accurate solution.

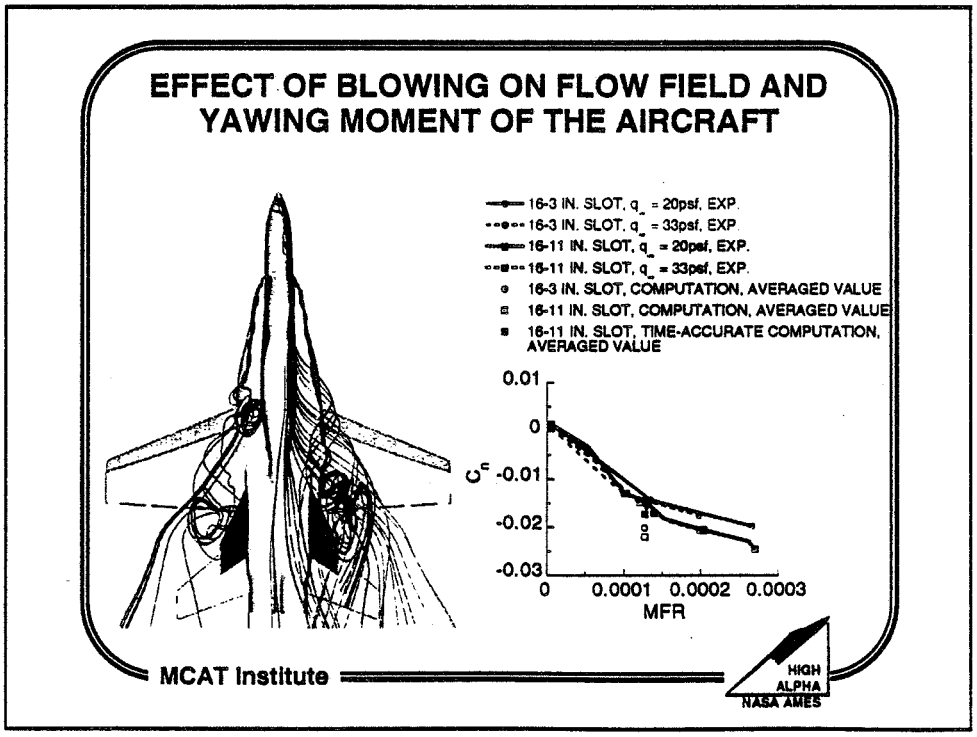

Time-accurate computations show that blowing has an effect on the frequency content of the aerodynamic loads on the vertical tails.[7] The computations were done using a rigid tail (i.e., no movement of the vertical tails due to the loads were simulated). The computed bending moment on the vertical tails show an oscillatory load on the tails. A Fast Fourier Transform analysis of the bending moment time history shows that the dominant frequency of aerodynamic loads on the vertical tails are 9 Hz for the blowing-side tail, and 12 Hz for the non-blowing-side vertical tail. These frequencies are slightly lower than that obtained in no-blowing computations and experiments. This indicates that blowing has an effect on the load frequencies, and therefore the tail buffet phenomenon .

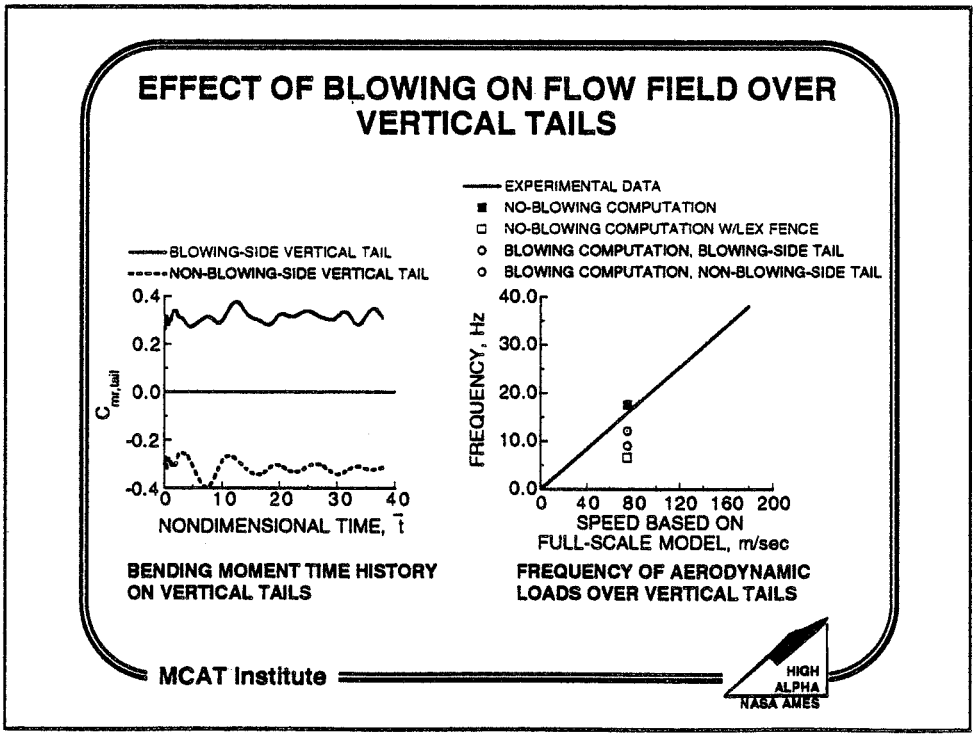

High performance fighter aircraft can maneuver in the high-angle-of-attack regime at transonic speeds. In order to determine the effect the freestream Mach number has on blowing, the problem is investigated numerically.[8] To best utilize available computational resources, the isolated forebody geometry is used in this part of the study. The smaller grid system requires less computer time, meaning more solutions can be obtained, allowing for a study at a variety of freestream velocities and jet conditions. Three freestream Mach number values are studied. At each freestream Mach number, different jet mass flow rates are used. The jet mass flow rate is determined by keeping the mass flow ratio (MFR) constant across the Mach number spectrum. The MFR is defined as the ratio of the jet mass flow rate and a reference mass flow rate based on freestream density, freestream velocity, and wing area.

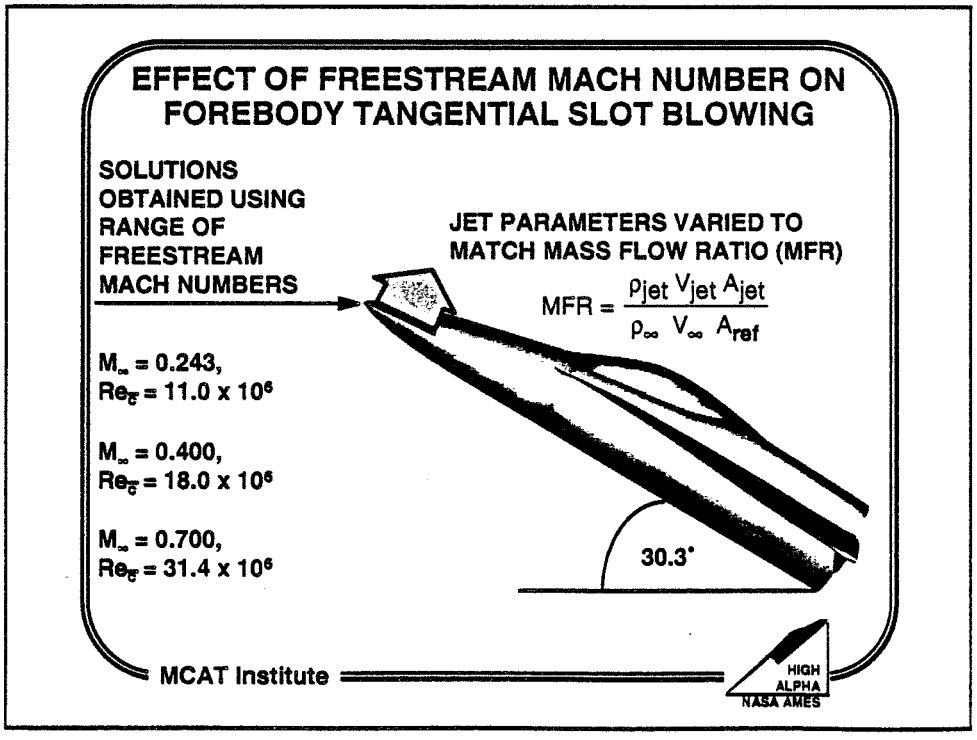

In order to determine the effectiveness of tangential slot blowing at higher freestream Mach numbers, computations are obtained using the F/A-18 isolated forebody with blowing at subsonic and transonic Mach numbers. At each freestream Mach number, solutions are obtained using a number of mass flow ratios. The correlation with MFR holds fairly well as the blowing rate increases and only breaks down at high blowing rates and high freestream Mach number. At high blowing rates and high freestream Mach number, overblowing occurs. Overblowing is characterized by a leveling off or drop in yawing moment with increasing blowing rates. Analysis of the computational results indicates the jet is underexpanded as it leaves the slot and separates fairly quickly. This early separation reduces the low pressure region caused by the jet and reduces the effect of the jet on the forebody vortices. Both of these effects contribute to a reduction in the yawing moment. This problem may be avoided by increasing the slot area, thereby reducing the total pressure required for a desired jet mass flow rate.

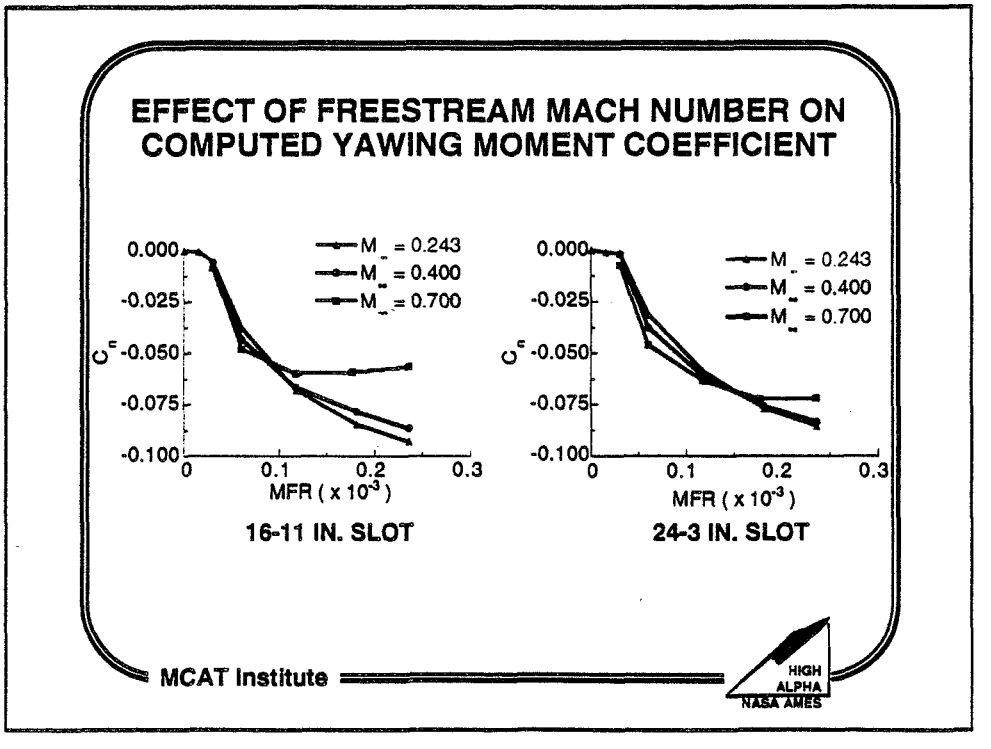

The effect that tangential slot blowing has on the flow field about the HARV can be seen using off-surface instantaneous streamlines. At very low blowing rates, the jet does not have enough energy or momentum to change the position of the vortices due to the nose. Instead, the jet becomes entrained in the blowing-side vortex and separates. Since the flow field remains essentially unchanged, there is little or no yawing moment produced. At moderate blowing rates, the jet remains attached to the surface due to the Coanda effect. The jet moves the blowing-side vortex and merges with the non-blowing-side vortex. This significantly alters the flow field near the nose, as well as the interaction of the vortices due to the nose and the LEX vortices. Therefore, significant yawing moment is obtained. At very high blowing rates, overblowing occurs. In order to obtain the high jet mass flow rate, the total pressure of the jet is increased such that the jet chokes at the exit, and the jet exit pressure is almost five times the local static pressure. Consequently, the jet is underexpanded. As the jet exits the slot, it rapidly expands, causing it to separate from the surface. This early separation limits the ability of blowing to generate yawing moment, leading to the leveling off of the yawing moment with increasing mass flow ratio.

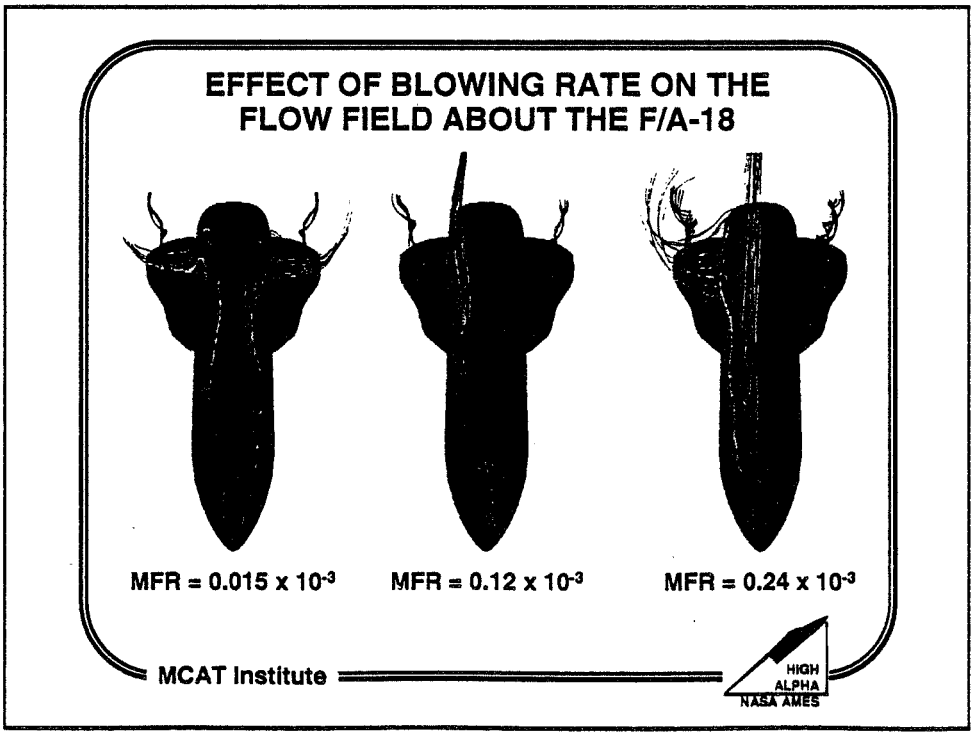

The time required for the yawing moment to fully develop from the onset of blowing must be known in order to determine the usefulness of forebody tangential slot blowing on a flight aircraft. Large force onset time lags would render the system useless. Full-scale[5] and sub-scale[9] wind tunnel tests have been conducted to quantify the force onset time lag associated with blowing. The results indicate time lags on the order of 0.1 second real time, or 1.0 non-dimensional time unit. Computations are obtained in a time-accurate mode using the isolated F-18 forebody to determine if the time lags can be resolved numerically and to extend the experimental data to higher freestream Mach numbers.[8] The computed results indicate the time required to fully establish the yawing moment is approximately 1.0 non-dimensional time unit, or the time it takes for a particle to travel the length of the forebody. This result is consistent with the experimental data. The response of the surface pressure coefficient at two fuselage stations on the forebody are also presented. At F.S. 142, there is a slight delay before the pressure drops in response to the blowing. This delay is larger at F.S. 184 since the disturbance requires more time to convect downstream. However, the time lag associated with blowing are well within acceptable limits and do not present a problem in implementation of blowing on a flight vehicle.

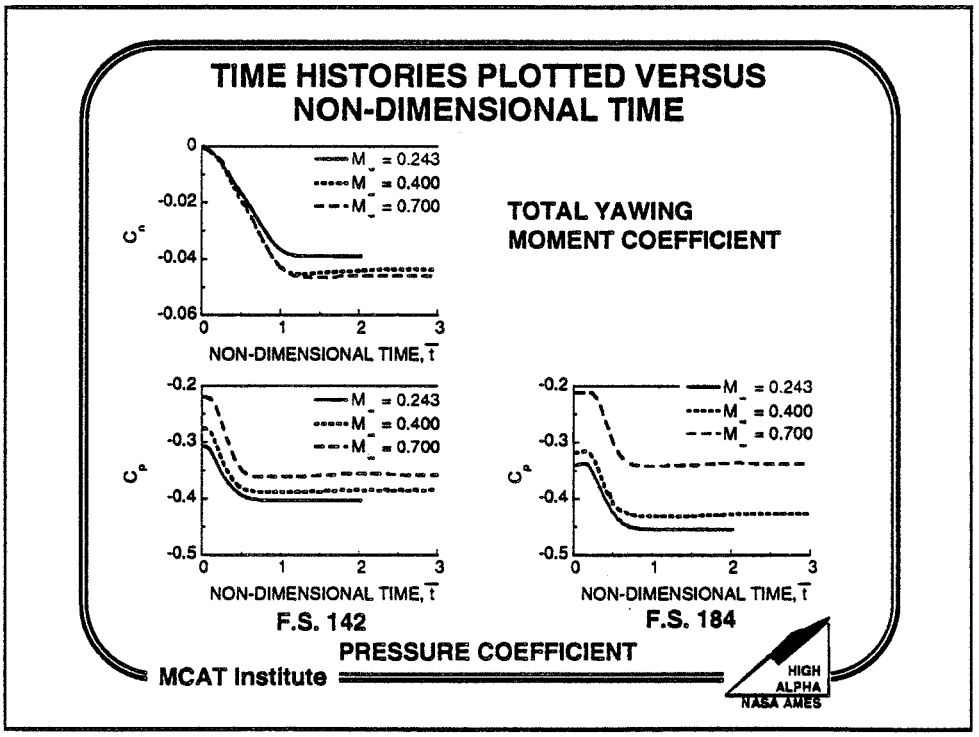

Future aircraft designs will differ from current aircraft designs. One such difference is the use of chined forebodies in future aircraft, compared to the smooth forebodies in use today. The use of tangential slot blowing on future aircraft designs will depend on its effectiveness in conjunction with the chined forebody. To address this question, an experimental investigation was undertaken at Cal Poly, San Luis Obispo, using a model of a chined forebody in the low-speed 3 by 4 ft. wind tunnel.[10] The model contained a slot located on the top surface. As in the full-scale F/A-18 model, the slot was divided into sections, with each section connected to a valve, so that the length of the active slot region can be controlled. Force and moment data were obtained using a sting balance. A numerical study was undertaken to compliment and extend the wind tunnel experiment.[11] A computational model of the wind tunnel model was developed, with the slot geometry modeled, using the overset grid method, hyperbolic grid generator, and grid communications software used to develop the HARV grid system.

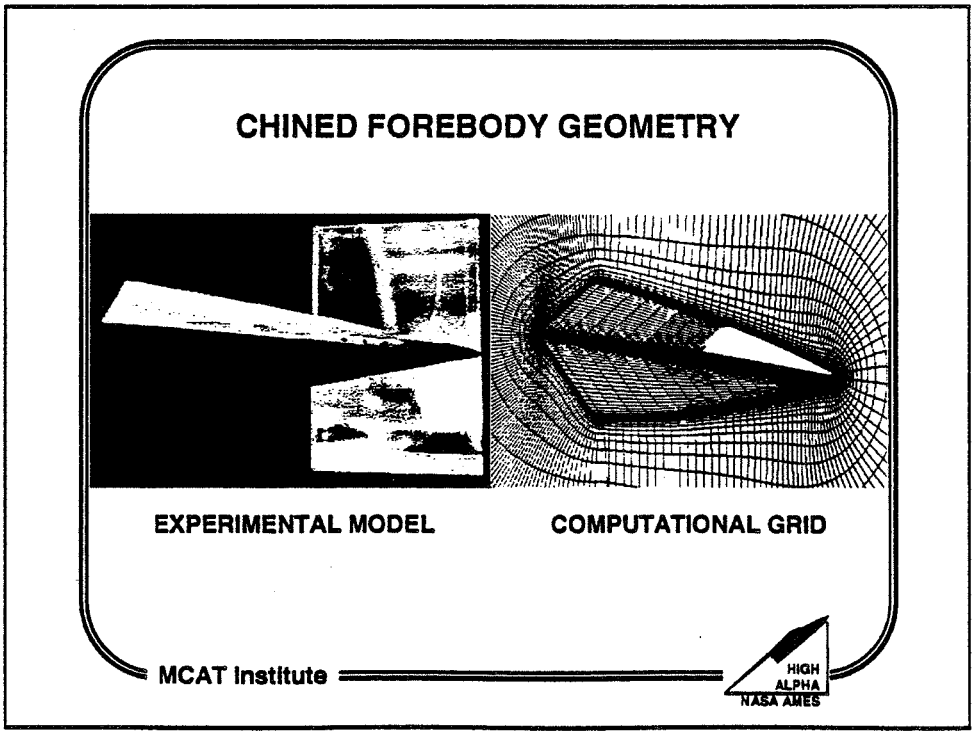

In a "conventional", smooth forebody, tangential slot blowing moves the primary crossflow separation location toward the leeward symmetry plane on the blowing side, and there may or may not be a secondary separation on the blowing side. For a chined forebody, the primary separation occurs at the chine for the no-blowing case. Unlike a "conventional", smooth forebody, blowing from a slot located on the top surface of the chined forebody does not move the primary separation line from its location at the chine line, but it does disturb the no-blowing flowfield, and draws the blowing-side vortex toward the surface while the non-blowing-side vortex moves away from the surface. Blowing outboard from a slot located on the bottom surface has a similar, but mirror-image effect. Here the jet forces the blowing-side vortex away from the body surface, while the non-blowing-side vortex moves closer to the body. In contrast to a conventional forebody, the primary crossflow separation remains located at the chine and a secondary separation does exist. These changes in the flowfield generate side forces and yawing moments which have the potential of being employed to control the aircraft at high angles of attack.

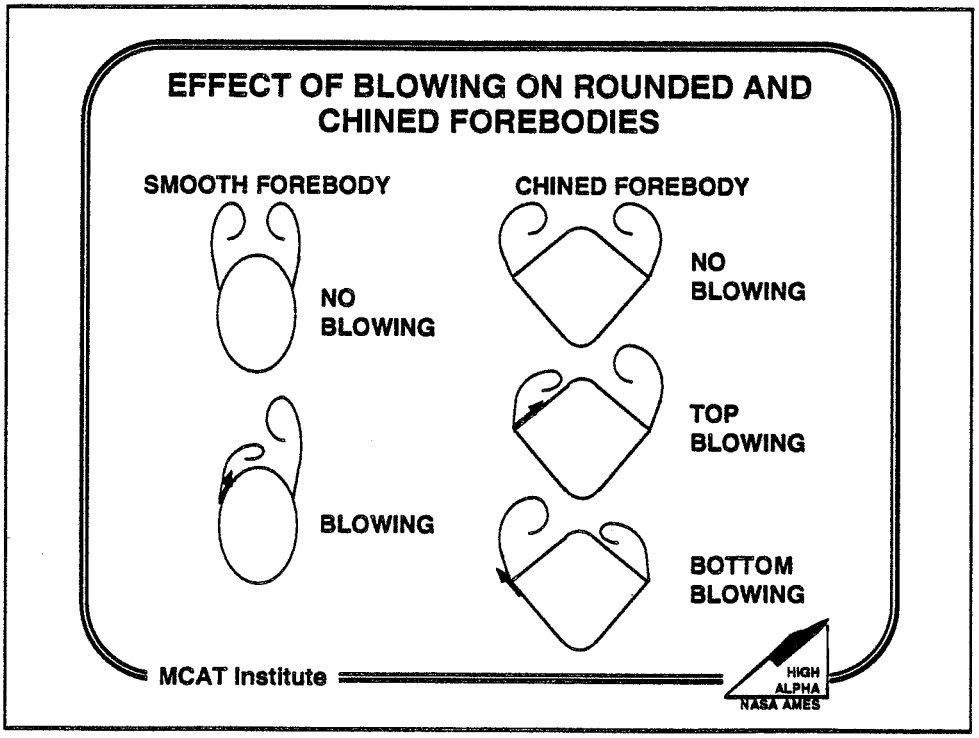

Solutions were computed for flow about the chined forebody with tangential slot blowing from the starboard side (pilot's view) of the body.[11] The blowing slot is one inch in length, starting 0.5 inch from the nose tip and extending aft. Here is the surface flow pattern and helicity density contours for the solution with MFR = 1.49×10^{-3}. Primary crossflow separation lines occur at the chine line, and extend along the entire length of the body. In addition, the secondary and tertiary crossflow separation lines extend from the nose of the forebody to the end of the forebody. Further, a fourth crossflow separation line appears near the back of the forebody. The surface flow pattern shows that the largest changes in the flowfield occur in the blowing region near the nose. The separation lines aft of the blowing region do not appear to greatly change positions.

The helicity density contours are shown in crossflow planes at three axial stations on the forebody. The helicity density contours grow larger and more diffuse in the axial direction. The first axial station is located in the middle of the blowing region. It shows that the primary vortex on the blowing side is entrained by the jet and moves downward towards the surface due to the Coanda effect. The non-blowing-side vortex moves away from the surface. Here the movement of the vortices, and the resulting lower pressure region on the blowing side cause a side force and yawing moment toward the blowing-side. The helicity density contours at the other two axial stations show that the blowing-side vortices move closer to the surface and the non-blowing-side vortices move away from the surface when compared to the no-blowing solution which causes tangential slot blowing to be effective in this region.

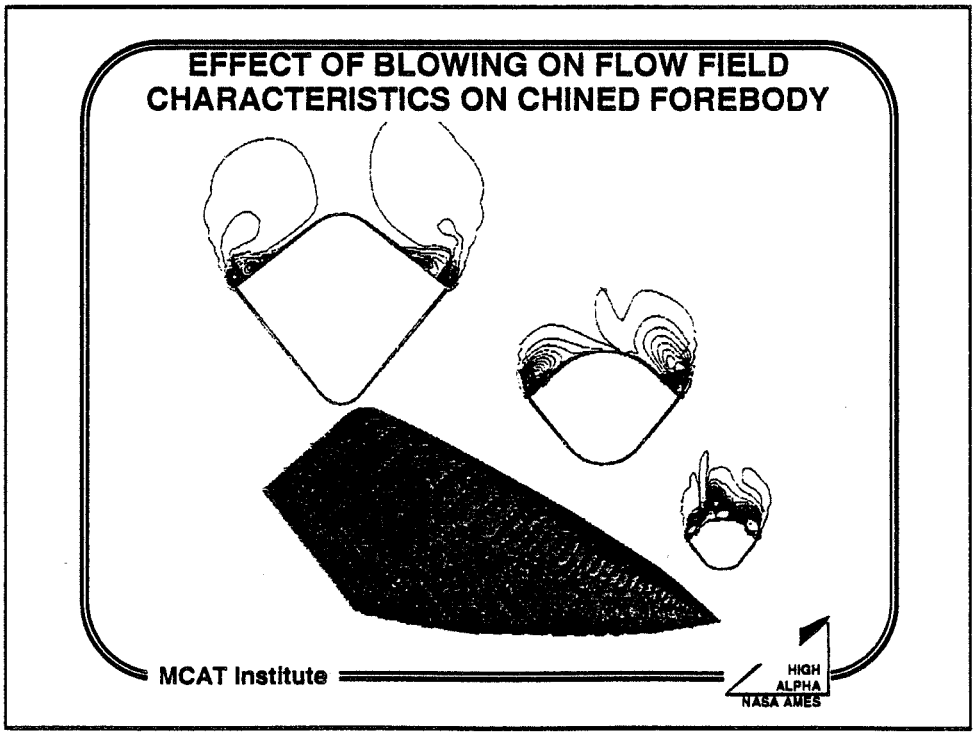

For $\alpha = 30°$, both the experimental and computational results show that the incremental yawing moment increases smoothly as the mass flow ratio increases. The computational results underpredict the experimentally-measured yawing moment. At $\alpha = 40°$, however, the computed results show three distinct regions of effectiveness. In the first region, low blowing rates produce a negative ΔCn. This is caused by the low-energy jet moving the primary blowing-side vortex away from the surface. This results in a higher pressure region on the blowing side which causes the negative yawing moment. In Region II, this trends reverses, and ΔCn increases with increasing MFR until a maximum is reached. The jet remains attached to the surface due to the Coanda effect, resulting in the positive yawing moment. In Region III, further increases in MFR causes a reduction in ΔCn. At the higher mass flow ratios, the pressure at the jet exit is greater than the freestream pressure. The jet rapidly expands after leaving the blowing slot, causing the jet to separate, pushing the primary vortex away from the surface. Similar trends have been observed in experiments using the F/A-18 with jet and slot blowing.[9] At the higher angle of attack, the computed results are generally in better agreement with the experiment, except at the low MFR values.

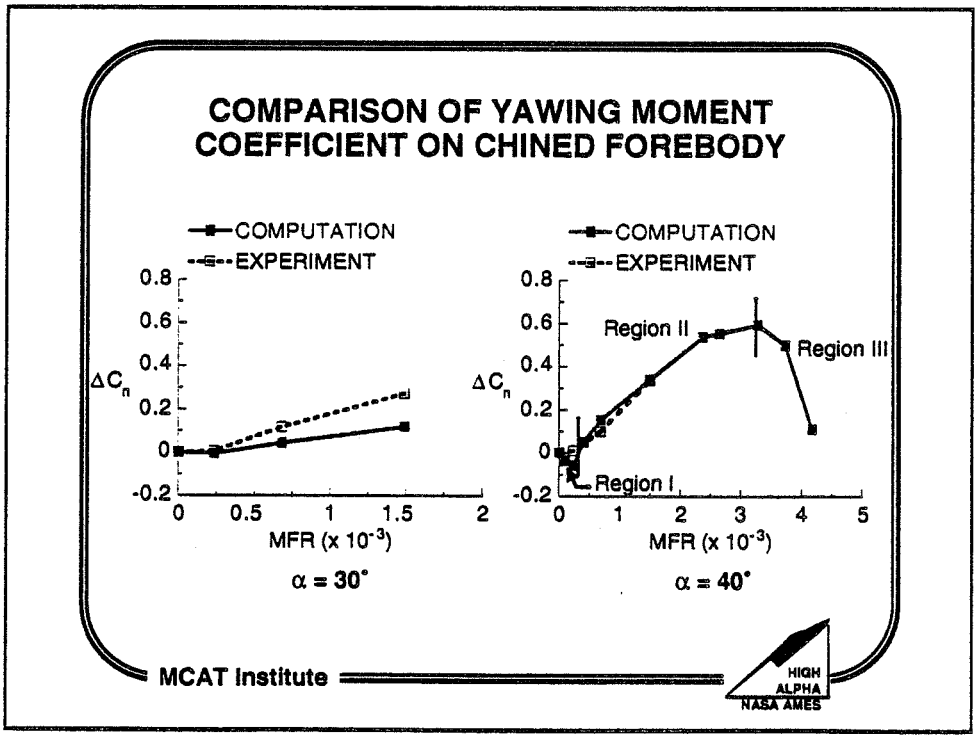

Experimentally, it was found that the most effective slot configuration of those tested on the generic chined forebody was a slot one inch long located 0.5 inches from the tip of the nose (referred to as Slot 1) and blowing tangentially toward the leeward symmetry plane. To investigate the effect of axial slot location computationally, solutions were obtained for an additional slot configuration (Slot 2), which had the same one inch length as Slot 1, but extended rearward from a point 1.5 inches from the tip of the nose. The variation of ΔCn with MFR for the two slot configurations is similar. The computed results for both slot configurations show a force reversal at low MFRs, followed by increasing ΔCn with increasing MFR. Slot 1 produces a larger magnitude of ΔCn for a given MFR than does Slot 2. This trend is clearly seen at the higher MFRs, and was seen in both the numerical and experimental results. It is also consistent with results obtained by Degani and Schiff,[12] who found that small disturbances near the tip of the nose produce greater effects on the flowfield than disturbances placed further aft.

In order to determine whether an alternative circumferential slot location could be more effective in developing side forces and yawing moments on the body, computations were carried out for a slot located on the lower chine surface and blowing tangentially outboard. This slot had the same axial location and extent of Slot 1. For the configurations investigated, it was found that blowing from the bottom slot produces a side force and yawing moment directed away from the blowing side. It was determined that blowing from the upper slot produces a greater change in yawing moment for a given MFR than does blowing from the bottom slot.

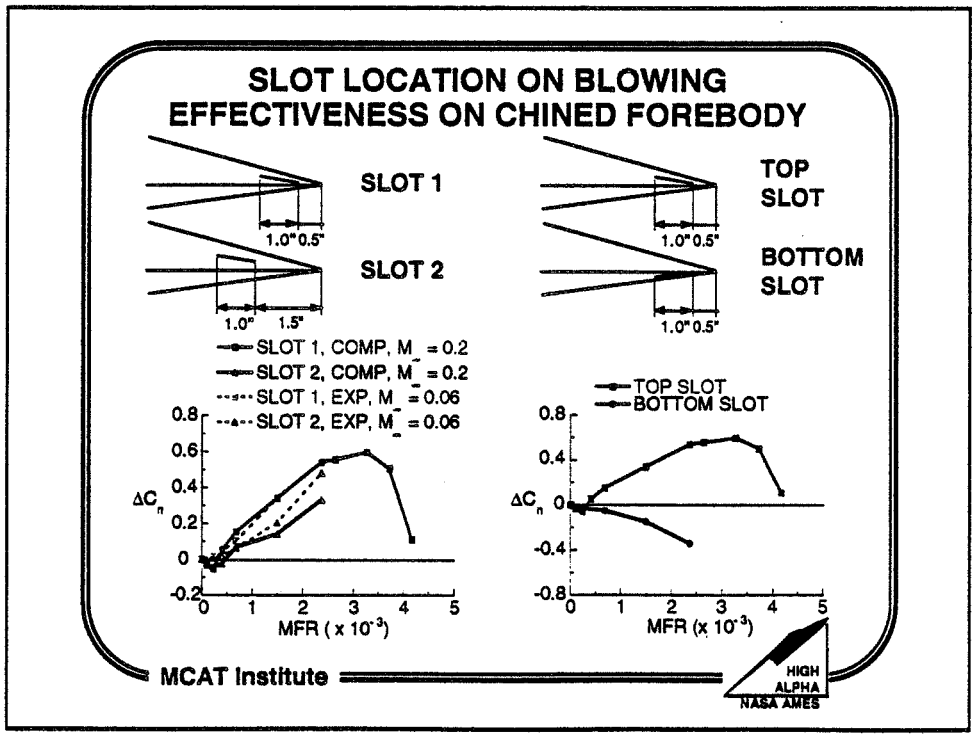

Forebody tangential slot blowing has been shown to be viable method of generating forces and moments on an aircraft flying at high angle of attack. Computational fluid dynamics is used to analyze forebody blowing about the F/A-18 aircraft geometry. The results obtained from this analysis compliments the data generated by sub-scale and full-scale wind tunnel tests. Comparison of computed results with experimental data show good comparison in such areas as surface pressure coefficient. The detailed flow picture obtained from computational solutions show the asymmetric LEX vortex burst caused by blowing, as well as the changes in the frequency of the aerodynamic loads impinging on the vertical tails. Computed results also show that blowing can be effective over a range of freestream Mach numbers and blowing rates. High blowing rates, however, can lead to overblowing, where a leveling off or reduction in yawing moment occurs.

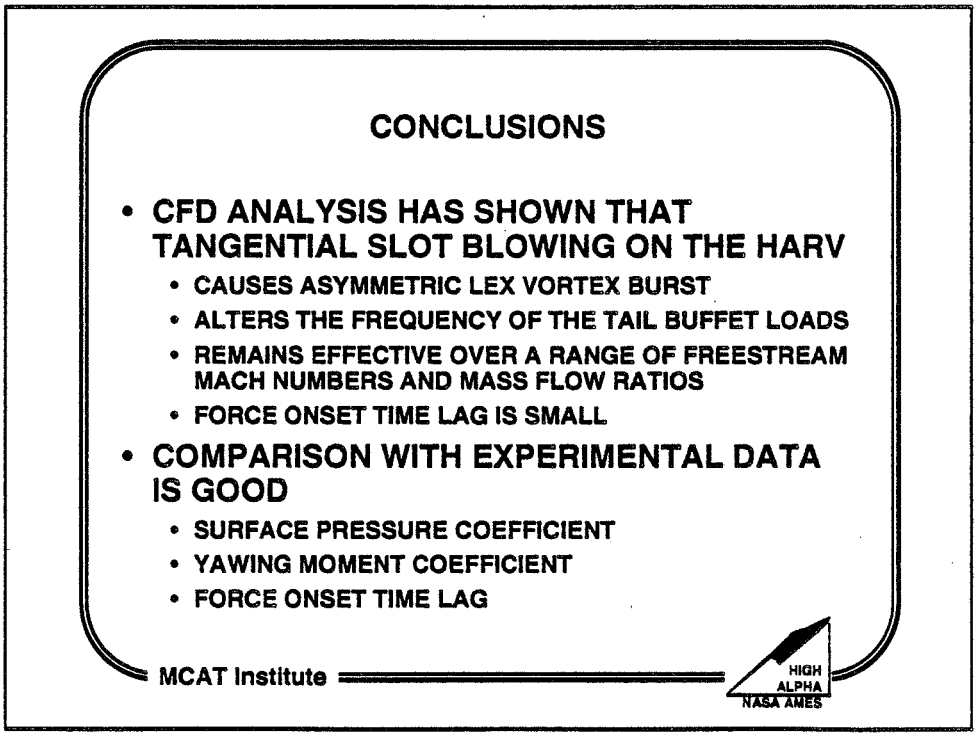

The computational investigation shows that forebody tangential slot blowing can generate significant side force and yawing moment on a generic chined forebody. The computed yawing moment compares well with the available experimental data, although slight discrepancies do exist, especially at the lower angle of attack. At the higher angle of attack, force reversal and the effects of overblowing are observed computationally. Force reversal occurs when the jet pushing the blowing-side vortex away from the surface, instead of entraining it closer to the surface, which happens at higher blowing rates. In the case of the chined forebody, overblowing causes a significant reduction in the yawing moment, instead of the leveling off observed in the F-18 isolated forebody computations. The flow mechanisms involved are the same, however, with the jet being underexpanded at the slot exit, which causes a rapid expansion and separation of the jet from the surface. Slot location also has a role in the effectiveness of blowing. A slot located further forward generated more yawing moment, as observed in the experiment. A slot located on the top surface is more effective than a slot located on the bottom surface. The computational analysis serves as a means of enhancing and extending the information obtained from experiments. Using both in conjunction, a more complete understanding of forebody tangential slot blowing is obtained.

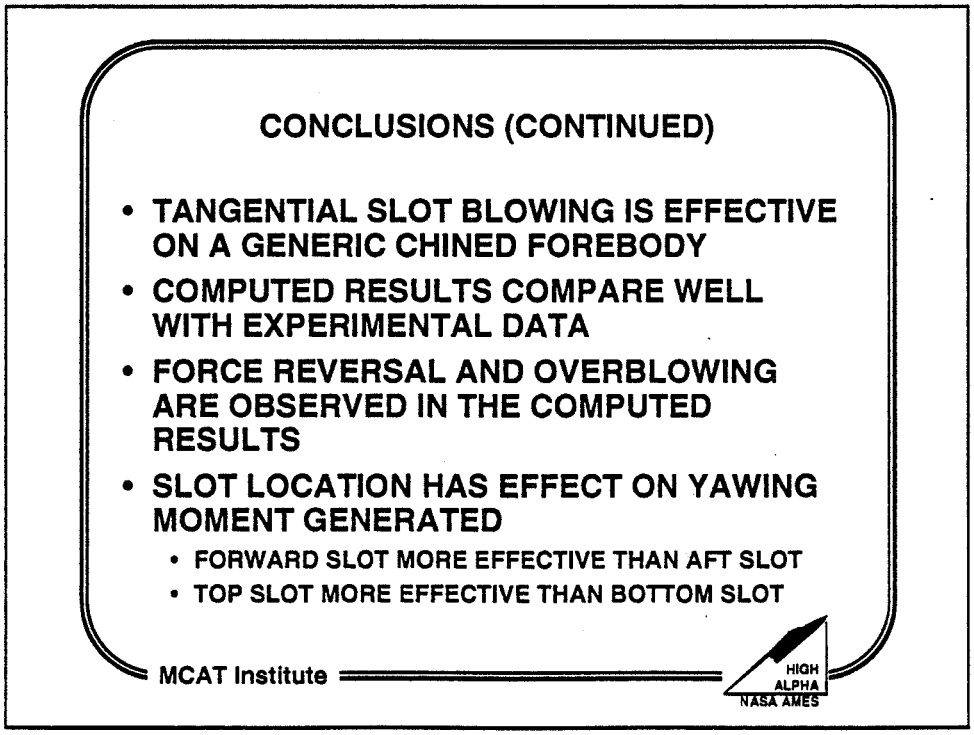

References

1. Benek, J. A., Steger, J. L., Dougherty, F. C., and Buning, P. G., "Chimera: A Grid Embedding Technique," AEDC-TR-85-64, Arnold Air Force Station, TN, 1986.

2. Steger, J. L., Ying, S. X., and Schiff, L. B., "A Partially Flux-Split Algorithm for Numerical Simulation of Compressible Inviscid and Viscous Flow," Proceedings of a Workshop on Computational Fluid Dynamics, University of California, Davis, 1986.

3. Baldwin, B. and Lomax, H., "Thin-Layer Approximation and Algebraic Model for Separated Turbulent Flows," AIAA Paper 78-0257, January, 1978.

4. Degani, D. and Schiff, L. B., "Computation of Turbulent Supersonic Flows About Pointed Bodies Having Crossflow Separation," *Journal of Computational Physics*, Vol. 66, No. 1, 1986, pp. 183-196.

5. Lanser, W. R., Meyn, L. A., and James, K. D., "Forebody Flow Control on a Full-Scale F/A-18 Aircraft," AIAA Paper 92-2674, June, 1992.

6. Gee, K., Rizk, Y. M., Murman, S. M., Lanser, W. R., Meyn, L. A., and Schiff, L. B., "Analysis of a Pneumatic Forebody Flow Control Concept About a Full Aircraft Geometry," AIAA Paper 92-2678, June, 1992.

7. Gee, K., Rizk, Y. M., and Schiff, L. B., "Effect of Forebody Tangential Slot Blowing on Flow About a Full Aircraft Geometry," AIAA Paper 93-2962, July, 1993.

8. Gee, K., Rizk, Y. M., and Schiff, L. B., "Analysis of Tangential Slot Blowing on F/A-18 Isolated Forebody," AIAA Paper 94-1831, June, 1993.

9. Kramer, B., Suarez, C., and Malcolm, G., "Forebody Vortex Control with Jet and Slot Blowing on an F/A-18," AIAA Paper 93-3449, August, 1993.

10. Cummings, R. M., Schiff, L. B., and Duino, J. D., "Experimental Investigation of Tangential Slot Blowing on a Generic Chined Forebody," AIAA Paper 94-3477, August, 1994.

11. Agosta-Greenman, R. M., Gee, K., Cummings, R. M., and Schiff, L. B., "Numerical Analysis of Tangential Slot Blowing on a Generic Chined Forebody," AIAA Paper 94-3475, August, 1994.

12. Degani, D. and Schiff, L. B., "Numerical Simulation of the Effect of Spatial Disturbances on Vortex Asymmetry," *AIAA Journal*, Vol. 29, No. 3, 1991, pp. 344-352.

19950078 40
352066
2:24

N95-14254

16103
P. 22

F/A-18 AND F-16 FOREBODY VORTEX CONTROL, STATIC AND ROTARY-BALANCE RESULTS

BRIAN KRAMER
BROOKE SMITH
EIDETICS AIRCRAFT, INC
TORRANCE, CALIFORNIA

NASA FOURTH HIGH-ANGLE-OF-ATTACK CONFERENCE
DRYDEN FLIGHT RESEARCH CENTER, EDWARDS, CA
JULY 12-14, 1994

OUTLINE

The results of research on forebody vortex control on both the F/A-18 and the F-16 aircraft will be shown. Several methods of forebody vortex control, including mechanical and pneumatic schemes, will be discussed for the F/A-18 with examples of the force and moment data obtained. The wind tunnel data includes both static and rotary balance data for forebody vortex control. Time lags between activation or deactivation of the pneumatic control and when the aircraft experiences the resultant forces are also discussed. The static (non-rotating) forces and pressures are then compared to similar configurations tested in the NASA Langley and DTRC Wind Tunnel, the NASA Ames 80'x120' Wind Tunnel, and in flight on the High Angle-of-Attack Research Vehicle (HARV).

Similar experiments were conducted on the F-16 using both mechanical and pneumatic forebody vortex control methods. The F-16 wind tunnel results will be reviewed briefly followed by a discussion of simulation studies focused on evaluating the advantages of incorporating forebody vortex control capability into the flight control system of an F-16.

Finally, conclusions from these two programs will be highlighted.

PRESENTATION OUTLINE

I INTRODUCTION

II F/A-18 WIND TUNNEL RESULTS
- EXPERIMENTAL SETUP
- FOREBODY VORTEX CONTROL TECHNIQUES
- TIME LAG
- PRESSURE DATA
- COMPARISON TO OTHER TEST DATA AND FLIGHT TEST

III ENHANCED F-16 SIMULATION RESULTS
- YAW CONTROL POWER
- 1v1 AIR COMBAT RESULTS

IV CONCLUSIONS

INTRODUCTION

The presentation covers the work conducted under two SBIR Phase II programs. The first, sponsored by NASA Ames (Technical Monitors Dr. Lewis Schiff and Dr. James Ross), was an investigation of forebody vortex control on a 6% F/A-18 model, with and without the influence of a rotary flow field. This research was part of the High Alpha Test Program (HATP), and was conducted in the NASA Ames 7'x10' Wind Tunnel.

The second SBIR Phase II program was sponsored by NASA Langley (Technical Monitor Mr. Daniel Banks). This program investigated forebody vortex control on the F-16, with three different forebodies. Static wind tunnel tests were conducted on a 10% F-16 model in the University of Toledo 3'x3' Wind Tunnel (forebody only) and in the NASA Langley 14'x22' Wind Tunnel. These results were then incorporated into a manned simulation.

INTRODUCTION

F/A-18

- STATIC AND ROTARY BALANCE TESTS WERE PERFORMED ON A 6% F/A-18 DURING AN SBIR PHASE II PROGRAM SPONSORED BY NASA AMES (HATP).
- PRIMARY OBJECTIVE: DETERMINE EFFECTIVENESS OF SEVERAL TYPES OF FVC IN A ROTARY FLOW FIELD

F-16

- NASA LANGELY SBIR PHASE II LOW-SPEED WIND TUNNEL TESTS WITH A 10% F-16 MODEL
- PRIMARY OBJECTIVE: SYSTEMATIC EVALUATION OF MECHANICAL AND PNEUMATIC FOREBODY VORTEX CONTROL.
- SECONDARY OBJECTIVE: EVALUATION OF FVC UTILITY WITH F-16

F/A-18 WIND TUNNEL MODEL

The model for these experiments is a new 6%-scale F/A-18 model designed and built by Eidetics International. The model exterior lines were determined by borrowing the Navy/McAir 6%-scale force and moment steel model to make a pattern and permanent mold. From this mold, a fiberglass shell with an accurate external shape was fabricated. The forebody part of the mold was then also used to make several forebody (nose portion only) model pieces.

The model structural design was required to accommodate the loads of both the static test and the rotary-balance tests. The fiberglass shell of the model attaches to a structure that consists of base plates, six aluminum bulkheads and stringers. The structural center of the model is a stainless steel balance block with mounting tabs for the wing and the base plates. The wings have a steel core to carry the aerodynamic loads, and the airfoil shape is built up with wood and fiberglass around the structural center. The leading and trailing-edge flaps and ailerons were all deflectable; however, the test was conducted with the leading edge flaps only in the maneuver position (34°) and the trailing-edge flaps undeflected. The ailerons were tested in the plus and minus 10° positions to estimate roll control power. The vertical tails have an aluminum core and rudders that can be deflected plus and minus 30°. The horizontal tails were fixed at 0° for the entire test.

6% F/A-18 WIND TUNNEL MODEL

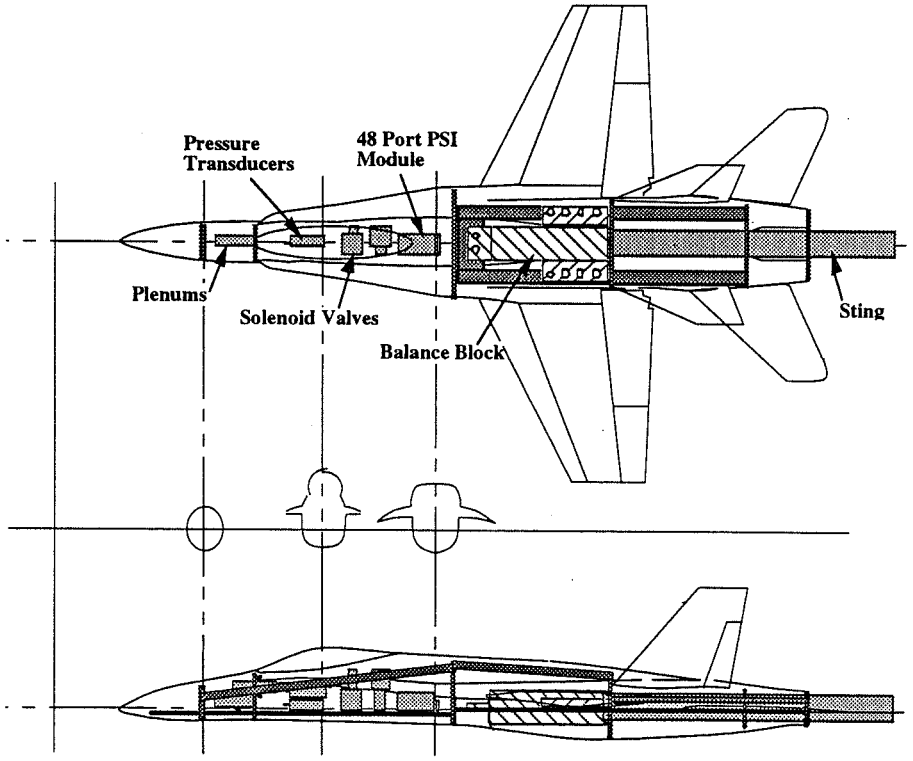

STATIC WIND TUNNEL TEST INSTALLATION

The model was sting mounted on a dog-leg and turntable system. The model was mounted on the sting at a 90° roll angle (wings vertical) and the model was pitched in the horizontal direction with the floor mounted turntable. Sideslip angles were introduced by inserting angled wedges between the sting base and the vertical strut. The tests were run at a dynamic pressure of 27 psf (approximately 150 ft/sec) and a Reynolds number of 0.92 x 10^6 per foot. A few runs were made at dynamic pressures of 10 psf (V=90 ft/sec and R_N=0.56 x 10^6 per foot) and 20 psf (V=131 ft/sec and R_N=0.8 x 10^6 per foot) to explore Reynolds number differences. The angle of attack was varied from 0° to 60°, and the sideslip angle at 0° or -10°.

STATIC WIND TUNNEL TEST INSTALLATION

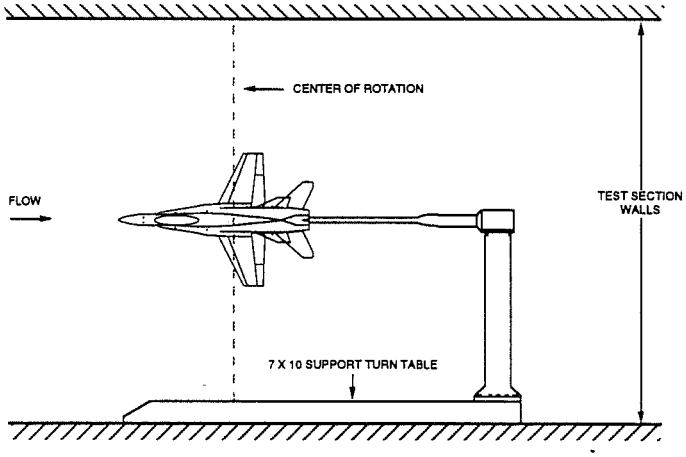

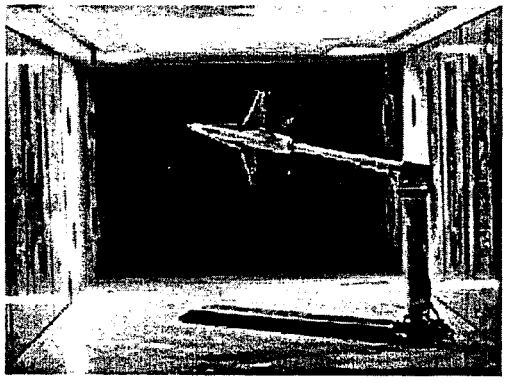

ROTARY BALANCE WIND TUNNEL TEST INSTALLATION

Rotary-balance experiments determine the forces and moments of a model in a steady rotational motion about the velocity vector at fixed angles of attack and sideslip. Rotation around the velocity vector is considered to be a key maneuver for enhanced agility in combat for modern fighter aircraft. In order to properly assess the control power to produce a robust velocity vector roll (known as a loaded roll because the aircraft is rolling with significant lift forces due to angle of attack), it is necessary to not only determine the yaw and roll moments statically, but dynamically at the appropriate roll rates.

The focus of the present rotary-balance wind tunnel experiments was to evaluate in a rotary motion the best forebody vortex control techniques determined from the previous static tests. The maximum rotation rate required in the wind tunnel is determined by matching the non-dimensional roll rate, expressed as $\omega b/2V$, where ω is the rotation rate (rad/sec), b is the wing span and V is the free stream velocity. If we choose a typical condition for a full-scale F/A-18 as velocity-vector roll rate of 60°/sec (up to 60° AOA) and free stream velocity of 150 ft/sec, then the non-dimensional rotation rate around the velocity vector would be 0.1396. For higher velocities, the non-dimensional parameter would be even less. The maximum rate of the rig during the experiments was 200 rpm, which resulted in maximum non-dimensional rotation rates of 0.175 for V=150 ft/sec.

The rotary rig was based on the hydraulics of the system last used in the Ames 6 x 6-Ft Wind Tunnel in 1984. New hardware was designed to provide manual changes in angle of attack and sideslip by moving and pinning the sting assembly to pre-drilled hole locations (every 3° from 0° to 60°) on the C-strut. Angles of sideslip at specific angles of attack are provided by rolling the straight sting around its own axis in the strut arm in combination with the appropriate angle setting on the C-strut.

ROTARY BALANCE WIND TUNNEL TEST INSTALLATION

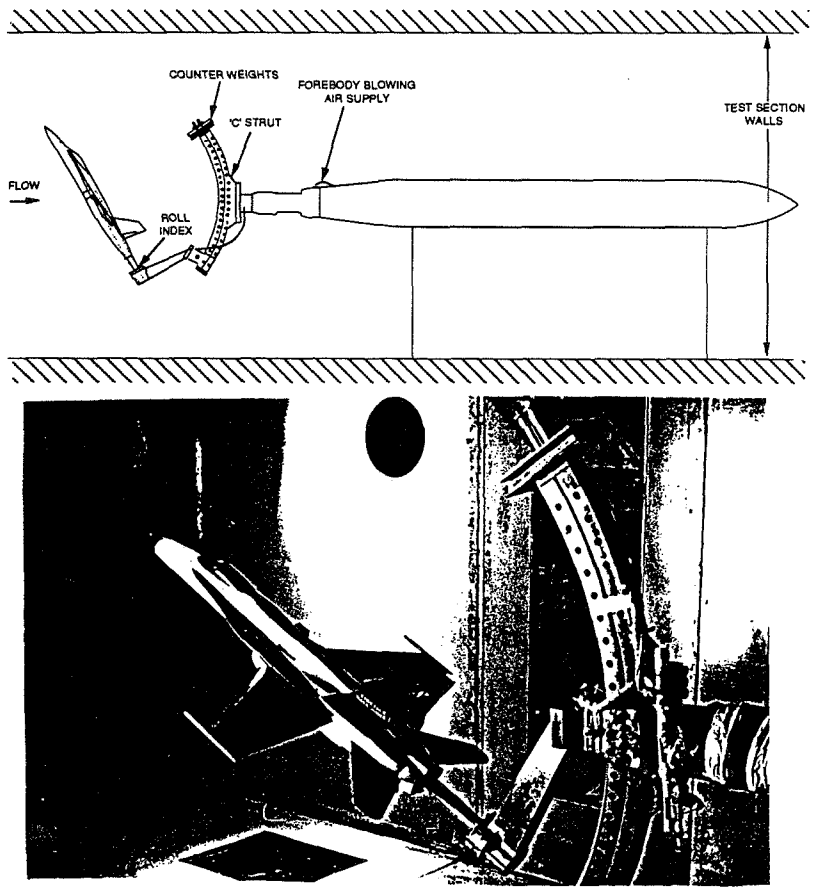

FOREBODY VORTEX CONTROL CONFIGURATIONS

The nose section of the model was removable so that different forebody vortex control devices could be studied by replacing the nose section. There were five blowing jet positions, three of which were at 135° azimuth from the windward meridian, at three fuselage stations (Noses 1, 2, 3). The middle position (x = 0.93 inches model scale) corresponded to the furthest aft fuselage station that was tested in the 1992 test of the F/A-18 in the 80x120 Foot Wind Tunnel at NASA Ames. The furthest aft position (x = 1.30 inches) corresponds to 0.5 equivalent nose diameters aft of the nose tip. At this fuselage station, in addition to the jet at 135°, there were jets at 150° and 120° (Noses 4 and 5). Only the results from the most effective jet configuration (Nose 4 with the jets angled inboard 60°) will be shown.

In addition to the jet blowing noses, there was a slot blowing nose. The slot width was held to a reasonably constant width (0.006 inches) with small metal shims between each of the four segments (A,B,C and D) . Unlike the full scale aircraft, size constraints made it impossible to have separate supply pressure lines to each slot segment. Instead, the interior of the nose was made into two plenums, one for the left side and one for the right, that supplied all of the segments. The slot size tested was 0.006 inches wide with a length of 2.58 inches beginning 0.56 inches from the nose tip. This was the slot configuration that showed the highest effectiveness in a 1992 test of the F/A-18 in the 80x120 Foot Wind Tunnel at NASA Ames. Different slot lengths were tested by taping over portions of the slot. The most effective slot configuration was with segments A and B blowing.

In addition to the pneumatic control systems, several mechanical, miniaturized strake configurations were tested. Only the results from the single rotating nose tip strake, and a vertical, pivoting, nose strake (the Rhino Horn) will be shown here. Although similar in shape to the rotating nose tip strake, the Rhino Horn is mounted on the leeward meridian line of the forebody and pivots about an axis perpendicular to the surface of forebody.

FOREBODY VORTEX CONTROL CONFIGURATIONS

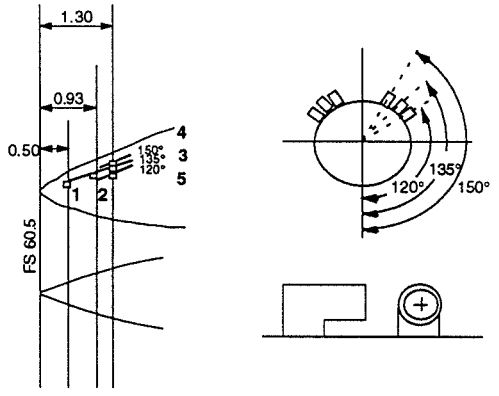

JET BLOWING

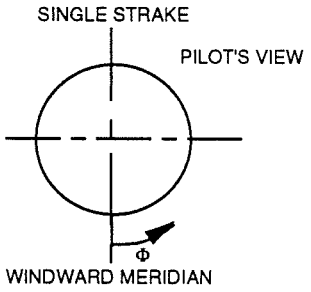

SINGLE STRAKE

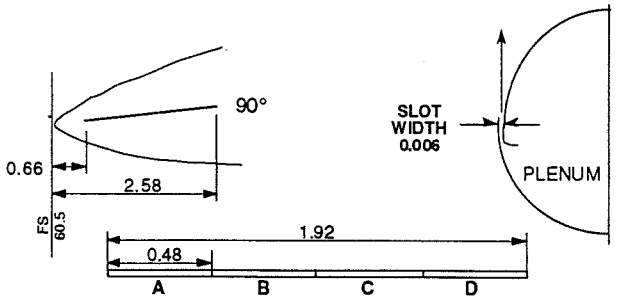

SLOT BLOWING

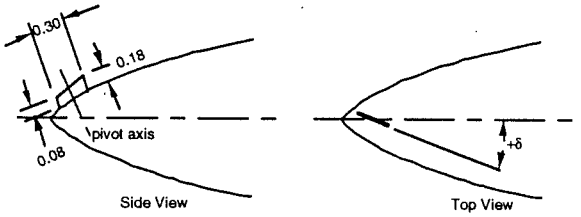

RHINO HORN

BASELINE RUDDER EFFECTIVENESS

The static wind tunnel test results show the primary reason for the interest in forebody vortex control. As the angle of attack is increased above 20°, the rudder effectiveness drops rapidly to near zero at 50°. The rotary balance results show that the static level of rudder effectiveness remains the same, and in fact, the increment from the baseline stays basically constant. The slope of the line with different dimensionless rotation rates indicates that the baseline F/A-18 has an anti-spin characteristic that is not effectively changed by the rudder deflection (the lines are parallel).

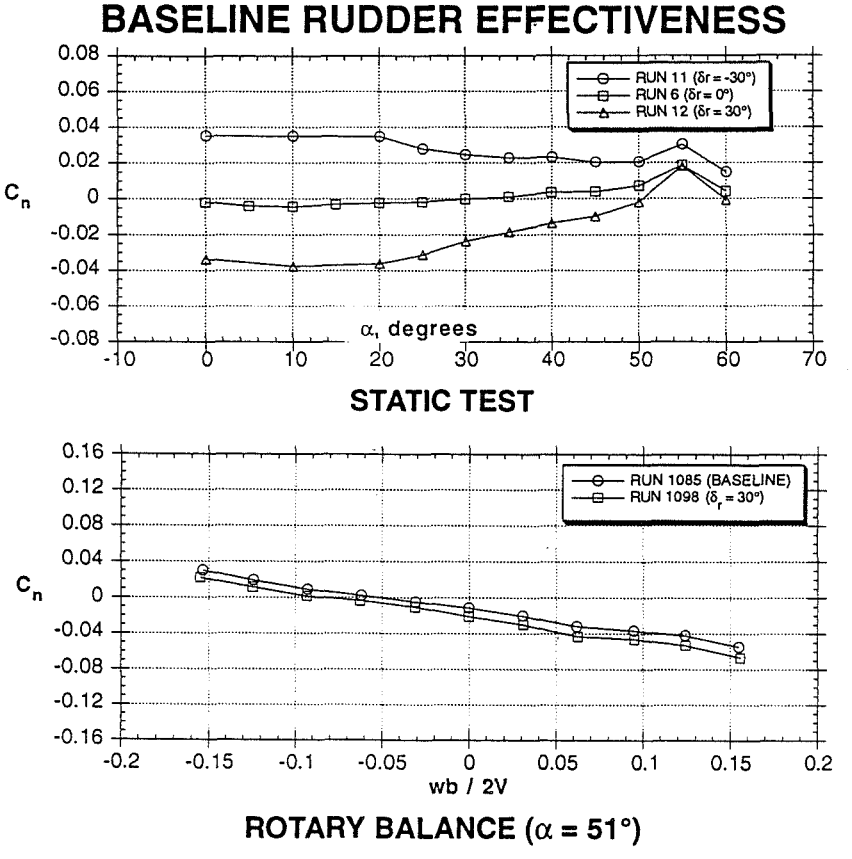

JET BLOWING

Jet blowing proved to be effective beginning at 20° to 30° AOA in the static test. As the angle of attack was increased, the effectiveness increased as the forebody vortex strength increased. Increasing the blowing rate tended to increase the yawing moment in a well behaved manner and, as previously observed, blowing on the right hand side of the body produced a positive yawing moment (and vise-versa). The rotary balance data showed very similar behavior, with very little degradation due to the rotating flow field. The blowing cases are similar to the rudder in that they only cause an offset to the baseline without effecting the slope (anti-spin tendency).

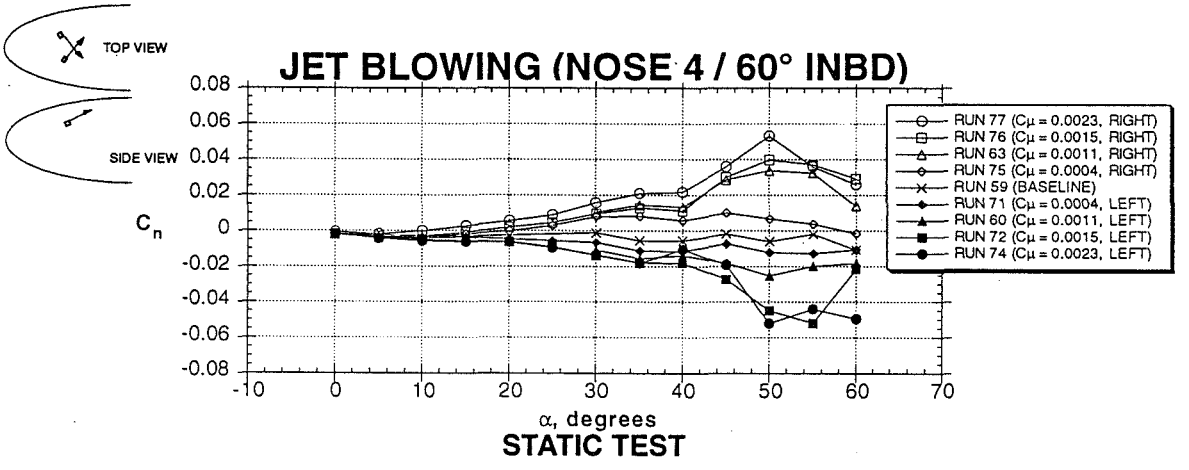

STATIC TEST

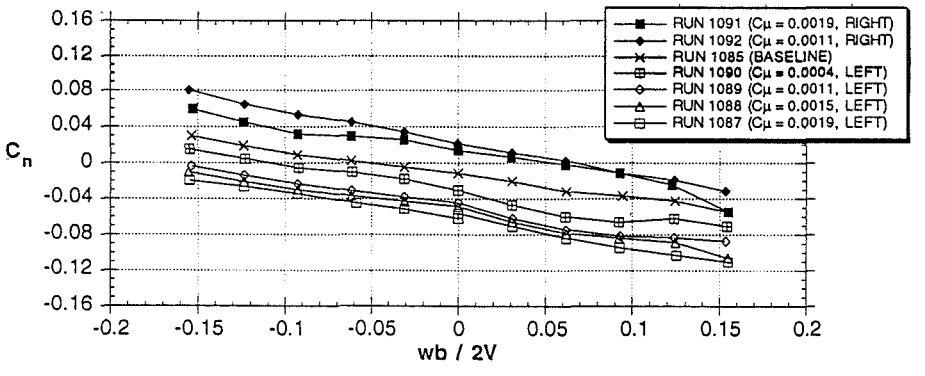

ROTARY BALANCE (α = 51°)

TIME LAG

An investigation was made to determine whether there is a significant time delay from activation of jet blowing to the time when the aircraft experiences a "fully transitioned" change in the yawing moment. The time lag is important not only for the onset of blowing control, but also for the decay time after the jet is turned off. The time lag was measured by looking at the pressure field response on the surface of the model with Endevco dynamic pressure sensors. In addition, the balance outputs were recorded in raw counts, but not reduced to forces or coefficients. As a reference point, the time that it takes the flow to traverse the length of the model fuselage (convective time) is 22 msec.

When the solenoid valve opens (at 0.065 sec), there is a finite period of time required for the plenum pressure to establish (~45 msec). At about 0.090 sec, Endevco #1 begins to respond. Because of the proximity of Endevco #1 on the forebody to the blowing jet, it is apparent that there is a pneumatic lag from not only the plenum filling but also the tubing length from the plenum to the jet exit. By 0.140 sec, Endevco #1 indicates that the flow is fully established at this point on the body. The other Endevcos shown, as well as those not shown, do not sense any change in the flow field caused by the blowing. This is in agreement with the static pressure data discussed above which also saw most of the effect only on the forebody. Perhaps more conclusive evidence of the time lag period is seen by examining the balance output. Here it is clear that by 0.130 sec the new steady state yawing moment has been established. Therefore, a conservative estimate of the time lag for the onset of control (including large pneumatic lags) would be 65 msec (just over 3 convective times). If the pneumatic lags were removed, the time lag would be on the order of 40 msec or about 2 convective time units.

The behavior is very similar for the decay of the yawing moment when the blowing valve is closed (at 0.500 sec.). In about 80 msec, the yawing moment has returned to the pre-blowing level. If the pneumatic lags were once again removed, the time lag would be on the order of 60 msec or about 3 convective time units.

As a point of reference, the full scale F/A-18 requires approximately 2 convective time units to fully deflect its rudder (moving at 60°/sec).

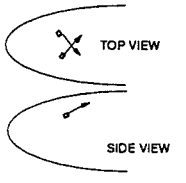

TIME LAG OF FVC COMMAND
(α = 51°)

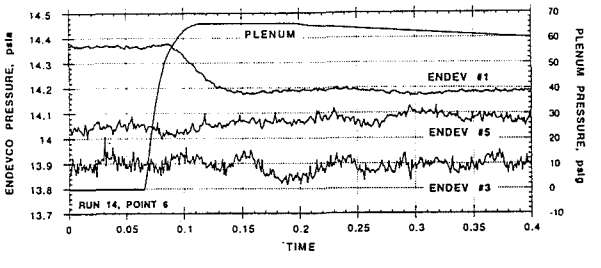

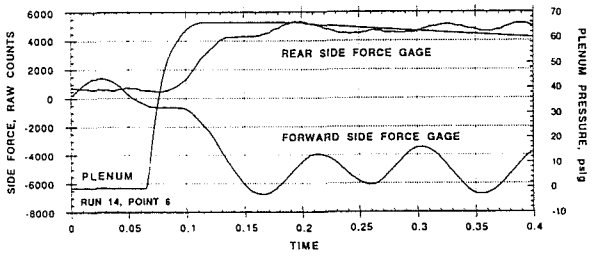

ONSET

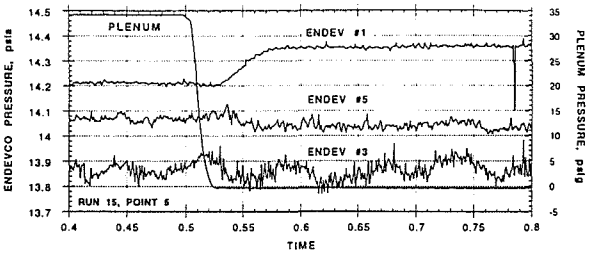

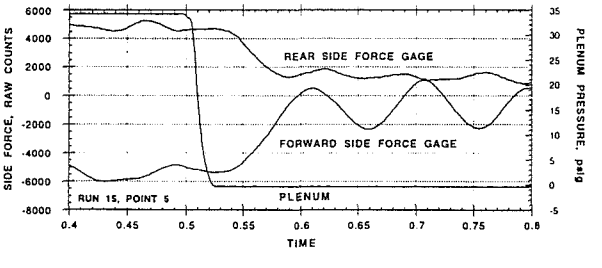

DECAY

SLOT BLOWING

The blowing slot is shown for left side blowing only. When low blowing rates are applied, the yawing moment is positive, or to the right side. As the blowing rate is increased, the yawing moment shifts over to the negative, or left side. This behavior is probably due, at least in part to the difficulty in building the slot at this scale. Flow visualization revealed that there was a fairly large forward component in the slot velocity, as well as the desired tangential flow. The rotary balance results yield the same results at zero rotation, but the effect of rotation direction is seen to have a relatively large effect. As the model is rotated in the negative direction, the left hand blowing slot is on the windward side of the fuselage, and the level of maximum of incremental yawing moment reduces. Likewise, as the model is rotated in the positive direction, the slot becomes more effective. It should be noted that blowing on the right side had the opposite effect.

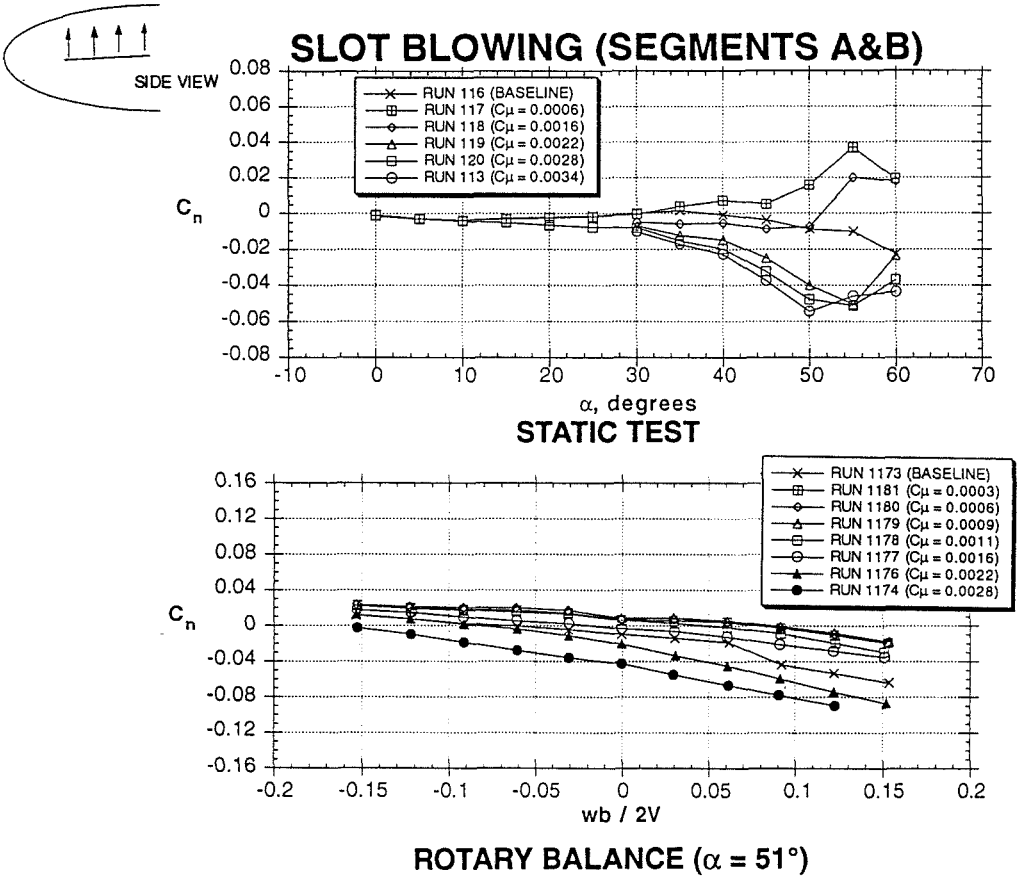

SINGLE ROTATING NOSE TIP STRAKE

The single rotating nose tip strake had very well behaved incremental yawing moment trends with angle of attack about the leeward side of the nose (top). In a rotary flow field, the strake has an increased level of anti-spin damping, when the strake is in the 180° position. However, when the strake was deflected, it could arrest or initiate a rotary motion throughout the range of rotations that were tested.

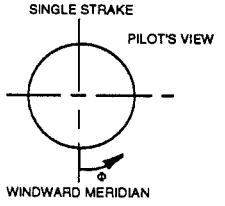

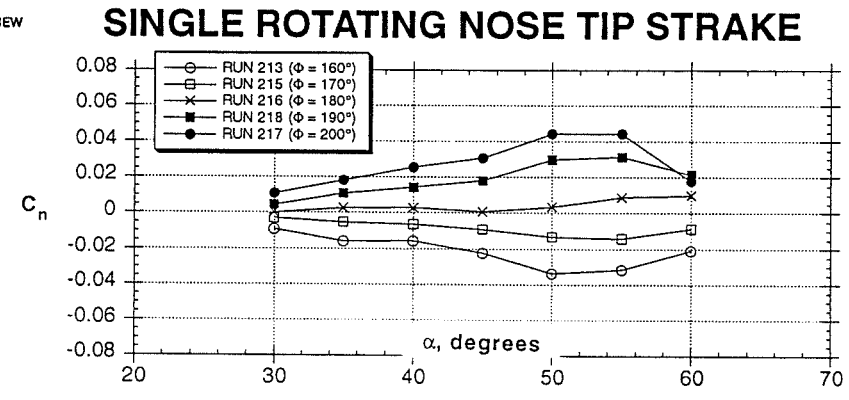

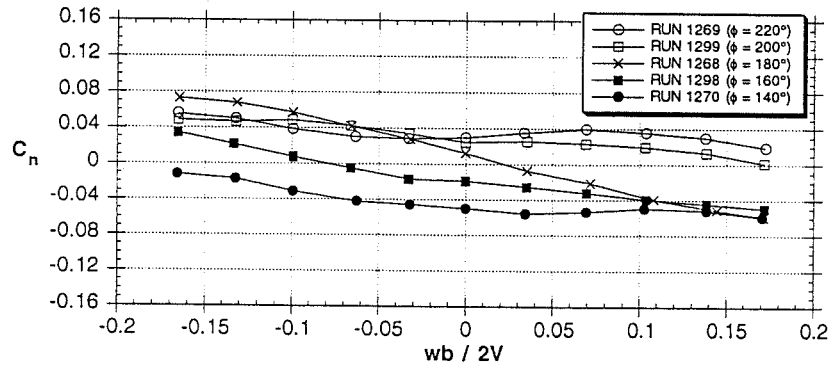

RHINO HORN

The Rhino Horn behaved similarly to single rotating nose tip strake and was well behaved up to 60° AOA. The rotary test showed that the presence of the strake increased the anti-spin tendency (greater negative slope) as well. At the maximum negative rotation rate, the Rhino Horn is unable to generate any additional positive yawing moment. However, the yawing moment generated in the undeflected case is greater than 0.08, which is considerably greater than the baseline aircraft's 0.04. This indicates that an active control system could be used to obtain a large envelope of control power, which will be discussed later. The Rhino Horn produced a larger range of achievable yawing moments across the range of reduced rotation rates than any other device tested.

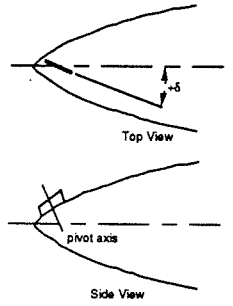

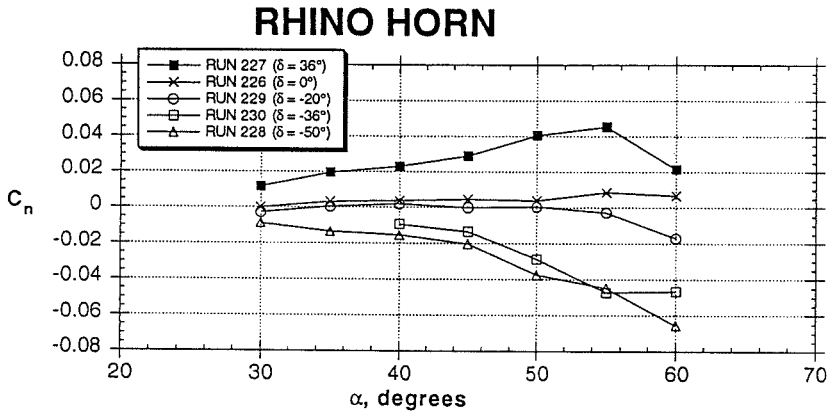

STATIC TEST

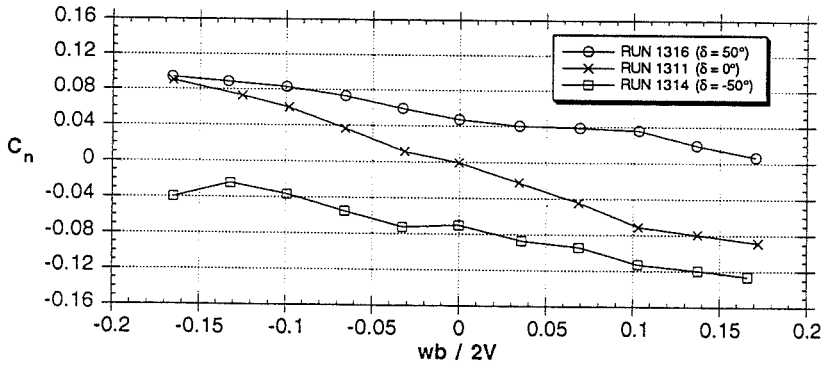

ROTARY BALANCE (α = 51°)

YAWING MOMENT COMPARISON

The comparison of the slot blowing data to that obtained in the 80'x120' wind tunnel shows some significant differences. The most probable culprit is the quality of the flow out of the 6% model slot. A better system of baffling the air in the plenum could help prevent some of the poor exit conditions from the slot. The jet blowing data compares somewhat better. The mass flow ratio achieved in the 6% test was even less than that obtained in the full scale test, but neither one is very effective at producing yawing moment at any angle of attack. The comparison of the rudder power generated by a 30° deflection is good.

YAWING MOMENT COMPARISON WITH NASA AMES 80'X120'

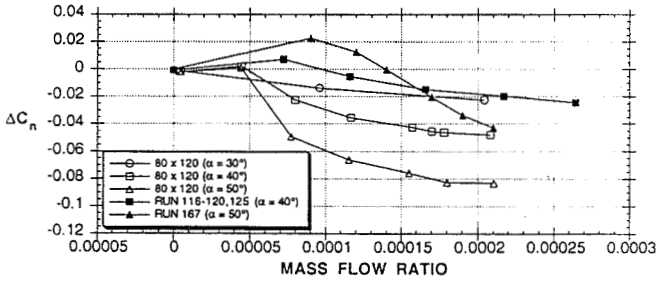

SLOT BLOWING SLOT AB

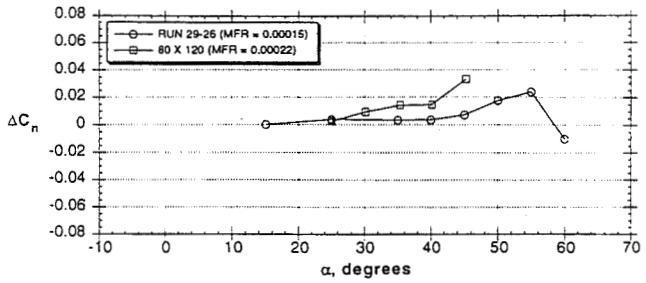

JET BLOWING
STRAIGHT AFT, NOSE

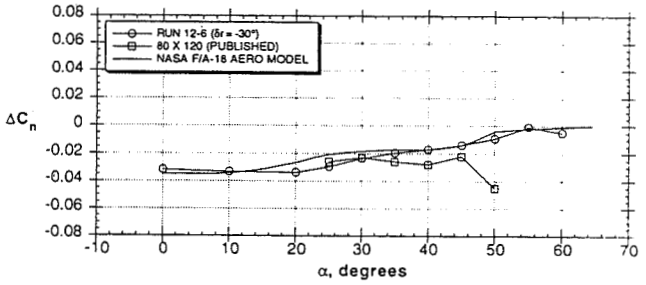

30° RUDDER

FOREBODY PRESSURE COMPARISON

The pressure distribution on the forebody is compared with the HARV F/A-18 and another 6% model tested by NASA Langley at the Navy's DTRC facility. The density of pressure ports was much greater for both of these than for the present test. The agreement overall is very good, however the HARV shows very clearly the location of the primary and secondary vortices. The sub-scale models fail to capture these peaks, although some of this could be due to a lack of density of the pressure ports. The current test also shows a slightly greater negative pressure than the other two tests.

FOREBODY PRESSURE COMPARISON TO HARV AND NASA LANGLEY

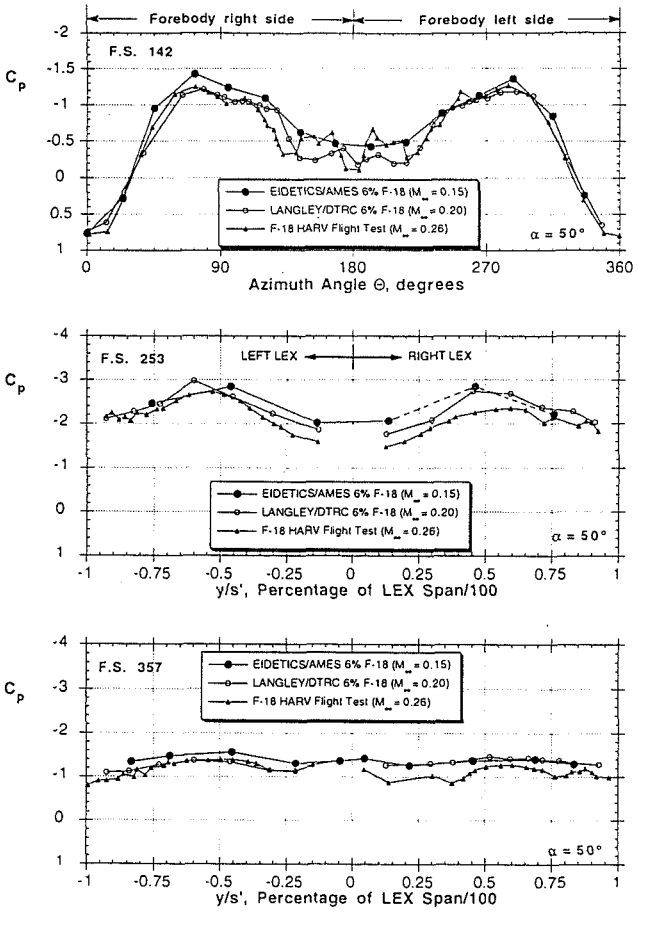

YAW CONTROL POWER ENVELOPE

The yaw control envelopes for all of the devices tested were created by simply shading in the area that corresponded to the largest positive and negative yawing moments achieved by each device. The baseline F/A-18 is shown as the white line. The Rhino Horn had the largest envelope of effectiveness, with the ability to create large (>0.04) yawing moment increments in either direction at any rotation speed. These envelopes show the possibilities for control that are available for either a stability augmentation system (SAS) or command augmentation system (CAS).

YAW CONTROL POWER ENVELOPE OF FVC DEVICES

$\alpha = 51°$

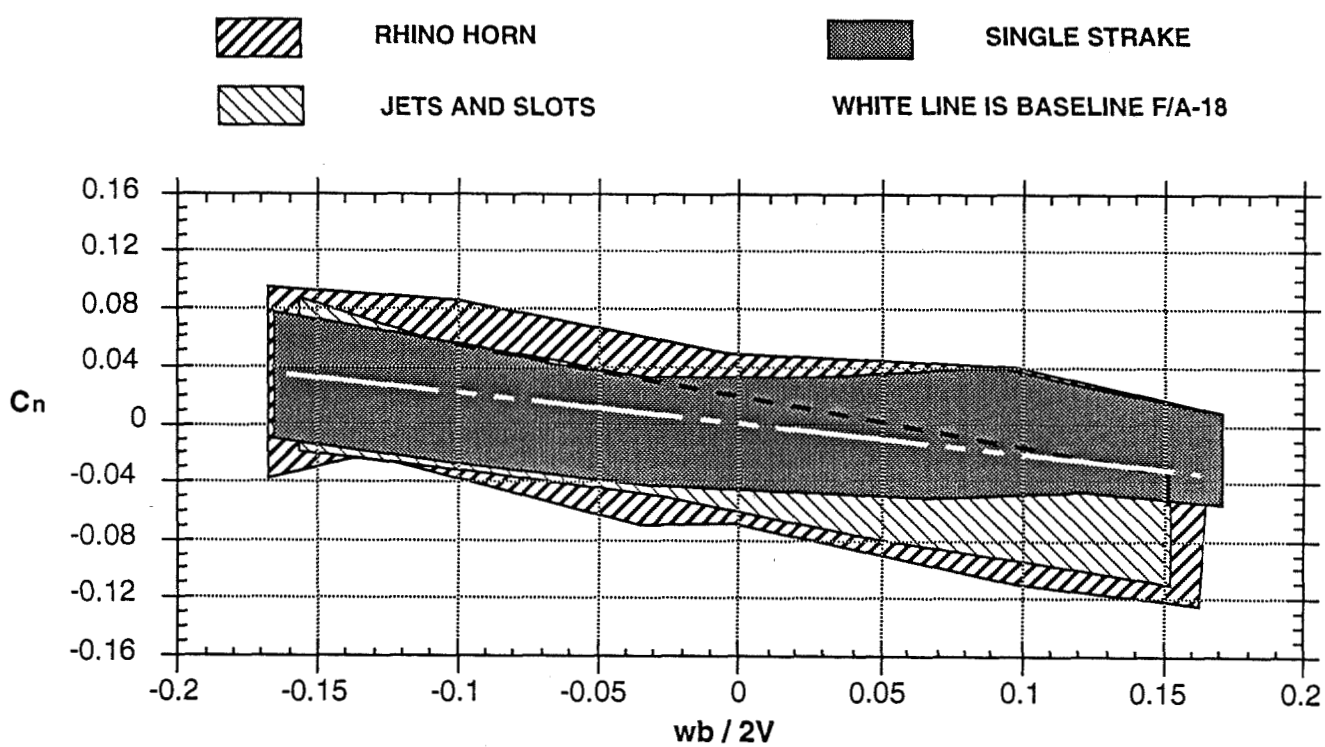

F-16 CONFIGURATION AND CONTROL TEST MATRIX

The methods of forebody vortex control (FVC) investigated during the F-16 wind tunnel tests were similar to those tested with the F/A-18. The tests parametrically varied a range of FVC characteristics, including blowing jets and slots and rotating miniature noseboom strakes, in an attempt to systematically sort out the design sensitivities and establish some guidelines for application.

The overall control characteristics of the F-16 FVC devices were similar to the F/A-18, in spite of a few geometry differences. For example, the mechanical rotating strakes were mounted on the F-16 nose boom instead of on the tip of the nose as with the F/A-18. And of course, the F/A-18 forebody cross-section is roughly elliptical with a vertical major axis whereas the F-16 forebody is horizontally oriented. The Shark and Chine nose geometries are even more flattened horizontally. Generally, the FVC behavior already presented for the F/A-18 configuration also is applicable to the F-16 (and derivatives) and will not be reviewed again. Instead, the focus of the following discussion will be the evaluation of FVC on the F-16 using manned simulation.

F-16 CONFIGURATION AND CONTROL MATRIX

		DIFFERENT FOREBODY GEOMETRIES		
		BASELINE F-16	USAF CHINE	EIDETICS SHARK NOSE
FOREBODY VORTEX CONTROL SCHEMES	ROTATABLE NOSE BOOM STRAKES	EFFECT OF ROTATION ANGLE (±180°) ON-AXIS AND OFFSET CONFIGURATIONS DIFFERENT PLANFORM SHAPES AND AREAS EFFECTS OF LONGITUDINAL POSITION ON BOOM		
	BLOWING JETS	DIFFERENT BLOWING RATES 4 LONGITUDINAL LOCATIONS ALONG NOSE 2 RADIAL POSITIONS MULTIPLE BLOWING ANGLES		
	BLOWING SLOTS	DIFFERENT BLOWING RATES 2 RADIAL POSITIONS VARYING SLOT LENGTH		

SIMULATION CONFIGURATIONS

After completing the static wind tunnel study, the F-16 project turned to a simulator study of the in-flight utility of FVC. The "best" FVC techniques from the wind tunnel tests were selected, new flight control systems designed, agility metrics quantified, and then 1v1 air combat trials were conducted.

Before the F-16 can be an effective high-angle-of-attack aircraft some other modifications must be made. Shortening the wing leading-edge extension (LEX) and adding a larger speedbrake (LSB) eliminates the deepstall, provides greater nose-down pitch agility and improves the lateral/directional characteristics (through coupling of the forebody, LEX and wing vortices). The baseline F-16 has a static directional instability at angles of attack above 32° and also develops large yaw moments at zero sideslip due to asymmetric forebody vortex formation at higher angles of attack. The Chine and Shark nose variants stabilize the forebody vortices and passively eliminate the yaw instability.

The five configurations shown in the figure were investigated in the simulation task.

STANDARD F-16:	Benchmark for enhancements
HI-AOA F-16:	Deepstall eliminated, AOA limit removed. Still directionally unstable.
PASSIVE CHINE:	Directionally stable, a true conventionally controlled high AOA airframe.
CHINE + JET:	Pneumatic FVC added for hi-AOA maneuverability.
STD + RNBS:	Standard forebody with cut-back LEX and LSB. Uses rotating nose boom strake for control and active yaw stabilization.

F-16 CONFIGURATIONS FOR SIMULATION

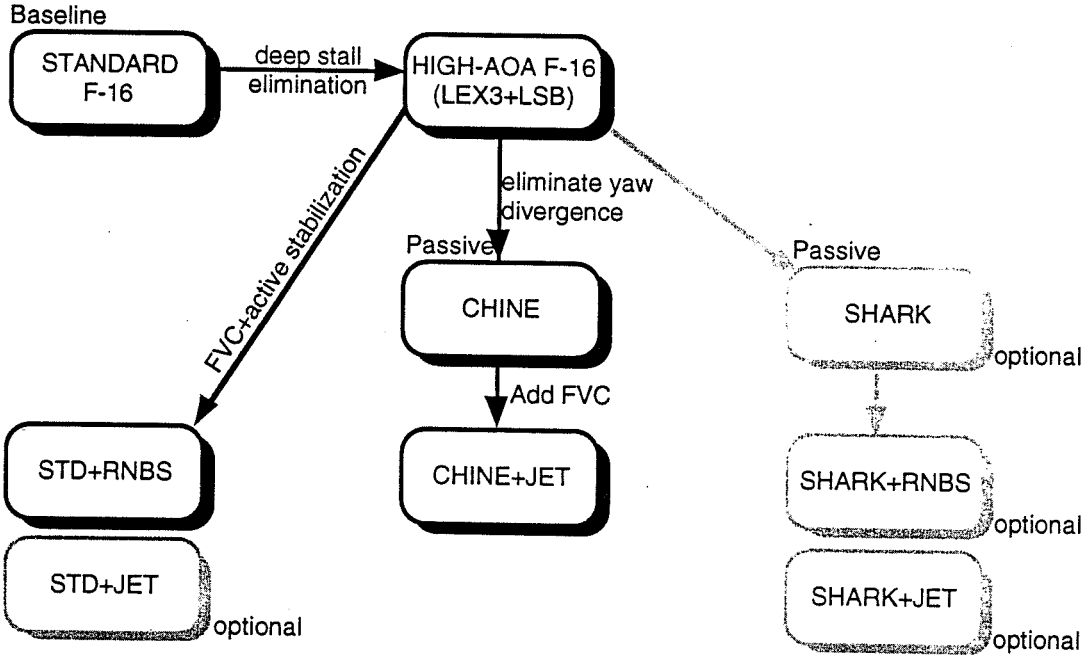

YAW CONTROL POWER

STANDARD F-16

The yaw moment due to ±maximum deflections of the rudder are shown in the central figure. The rudder control power is constant up to 30° angle of attack where it begins to decrease. The rudder is virtually ineffective above 50° angle of attack. Note that the yaw moment magnitude is 0.045. This model developed a yaw moment asymmetry at high angles of attack.

STD NOSE + RNBS

The yaw control power developed by the rotating nose boom strake (RNBS) is shown on the left hand plot for various strake rotation angles. Like the F/A-18 the strake does not become effective until the angle of attack is greater than 30°. Note that this configuration includes the cut-back LEX and large speed brake as shown in the sketch.

CHINE + JET

Mechanical FVC was not effective when used in combination with the Chine. The effectiveness of jets angled across the forebody is shown in the right figure. The jets produce yaw control moments over a larger angle of attack range than the RNBS. Note that the magnitudes of the yaw control power at high angles of attack are roughly equal to that produced by the rudder at low AOA.

F-16 YAW CONTROL POWER

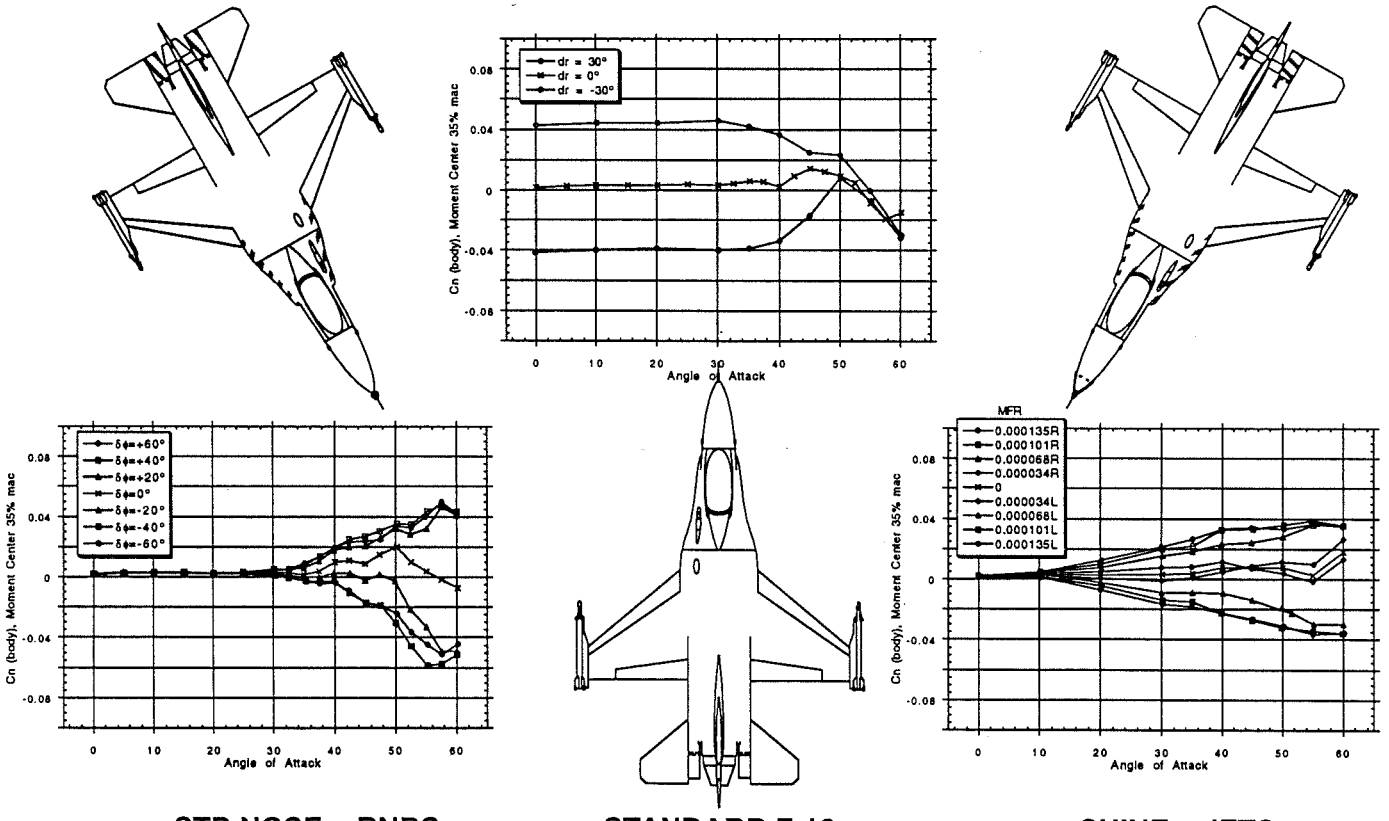

STD NOSE + RNBS STANDARD F-16 CHINE + JETS

TYPICAL TRACKING MANEUVER

These plots illustrate a typical change of maneuver plane during a tracking task as performed by the standard F-16 and an FVC enhanced configuration. The plot shows the angular orientation of the aircraft's body axis (θ and ψ) at discrete moments during the maneuver. The long line extending from the aircraft symbol represents the angle of attack and the shorter leg is sideslip. The end of the "L" opposite the aircraft symbol shows the velocity vector (γ and σ). The numbers show the flight time in seconds. This technique of presenting flight data was developed by Yuri Kalviste (AIAA-86-2283).

The most striking difference between the two examples is that the FVC aircraft is much smoother in its maneuvering to acquire and track the target. The use of higher angles of attack and sideslip are apparent, as is the use of velocity vector maneuverability at high angles of attack. The standard F-16 maneuver plot reflects the pilot's explanation of the maneuver technique as, "pull - unload - roll - pull -unload - roll, repeat."

Other pilot comments from the post-flight de-briefs and questionnaires were that the FVC aircraft required a different piloting technique that was much smoother than used with the baseline aircraft. The smoother technique made it easier to set-up for a shot, allowed adjustments of the maneuver plane, and would provide additional shot opportunities during air combat. Other differences between the configurations that were seen during the air combat trails were the use of the increased nose-down pitch agility and rapid deceleration in a defensive position to force an overshoot. Rapid deceleration is possible due to the high drag associated with post-stall angles of attack.

By and large, these were the expected benefits to be obtained with capability to maneuver at high angles of attack. These advantages became apparent during a prolonged engagement -- typically when the pilot was maneuvering for a guns kill instead of a missile shot.

F-16 FVC 1v1 WVR - TYPICAL TRACKING MANEUVER

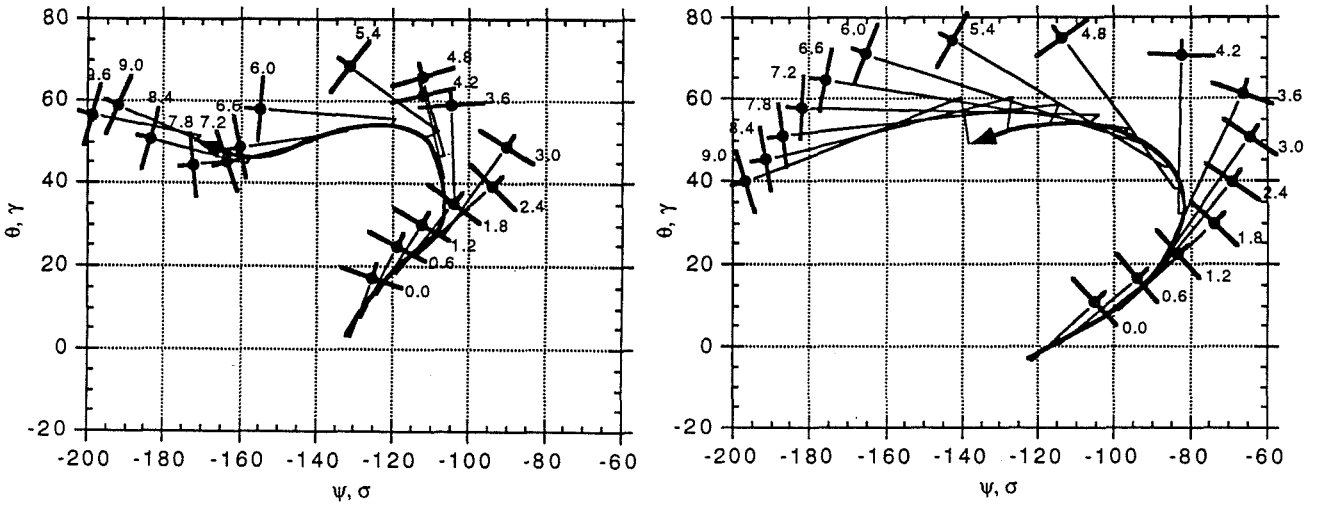

STANDARD F-16

STD NOSE + RNBS

INITIAL ENCOUNTER

While the differences observed during prolonged WVR air combat were not particularly surprising given the increased aerodynamic capability of the FVC enhanced aircraft, some interesting results developed from the initial engagement. The 1v1 scenario begins with both aircraft at the same altitude and speed on reciprocal headings. The aircraft were offset laterally approximately 0.9 miles from one another. The engagements began with both aircraft turning toward the other to obtain a missile or gun solution.

The initial engagements fell into three groups as sketched in the figure. The standard F-16 had roughly the same turn rate as the opposing aircraft and the first pass would be close to nose-to-nose. The two conventional control modifications had a moderate turn rate advantage and would acquire the target earlier. The FVC enhanced configurations had a tremendous turn rate and turn radius advantage and would be in a missile firing position long before the other aircraft.

Examination of the angles of attack used during the turn explains the turn rate difference.

Configuration	Maximum AOA Used
Std F-16	26-28°
Passive Hi-AOA	30-35°
FVC Config's	40-45°

The trimmed lift coefficient of the five configurations over these angles of attack are very close to the same. The large difference in turn rate is due to the additional thrust component (≈40%) at higher angles of attack.

The passive airframes have the same high angle of attack capability as the FVC airframes but the pilot was unwilling to use the capability, citing a bad feel and lack of confidence in the aircraft response. The passive chine configuration was stable at high angles of attack, but not controllable. The pilot soon learned to manually limit the angle of attack to a more moderate level where some degree of lateral-directional control remained. Even though the initial encounter was mostly a pure roll and pull maneuver, not requiring agile velocity vector rolls, the added control provided by FVC gave the pilot the confidence to fully utilize the pitch plane agility offered by the hi-AOA modifications.

F-16 FVC 1v1 WVR - INITIAL ENCOUNTER

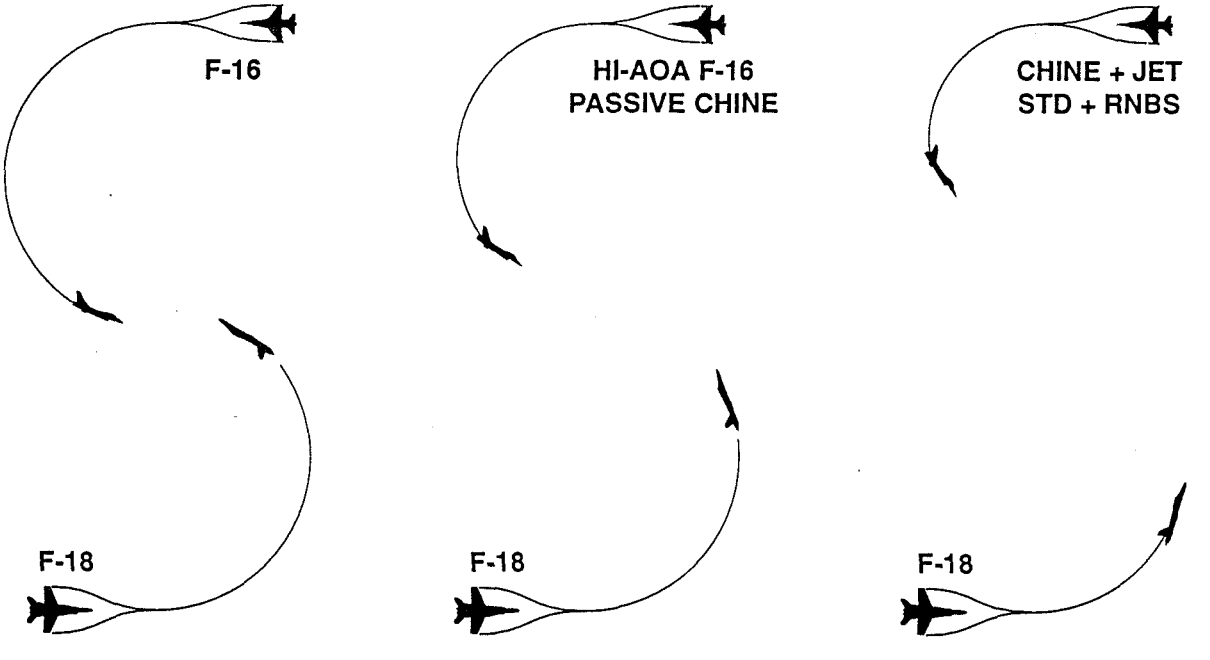

CONCLUSIONS

FVC FROM STATIC AND ROTARY WIND TUNNEL TESTS:

Forebody vortex control is effective at angles of attack above 30°

Jet blowing is not greatly effected by a rotary flow field

Slot blowing is more effective on the leeward side during rotation.

Both the single rotating strake and the Rhino Horn increase the anti-spin tendency when undeflected.

The time lag due to onset and decay of blowing is on the order of the time it takes to deflect a conventional rudder.

FVC GAVE LARGE COMBAT ADVANTAGE:

ENVELOPE OPENED TO HI AOA
The configurations were stable, controllable and had predictable responses. The increased angle of attack envelope resulted in a large turn rate and turn radius advantage.

INCREASED CONTROL OF MANEUVER PLANE
Forebody vortex control gave velocity vector roll control allowing the maneuver plane to be changed without unloading from high angle of attack.

DIFFERENT FLYING TECHNIQUE, EASIER
This resulted in a smoother, more continuous approach to the target. Adjustments to the plane of the primary maneuver could be made during the approach to capture.

MORE MANEUVER OPTIONS
A larger variety of defensive and offensive maneuvers are available for the pilot to choose from allowing more shot opportunities.

CONCLUSIONS

F/A-18 -- FVC IN ROTARY FLOW FIELD

- FOREBODY VORTEX CONTROL IS EFFECTIVE AT ANGLE OF ATTACK ABOVE 30°.
- JET BLOWING IS NOT GREATLY EFFECTED BY A ROTARY FLOW FIELD.
- SLOT BLOWING IS MORE EFFECTIVE ON LEEWARD SIDE DURING ROTATION.
- SINGLE STRAKE AND RHINO INCREASE THE ANTI-SPIN TENDENCY.
- BLOWING TIME LAG IS ON THE ORDER OF CONVENTIONAL CONTROL DEFLECTION TIMES.

F-16 -- FVC IN COMBAT

FOREBODY VORTEX CONTROL GAVE A LARGE COMBAT ADVANTAGE DUE TO:

- FLIGHT ENVELOPE OPENED TO HIGH ANGLE OF ATTACK.
- INCREASED CONTROL OF MANEUVER PLANE.
- A DIFFERENT, EASIER FLYING TECHNIQUE.
- MORE MANEUVER OPTIONS AVAILABLE.

1995107842

N95-14255

– Ames Research Center

16104

19

29p

3500067

Comparison of Full-Scale, Small-Scale, and CFD Results for F/A-18 Forebody Slot Blowing

by
Wendy R. Lanser
Larry A. Meyn
NASA Ames Research Center
Moffett Field, CA

Kevin D. James
Sterling Federal Systems, Inc.
Moffett Field, CA

1994 High Alpha Conference July 12-14, 1994

Abstract

It has been shown experimentally that pneumatic forebody flow control devices provide a significant increase in yaw control for fighter aircraft at high angle-of-attack. This study presents comparisons of the various experimental and computational results for tangential slot blowing on the F/A-18 configuration. Experimental results are from the full-scale and 6%-scale model tests and computational solutions are from both isolated forebody and full aircraft configurations. The emphasis is on identifying trends in the variation of yawing moment with blowing-slot exit conditions. None of the traditional parameters (mass flow ratio, blowing momentum coefficient, velocity ratio) succeeded in collapsing all of the results to a common curve. Several factors may affect the agreement between the 6%- and full-scale results including Reynolds number effects, sensitivity of boundary layer transition from laminar to turbulent flow, and poor geometric fidelity, particularly of the blowing slot. The disagreement between the full-scale and computed yawing moments may be due to a mismatch in the slot exit conditions for the same mass flow ratio or aircraft configuration modeling. The general behavior of slot blowing on the 6%-scale and computational models is correct, but neither match the full-scale results.

Introduction

Wind tunnel testing has been and continues to be the best way to obtain accurate estimates of the aerodynamic performance of a vehicle before building a prototype. For many applications, small-scale model testing is appropriate and sufficient. In some cases, for example when model fidelity is critical or significant amounts of flow separation are present, results may be sensitive to Reynolds number, and large-scale testing is in order. Along with wind-tunnel testing, computational fluid dynamic (CFD) solutions are a useful tool in generating estimates of aerodynamic performance before a prototype is built.

It has been shown experimentally that pneumatic forebody flow control devices provide a significant increase in yaw control for fighter aircraft at high angles-of-attack. This control capability has been demonstrated in small-scale and full-scale experiments as well as in computational solutions using Navier Stokes equations. This study presents comparisons of the various experimental and computational results for tangential slot blowing on the F/A-18 configuration. Experimental results are from full-scale and 6%-scale model tests and the computational results are from both the isolated forebody and the full aircraft configurations. The full-scale experiment was conducted in the 80- by 120-Foot Wind Tunnel, the 6%-scale model was tested in the 7- by 10-Foot Wind Tunnel, and the computations performed at the Numerical Aerodynamic Simulation Facility at NASA Ames Research Center. The emphasis is on identifying trends in the variation of yawing moment with blowing-slot exit conditions. Definition of an appropriate non-dimensional slot-exit parameter may allow direct comparisons of the CFD and the small-scale experimental results with the full-scale experimental results. The traditional non-dimensional parameters: mass flow ratio, blowing momentum coefficient, and velocity ratio will be evaluated in an attempt to collapse all of the results to a common curve. Additionally, the comparison of experimental and computed surface pressure distributions will be presented. The test conditions included variation in angle-of-attack from 25 to 60 deg, and free-stream velocities from 95 to 157 ft/sec for the 6%-scale model and 40 to 168 ft/sec for the full-scale model. The Reynolds number based on wing mean aerodynamic chord ranged from 0.387×10^6 to 0.636×10^6 for the 6%-scale model, from 4.5×10^6 to 12.0×10^6 for the full-scale aircraft, and 11×10^6 for the computational solutions.

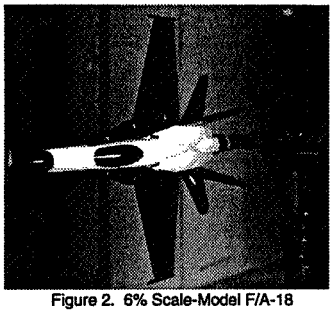

Figure 2. 6% Scale-Model F/A-18

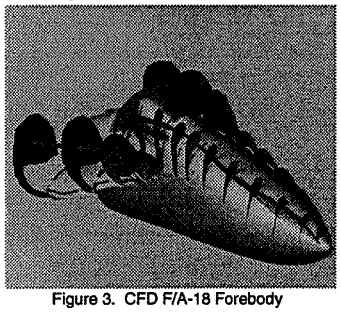

Figure 3. CFD F/A-18 Forebody

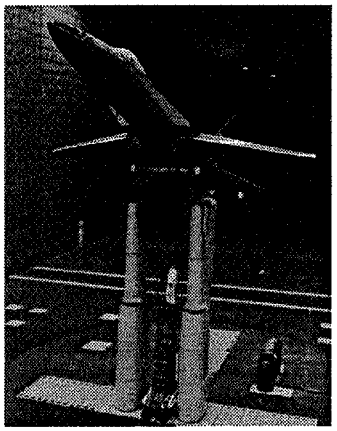

Figure 1. Full-Scale F/A-18

Model Descriptions

Full-scale Aircraft

The full-scale F/A-18 aircraft tested was a single-seat aircraft built by the McDonnell Douglas Aircraft and the Northrop corporations. The F/A-18 fighter aircraft has two vertical stabilizers canted 20 deg outboard from the vertical and has leading edge extensions (LEXs) on each side of the fuselage just forward of the wing. The LEXs used for this experiment were instrumented for surface pressures and were flown on the High Alpha Research Vehicle at the Dryden Flight Research Facility in 1990, reference 1. During the wind-tunnel test, the aircraft had both engines removed, air flow through the engine inlets, the wingtip missile launch racks mounted, and the control surfaces configured for high-angle-of-attack flight. The high angle-of-attack configuration has the leading-edge flaps set at 33 deg and the trailing-edge flaps set at 0 deg. The horizontal tails operated on a flight control schedule that was a function of the angle-of-attack to simulate trimmed flight conditions. The rudders were positioned at 0 deg deflection unless noted otherwise.

The radome designed for these experiments incorporated a variable-length slot, pneumatic forebody-flow-control mechanism interior to the radome structure. This radome was a composite laminate of fiberglass/foam/fiberglass fabricated from a plastic mold formed on a production-aircraft radome. Figure 1 above shows the slot highlighted with a white stripe on the radome; only the port slot was active. Care was taken to assure symmetry by incorporating a dummy slot on the starboard side.

The blowing slot had a total length of 48 inches and began 3 inches aft of the radome apex. The slots were positioned at 90 deg and 270 deg from the windward side (bottom) of the radome. The active slot was at the 270 deg position (port-side) and was designed to blow tangentially to the surface toward the leeward side of the radome. The 48 inch slot was divided into 24 separately controlled segments with each segment measuring 2 inches long. The slot height was 0.10 inches. Air for the slot was supplied by several 125 psi compressors, totaling 1550 CFM. The mass flow rate of the blowing air was measured using a turbine flow meter.

A three-strut configuration was used to mount the F/A-18 aircraft in the 80-by 120-Foot Wind Tunnel test section. The aircraft was attached to a circular cross beam at the two main landing gear positions, which in turn was attached to the wind-tunnel main struts. A tail boom assembly, connected to the

aircraft at each engine mounting pin and at the arresting tail hook hard point, was used to attach the aircraft to the third wind-tunnel tail strut. The angle-of-attack was varied by altering the length of the tail strut. The angle-of-attack range for the full-scale forebody flow control experiment was from 20 to 50 deg. Additional details can be found in references 2-4.

6%-scale Model

The 6% model (fig. 2) for this experiment was a new model designed and built by Eidetics International. A fiberglass model was made from a mold made from a Navy/McAir 6% model. During the wind tunnel test, the engine inlet was faired over, the leading-edge flaps were deflected 34 deg, the trailing edge flaps at 0 deg, the horizontal tails fixed at 0 deg, and the rudders were positioned at 0 deg deflection unless otherwise noted.

The radome on this model had blowing slots on both sides made up of four segments. The slot had a total length of 1.92 inches, a width of 0.006 inches, and began 0.66 inches aft of the radome apex. This slot configuration corresponded to a 32 inch long slot located 11 inches aft of the radome apex at full-scale. The slots were positioned at 90 deg and 270 deg from the windward side (bottom) of the radome. Various slot lengths were tested by taping over portions of the slot segments. The interior of the nose contained two plenums, one on the starboard side and one on the port side that supplied air to the blowing slots. The mass flow rate of the blowing air was measured with an Omega volumetric flow meter. The volumetric flow meter was calibrated using an extremely sensitive (0.1 gram) scale and a regulated supply tank.

The 6%-scale model was sting mounted with the wings vertical, and the model was pitched in the horizontal direction with the floor mounted turntable. The angle-of-attack range for this experiment varied from 20 to 60 deg. Further details of this experiment can be found in reference 5.

Computational Analysis

The computational results presented here for the yawing moment coefficient as a function of blowing rate are for both the isolated forebody (fig. 3) and the full aircraft geometry. The computed pressure distributions presented are for the full aircraft geometry only. The aircraft and slot geometry were modeled using an overset grid technique, references 6-8. The full computational aircraft geometry had a faired-over engine inlet. The computational slot geometry is identical to the geometry used in the full-scale wind tunnel test. For both of these computations, a three-dimensional, thin-layer, implicit Navier-Stokes code with the Degani-Schiff modified Baldwin-Lomax algebraic turbulence model was used, references 6-8. The solutions for the forebody blowing conditions were computed at 30 deg angle-of-attack.

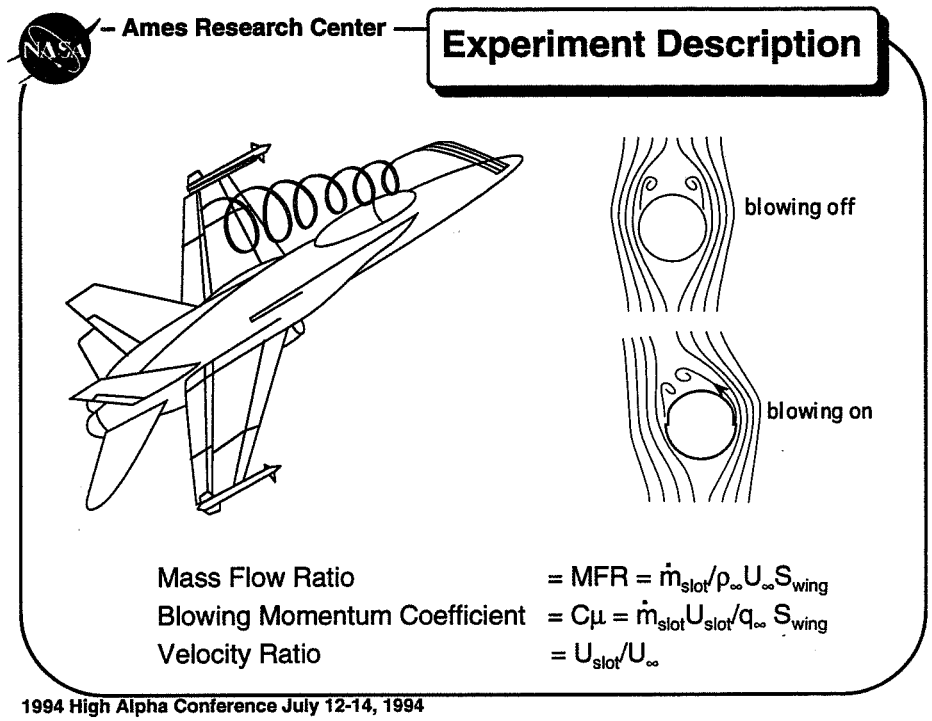

Experiment Description

These experiments measured the forces and moments on the aircraft due to the tangentially blowing slot. The tangentially blowing slot concept is based on the flow phenomenon called the coanda effect. The coanda effect delays the flow separation over a curved surface. This phenomenon creates a low pressure on the blowing side of the radome resulting in a suction force. The results presented show the yawing moment generated by the slot blowing for several slot configurations. In some cases the effect of the tangentially blowing slot was evaluated as the difference between the blowing-off and blowing-on conditions, ΔCn.

In the full-scale experiment, the yawing moment was measured using the external wind-tunnel balance system. During the 6%-scale wind tunnel test, the yawing moment was measured with an internal sting-mounted six-component balance. The moment reference was located at the 25% mean aerodynamic chord for both experiments and the CFD analyses.

Data from the full-scale wind-tunnel test have been corrected for blockage effects using techniques described in reference 9. The correction for blockage varied with the angle-of-attack. For example, at 50 deg angle-of-attack and q_∞ of 33 psf, the dynamic pressure had a correction of 3.8%, and a measured pressure coefficient of -1.0 at 30 deg angle-of-attack had a correction of 0.058.

In order to compare results from the 6%-scale test, the full-scale test, and the computational solutions non-dimensional slot exit parameters are required. As a result, the 6%-scale and the full-scale tests measured the blowing mass flow rate to determine the mass flow ratio, MFR. MFR is defined as the ratio of the mass flow rate through the slot to a reference mass flow rate. The reference mass flow rate is based on free-stream density, velocity, and the wing reference area. For both the full-scale and 6%-scale tests measured mass-flow rate, slot-exit area, and wind-tunnel static pressure were used to determine the slot exit conditions. In the full-scale test the total temperature in the plenum was used to determine slot exit conditions while the wind-tunnel total temperature was used in the 6%-scale test. Based on these measurements, the exit Mach number, the velocity, and the blowing momentum coefficient were determined using the continuity relationships for compressible flow defined in reference 10. This relationship assumed a uniform exit velocity and slot exit area.

To better understand the influence of the pneumatic forebody flow control on the flow-field structure, time-averaged pressures were measured on the forebody. The pressure orifices were located at five fuselage stations (FS): three circumferential rings on the radome at FS 70, 85, and 107, and two circumferential rings on the forebody at FS 142 and 184. The radome apex was located at FS 60.5, and the fuselage stations were measured in inches from that point.

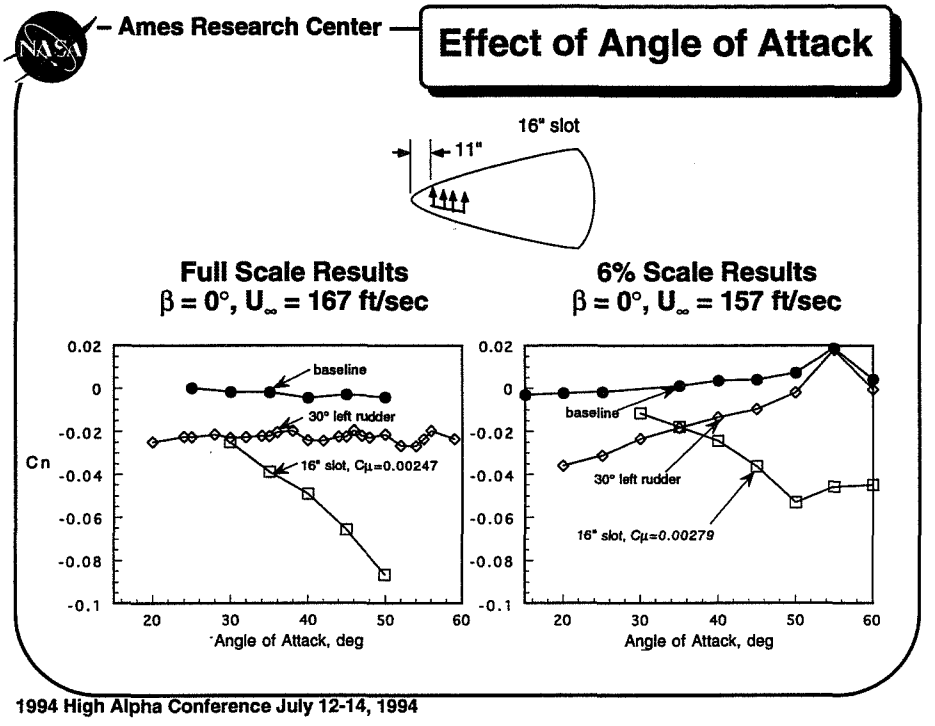

Results: Effect of Angle-of-Attack

The figure above shows the yawing moments generated by the baseline, no blowing, configuration, 30 deg of left rudder deflection, and blowing through a 16 inch slot located 11 inches aft of the radome apex for full-scale experiment and the corresponding configuration for 6%-scale experiment (0.96 inch slot located 0.66 inches aft). These results show that for a similar blowing momentum coefficient, $C\mu$, the small-scale model is less effective than the full-scale model. Also of interest, the small-scale results show an asymmetry above 50 deg angle-of-attack. Additionally, the rudder effectiveness decreased as angle-of-attack increased, which has been seen in other small-scale tests. However, the full-scale experiment shows the rudder effectiveness to be nearly constant across the angle-of-attack range from 20 to 60 deg. At 35 deg angle-of-attack, nearly the same magnitude of yawing moment was generated due to the rudder deflection at full-scale as was generated in the small-scale experiment. One noted difference was that the 6%-scale model had the horizontal tail fixed at 0 deg, and the full-scale experiment operated the horizontal tails on a flight control schedule that was a function of the angle-of-attack to maintain trimmed flight conditions. During the full-scale experiment, the 30 deg rudder case was re-run with the horizontal tails fixed at 0 deg and the same trend in the yawing moment was observed. As previously mentioned, the full-scale blowing experiment was limited to 50 deg angle-of-attack. The additional 30 deg rudder deflection data from 50 to 60 deg angle-of-attack was obtained during a second full-scale wind tunnel entry.

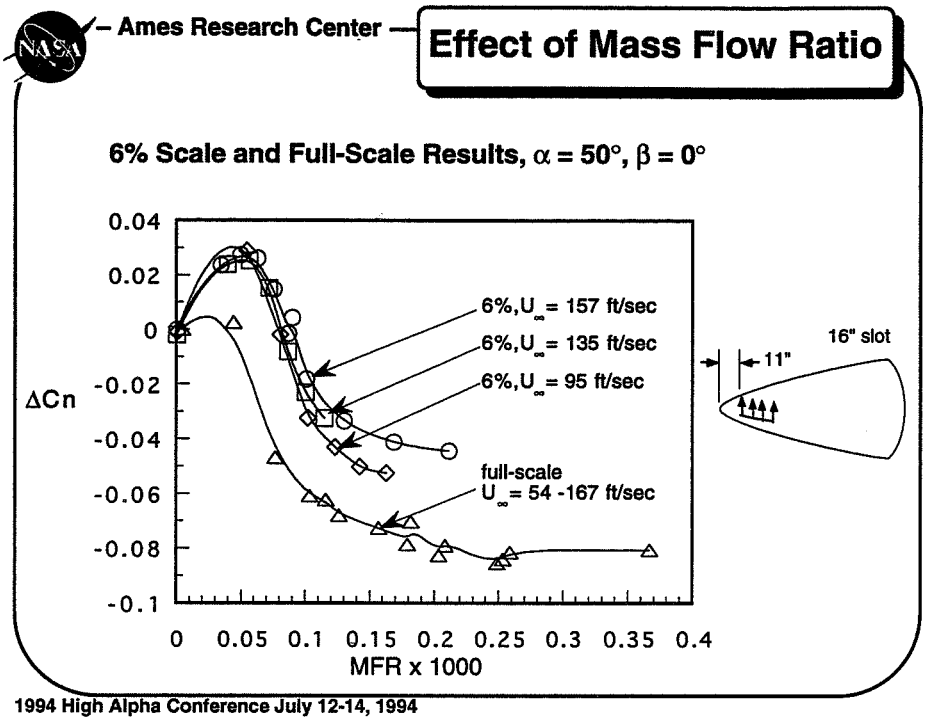

Results: Effect of Mass Flow Ratio

The results shown above are for the 16 inch long slot positioned 11 inches aft of the radome apex for the full-scale experiment and the corresponding 6%-scale configuration (0.96 inches long 0.66 inches aft). The figure above shows the yawing moment generated by the slot blowing as a function of the mass flow ratio (MFR) at 50 deg angle-of-attack. The 6%-scale data show a less effective slot than the full-scale slot for the same MFR. The full-scale data collapses fairly well to a single curve for the MFR range investigated, which included a free-stream velocity range from 40 ft/sec to 167 ft/sec. Whereas, the 6%-scale slot does not collapse the data to a single curve for the free-stream velocity range tested. The small-scale data also show an amplified moment reversal at low blowing rates when compared to the full-scale results. A few possible explanations for the differences found between the two sets of results are forebody geometry fidelity, surface roughness, and Reynolds number effect. Any one of these explanations or a combination of them may cause the flow in the boundary layer on the forebody region of the aircraft to transition from laminar to turbulent differently from the small-scale test to the large-scale test and more importantly to separate at different points on the forebody.

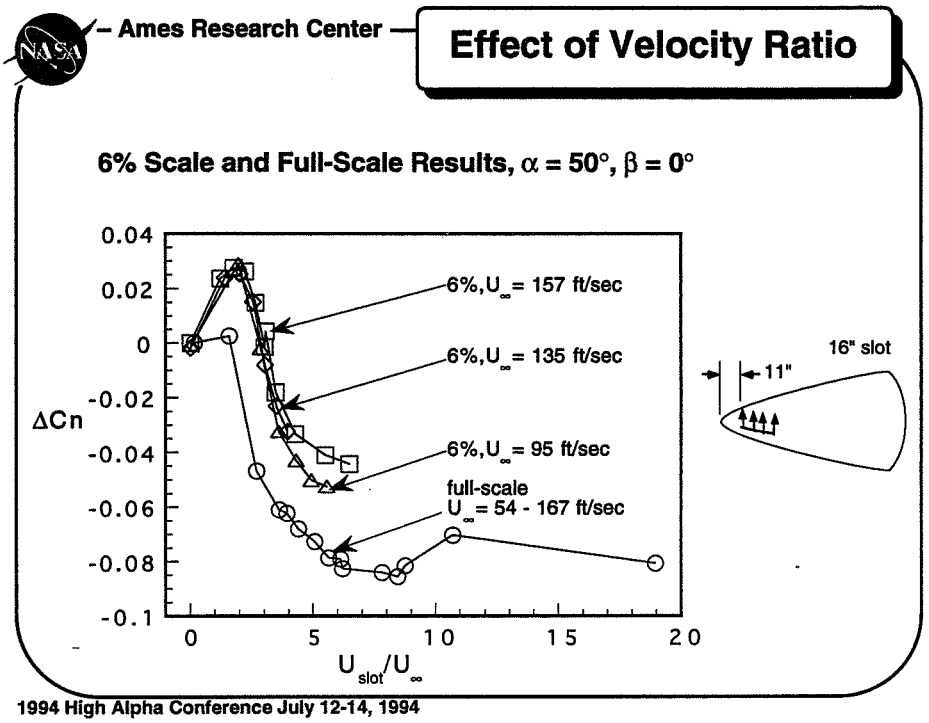

Results: Effect of Velocity Ratio

The yawing moment generated by the slot blowing for the same slot configurations and angle-of-attack are shown above as a function of the velocity ratio. The velocity ratio is defined as the ratio of the slot exit velocity to the free-stream velocity. The data from the 6%-scale model test appear to collapse slightly better as a function of the velocity ratio than when plotted as a function of the MFR. Similar to the previous comparison using MFR to non-dimensionalize the blowing slot-exit conditions, the small-scale test produced less yawing moment than the full-scale test for the same velocity ratio and showed an amplified moment reversal at the low blowing rates.

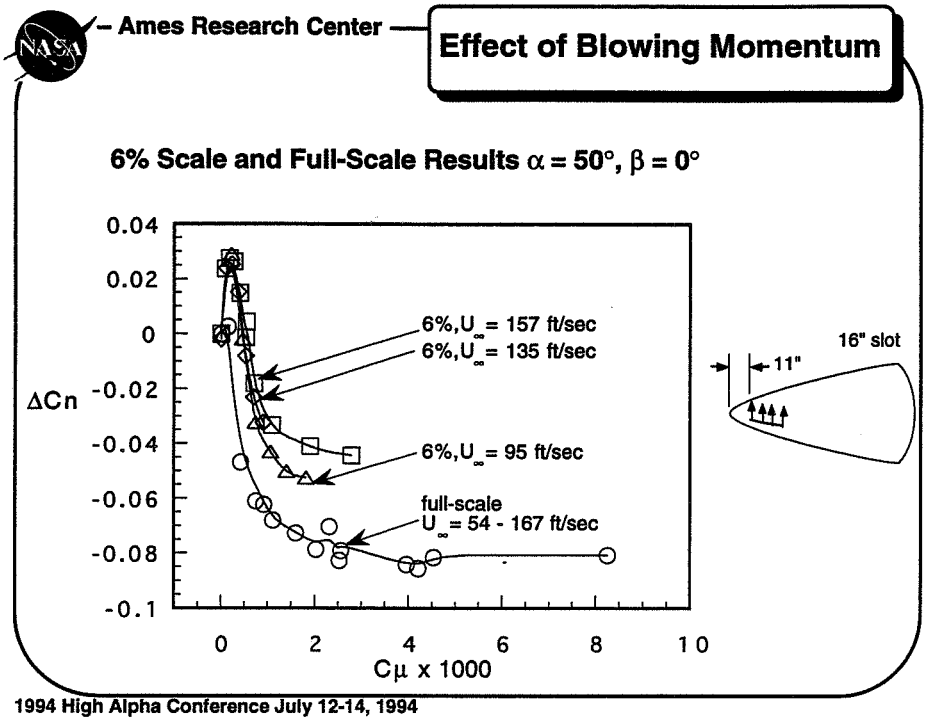

Results: Effect of Blowing Momentum Coefficient

Again for the 16 inch slot positioned 11 inches aft of the radome apex for the full-scale configuration and the corresponding 6%-scale model configuration, the yawing moment due to slot blowing is shown as a function of the blowing momentum coefficient. The blowing momentum coefficient, $C\mu$, is a velocity squared function as defined in the experiment description figure. The full-scale results collapse to a common curve better as a function of the $C\mu$ than as a function of the velocity ratio. The 6%-scale data appears to collapse slightly better at the lower blowing rates as a function of $C\mu$ than as function of velocity ratio; however, at higher blowing rates the velocity ratio parameter appears slightly better than the $C\mu$ parameter. The comparison of the yawing moments as a function of $C\mu$ for the small-scale with the full-scale yields similar results to those seen for the MFR and velocity ratio parameters.

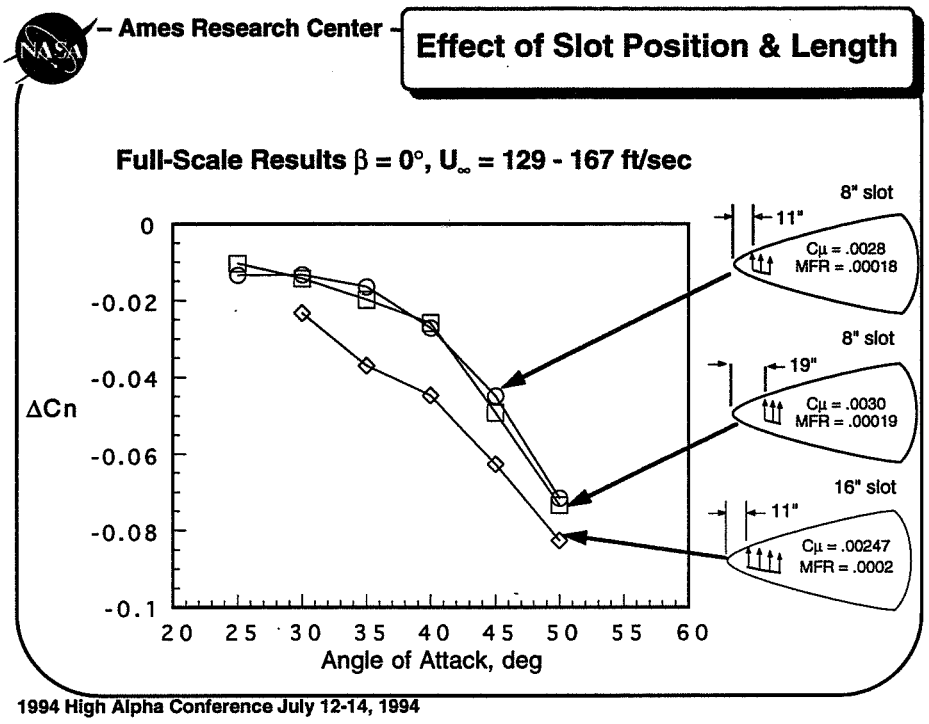

Results: Effect of Slot Position and Length for the Full-scale Results

In the figure above, the yawing moment generated by three full-scale slot configurations for similar Cμ values over an angle-of-attack range from 20 to 50 deg are shown. The slot configurations shown are the 8 inch long 11 inches aft, 8 inch long 19 inches aft, and 16 inch long 11 inches aft. The position of the slot relative to the radome apex had no effect on the 8 inch slot configurations. However, the 16 inch long slot positioned 11 inches aft produced more yawing moment than either one of the 8 inch long slot configurations for a lower Cμ value. Even though the MFR did not change in going from the 8 inch slot to the 16 inch slot, the yawing moment increased significantly.

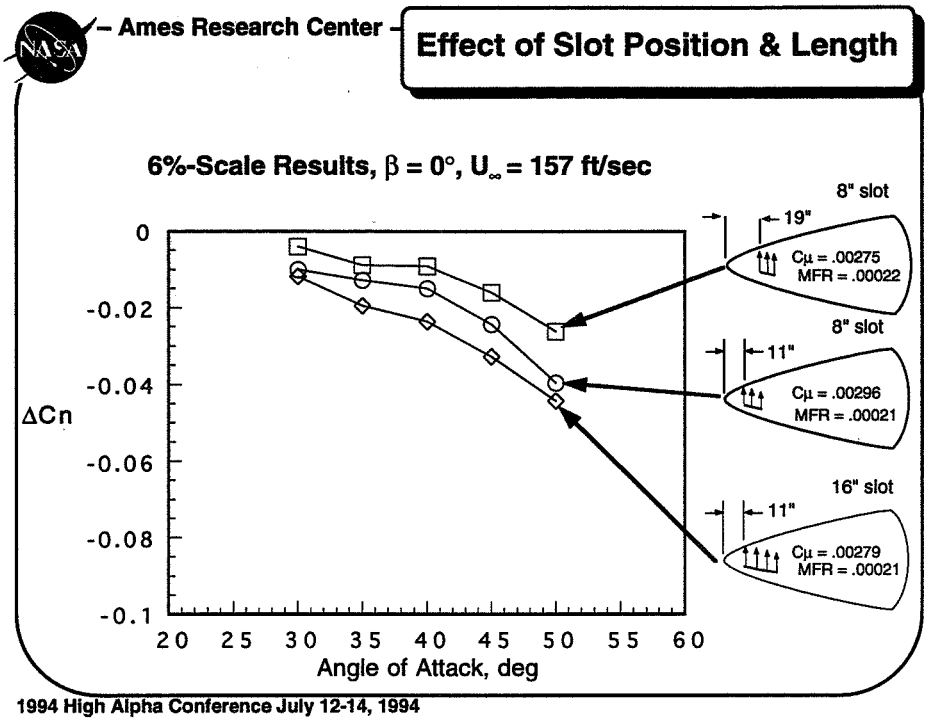

Results: Effect of Slot Position for the Small-scale Results

Shown above are the yawing moments generated by the the three 6%-scale model configurations that correspond to the three full-scale configurations shown on the previous page for similar Cμ values over the angle-of-attack range from 20 to 50 deg. Again, the slot configurations shown are the 0.48 inches 0.66 inches aft (8 inch long 11 inches aft full-scale) , 0.48 inches 1.14 inches aft (8 inch long 19 inches aft full-scale), and 0.96 inches 0.66 inches aft (16 inch long 11 inches aft full-scale). In contrast to the full-scale experiment, the 6%-scale model showed an effect of the slot position relative to the radome apex on the amount of yawing moment generated. The discrepancy shown between the 6%-scale model configurations of the 8 inch slots combined with test notes indicating poor flow quality from the forward slot position suggest that there was non-uniform flow at the slot exit. These results for the 8 inch slots could also indicate that the location of the boundary layer transition from laminar to turbulent flow differ on the 6%-scale model than on the full-scale model. Similar to full-scale results, the 6%-scale model of the 16 inch slot positioned 11 inches aft produced more yawing moment than both the 8 inch slots.

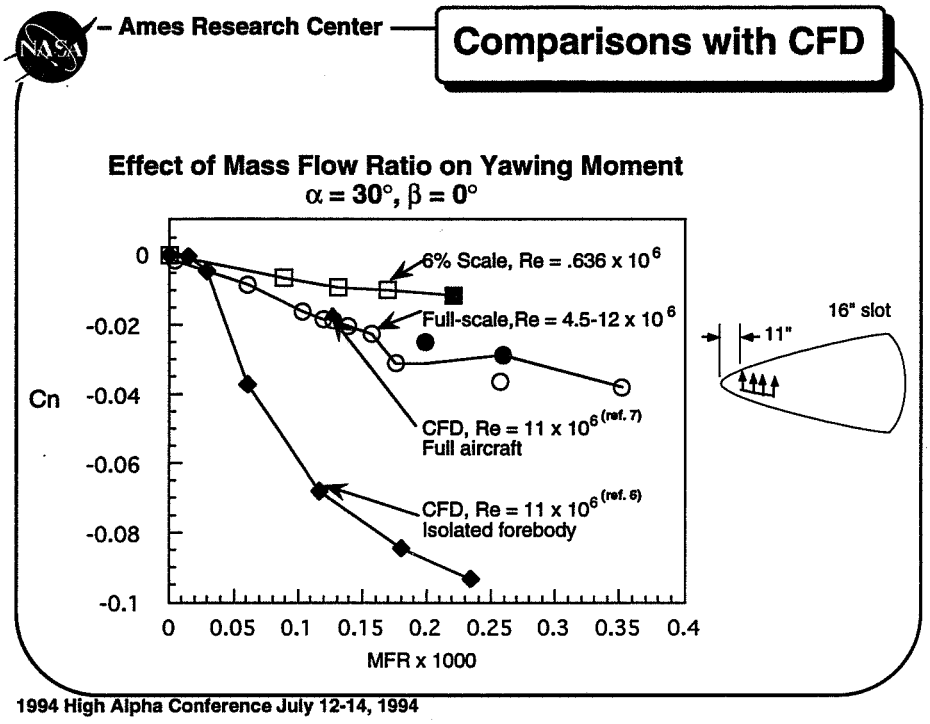

Results: Comparison of Small-scale, Full-scale, and CFD Results

The figure above shows the yawing moment as a function of MFR for the 16 inch slot positioned 11 inches aft at 30 deg angle-of-attack for both the small-scale and full-scale wind tunnel tests, as well as computational solution for the isolated forebody and full aircraft-configuration. In the figure above, the data points shown in black indicate that the exit velocity conditions were sonic. As seen in previous comparisons of the small-scale to full-scale results, the small-scale tests produced smaller yawing moments than the full-scale tests did at the same mass flow ratio. The computational analyses for the isolated forebody significantly over predicted the yawing moment produced in either one of the experiments. However, the computational analyses for the full-aircraft configuration yields a time-accurate solution that falls on the curve with the full-scale experimental results. It is important to note that for the isolated forebody and full-aircraft configuration computational solutions there was a mismatch in both the slot exit conditions and the free-stream Mach numbers. The maximum Mach number for the full-scale experiment was 0.15 whereas the computed solutions had a free-stream Mach number of 0.243. These computational solutions suggest that while the full-aircraft may not be critical for qualitatively capturing the global flow physics it is critical for accurate predictions of force magnitudes and blowing strengths.

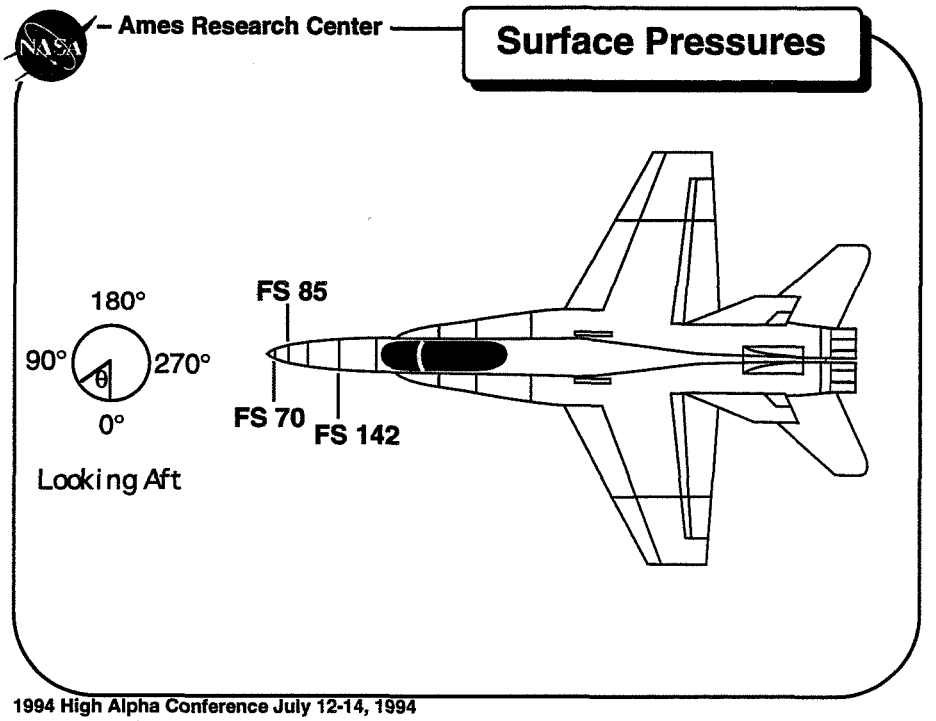

Forebody Fuselage Stations

As previously mentioned, time-averaged pressures were measured on the forebody to better understand the flow-field. Pressure orifices were located at five fuselage stations (FS): three circumferential rings on the radome at FS 70, 85, and 107, and two circumferential rings on the forebody at FS 142 and 184 for the full-scale model and the corresponding FS on the 6%-scale model. The radome apex was located at FS 60.5, and the fuselage stations were measured in inches from that point. Pressure distributions will be shown at FS 70, 85, and 142.

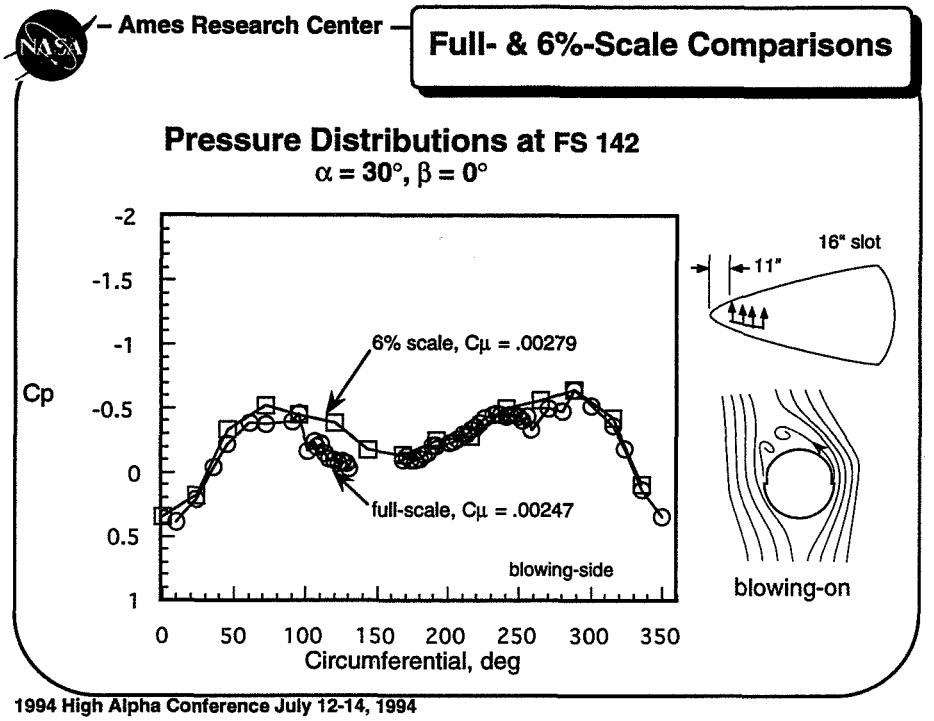

Results: Full-scale and 6%-Scale Pressure Distribution Comparisons

The figure above shows the pressure distributions for FS 142 on the aircraft at 30 deg angle-of-attack for both wind tunnel experiments at similar slot-blowing conditions. Agreement of data was within a reasonable range. As was expected, there is a decrease in pressure on the blowing side of the radome and an increase in pressure on the non-blowing side of the radome. The full-scale experiment showed a higher pressure on the non-blowing side of the radome. This result supports the larger forces seen in the full-scale data for the yawing moment comparisons. The discontinuities in the full-scale data at circumferential angles of approximately 95 deg and 265 deg are due to an antenna fairing which protrudes just forward of the orifice. Also, pressure taps could not be located between the circumferential angles of 131 deg and 167 deg due to structural obstructions inside the aircraft.

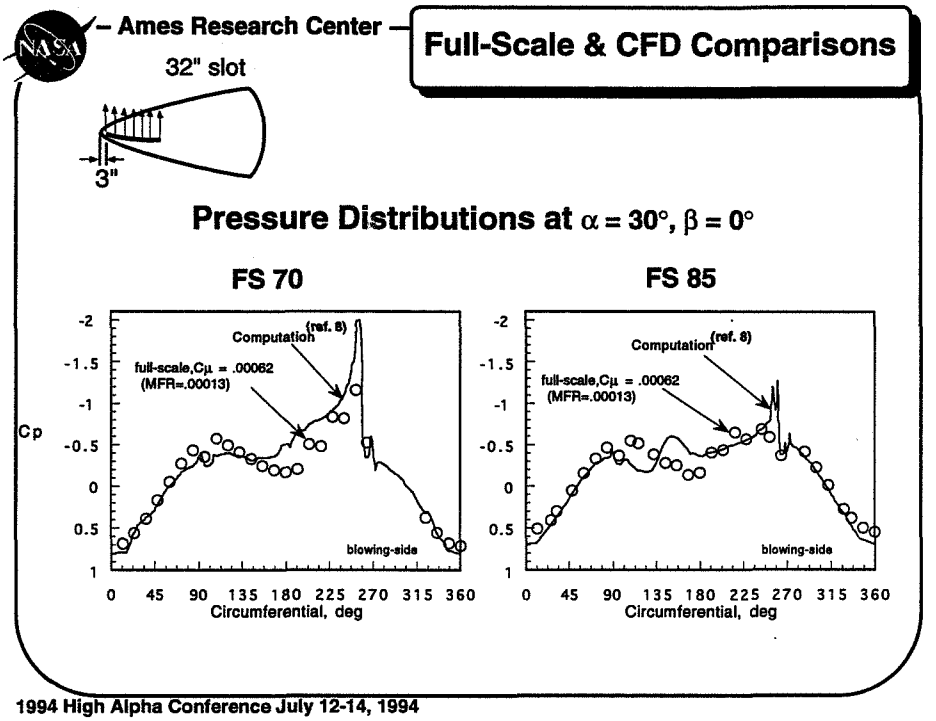

Results: Full-scale and CFD Pressure Distribution Comparisons

For the 30 deg angle-of-attack condition and the 32 inch long slot position 3 inches aft, the pressure distributions are shown for FS 70 and FS 85. The computed pressures are for the full-aircraft configuration, reference 8. Reasonable agreement is shown: the essential flow characteristics seen in the wind tunnel are captured in the computed solution. For these datasets, there is closer agreement in pressure distributions between the full-scale measurements and the computational solution on the leeward side than on the windward side of the radome.

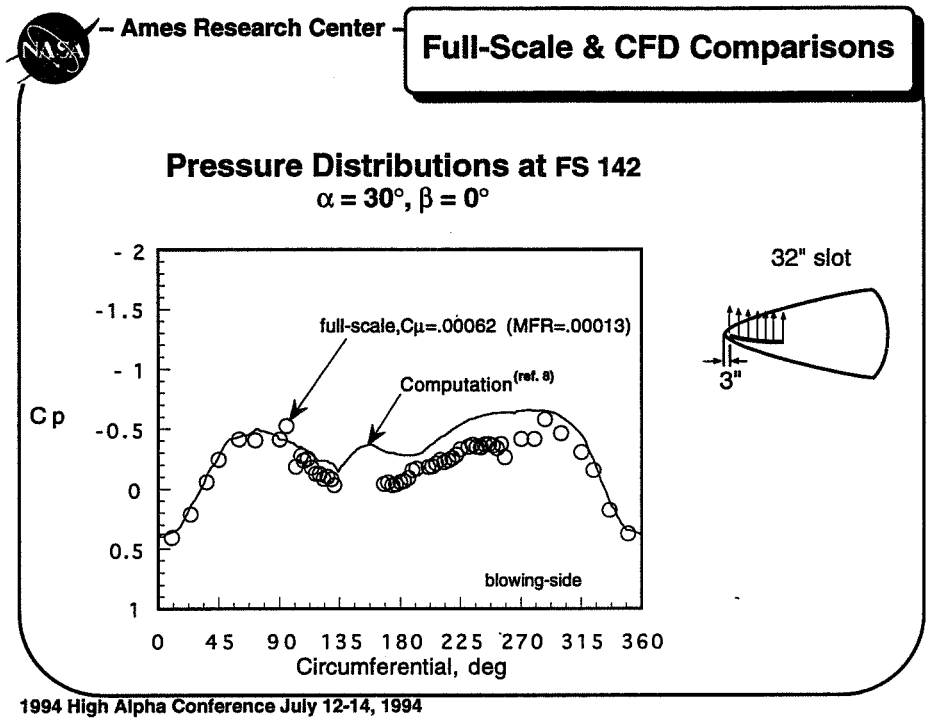

Results: Full-scale and CFD Pressure Distribution Comparisons

The data above shows pressure distributions at FS 142 on the aircraft for the 32 inch slot positioned 3 inches aft of the radome apex at 30 deg angle-of-attack. The computed solution includes the full-aircraft geometry. While the correspondence in the data between the computed solution and the full-scale wind tunnel measurements is promising, there are some differences in the magnitudes. As noted previously, the discontinuities in the full-scale data at circumferential angles of approximately 95 deg and 265 deg are due to an antenna fairing which protrudes just forward of the orifice, and the gap in the data between circumferential angles of 131 deg and 167 deg due to structural obstructions inside the aircraft.

Summary

This study presented comparisons of the various experimental and computational results for tangential slot blowing on the F/A-18 configuration. Experimental results are from full-scale and 6%-scale model tests and the computational results are for both the isolated forebody and full aircraft configurations. The emphasis was on identifying trends in the variation of yawing moment with slot-exit conditions. None of the traditional parameters (mass flow ratio, blowing momentum coefficient, velocity ratio) succeeded in collapsing all of the results to a common curve. For the conditions investigated, the 6%-scale tangential slot blowing experiment generated smaller yawing moments than the full-scale experiment, as well as showing an amplified moment reversal at the low blowing rates. Several factors may affect the agreement between the 6%- and full-scale results including Reynolds number effects, sensitivity of boundary layer transition from laminar to turbulent flow, and poor geometric fidelity particularly of the blowing slot. More detailed data are required to identify the cause of the disagreement between these two experiments.

The comparisons of the computational solutions with the full-scale experiment show some interesting results. The computations with the isolated forebody significantly over predicted the yawing moment generated for the slot blowing and the blowing strength required, but the full-aircraft configuration yielded a time-accurate solution that matched the full-scale experimental results. Another important point in these comparisons was that the slot-exit conditions and free-stream Mach number did not match. The disagreement between the full-scale and CFD yawing moments, particularly for the isolated forebody, may be due to a mismatch in the slot exit conditions for the same mass flow ratio or aircraft configuration modeling.

The general behavior of slot blowing on the 6%-scale and computational models is correct, but neither match the full-scale results. It appears that modeling of this flow field requires greater fidelity than currently feasible for both the small-scale test and CFD.

References

1. Fisher, D., Banks, D., and Richwine, D. M., "F-18 High Alpha Research Vehicle Surface Pressures: Initial In-Flight Results and Correlation With Flow Visualization and Wind-Tunnel Data," AIAA Paper 90-3018, Aug. 1990.
2. Lanser, W. R. and Meyn, L. A., "Forebody Flow Control on a Full-Scale F/A-18 Aircraft," AIAA Paper 92-2674, June 1992.
3. Meyn, L. A., Lanser, W. R., and James, K. D., "Full Scale High Angle of Attack Tests of an F/A-18," AIAA Paper 92-2676, June 1992.
4. Lanser, W. R., "Wind Tunnel Measurements on a Full-Scale F/A-18 With a Tangentially Blowing Slot," NASA CP-10134, Feb. 1994.
5. Kramer, B. R., Suarez, C., Malcolm, G., and Ayers, B.F., "F/A-18 Forebody Vortex Control Volume 1 - Static Tests," NASA CR 4582, March 1994.
6. Gee, K. and Rizk, Y. M., "Analysis of Tangential Slot Blowing on F/A-18 Isolated Forebody," AIAA Paper 94-1831, Jan. 1994.
7. Gee, K. and Rizk, Y. M., "Effect of Forebody Tangential Slot Blowing on Flow About a Full Aircraft Geometry," AIAA Paper 93-2962, July. 1993.
8. Gee, K. and Rizk, Y. M., "Analysis of of a Pneumatic Forebody Flow Control Concept About a Full Aircraft Geometry," AIAA Paper 92-2678, June. 1992.
9. Rae, W. H. Jr, and Pope, A., Low Speed Wind Tunnel Testing, Second Edition, 1984.
10. Society of Automotive Engineers, Inc., "Thermodynamics of Incompressible and Compressible Fluid Flow," AIR1168/1, Mar. 1990, pp. 85-87.

19950784 2

N95-14256

Low-Energy Pneumatic Control of Forebody Vortices*

35-02
16105
p. 16
350068

Frederick W. Roos

McDonnell Douglas Corporation

Presented at the Fourth NASA High-Angle-of-Attack Conference, Dryden Flight Research Center, CA, July 12-14, 1994.

* This research was conducted under the McDonnell Douglas Independent Research and Development program.

Motivation

Highly maneuverable combat aircraft and missiles often fly at sufficiently high angles of attack that their slender (usually pointed) forebodies develop asymmetric separated-flow vortex configurations. Management of this vortex (and associated aerodynamic force) asymmetry is essential to controlled flight under such conditions. Furthermore, the ability to generate and suppress this flow asymmetry at will holds promise of serving as a powerful high-angle-of-attack control technique for these vehicles.

Approach

Explore the prospect of employing bluntness, known to suppress the tendency toward flow asymmetry on slender forebodies, jointly with pneumatic vortex manipulation as a system of forebody flow asymmetry control. Evaluate influences of jet location and direction, blowing rate, relative nose bluntness, angle of attack, and state of flow separation feeding the vortices (laminar vs. turbulent).

Effect of Blunting on Side Force for 3.5-Caliber Tangent Ogive

Slender, pointed forebody shapes are well known to develop large side forces and yawing moments at high angles of attack as a consequence of the development of asymmetry of the vortex system formed by flow separation on the leeward side of such bodies. It has been demonstrated that the blunting of such a forebody shape suppresses the tendency of that body to develop asymmetric flow (and corresponding side forces) at high angles of attack. The figure shows the suppression of asymmetric forces achieved by 20% bluntness on the tangent ogive nose (dotted nose shape in plan view). But introduction of slight geometric asymmetry onto the blunted nose (small bump indicated by the spot on the nose in plan view) reintroduces asymmetry of approximately the same magnitude as that of the original (pointed) forebody.

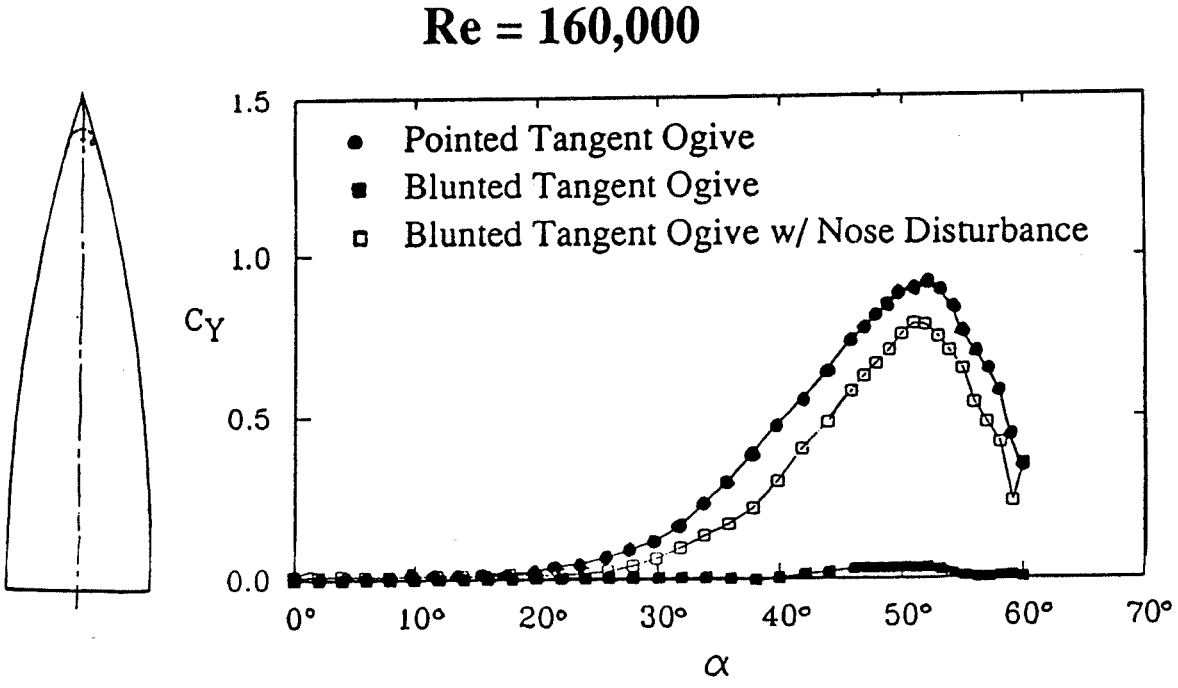

Nose Jets for Side Force Control

The foregoing leads to the concept of combining nose blunting (to suppress flow asymmetry) with blowing through small, symmetrically positioned nose jets to introduce flow perturbation leading to controllable side forces. As suggested by the sketch, the local displacement effect of slight blowing through a jet on the right side of the nose would promote detachment of the separated-flow vortex on the right side of the forebody, leading to a leftward side force. (Here and elsewhere, right and left are intended in the sense of the view forward over the forebody nose.)

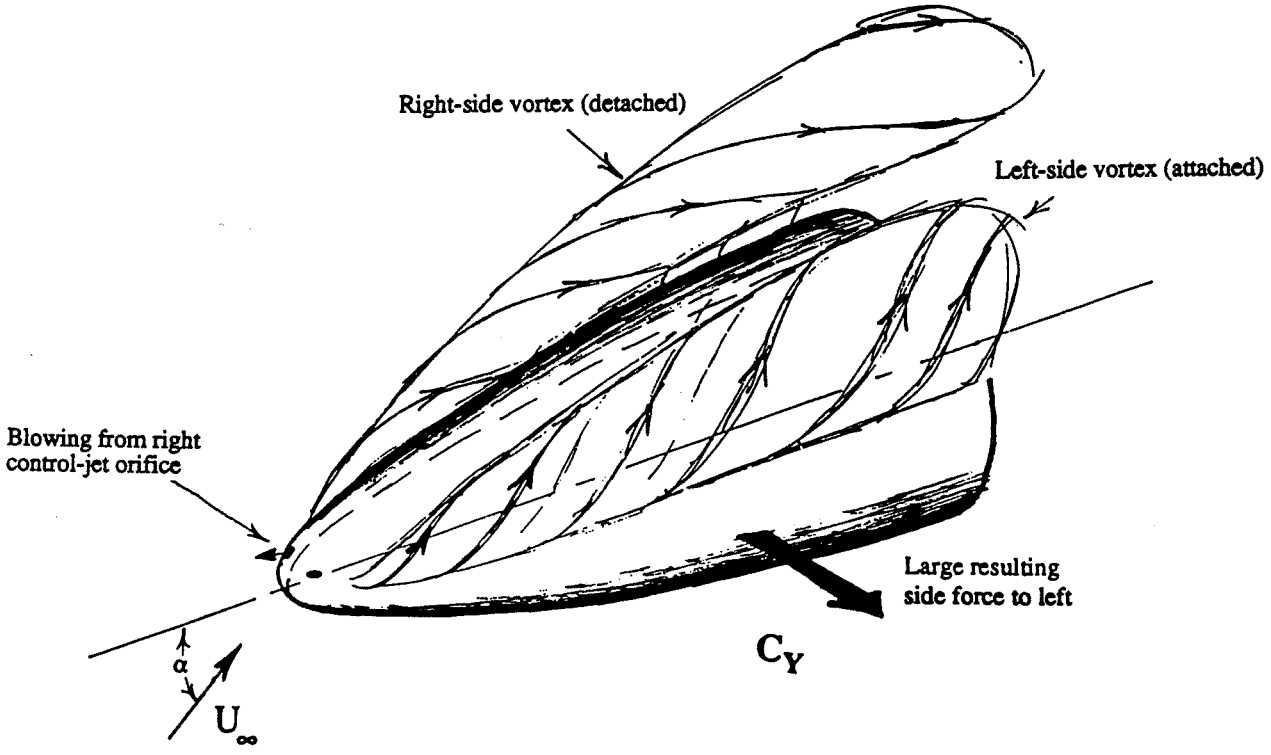

Forward-Blowing Nose Jet Configuration on 20% Blunt, 3.5-Caliber Tangent Ogive

The model forebody studied experimentally (at low speed) was a 3.5-caliber tangent ogive having a base diameter, D, of 7.62 cm. For the bulk of this study, the nose of the body was hemispherically blunted to a radius that was 20% of the base radius. Several control-jet configurations were evaluated; in all cases, jet orifices were located axially at the point of tangency of the hemispherical nose and the tangent ogive surface. Azimuthally, the jets were usually positioned at ±135° from the windward meridian. The figure is a photograph of the nose of this model configured with flush, forward-facing jet orifices.

Additional details of the experimental setup and effort can be found in Roos, F.W. and Magness, C.L., "Bluntness and Blowing for Flowfield Asymmetry Control on Slender Forebodies," AIAA Paper No. 93-3409, August 1993.

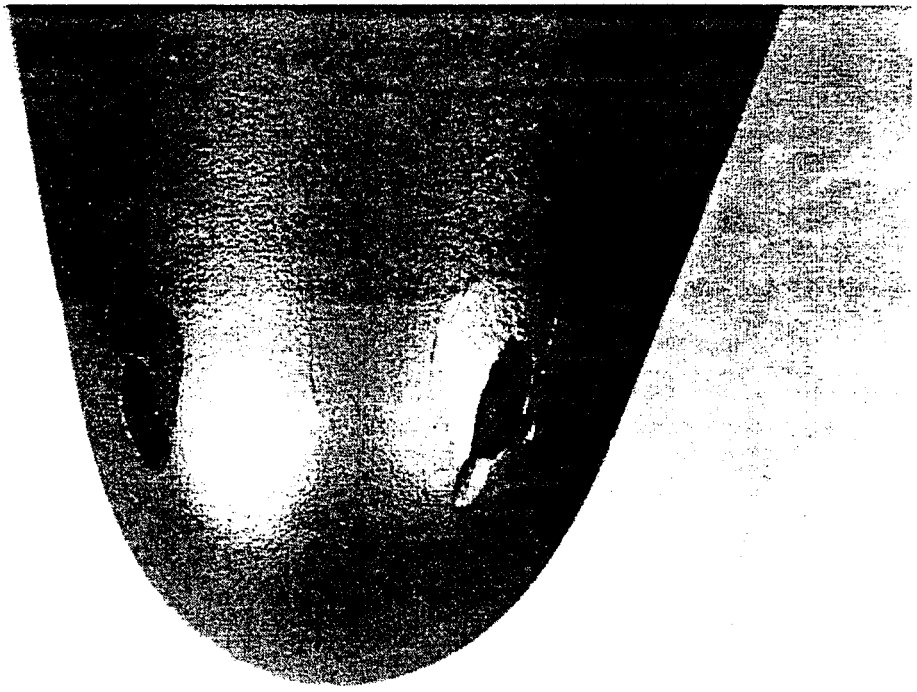

Mass-Flowrate Coefficient

Blowing rates are all defined in terms of a mass-flowrate coefficient, $C_{\dot{m}}$, rather than a momentum coefficient, C_{μ}, to emphasize the fact that it is the displacement effect of the jet flow, rather than any momentum-related entrainment and/or energizing effect, that is responsible for the phenomena demonstrated here.

$$C_{\dot{m}} = \dot{m}_j / \rho_\infty U_\infty A$$

$\dot{m}_j$ = **mass flowrate of control jet**

A = **planform area of 3.5 caliber tangent ogive**

Side-Force Control via Forward-Blowing Jets on Blunt Tangent Ogive (Laminar Separation)

Cross-plotting ΔC_Y vs. blowing rate (+ for right jet, - for left jet) for several angles of attack shows the basic characteristics of the low-energy pneumatic control. Within a range about $C_{\dot{m}} = 0$, the effect of blowing is proportional, up to limiting levels of ΔC_Y (with different maxima for each α).

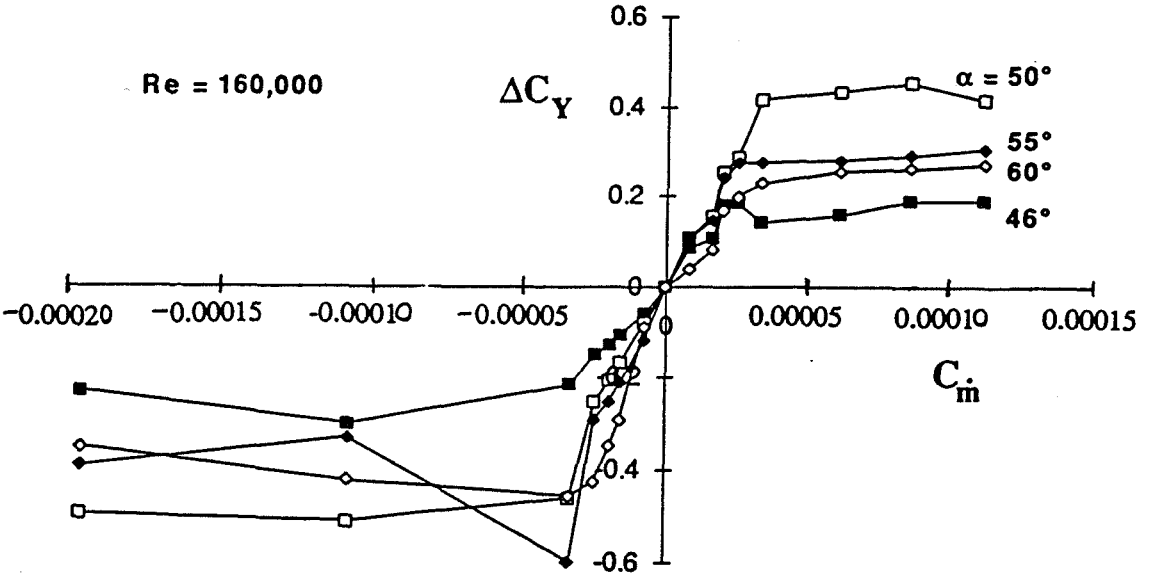

Influence of Bluntness Ratio on Blowing Effectiveness
(Laminar Separation)

Limited studies were conducted with a 5%-blunted forebody, also equipped with forward-blowing jet orifices. C_Y vs. $C_{\dot{m}}$ results were similar to those for the 20%-blunted body, although it appears that the less-blunt shape is more sensitive to blowing rate. This is evident in the figure, which compares blowing-effectiveness curves for the two blunted forebodies at the same angle of attack ($\alpha = 50°$).

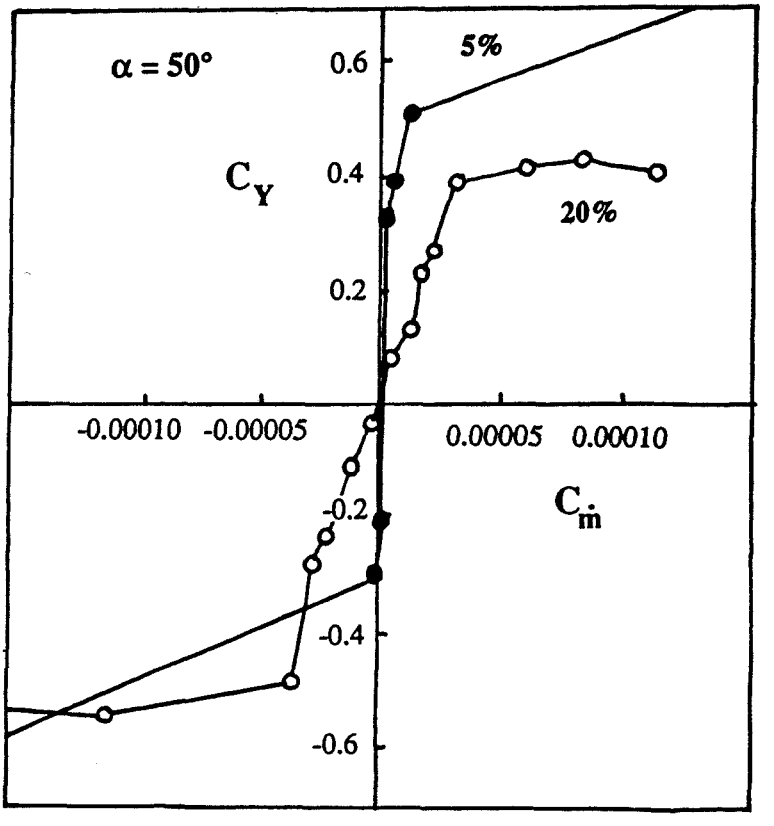

Comparison of Forward-Blowing-Jet Effectiveness with Laminar and Turbulent Separation, 20%-Blunt Tangent Ogive

The sensitivity of pneumatic-vortex-control results to the state (laminar or turbulent) of the separating forebody boundary layers was explored via experiments conducted with longitudinal grit strips employed to trip the crossflow boundary layer before separation. Further details concerning the tripping are given in Roos and Magness. The figure compares ΔC_Y vs. $C_{\dot{m}}$ curves at $\alpha = 55°$ with laminar and turbulent separation. At this α, the pneumatic-control effectiveness is clearly much greater when the separation is turbulent. This kind of variation emphasizes the importance of properly simulating the anticipated (full-scale) type of boundary-layer separation when attempting to evaluate unconventional flow-control methodologies.

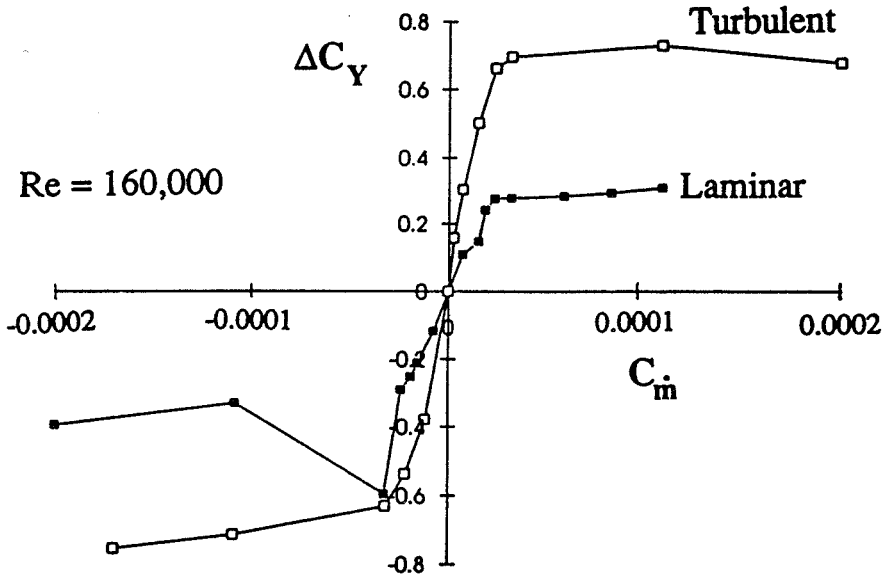

Effectiveness of Various Jet Configurations on 20%-Blunted Tangent Ogive

Turbulent Separation, $\alpha = 50°$

Several pneumatic-control jet configurations were studied with turbulent flow separation on the 20%-blunted tangent ogive. Blowing-flow-control effectiveness is compared for three jet configurations, all with fully turbulent separation, at $\alpha = 50°$ in the figure. The forward-blowing jets at $\phi_j = \pm 135°$ produce the strongest response at low $C_{\dot{m}}$, whereas the forward-blowing jets at $\phi_j = \pm 105°$ appear to yield the greatest overall ΔC_Y. The jets issuing normal to the surface evidently reach an "overblowing" condition.

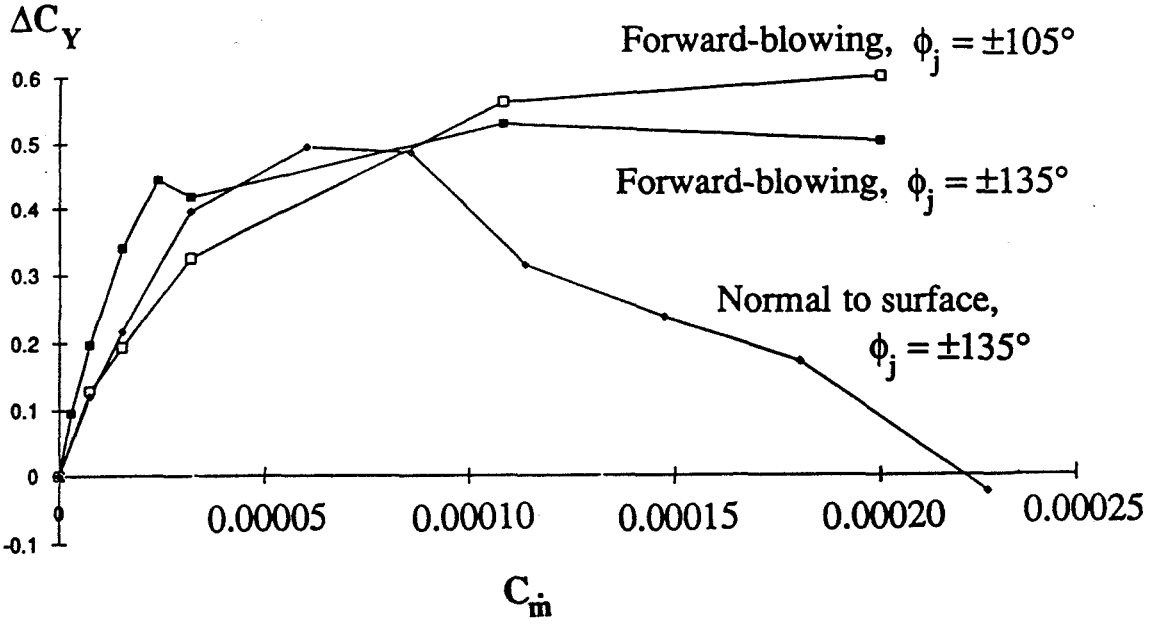

Forward-Blowing Control-Jet Orifices at Nose of 3.5-Caliber Tangent Ogive

Limited studies have been conducted of the forward-blowing concept applied to the basic 3.5-caliber (pointed) tangent ogive forebody shape. The flush, forward-facing control-jet-orifice configuration at the pointed nose is shown in the figure.

1.0 in

Forward-Blowing Results for Pointed Tangent Ogive
(Laminar Separation)

The no-blowing flow asymmetry shown in the previous figure is readily reversed at moderate mass flow, as this cross-plot of C_Y vs. $C_{\dot{m}}$ indicates.

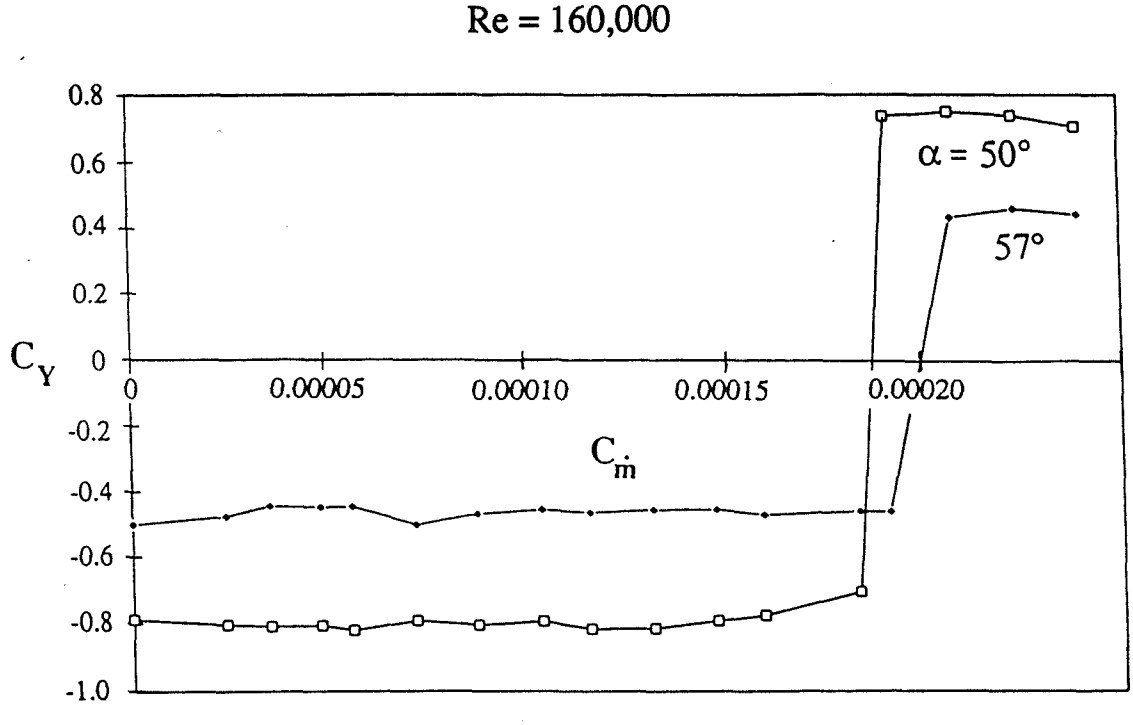

Forward-Blowing Effectiveness for Pointed Tangent Ogive
(Laminar Separation)

Side-force (C_Y vs. α) results for the pointed forebody (with laminar separation), shown in the figure, are similar to those from the blunted forebody except that the pointed body develops asymmetric flow naturally when $C_{\dot{m}} = 0$.

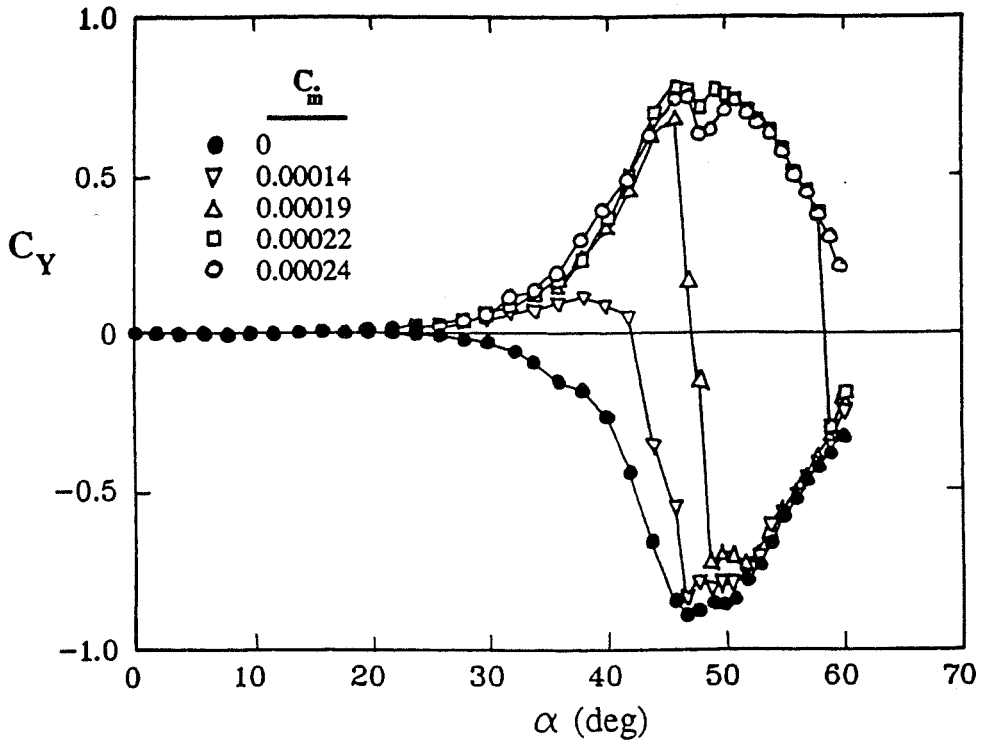

Forward-Blowing Effectiveness on Blunted and Pointed Forebodies (Laminar Separation)

This comparison of blowing-effectiveness curves for the pointed and blunted tangent ogives at $\alpha = 50°$ shows that the pointed forebody with forward–blowing control jets develops side-force-control characteristics comparable to the blunted forebody, continuing the trend indicated earlier of greater extremes of C_Y and greater sensitivity to blowing rate with reduced nose bluntness.

Note that minimal mass flowrates produce the pneumatic vortex control described here: a quick calculation based on data from this study shows that just 0.04 lbm/s is needed to achieve maximum C_Y for an F/A-18 class vehicle at sea level, M = 0.5.

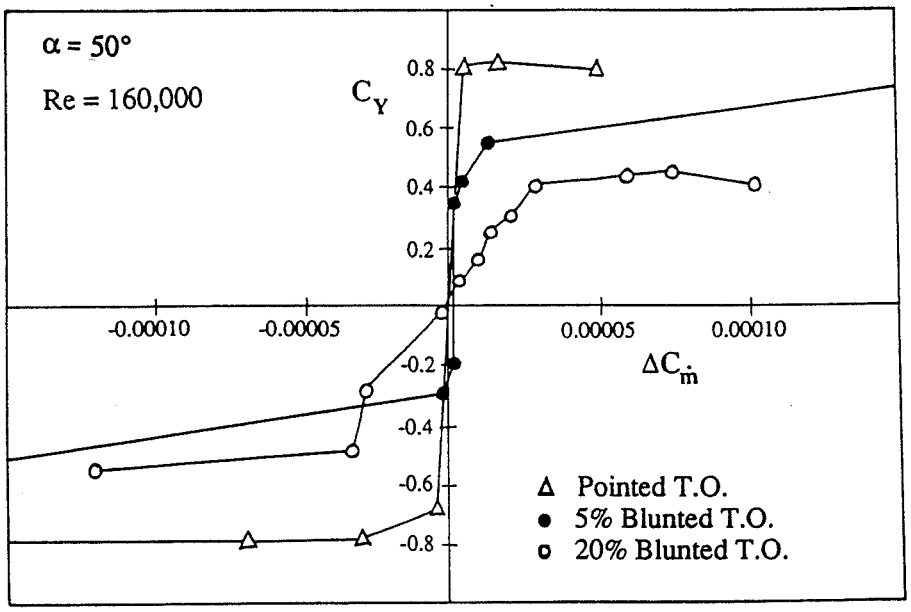

Yaw Influence on Pneumatic Side-Force-Control Effectiveness

(Laminar and Turbulent Separation)

Using the configuration with jets normal to the surface on the 20%-blunted tangent ogive forebody, sensitivity of pneumatic-side-force-control effectiveness to yaw was evaluated over the yaw-angle range $-15° \leq \psi \leq 15°$ with both laminar and turbulent separation. Results for $\alpha = 50°$ are shown in the figure, where it is evident that, regardless of the nature of the flow separation, the pneumatic control capability is retained throughout the indicated yaw range.

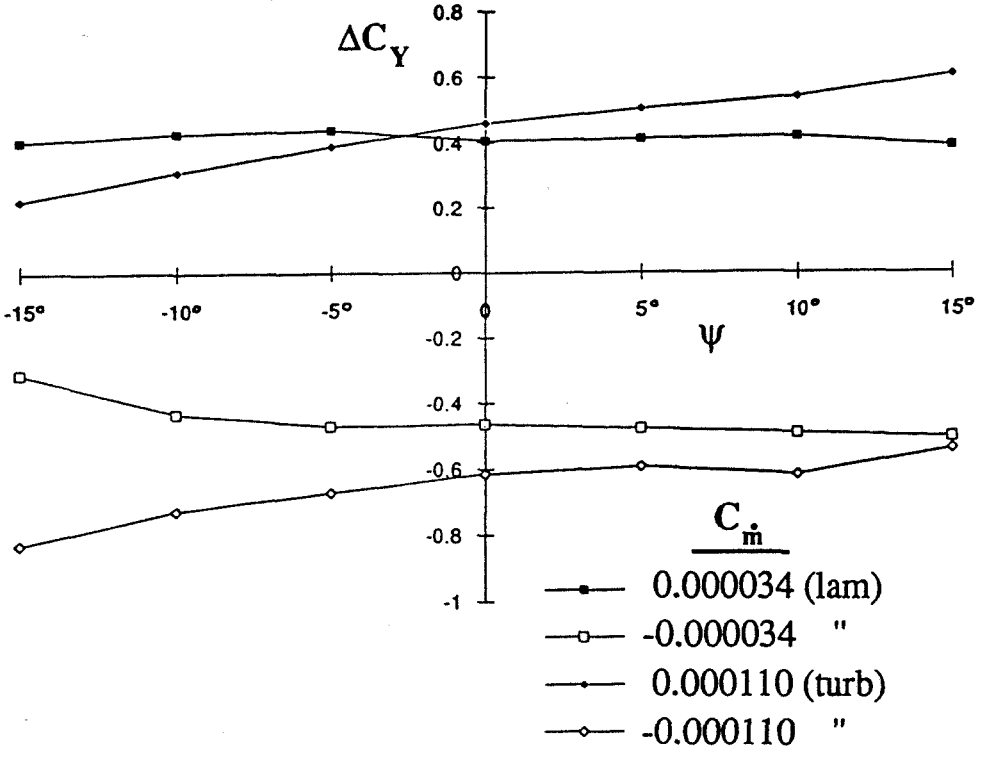

Lateral Pressure Difference Associated with Forebody Flow Asymmetry

Pressure data from experiments on high-α forebody flow fields (Roos, F.W. and Kegelman, J.T., "Aerodynamic Characteristics of Three Generic Forebodies at High Angles of Attack," AIAA Paper No. 91-0275, January 1991) suggests that a simple two-point C_p-difference measurement might suffice to serve as input for a side-force control system. The figure shows a nearly linear relationship between ΔC_p, the side-to-side C_p difference at a given axial station along the forebody, and C_Y, the side-force coefficient. This relationship suggests that the measured level of ΔC_p might be used to set $C_{\dot{m}}$, thereby controlling C_Y.

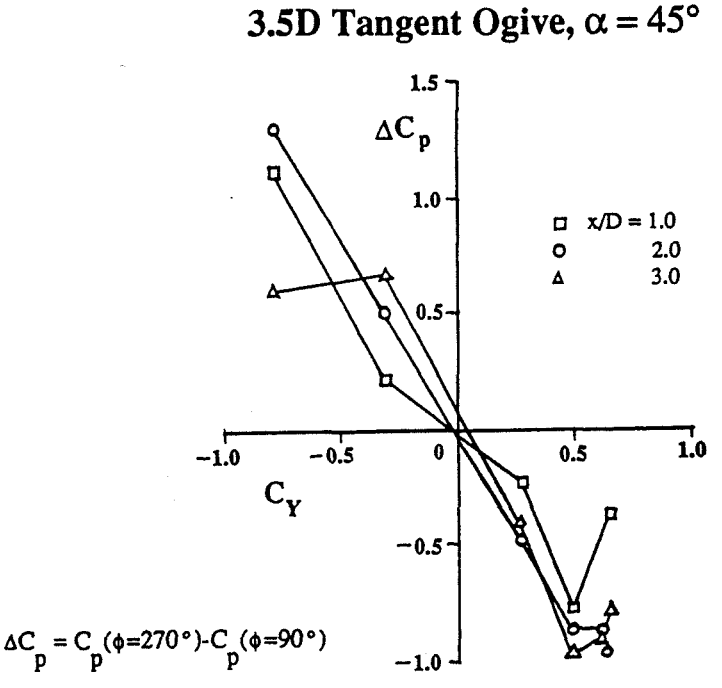

Conclusions

- A 20%-blunted, 3.5-caliber tangent ogive forebody develops no side force throughout the range $0 \leq \alpha \leq 60°$, for both laminar and turbulent separation.

- Slight blowing through either of two symmetrically positioned orifices at the blunt nose of the forebody produces flow asymmetry (and corresponding side force) that is proportional to jet mass flowrate within maximum and minimum limits that vary with α, the degree of nose bluntness, the specific jet configuration, and laminar vs. turbulent boundary-layer separation.

- Forward-blowing jets are generally more effective than jets normal to the forebody surface.

- Reducing the relative bluntness increases the magnitude of side force developable by blowing, and also increases sensitivity to blowing rate, at least for the laminar-separation cases studied.

- A simple, two-point pressure-difference measurement shows promise of serving as input for a pneumatic-side-force-control system.

In summary, a promising, very-low-energy concept for pneumatic forebody vortex-asymmetry control has been demonstrated, and a simple control input for the forebody blowing has been identified.

Examination of Vortex Control on a Chined Forebody During Manuevering Flight Conditions

John Ralston

Bihrle Applied Research, Inc.

4th NASA High Angle-of-Attack Projects and Technology Conference

Dryden Flight Research Center

July 12-14, 1994

Objectives

- Devise realistic application of chined forebody
- Establish test technique for rapid evaluation of vortex controller configuration parametrics
- Evaluate following controllers:
  - Mechanical
  - Conformal pneumatic slots
  - External pneumatic jets
- Initial evaluation of selected controller during velocity vector maneuver
- Evaluate feasibility of time dependant response measurement during dynamic conditions

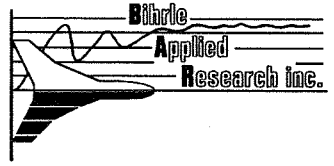

F-16 Chined Forebody

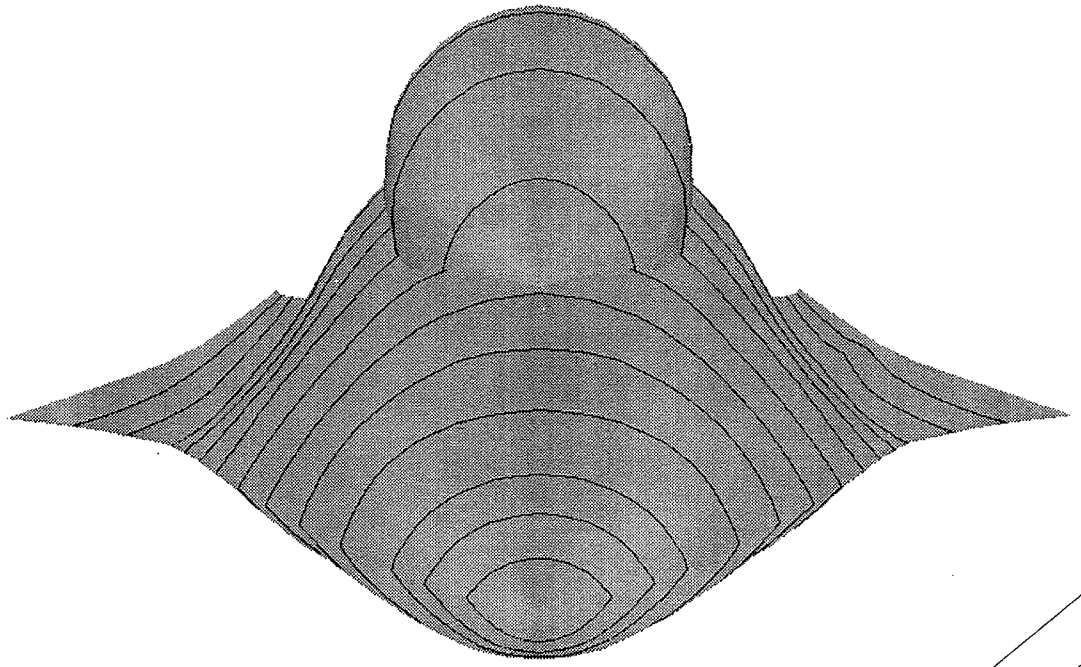

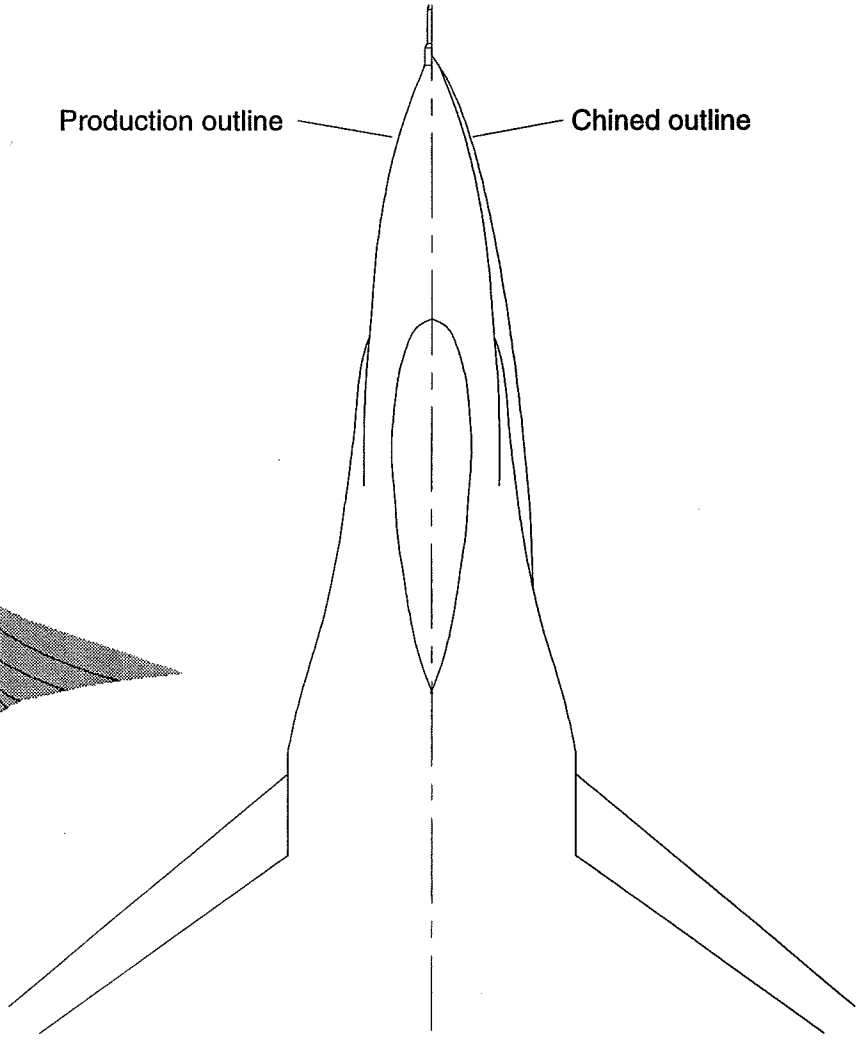

Bihrle Applied Research inc.

Basic Configuration Results

20 Static and dynamic runs made to identify the basic chined configuration characteristics

- Significant chine effect on baseline F-16
- Substantial increase in maximum lift
- Degradation of static pitch characteristics
- Pitching moment no longer nose-up with sideslip
- Improvement in static lateral stability, post stall directional stability
- Increase in post stall yaw damping
  - No spin mode

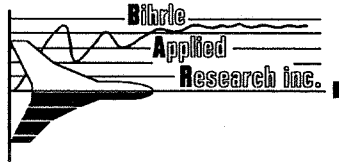

Blowing Test Apparatus Schematic

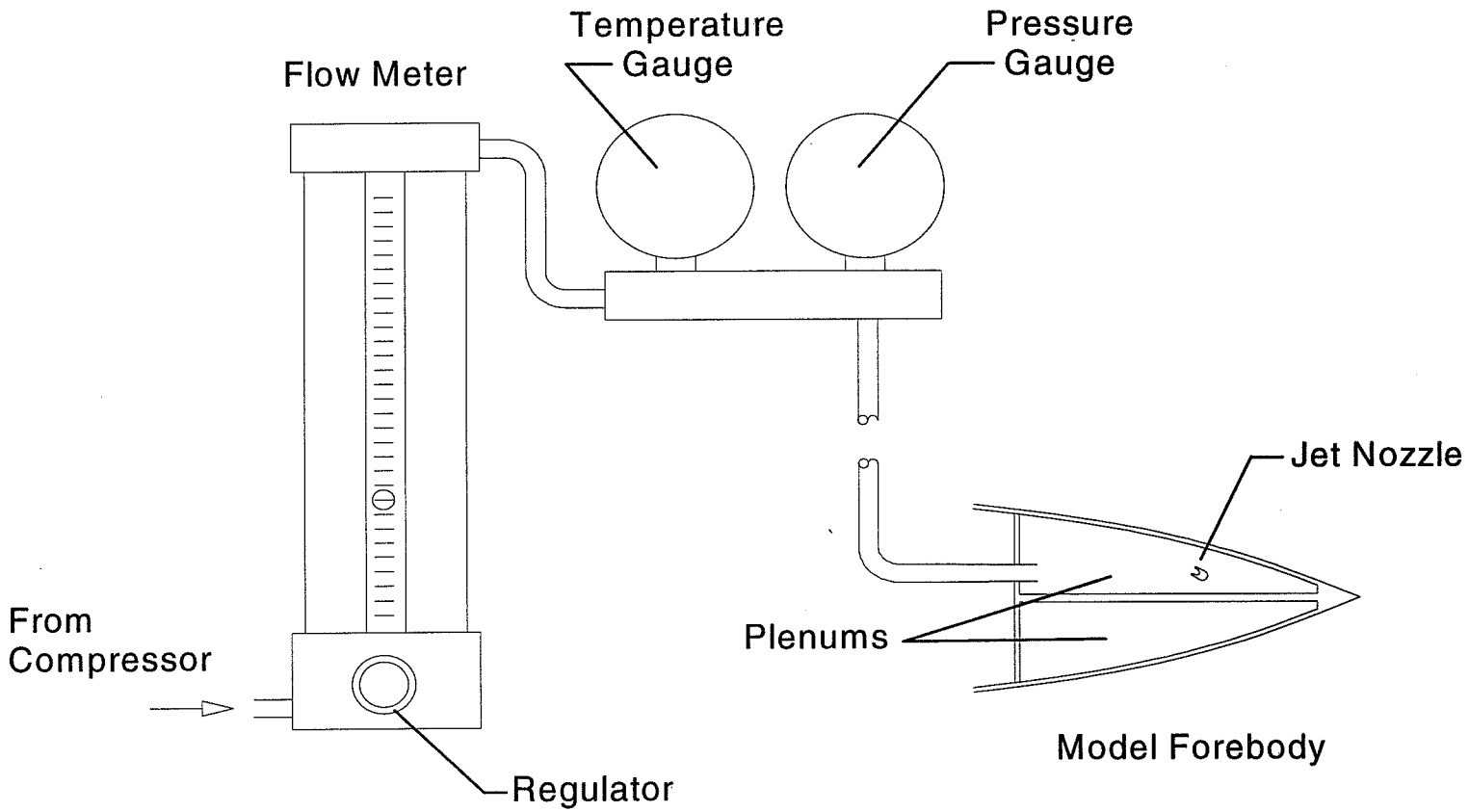

Bihrle Applied Research inc.

Longitudinal Slot Geometries

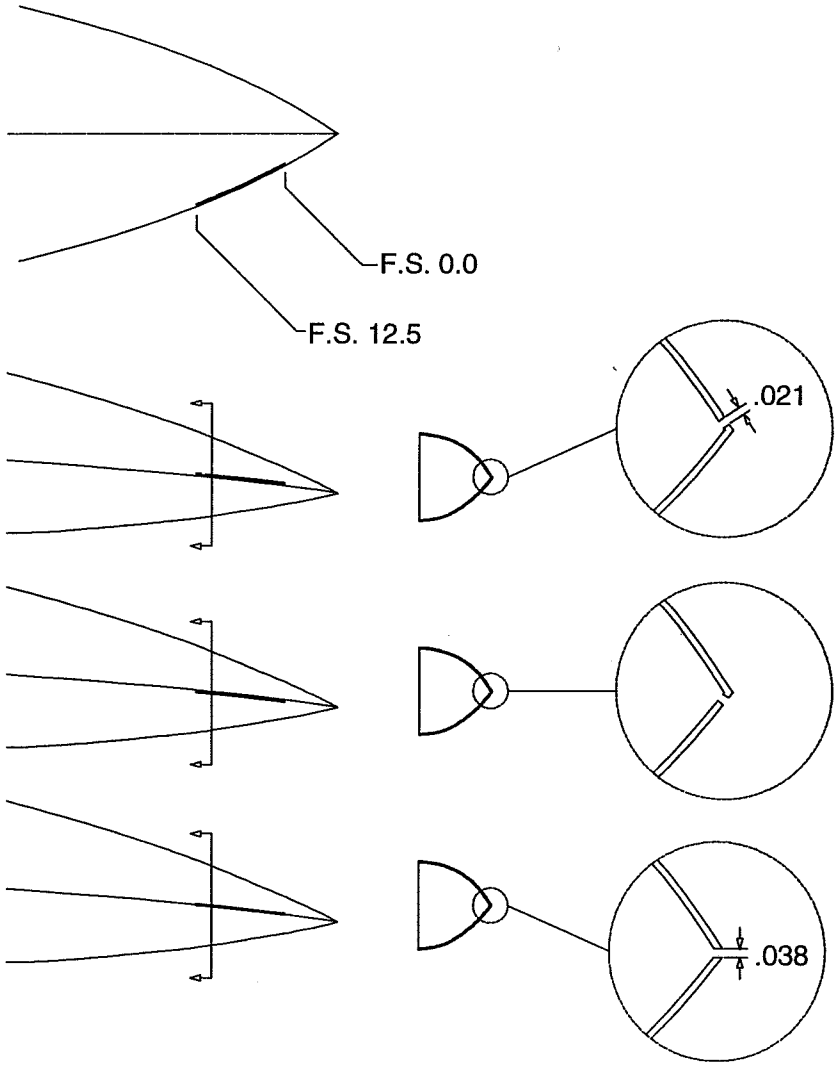

Bihrle Applied Research inc.

Jet Orientation and Dimensions

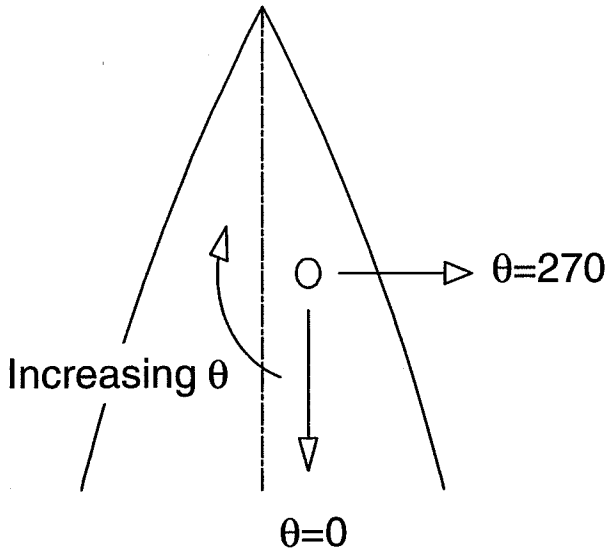

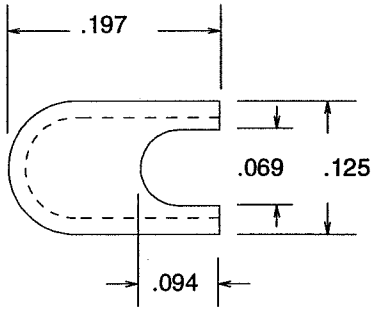

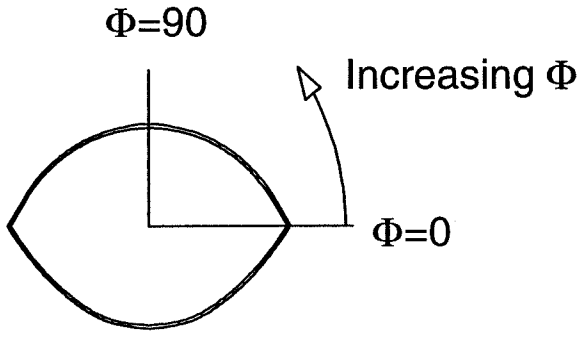

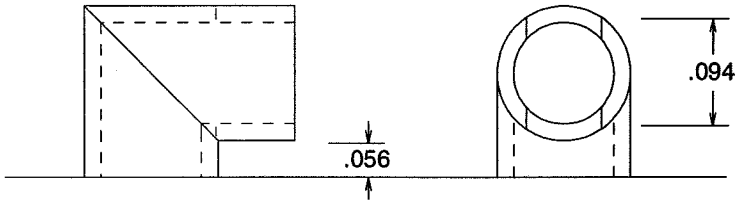

Bihrle Applied Research Inc.

Vertical Slot Geometries

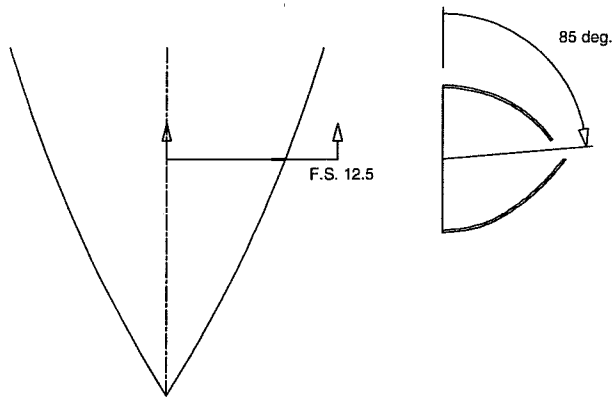

Slot 7

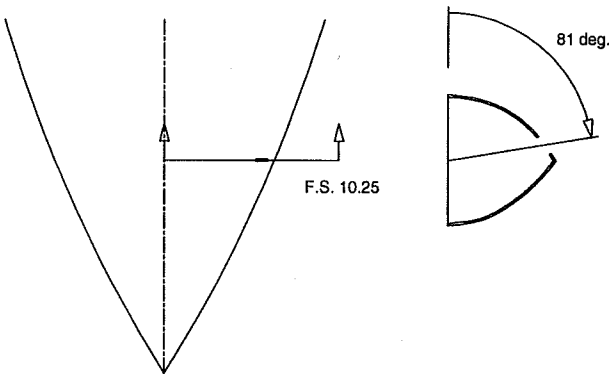

Slot 8

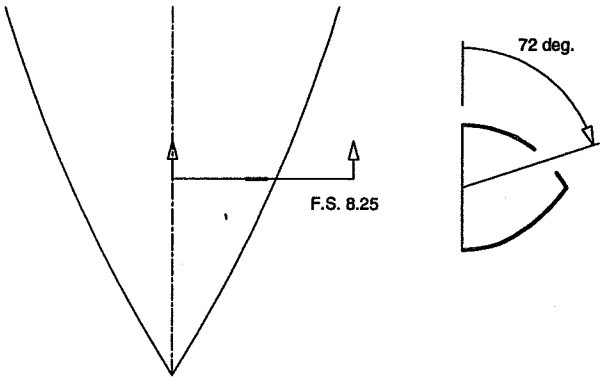

Slot 9

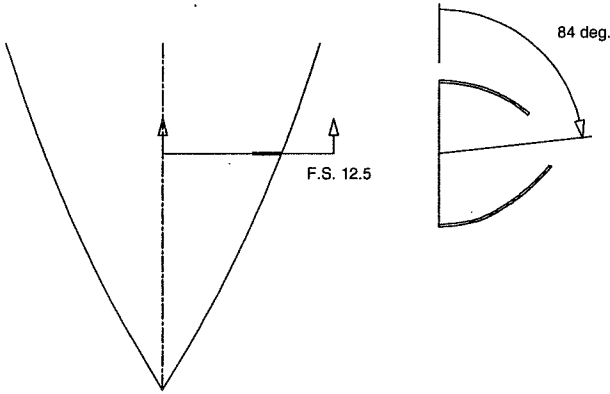

Slot 7a

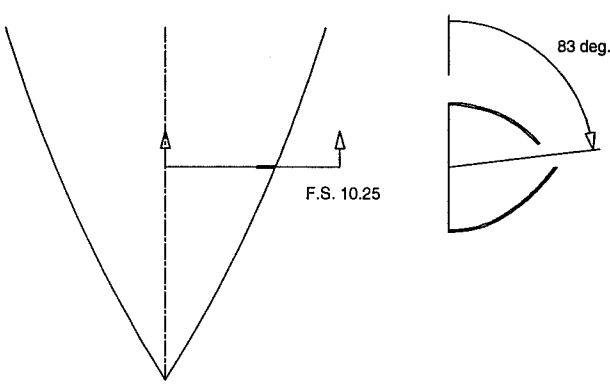

Slot 8a

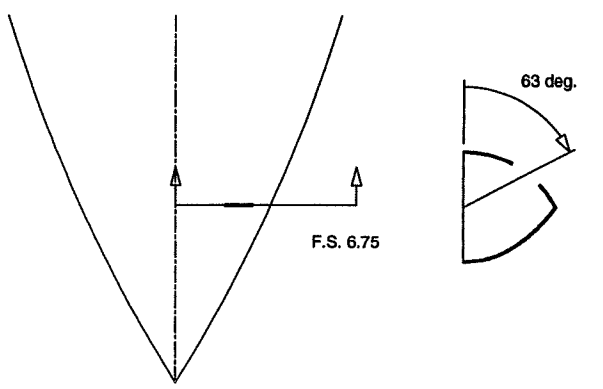

Slot 10

Bihrle Applied Research inc.

Vortex Control Results

3 Strake, 14 slot, and 12 jet configurations tested for 56 static and dynamic runs

- Forebody chines develop energetic vortex pair that is difficult to influence
  - Mechanical strakes tested ineffective
- Longitudinal slots effectiveness limited because of orientation of pneumatic sheet
- Oriented properly, slotted jet very effective controller
- Selected jet configuration effectiveness independent of sideslip, velocity vector roll rate
- Limited vertical slot testing reveals potential for conformal pneumatic controller

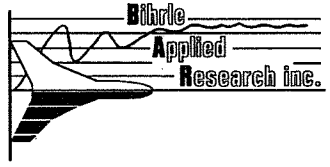

Effect of Longitudinal Slot Orientation

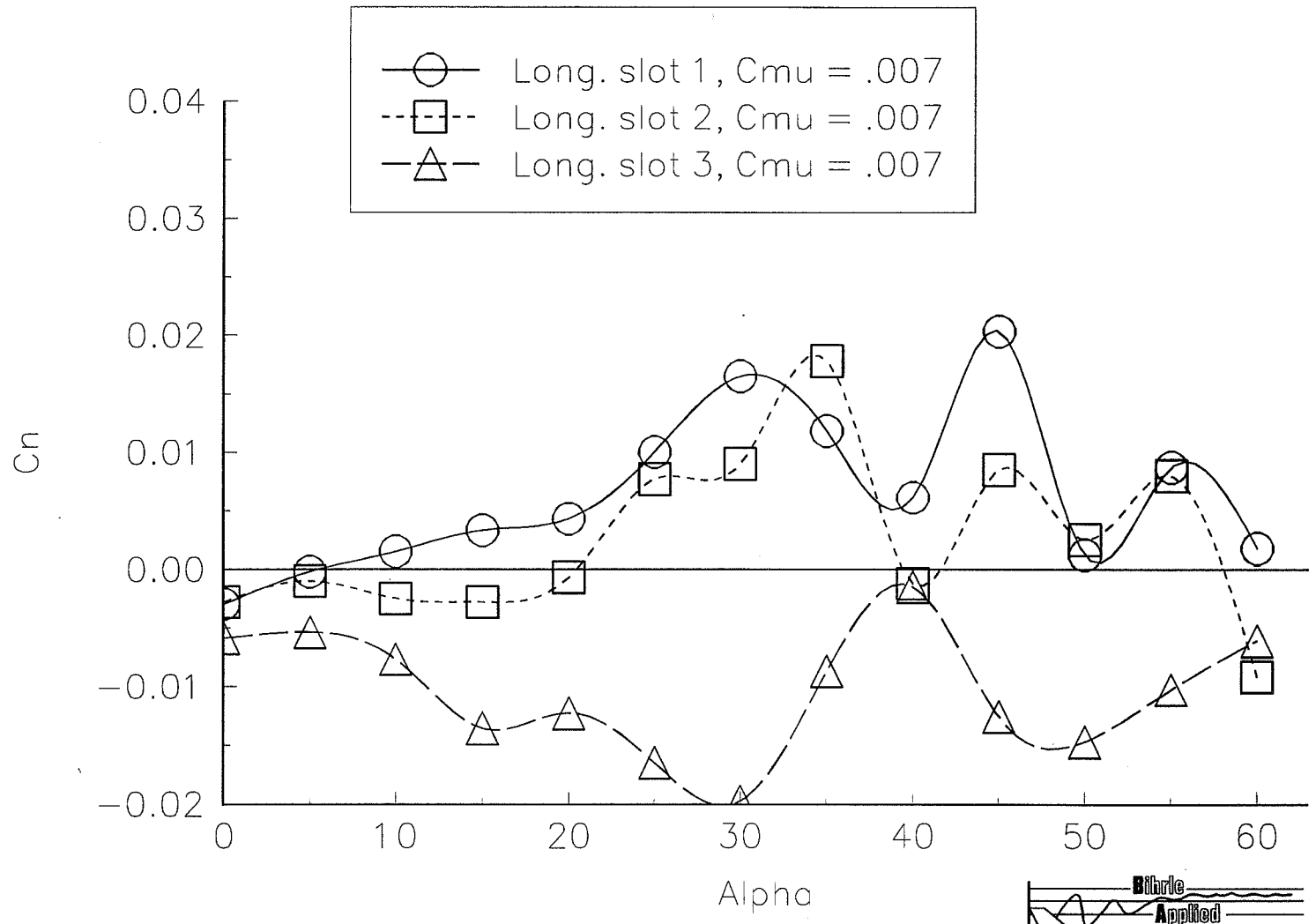

Bihrle Applied Research inc.

Effect of Orientation on Slotted Jet Effectiveness
(θ=270, F.S.=12.5, Cμ=.007)

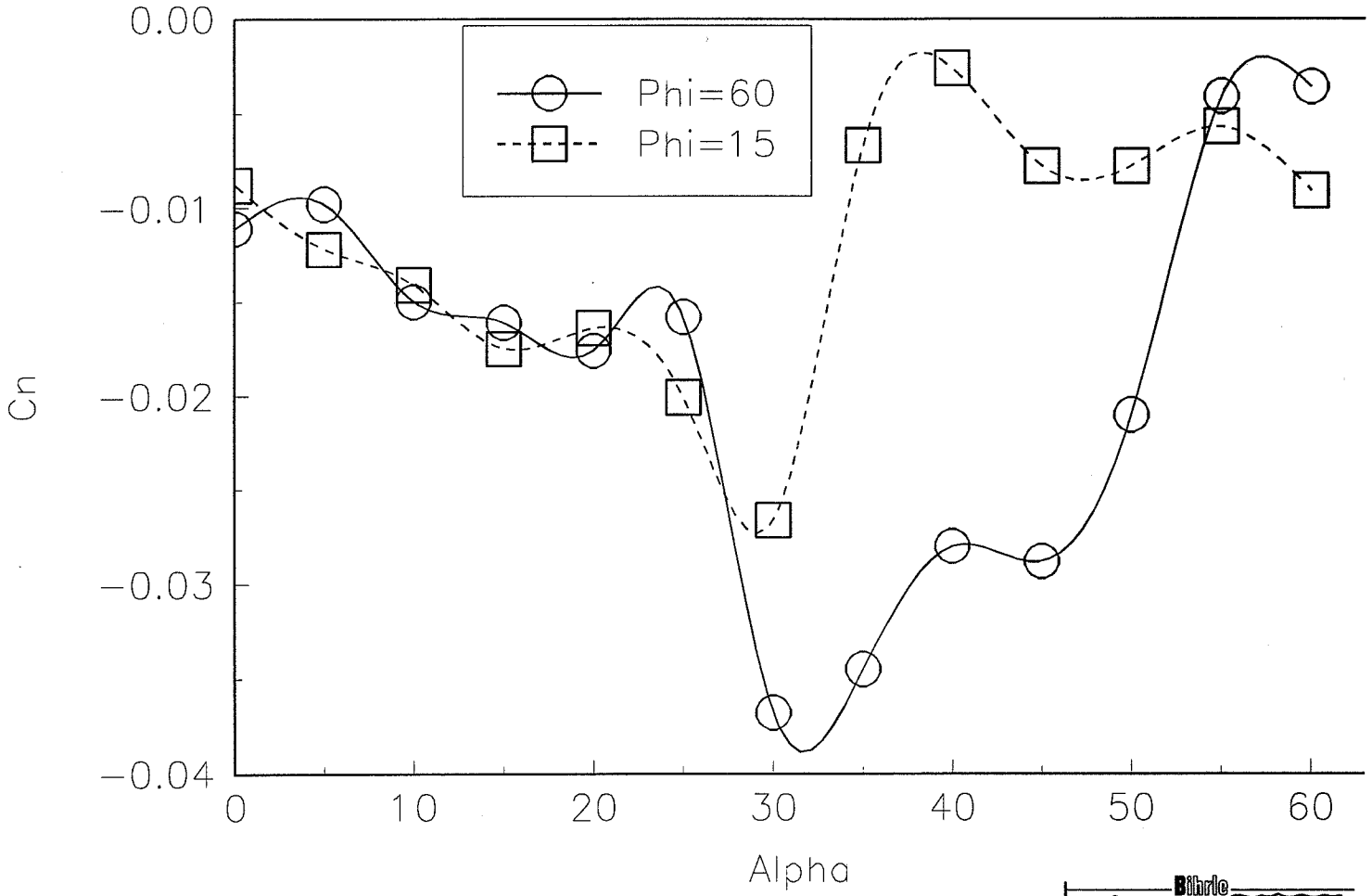

Bihrle Applied Research inc.

Effect of Fuselage Station on Slotted Jet Effectiveness (θ=270, ϕ=60, Cμ=.006)

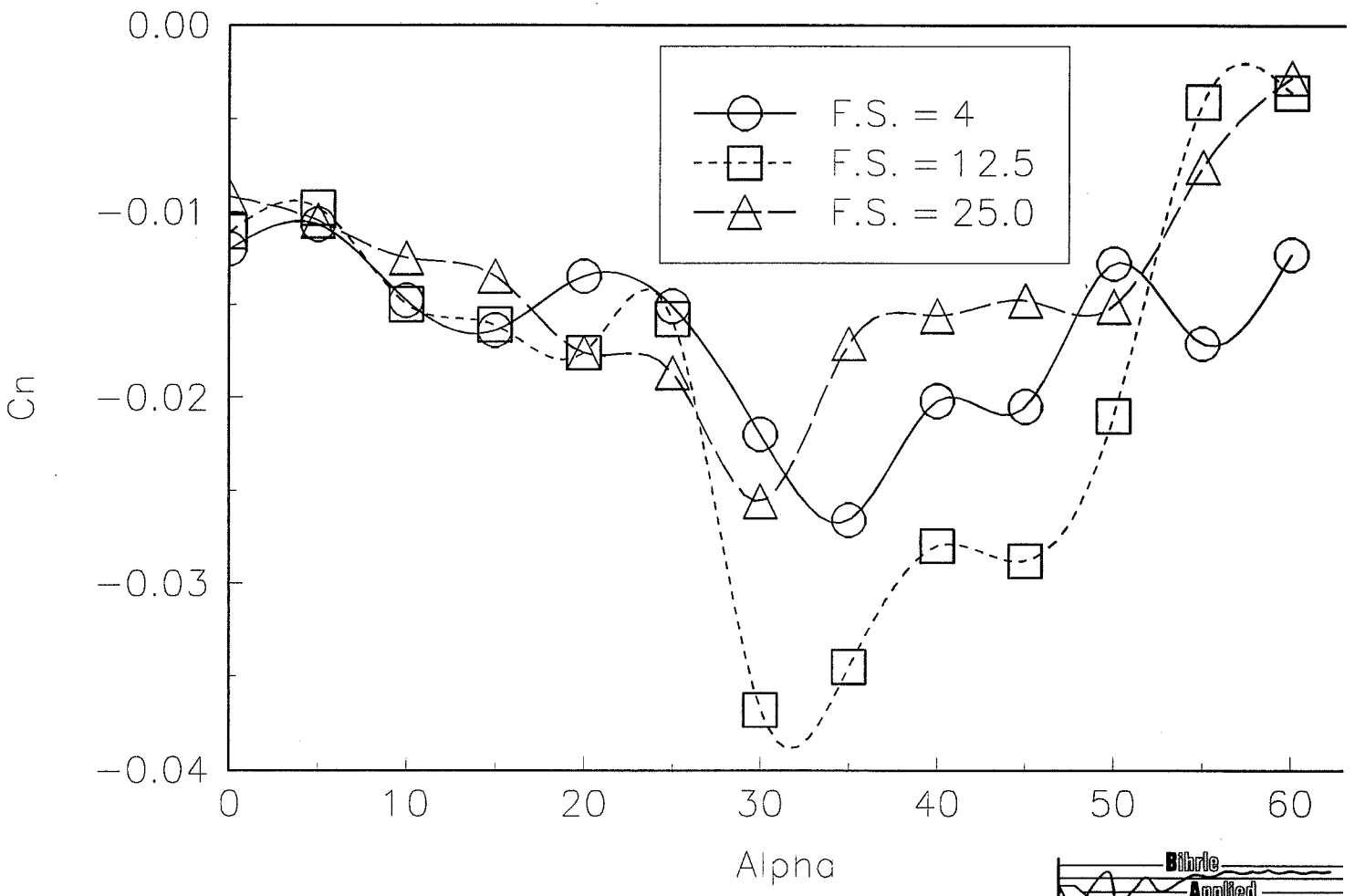

Bihrle Applied Research inc.

Effect of Blowing Rate on Slotted Jet Effectiveness (θ=270, ϕ=60)

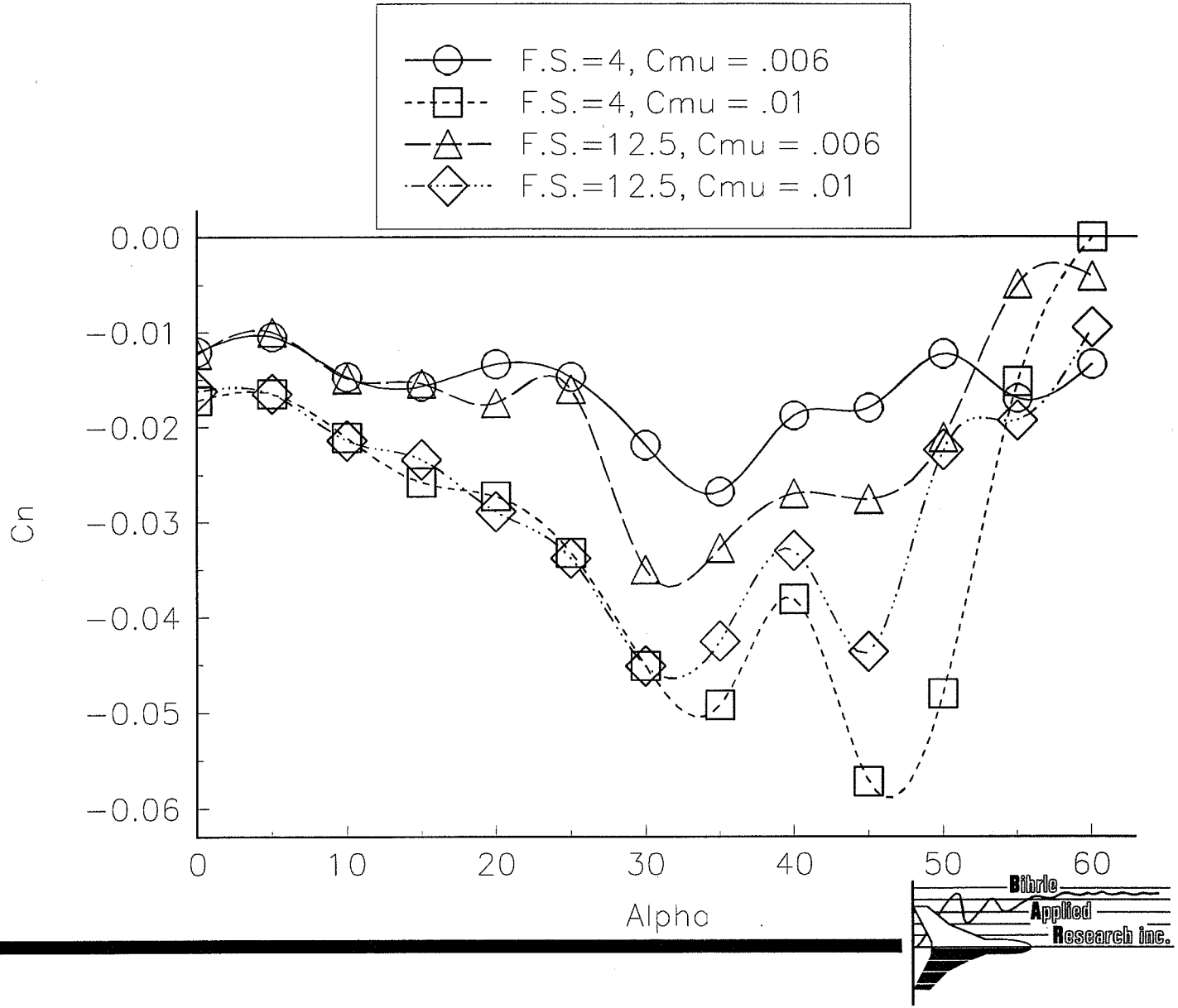

Effect of Blowing Configuration

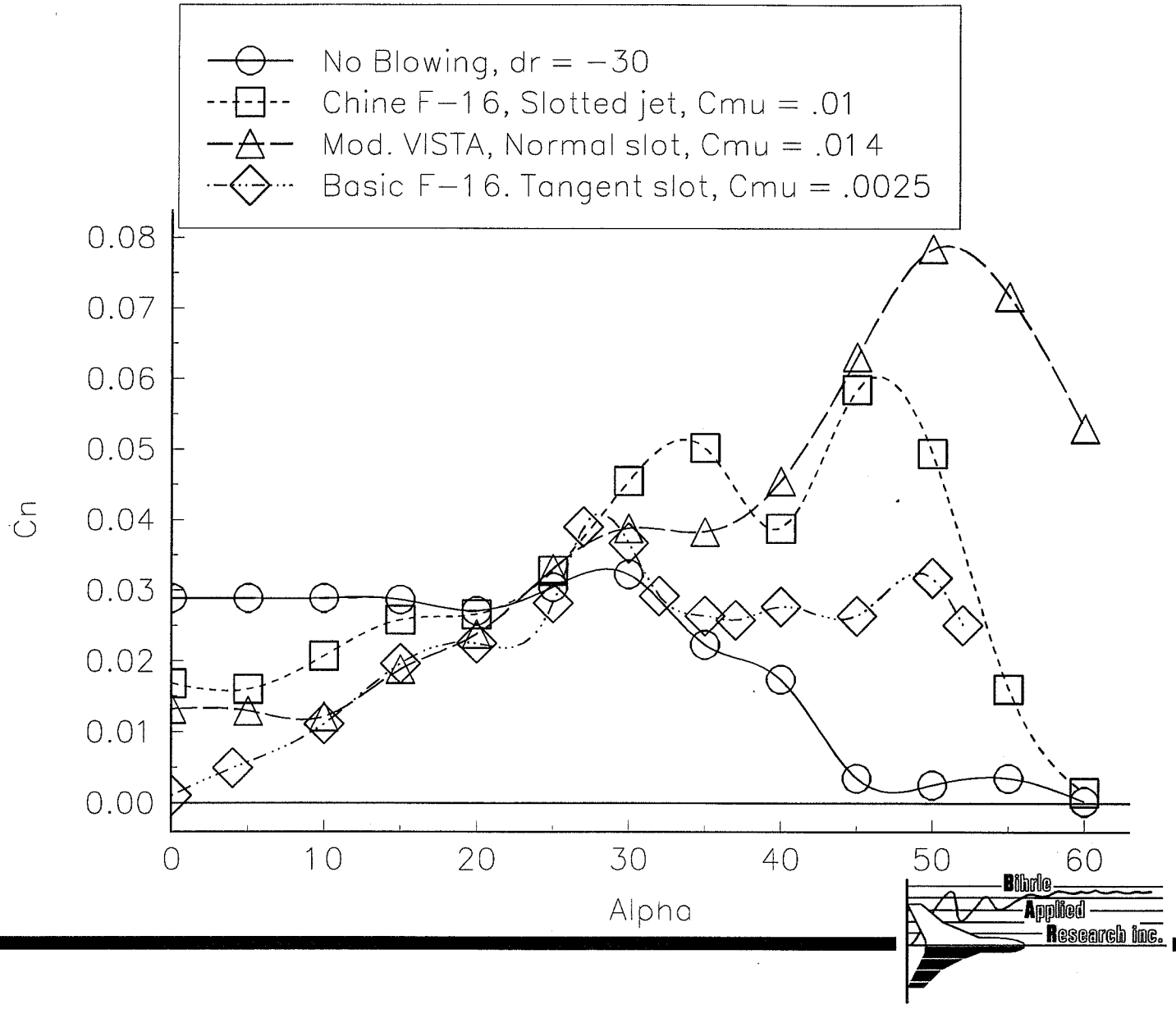

Bihrle Applied Research inc.

Effect of Rotation Rate & Blowing on Yawing Moment for Chined F-16

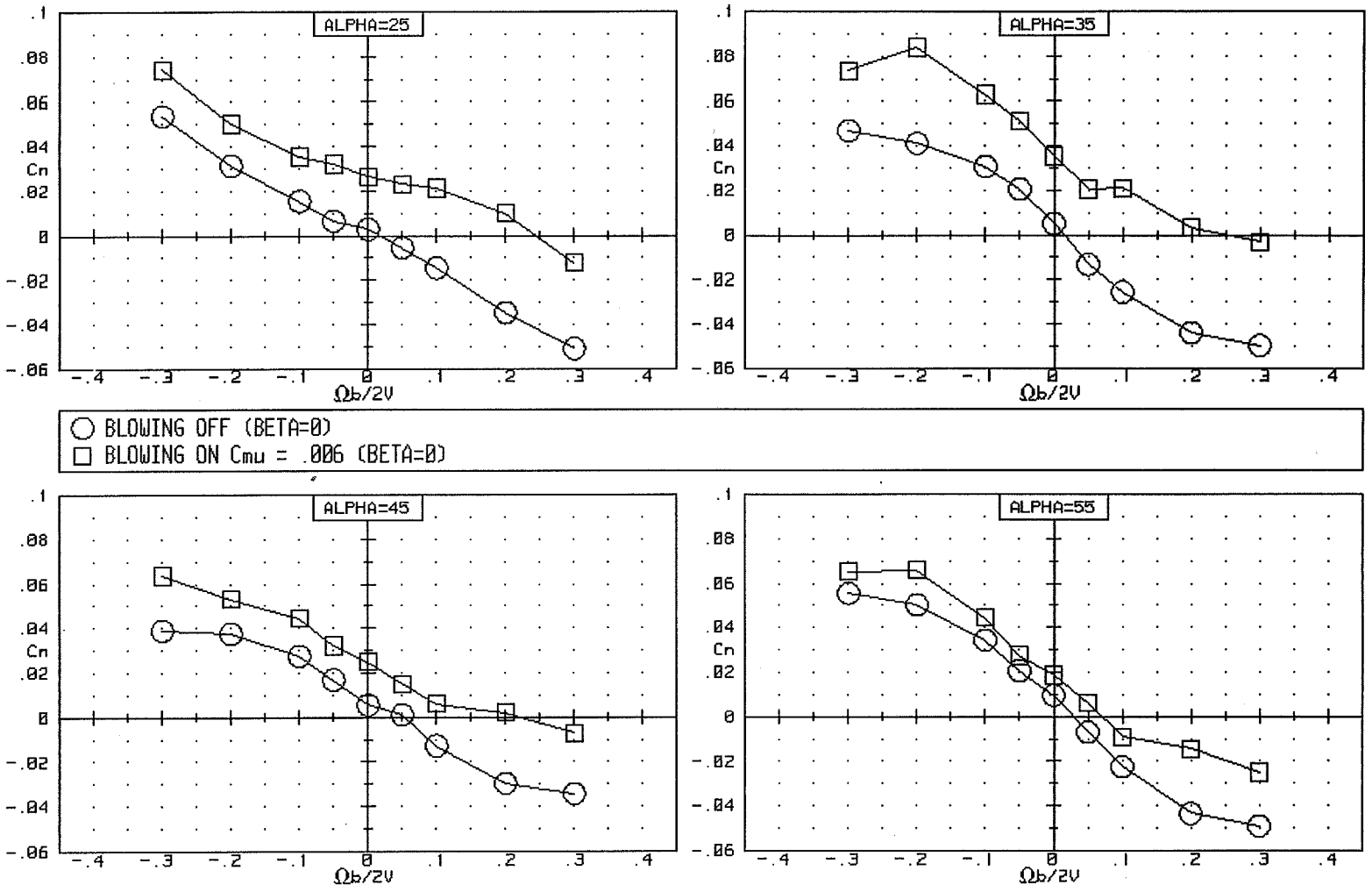

Bihrle Applied Research inc.

Effect of Conditions on Yaw Effectiveness
(Ωb/2V=0, β=0)

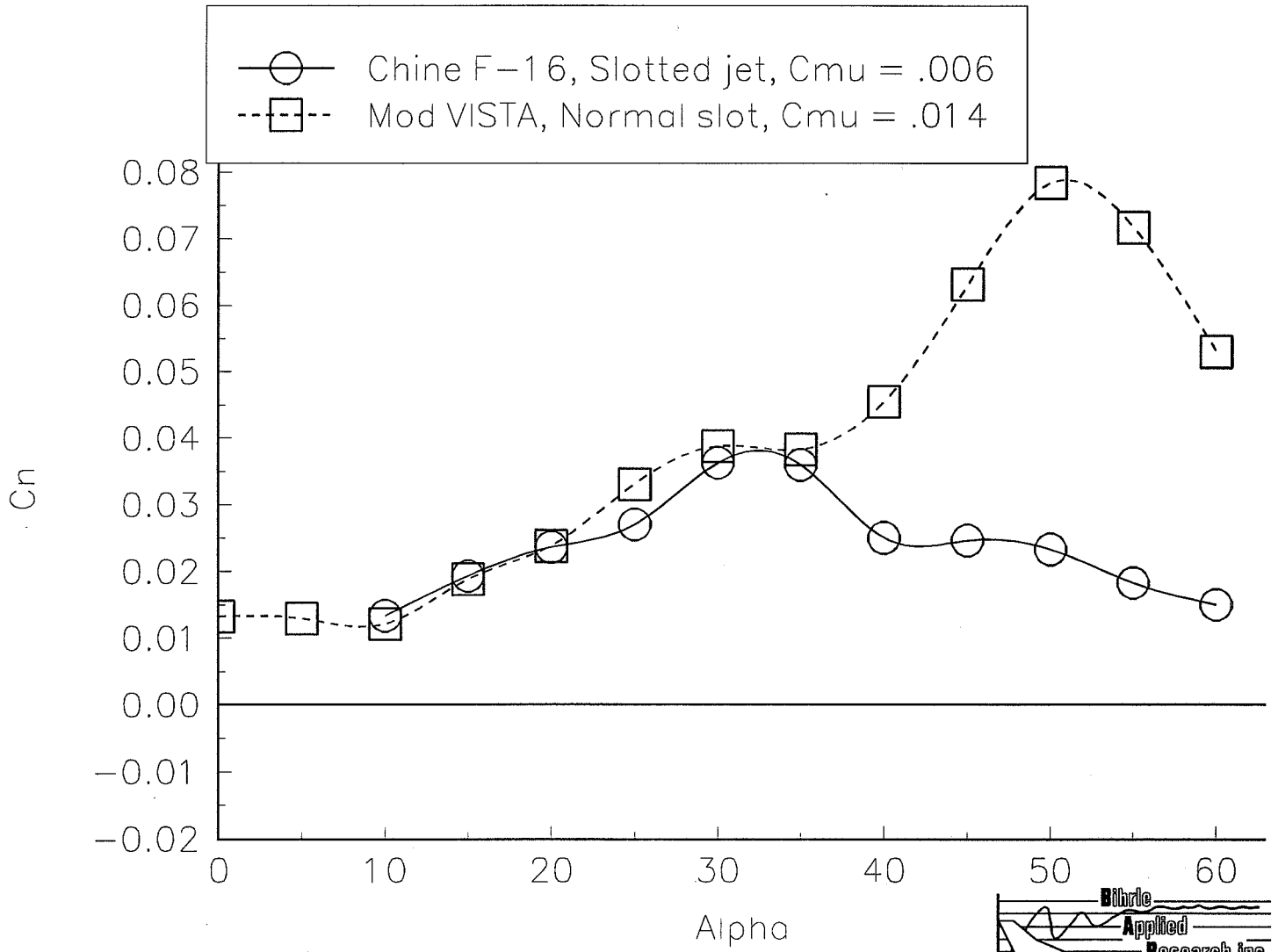

Bihrle Applied Research inc.

Effect of Conditions on Yaw Effectiveness
(Ωb/2V=.1, β=0)

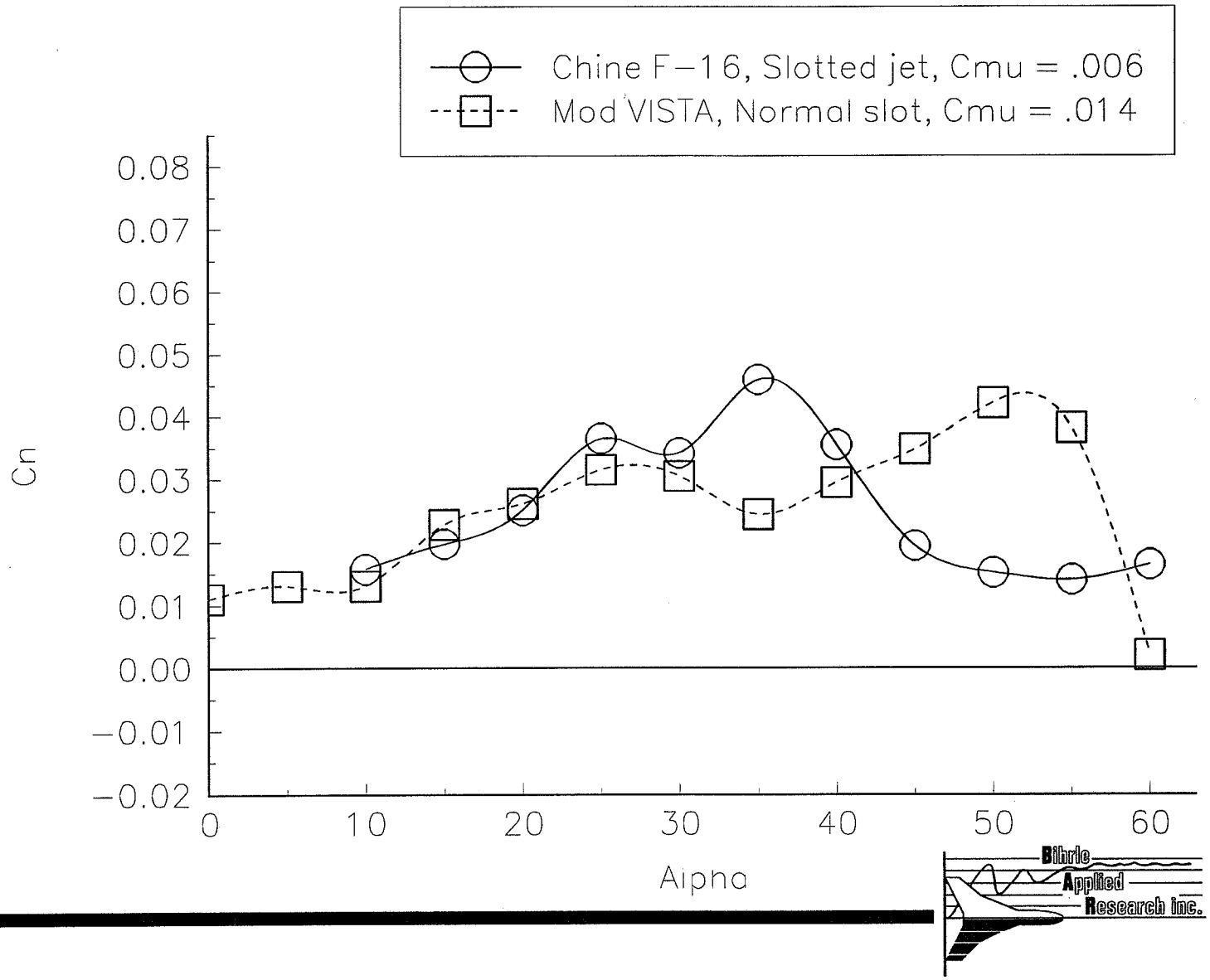

Bihrle Applied Research inc.

Effect of Conditions on Yaw Effectiveness
(Ωb/2V=.1, β=10)

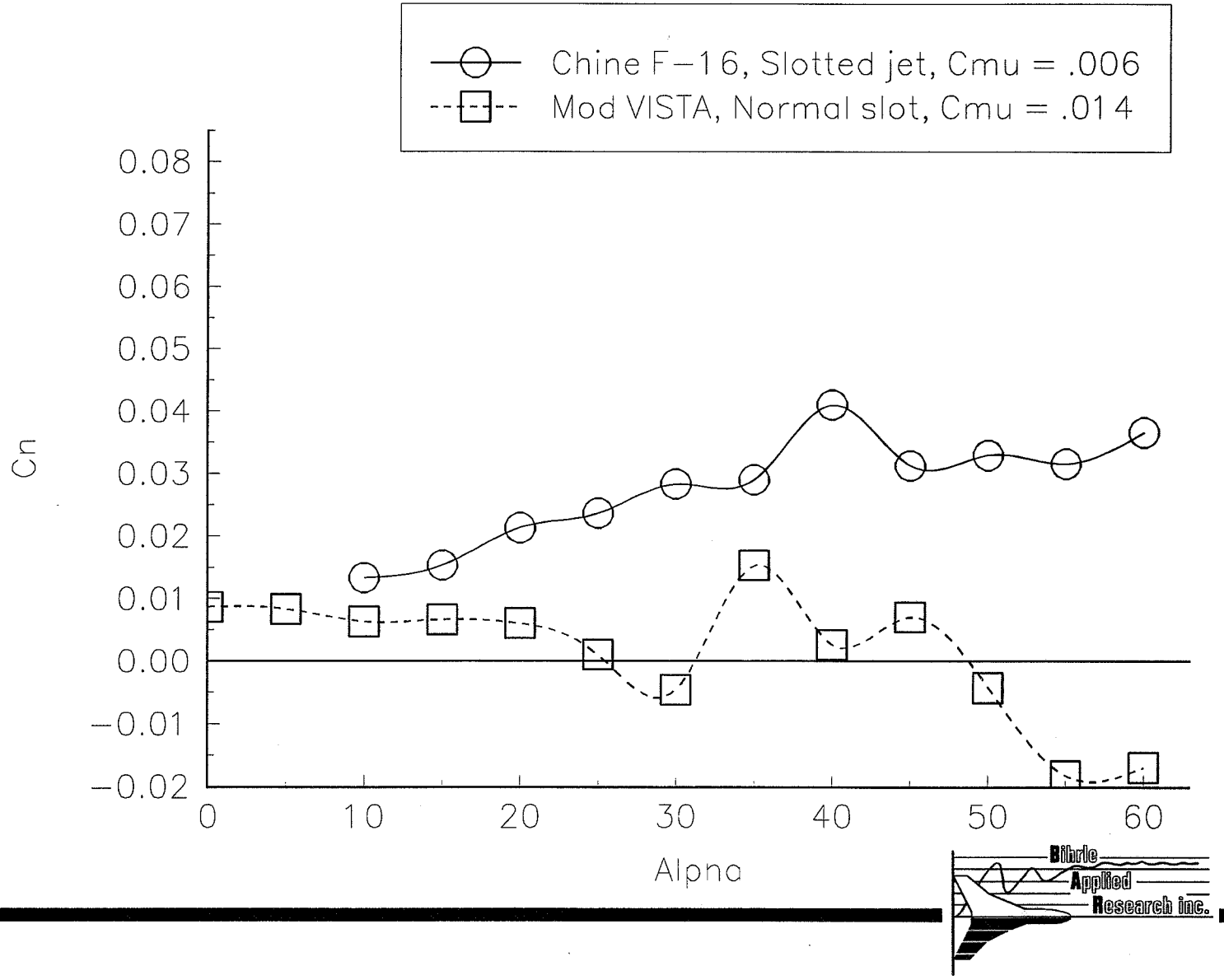

Bihrle Applied Research inc.

Effect of Vertical Slot Orientation
(Cμ=.012)

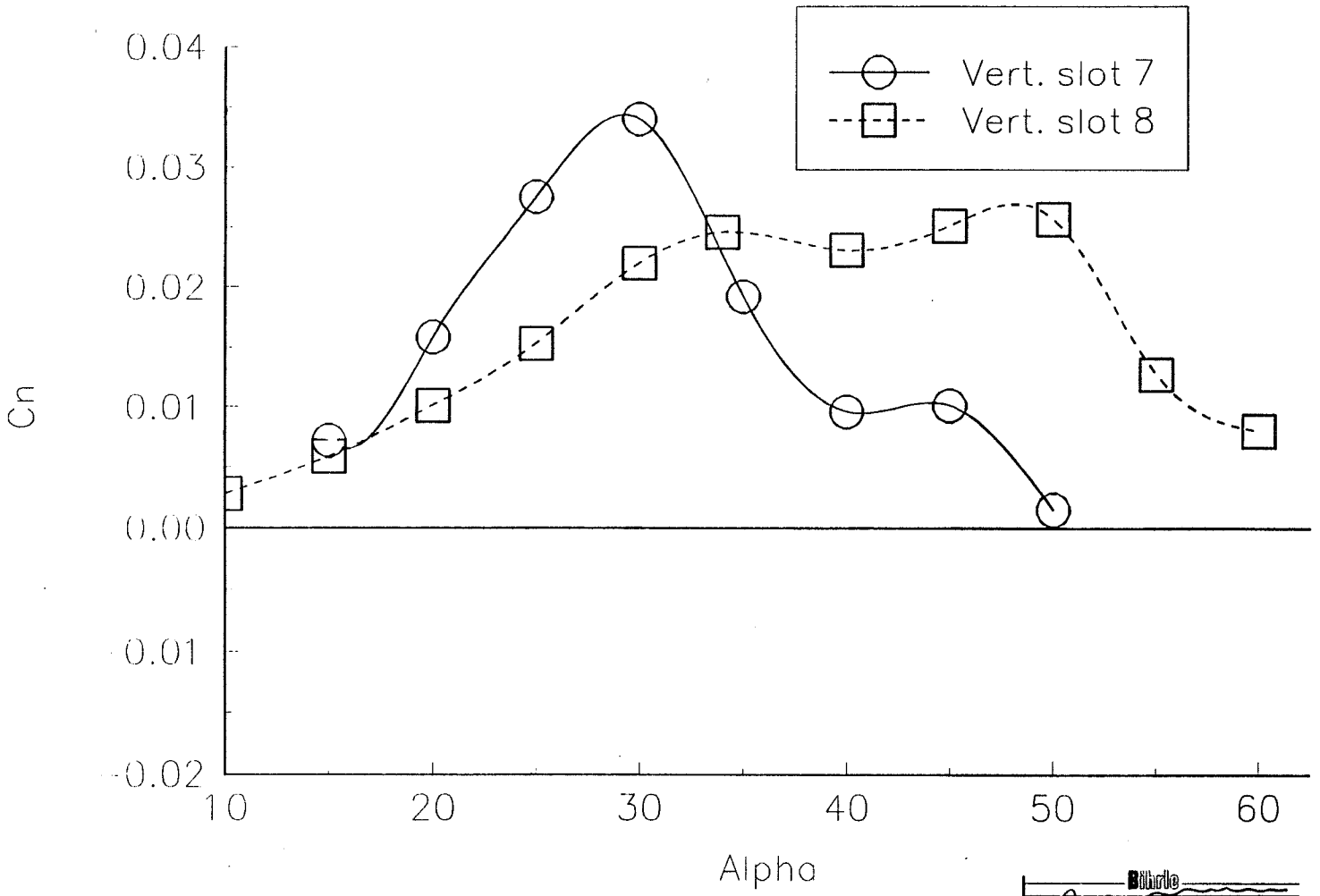

Bihrle Applied Research Inc.

Summary

- Influence of chine forebody on F-16 illustrates potential of future applications
- Chine forebodies vortex pair more difficult to manipulate than conventional bodies
- Yaw development very sensitive to jet plume orientation and location
- Properly located, pneumatic devices on chine bodies can be as effective as those seen on conventional bodies
- Selected configuration effectiveness not influenced by sideslip, velocity vector roll rate
  - Pneumatic vortex control on conventional bodies can exhibit attitude sensitivity
- Time dependant effects, particularly in dynamic conditions, require further evaluation

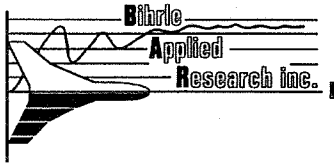

Acknowledgments

The work presented herein is reported in "A Feasibility Study of Forebody Vortex Control on a Chined Forebody", WL-TR-93-3027, January 1993.

The Author would like to acknowledge the the support and interest shown by Wright Labratory/FIMA personnel, as well as the generosity of the Lockheed Fort Worth Aerodynamics Stability and Control Group for the use of the model used to conduct these tests.

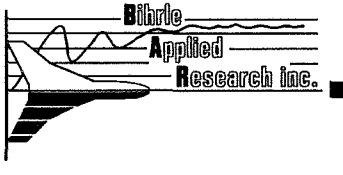

19951078 43
3500 70

N95-14257

PREPARATIONS FOR FLIGHT RESEARCH TO EVALUATE ACTUATED FOREBODY STRAKES ON THE F-18 HIGH-ALPHA RESEARCH VEHICLE

56-02
16106
P. 20

Daniel G. Murri

Gautam H. Shah

Daniel J. DiCarlo

NASA Langley Research Center
Hampton, VA

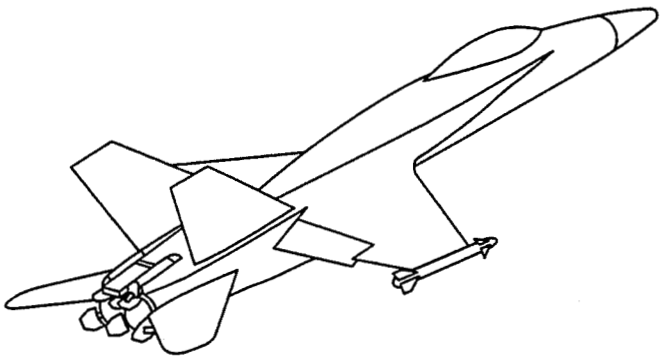

High-Angle-of-Attack Projects and Technology Conference
NASA Dryden Flight Research Center
Edwards, CA
July 12-14, 1994

INTRODUCTION

A major goal of the NASA High-Angle-of-Attack Technology Program (HATP) has been to help develop technologies that can significantly improve the high-angle-of-attack controllability and maneuvering effectiveness of fighter aircraft. A wide range of advanced control concepts have been investigated under this program including propulsive control concepts as well as advanced aerodynamic control concepts. As part of the NASA HATP, flight tests are currently being conducted with a multi-axis thrust vectoring system applied to the NASA F-18 High-Alpha Research Vehicle (HARV). A follow-on series of flight tests with the NASA F-18 HARV will be focusing on the application of actuated forebody strake controls. These controls are designed to provide increased levels of yaw control at high angles of attack where conventional aerodynamic controls become ineffective. The series of flight tests are collectively referred to as the Actuated Nose Strakes for Enhanced Rolling (ANSER) Flight Experiment. (The ANSER acronym refers to "rolling" since the strakes provide the critical yaw control required to coordinate rolling maneuvers about the velocity vector at high-angle-of-attack conditions.)

The development of the actuated forebody strake controls for the F-18 HARV is discussed in reference 1, and a summary of the ground tests conducted in support of the flight experiment is provided in reference 2. This paper presents a summary of the preparations for the flight tests. Topics include the objectives of the ANSER Flight Experiment, a brief review of the strake development and the ground-test results, a description of the flight hardware, a discussion of aircraft integration considerations, and the flight test plans and schedule.

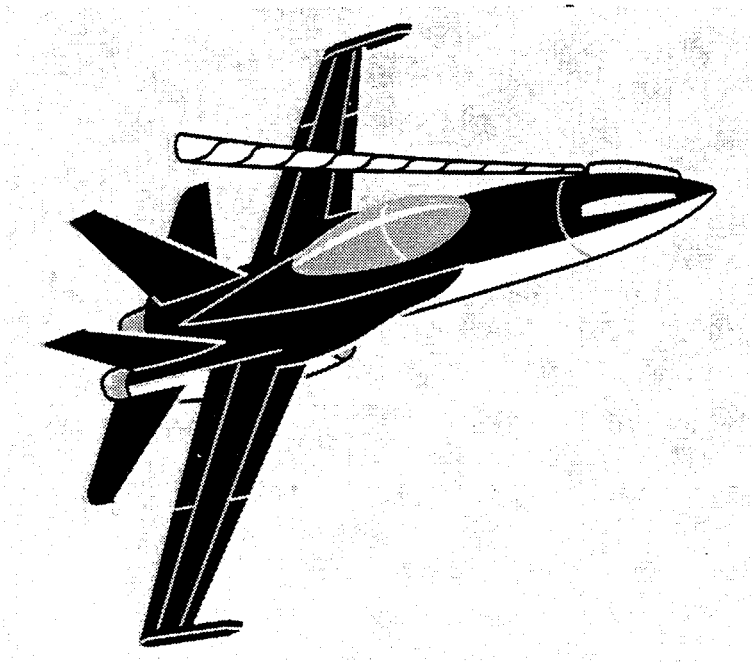

NOMENCLATURE

The moment reference for all of the wind-tunnel data presented is fuselage station 458.56 (25-percent mean aerodynamic chord) and water line 100.0.

b	reference wing span, 37.42 ft (full scale)
c_s	reference strake chord, .6775 ft (full scale)
C_h	strake hinge-moment coefficient (positive to close strake), hinge moment/$q_\infty S_s c_s$
C_n	body-axis yawing-moment coefficient, yawing moment/$q_\infty Sb$
C_p	static pressure coefficient, (local static pressure - free stream static pressure)/q_∞
FS	fuselage station, full scale, in
HARV	High-Alpha Research Vehicle
HATP	High-Angle-of-Attack Technology Program
M	Mach number
n_z	normal acceleration, g's
q_∞	free-stream dynamic pressure, lb/ft^2
S	reference wing area, 400 ft^2 (full scale)
S_s	reference strake area, 2.71 ft^2 (full scale)
TV	thrust vectoring
α	angle of attack, deg
β	angle of sideslip, deg
δ_s	strake deflection measured from the retracted position, deg

ANSER FLIGHT EXPERIMENT

The primary objectives of the ANSER Flight Experiment are to provide flight validation of a ground-test data base for a forebody control device and to evaluate the use of this type of control in enhancing fighter aircraft maneuverability.

In addition to the primary flight test objectives, many other important integration issues are being addressed that could aid in future application of forebody control concepts. Some of the issues that are being addressed include control law design implications, hydraulic/actuator requirements, structural loads, aircraft systems integration considerations, and pilot acceptance of the unique response characteristics of forebody controls.

ANSER FLIGHT EXPERIMENT
Objectives

- Obtain flight validation of ground-test data base for a forebody control device

- Evaluate the use of forebody controls in enhancing fighter aircraft maneuverability

DEVELOPMENT OF ACTUATED FOREBODY STRAKE CONCEPT

The overall development process of the actuated forebody strake concept has followed a successive series of studies from initial concept exploration to full-scale flight validation. The initial development tests of the actuated forebody strake concept were conducted using a generic fighter model and are described in references 3 and 4. These tests showed that the actuated forebody strake concept could provide high levels of yaw control over wide ranges of angle of attack and sideslip and that the yawing moment could be controlled by varying the strake deflections. The concept has been refined through a wide range of ground-based studies to develop the concept for application to the F-18 HARV and to support the planned flight tests[1, 2]. As mentioned previously, this paper presents a summary of the preparations for the upcoming flight research.

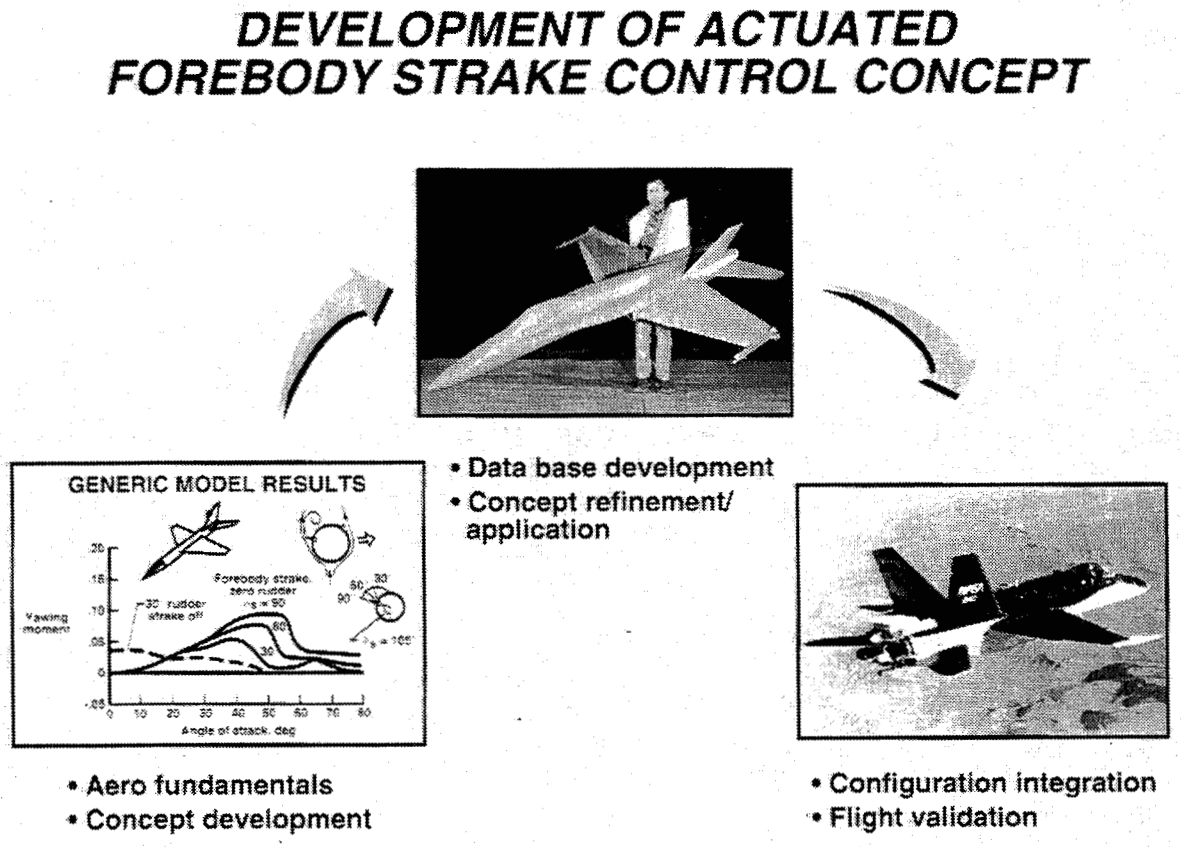

ANSER STRAKE DESIGN

A sketch of the conformal actuated forebody strakes designed for flight testing on the F-18 HARV is presented in the figure. This strake design includes a pair of conformal actuated strakes, each capable of a 90° deflection and positioned at a radial location of 120° from the bottom of the forebody. The term "conformal" indicates that when both strakes are retracted, the forebody retains the nominal F-18 HARV forebody contour.

It is recognized that implementation of actuated forebody strakes on the radome is probably not practical for current generation radar-equipped aircraft. However, actuated forebody strakes have been found to be very effective when located behind the radome, and many other forebody flow control devices (both mechanical and pneumatic) have been developed that minimize radar impact. In addition, the application of advanced (phased array) radars to future aircraft may relax the stringent radar-related requirements on the forebody.

The ANSER configuration has been designed to allow the evaluation of a wide range of issues applicable to forebody controls, while minimizing the cost and complexity of the aircraft modifications. Therefore, the strakes are positioned to remain within the length of the radome of the full-scale F-18 HARV. The aircraft will be modified by attaching a newly fabricated radome incorporating the strakes and actuators and making the appropriate connections to the aircraft systems.

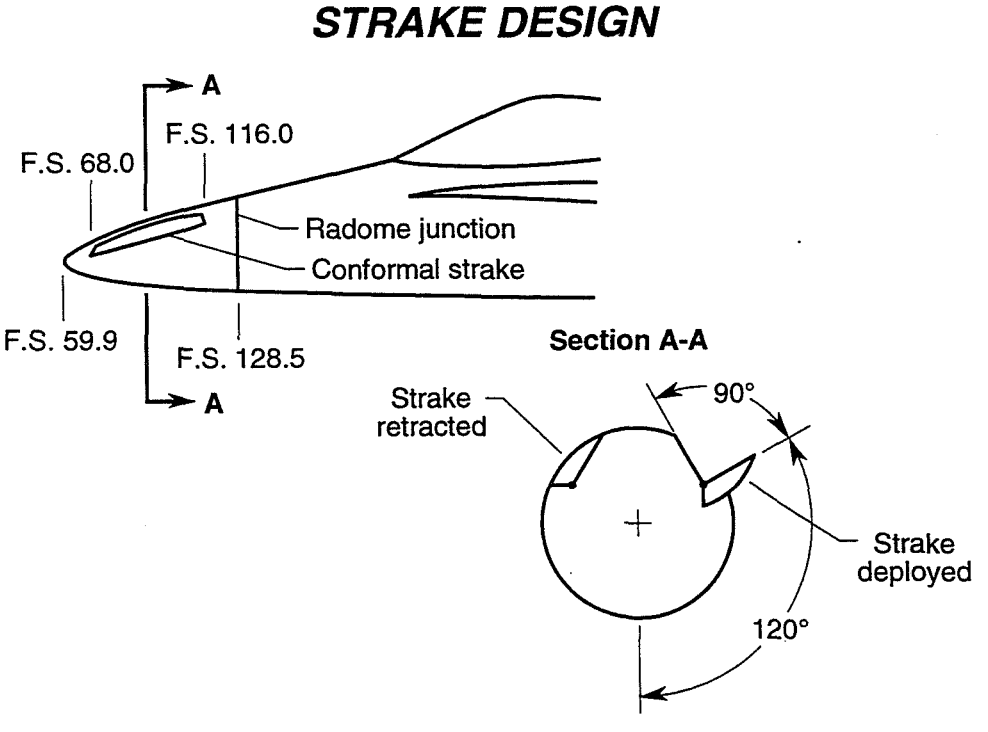

ANSER STRAKE DESIGN

Some of the features the ANSER strake design are evident in the two photographs which show the strakes applied to a full-scale F-18 forebody wind-tunnel model.

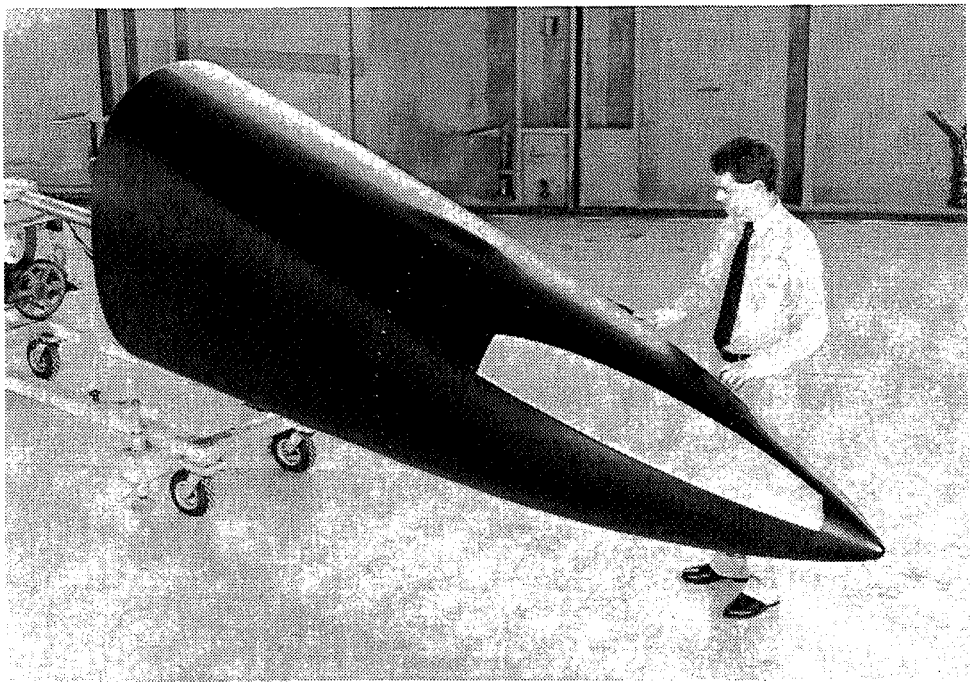

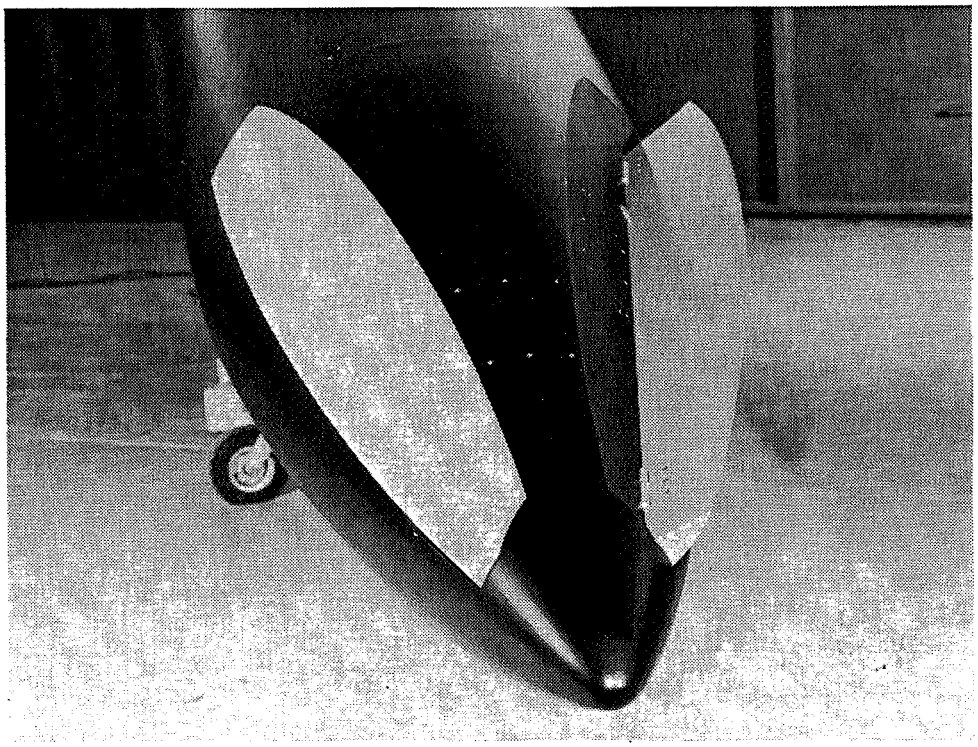

ANSER FLIGHT EXPERIMENT GROUND TESTS

The primary ground tests used in the analysis of the ANSER strake design are shown in the figure. The tests include low-speed static and dynamic force tests using a 16%-scale model in the Langley 30- by 60-Foot Tunnel, transonic tests using a 6%-scale model in the David Taylor 7- by 10-Foot Transonic Tunnel, rotary balance tests using a 10%-scale model in the Langley 20-Foot Vertical Spin Tunnel, full-scale F-18 forebody model tests in the Langley 30- by 60-Foot Tunnel, full-scale F-18 airframe tests in the Ames 80- by 120-Foot Tunnel, and free spinning tests using a 3.6%-scale model in the Langley 20-Foot Vertical Spin Tunnel.

During the strake development process, additional studies were conducted with a preliminary version of the ANSER strake design. These studies are described in reference 1 and included wind-tunnel free-flight tests and preliminary piloted simulation studies, both of which illustrated the enhancements in controllability and maneuverability provided by the strakes. Computational fluid dynamics studies have also been conducted for the same preliminary strake configuration (reference 5) and are continuing with the current ANSER strake design.

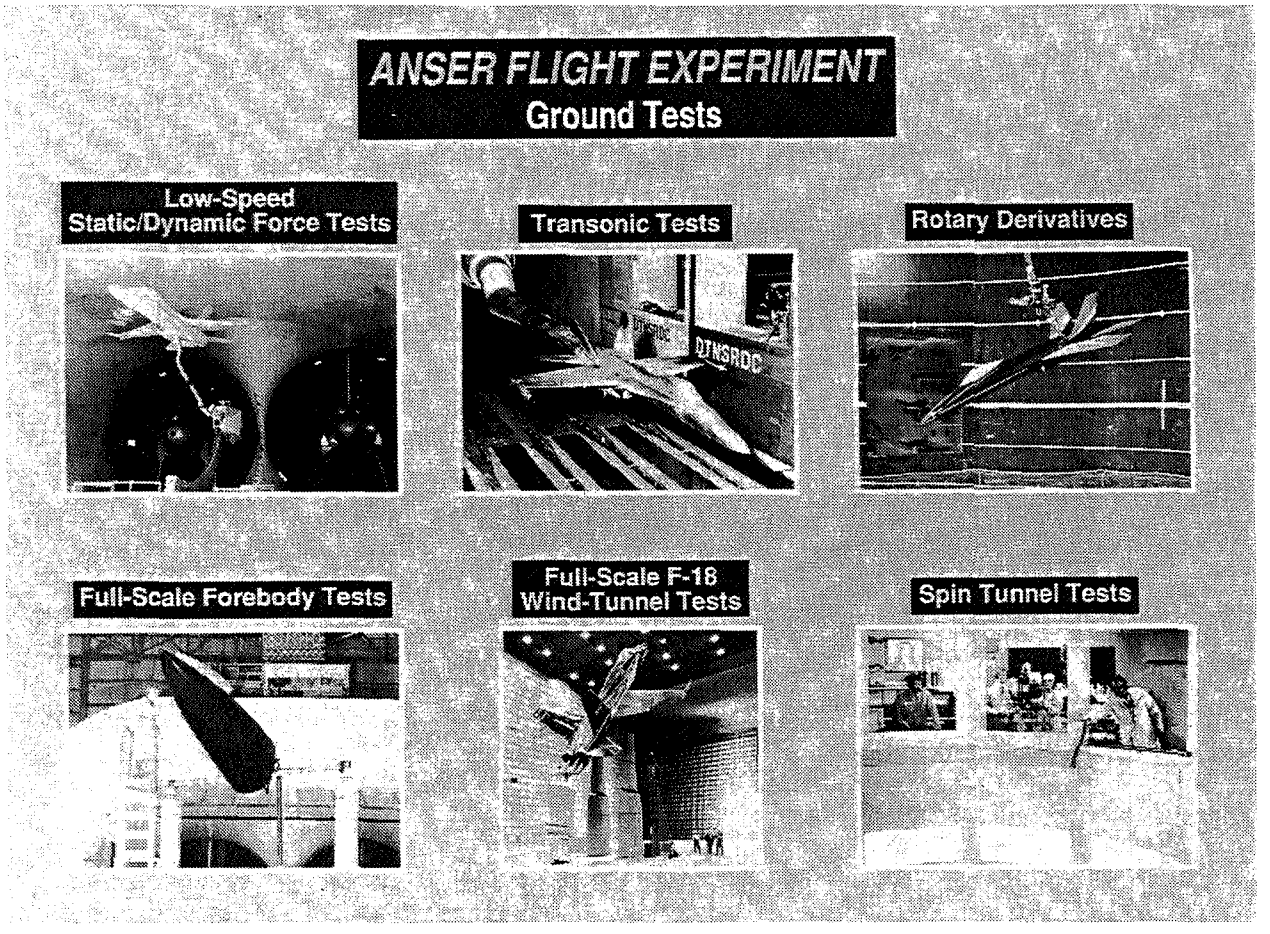

COMPARISON OF F-18 RUDDER AND
FOREBODY STRAKE YAW CONTROL POWER

The conventional rudders of the F-18 lose effectiveness as stall develops and the vertical tails become immersed in the low-energy stalled wake shed from the wings and fuselage. Although rudder effectiveness degrades rapidly above α=20°, the yaw control power provided by the strakes increases and produces very high levels of yawing moment at higher angles of attack. Although not shown here (see references 1, 2, 6, and 7), the results of all the ground-based studies indicate that the strakes also exhibit a number of other very desirable characteristics:

- The strakes remain effective over wide ranges of sideslip, Mach number, and aircraft rotation rate (about the velocity vector).
- They produce relatively small coupled rolling and pitching moments.
- They provide a well behaved variation of yawing moment with strake deflection.

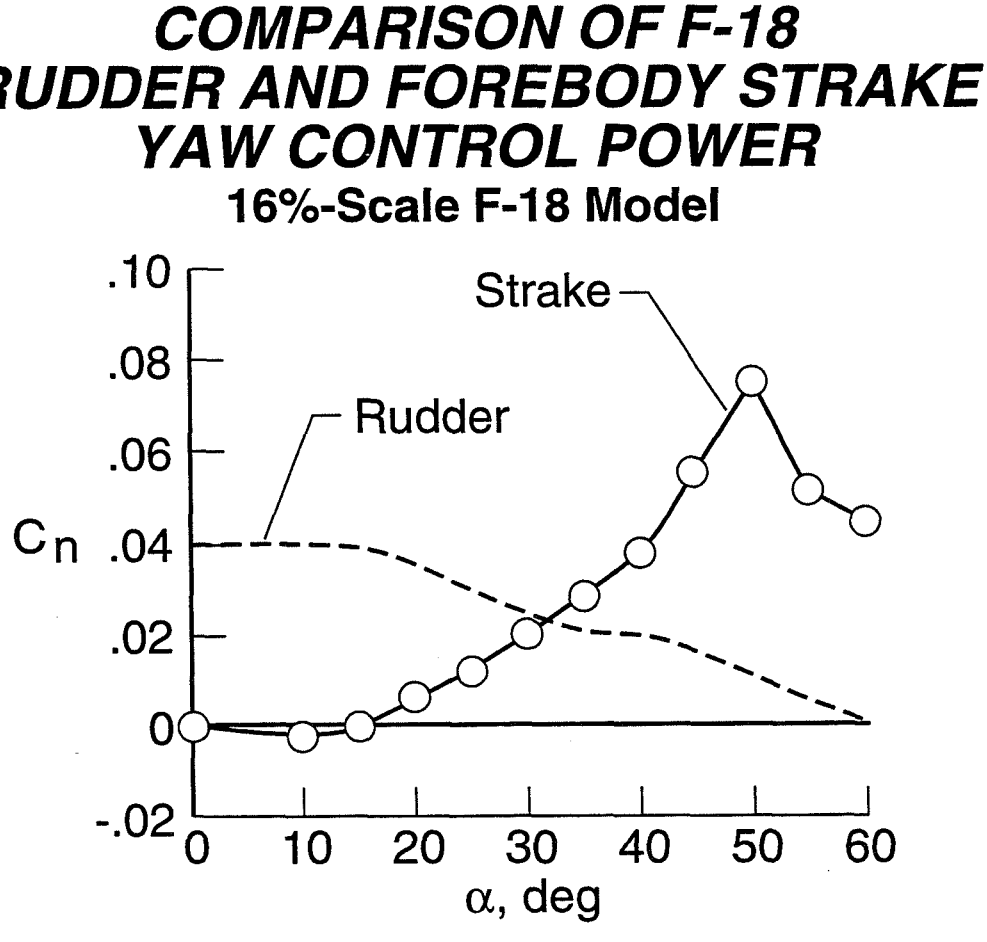

EFFECT OF STRAKE DEFLECTION ON
FOREBODY CROSSFLOW CHARACTERISTICS

Flow visualization and pressure distribution results were obtained with the full-scale F-18 forebody model and are used to describe the basic aerodynamic mechanisms that are responsible for the yawing moments generated by the strakes. The photographs show head-on views of the forebody cross-flow characteristics at α=50° and FS 107.0 (about 80-percent down the length of the strake) that were obtained using a laser light sheet technique. With the strakes retracted, the photograph shows that the flow has separated symmetrically to produce a pair of small counter-rotating forebody vortices located above the forebody. However, with a maximum strake deployment, the photograph shows that the strake generates a much larger vortex, located above the strake and displaced away from the forebody.

FULL-SCALE F-18 FOREBODY LASER SHEET FLOW VISUALIZATION

α = 50°

Strakes Retracted

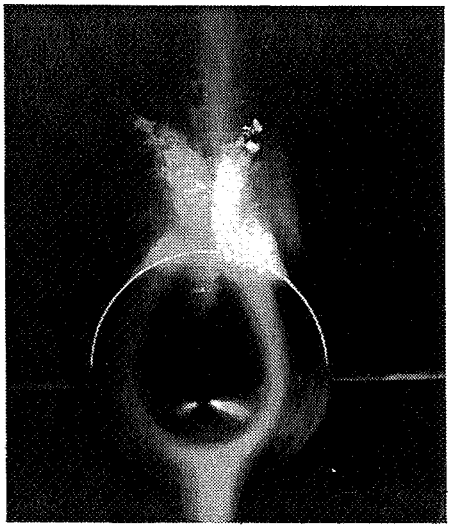

Strake Deployed 90°

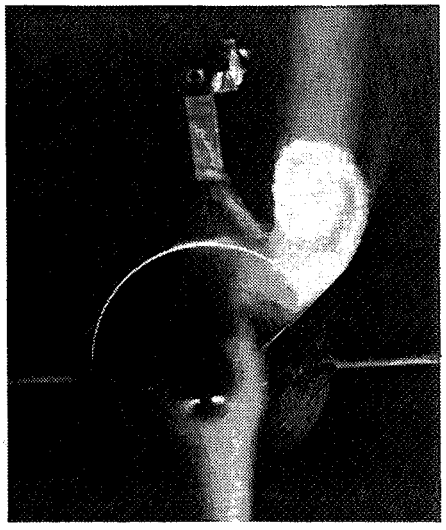

EFFECT OF STRAKE DEFLECTION ON
FOREBODY PRESSURE DISTRIBUTIONS

The sketches show pressure distributions measured around the forebody for the same conditions shown in the photographs. With the strakes retracted, large suction pressures develop as the flow accelerates around the sides of the forebody. The flow then separates and the "footprints" of the two small vortices are evident on the top of the forebody. When a strake is deployed, the suction pressures are reduced on the strake-deployed side of the forebody and the suction pressures are increased on the strake-retracted side. Although it is not shown here, the increased suction pressures on the strake-retracted side of the forebody are accompanied by a delay in the primary separation line (visualized using oil flow). Therefore, it appears that a strake deployment generates a dominant vortex that delays separation and accelerates the flow on the strake-retracted side and forces separation and decelerates the flow on the strake-deployed side. These changes in flow velocity generate differential suction pressures that produce side forces and yawing moments in the direction away from the strake deployment.

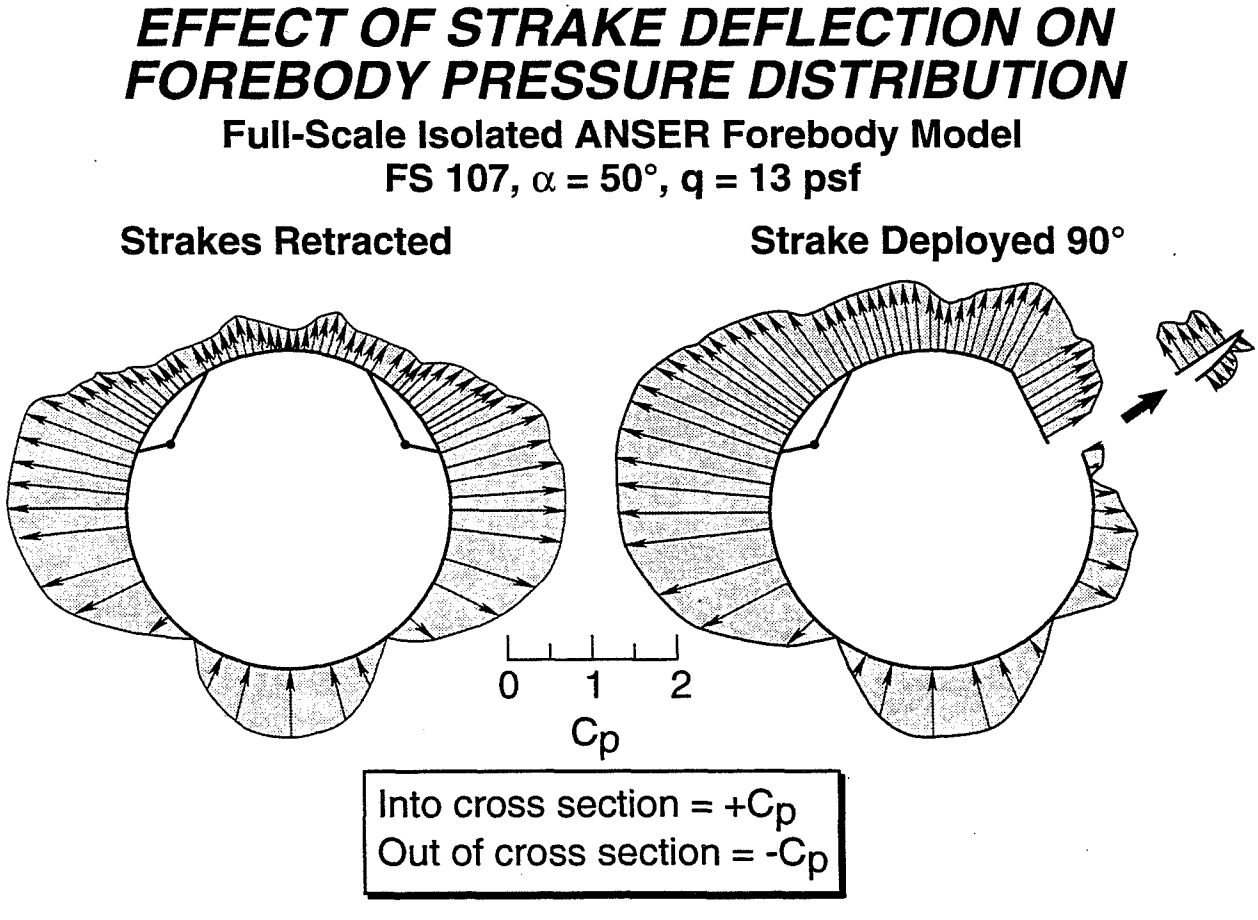

ANSER RADOME/STRAKE DESIGN

As shown in the figure, the approach being taken to modify the F-18 HARV for the ANSER Flight Experiment is to replace the basic radome with a newly fabricated radome that incorporates the strakes, actuators, and instrumentation. The flight radome and strake components have been designed and fabricated at NASA Langley and are shown on the following page. The radome and strake structures consist of aluminum skin panels that are riveted to aluminum stringers and bulkheads. Fiberglass fairings are used in several areas but are not used as load-bearing components. The hydraulic actuators used to drive the strakes consist of modified F-18 aileron actuators and are discussed in more detail in a subsequent figure.

In addition to the existing instrumentation system on the HARV, the newly fabricated radome incorporates specific instrumentation required for the ANSER Flight Experiment. A total of 215 pressure orifices have been installed to provide surface pressure distributions around the radome, on the strakes, and on the nosecap. Assessment of radome structural loads and strake hinge moments will be provided by strain gauge measurements, and vibration information associated with the strakes will be obtained using accelerometers. In addition, a smoke port will be incorporated on each side of the radome and will be connected to the existing HARV smoke generating system to allow visualization of the forebody and strake vortex flowfields.

The total weight of the research radome, including all components and instrumentation, is approximately 263 lbs (radome structure and fairings at 134 lbs, two strakes at 19 lbs each, two actuators at 20 lbs each, and instrumentation at 51 lbs). It should be noted that no effort was made to minimize weight of the research hardware since, when integrated onto the HARV, the radome will be ballasted up to a total weight of about 615 lbs to maintain the desired aircraft center of gravity. For comparison, the weight of a standard F-18 composite radome is approximately 121 lbs. A more detailed description of the flight test hardware is presented in reference 8.

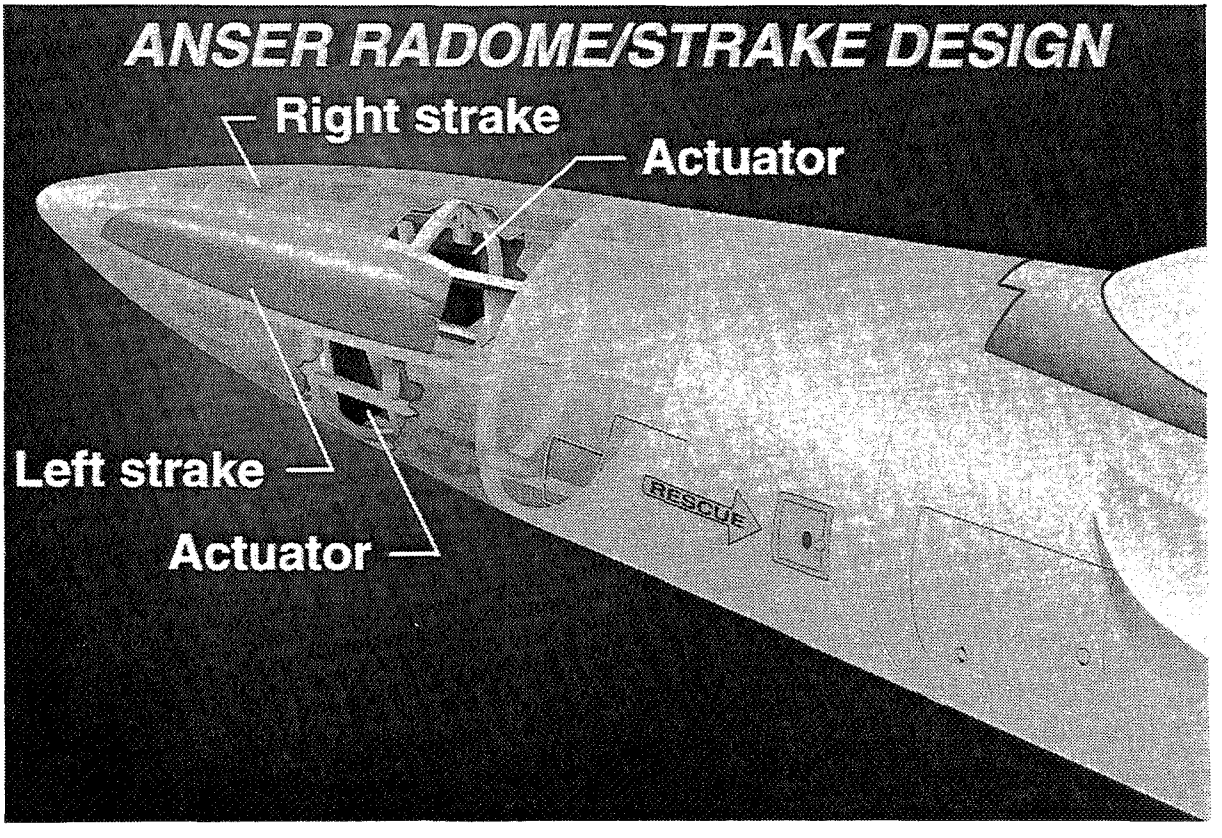

ANSER FLIGHT HARDWARE

The two photographs show various aspects of the ANSER flight hardware.

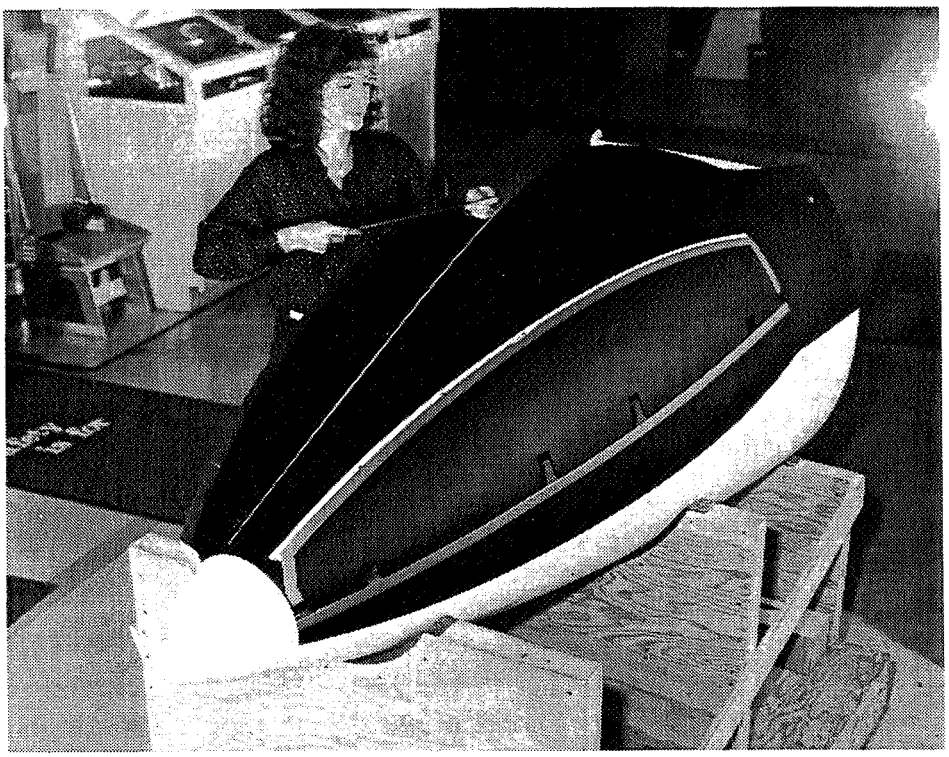

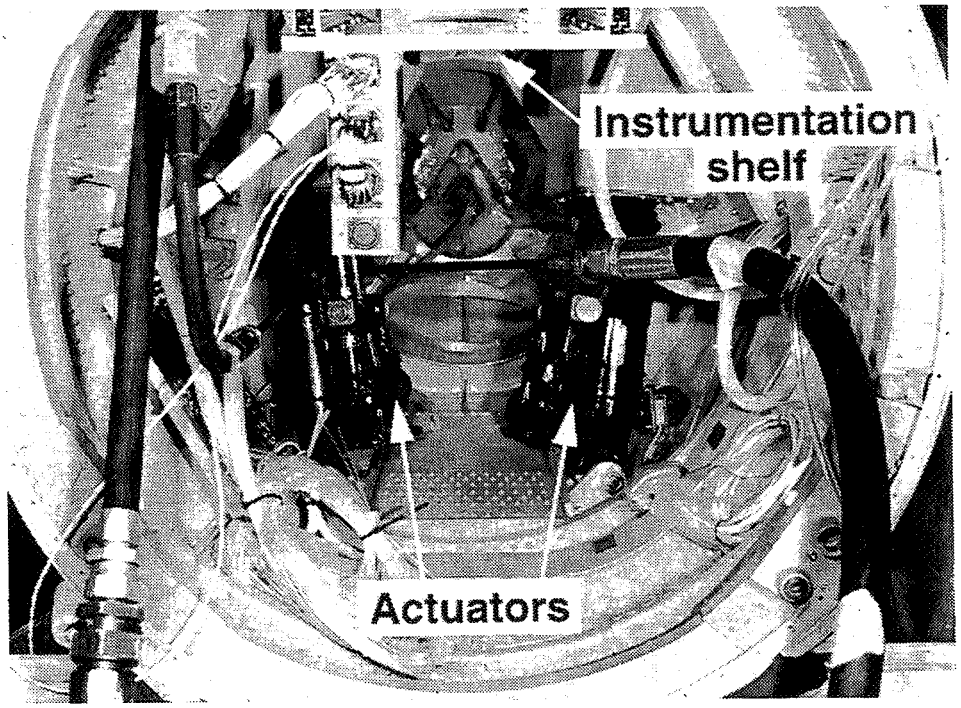

STRAKE HINGE MOMENT CHARACTERISTICS

Strake hinge moment measurements have been obtained during full scale F-18 forebody model tests in the Langley 30- by 60-Foot Tunnel and during full-scale F-18 airframe tests in the Ames 80- by 120-Foot Tunnel. All of the results have shown that the strakes produce maximum hinge moment coefficients at high angles of attack and sideslip with a full strake deflection on the windward side. An example of these results, shown in the figure, were obtained on a fully deployed left strake during full-scale F-18 forebody tests in the Langley 30- by 60-Foot Tunnel. Although the maximum hinge moment coefficient occurs at high angles of attack, the aircraft can only reach these conditions at relatively low dynamic pressures. When the dynamic pressure envelope of the aircraft is taken into account, the maximum hinge moment loads occur near an angle of attack of 20° and at relatively small sideslips. Under these conditions, the actuator force required to offset the hinge moment is approximately 1000 lbs.

With a projected area of 2.71 ft^2 (each), the strakes are much smaller than any other aerodynamic control surface on the F-18 HARV. For example, each F-18 aileron has an area of approximately 12.2 ft^2 and each rudder has an area of approximately 8.1 ft^2. The hydraulic actuators used to drive the strakes consist of F-18 aileron actuators that have been modified for longer stroke, higher rate, and less force capability. The strake actuators have a stroke of ±2.84 inches that provides each strake with a deflection of 0° to 90°. Based on the hinge moment measurements, the strake actuators have been designed to provide a rate capability of 180 deg/sec under the highest expected load (~1000 lb). This control surface rate allows a maximum strake deployment in 1/2 sec, which is the same time required for a maximum rudder deflection for this aircraft (30° deflection at 60 deg/sec).

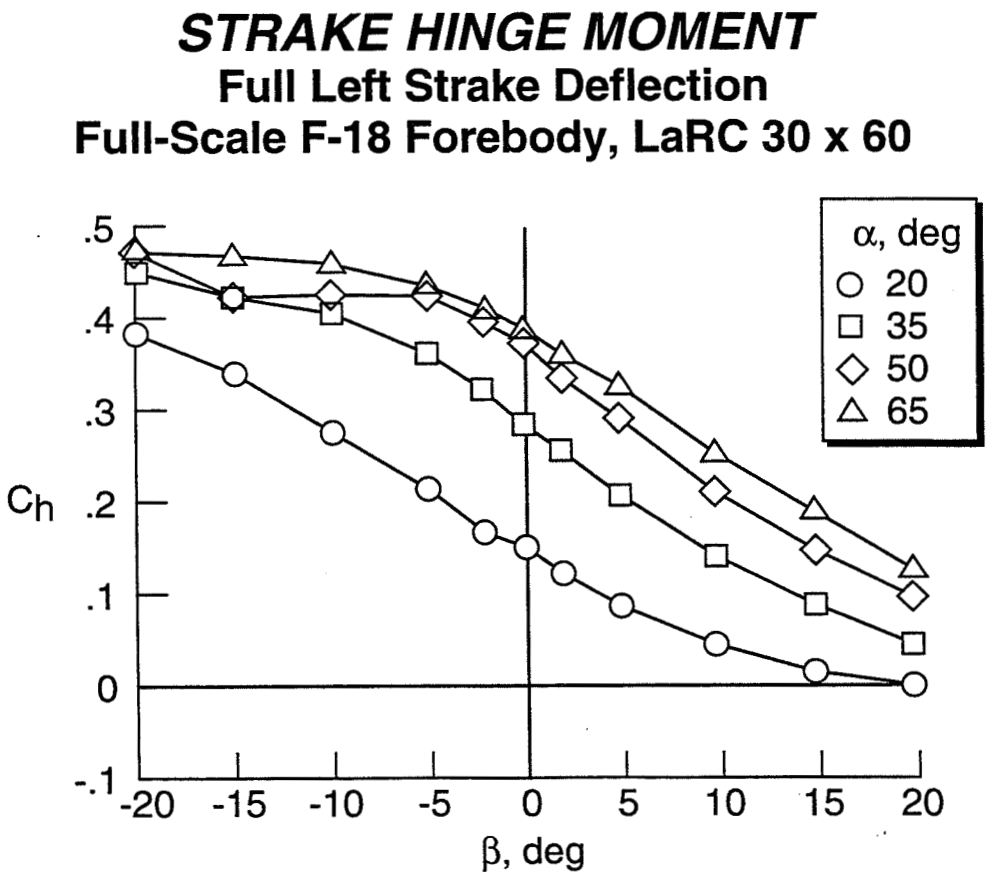

STRUCTURAL CONSIDERATIONS

A significant issue when integrating forebody controls on an aircraft involves the structural loads induced on the forebody. The strakes designed for the F-18 HARV, in general, produce much larger aerodynamic side forces on the forebody than would be obtained for the same flight condition without the strakes deployed. In addition, the anticipated higher maneuvering rates and accelerations provided by the strakes would be expected to induce larger inertial loads. In order to evaluate these structural considerations, a high-fidelity aerodynamic and inertial loads model for the forebody was incorporated into the existing HARV/ANSER simulation. The forward fuselage loads were then predicted through real-time piloted simulation where a wide matrix of maneuvers were flown that were expected to maximize the forebody loads.

A typical example of the results from the loads simulation is shown in the figure for an initial condition of α=30°, M=0.5 and n_Z=4.2. These results are presented as time histories of fuselage side bending loads for a maneuver consisting of a full right lateral stick input followed several seconds later by a full lateral stick reversal. The time histories show the aerodynamic, inertial, and total side bending load at fuselage station 190 (several inches in front of the canopy) during the maneuver, with and without the strakes operating. For the basic aircraft (with the strakes inactive), the aerodynamic load on the forebody opposes the direction of motion because of the sideslip generated by the maneuver. When the strakes are used for control, however, the result is a large aerodynamic load on the forebody in the direction of the maneuver. In both cases, the inertial loads act in the direction opposite the maneuver, but are higher with the higher accelerations provided by the strakes.

The net result, since the aerodynamic and inertial loads act in opposite directions, is that the total load on the forward fuselage is actually lower when using the strakes for control than with the basic radome. This result indicates that although the use of forebody controls can increase aerodynamic and inertial loads, the opposing nature of these loads can reduce or eliminate the need for a stronger aircraft structure and its inherent weight penalties.

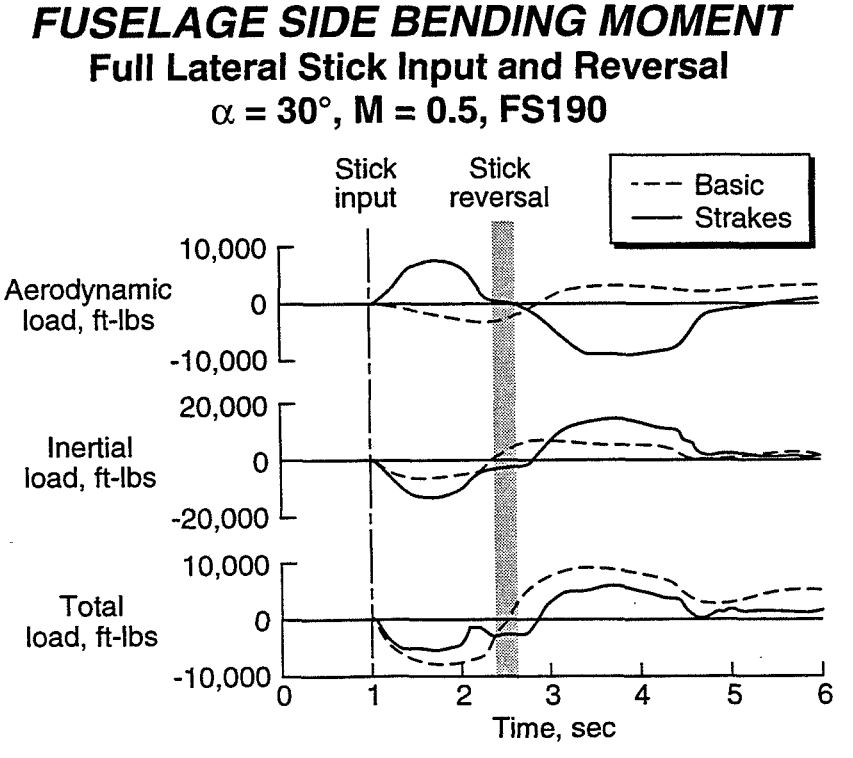

ANSER CONTROL LAWS

In addition to the actuated forebody strakes, the thrust vectoring control system that is currently being flown on the F-18 HARV will be retained during the ANSER Flight Experiment. Because of this, a versatile set of flight control laws have been developed that will allow several combinations of advanced control concepts to be compared directly with the basic F-18 capabilities. The control laws have been developed utilizing an advanced design methodology (ref 9) incorporating analytical synthesis techniques combined with nonlinear piloted simulation using the Langley Differential Maneuvering Simulator.

These flight control laws will be implemented using the existing Research Flight Control System on the F-18 HARV and will include 4 research modes: (1) control augmentation using strakes (including pitch thrust vectoring); (2) control augmentation using multi-axis thrust vectoring; (3) control augmentation using strakes and multi-axis thrust vectoring; and (4) a programmed strake mode. The first control law mode is designed to evaluate yaw-control augmentation using strakes only. Pitch thrust vectoring is used in this mode, however, to allow the aircraft to trim at higher angles of attack than possible with aerodynamic controls alone. The second control law mode (with strakes deactivated) is the same set of advanced thrust-vectoring control laws currently under evaluation on the F-18 HARV. This control law mode will be retained during the ANSER Flight Experiment to allow a direct comparison between strake augmentation and thrust vectoring augmentation. The third control law mode combines strakes and multi-axis thrust vectoring to provide the maximum potential agility. The fourth control mode is designed primarily to obtain aerodynamic data (control effectiveness, pressures, hinge moments, flow visualization) with varying strake deflections. This mode will allow pre-programmed deflections of the strakes and will use the thrust vectoring system to maintain a stabilized flight condition.

ANSER CONTROL LAWS

Mode	Flight Test Usage
• Strakes only (with pitch TV)	• Agility • Handling qualities
• Multi-axis TV	
• Strakes + Multi-axis TV	
• Programmed strakes	• Aerodynamic data

FLIGHT TEST PLANS

The primary objectives of the ANSER Flight Experiment are to provide flight validation of a ground-test data base for a forebody control device and to evaluate the use of this type of control in enhancing fighter aircraft maneuverability. One focus of the flight tests will be on obtaining aerodynamic measurements (strake control effectiveness, surface pressures, hinge moments, and flow visualization) for comparison with ground-test results. Another focus of the flight tests will be to evaluate the overall payoffs in agility and controllability obtainable with this type of control. A total of 60 to 70 flights are anticipated to accomplish the envelope expansion and research phases of the flight test program.

ANSER FLIGHT EXPERIMENT
Approach

- Obtain control effectiveness characteristics, pressures, hinge moments, and flow visualization

- Determine effects on aircraft response when using strakes for control and stability augmentation

PROJECT SCHEDULE

The flight hardware has been delivered to NASA Dryden where the preparations for integrating with the F-18 HARV are underway. Once the current flight test phase is completed, the aircraft will be available to begin the integration of the new research radome. This hardware integration is expected to begin by the latter part of June and continue through November 1994. Following this integration, several months of flight tests will be directed toward expanding the operational envelope of the F-18 HARV with the ANSER modification. The research flights will follow this period of envelope expansion and are expected to run through March 1995.

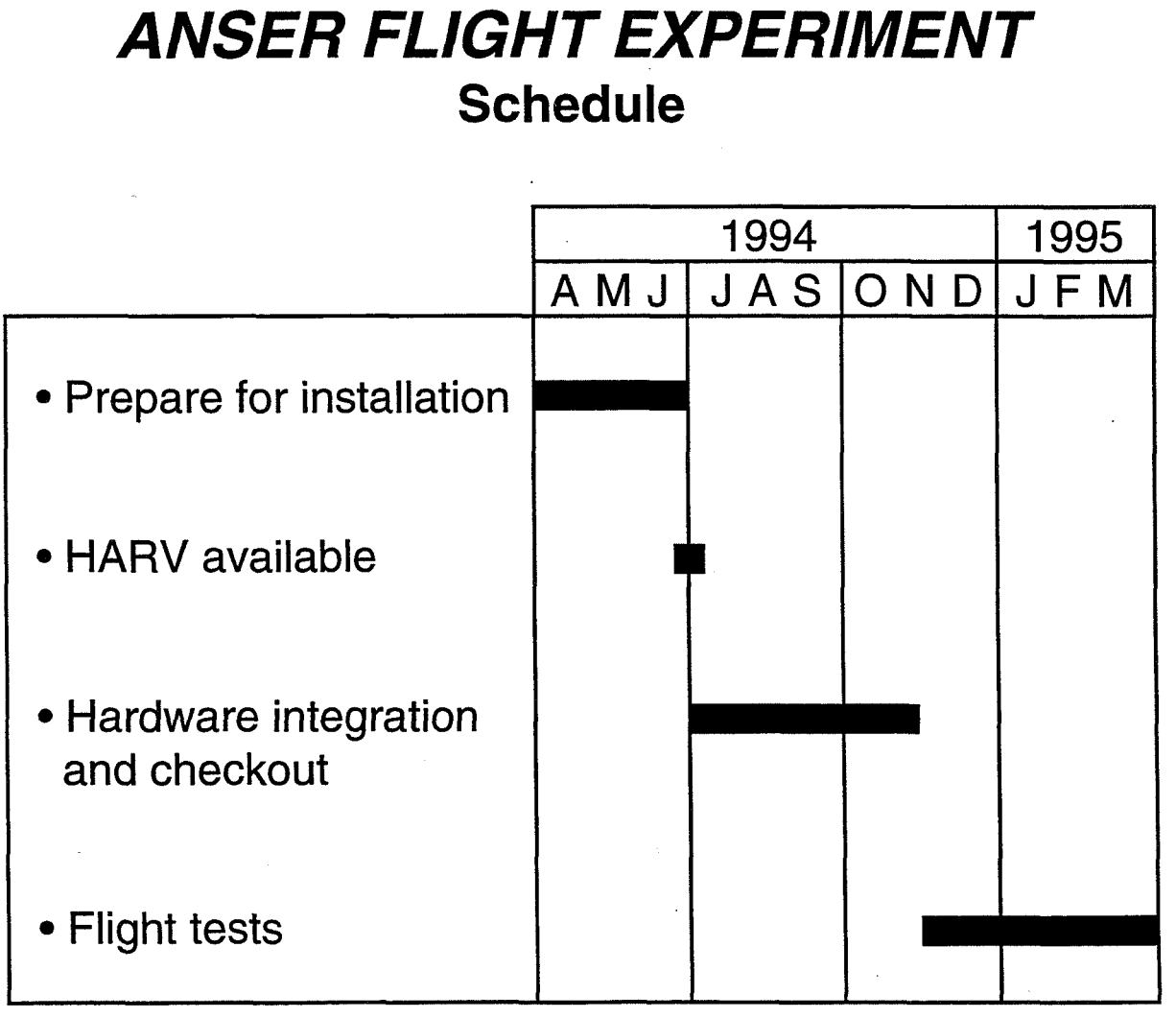

CONCLUDING REMARKS

A wide range of coordinated activities have been used to develop the actuated forebody strake control concept. Although directed toward a specific forebody control concept, these studies are providing an overall understanding of forebody controls characteristics and design implications. Favorable results from these efforts have provided confidence that the ANSER strake design will be a very effective yaw control device at high angles of attack, and can provide significant enhancements in maneuverability by providing the critical yaw control required to coordinate rolling maneuvers at these high-angle-of-attack conditions. The objectives of the flight tests using the F-18 HARV are to provide flight validation of the ground-based studies and to evaluate the use of forebody controls in enhancing fighter aircraft maneuverability. It is expected that the flight tests will begin during the latter part of 1994 and be completed in early 1995.

REFERENCES

1. Murri, Daniel G.; Biedron, Robert T.; Erickson, Gary E.; Jordan, Frank L., Jr.; and Hoffler, Keith D.: Development of Actuated Forebody Strake Controls for the F-18 High Alpha Research Vehicle. NASA CP-3149, pp. 335-380. November 1990.

2. Murri, Daniel G.; Shah, Gautam H.; DiCarlo, Daniel J.; and Trilling, Todd W.: Actuated Forebody Strake Controls for the F-18 High-Alpha Research Vehicle. AIAA 93-3675-CP. August 1993.

3. Murri, Daniel G.: Wind-Tunnel Investigation of Actuated Forebody Strakes for Yaw Control at High Angles of Attack. M.S. Thesis, George Washington University. May 1987.

4. Murri, Daniel G.; and Rao, Dhanvada M.: Exploratory Studies of Actuated Forebody Strakes for Yaw Control at High Angles of Attack. AIAA-87-2557-CP. August 1987.

5. Biedron, Robert T.; and Thomas, James L.: Navier Stokes Computations for an F-18 Forebody with Actuated Control Strake. NASA CP-3149, pp. 481-506. November 1990.

6. Erickson, Gary E.; and Murri, Daniel G.: Wind Tunnel Investigations of Forebody Strakes for Yaw Control on F/A-18 Model at Subsonic and Transonic Speeds. NASA TP-3360. September 1993.

7. Lanser, Wendy R.; and Murri, Daniel G.: Wind Tunnel Measurements on a Full-Scale F/A-18 with Forebody Slot Blowing or Forebody Strakes. AIAA-93-1018. February 1993.

8. DiCarlo, D. J.; Murri, D. G.; Shah, G. H.; and Lord, M. T.: Status of Hardware Preparation and Flight Test Plans to Assess Actuated Forebody Strakes. AIAA 94-2131. June 1994.

9. Davidson, John B.; Foster, John V.; Ostroff, Aaron J.; Lallman, Fredrick J.; Murphy, Patrick C.; Hoffler, Keith D.; and Messina, Michael D.: Development of a Control Law Design Process Utilizing Advanced Synthesis Methods with Application to the NASA F-18 HARV. NASA CP-3137, Volume 4, pp. 111-157. April 1992.

19951078 44
3500 74

N95-14258

16107
P 20

Integration of a Mechanical Forebody Vortex Control System Into the F-15

Richard E. Boalbey, Kevin D. Citurs, Wayne L. Ely,

Stephen P. Harbaugh, William B. Hollingsworth, and Ronald L. Phillips

of

McDonnell Douglas Corporation

Saint Louis, Missouri

4th NASA High Angle-of-Attack Conference
July 12-14, 1994 / Dryden Flight Research Facility

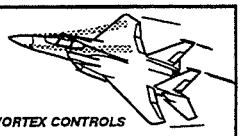

The F-15 Forebody Vortex Control (FVC) Program was initiated to improve the high angle of attack controllability of the F-15. The F-15 has more-than-adequate nose-down recovery margin, however it would be desirable to increase the yaw control available at high angles of attack in order to improve departure resistance as well as maneuverability.

The goal of the program is to develop a production FVC system for the F-15. The system may consist of either a mechanically actuated device such as the strakes developed for the HARV program, or a pneumatic device such as the port blowing system tested on the X-29. Both types of systems are being evaluated under this program.

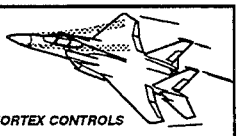

Integration of a Mechanical Forebody Vortex Control System Into the F-15

by

Richard E. Boalbey, Kevin D. Citurs, Wayne L. Ely,
Stephen P. Harbaugh, William B. Hollingsworth, and Ronald L. Phillips
of
McDonnell Douglas Corporation
Saint Louis, Missouri

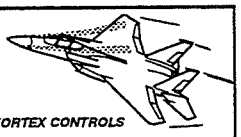

Background information on the F-15 aircraft will be presented, followed by a description and overview of forebody vortex controls (FVC) technology. Then the status and future plans of the F-15 Forebody Vortex Controls Program will be discussed.

Discussion Overview

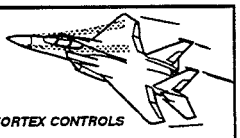

- Background
- Results of Phase I: Concept Exploration Study
- Results of Phase II: Concept Validation Study
- Status of Phase III: FVC Integration Study
- Future Plans

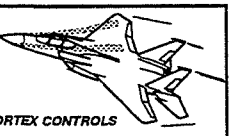

The F-15 flight control system consists of a mechanically controlled, hydraulic surface actuation system, supplemented by a high authority Control Augmentation System (CAS) which is implemented through the Flight Control Computer (FCC). The CAS is the primary means for implementation of flight control changes in the F-15. Early models of the F-15 utilized an analog FCC, whereas the F-15E has a digital FCC which is more adaptable to flight control changes.

Outer mold lines are similar for all F-15 models, with the major exception of the canopy. The A and C models have a single place canopy, and the B, D, and E models have a two place canopy. The models also have somewhat different main landing gear bumps, as well as different protuberances.

High angle of attack characteristics of the F-15 are similar to many other aircraft. At high angles of attack, the ailerons tend to produce adverse yawing moment. For the F-15, the adverse yawing moment makes it necessary to wash-out the aileron authority at high angles of attack. The rudders also lose effectiveness at high angles of attack due to tail blanking by the wing and fuselage.

A Short Course on the F-15

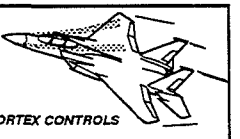

Main Features

- Mechanical Control System With High Authority Control Augmentation System (CAS)
- Analog FCC on F-15 A through D
- Digital FCC on F-15E
- Canopy and CFT's are the Only Major Outer Mold Line Changes Between Models
- High AOA Characteristics
  - Ailerons Produce Adverse Yaw
  - Rudders Lose Effectiveness

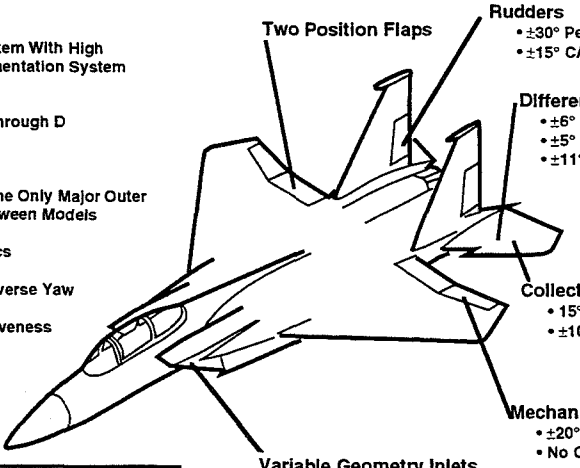

More Control Power Is Desired At High AOA

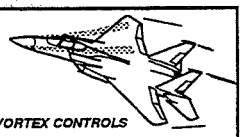

The aerodynamic benefits of forebody vortex control have been demonstrated under the HARV and X-29 programs, as well as many other studies. For vehicles such as the X-29, F-18, and F-15, forebody vortex controls produce primarily yaw control.

At high angles of attack, the tail surfaces are blanked by the wing and fuselage resulting in reduced stability and control. In contrast, the forebody flow field remains in a highly energized flow field throughout the angle of attack range, making forebody vortex control an attractive option.

Forebody vortex control utilizes small perturbations which modify the shear layer separation point and restructure the forebody vortex system. The perturbations may be accomplished through either a mechanical or pneumatic device, but the magnitude of the perturbation required to produce a given force increases rapidly as the perturbation is positioned at greater distances from the nose. Forebody vortex control has also been found to be controllable which means that the magnitude of the resulting force is proportional to the magnitude of the perturbation.

FVC Improves Hi-α Departure Resistance and Maneuverability

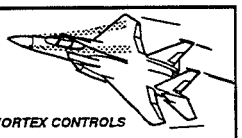

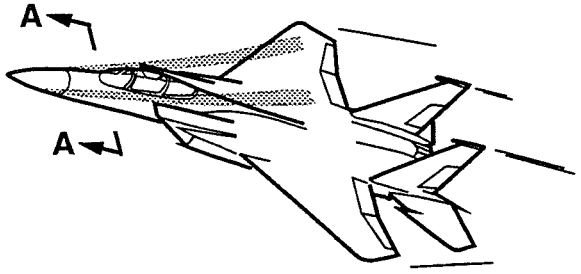

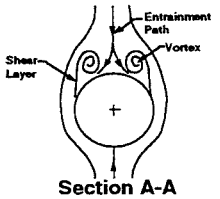

Section A-A
Without FVC

- Forebody Flow Field Remains Highly Energized at High Angles of Attack
- Forces Are Controlled By Manipulating Shear Layer Separation Point
- Perturbations Can Be Relatively Small . . . Perturbation Requirements Increase Aft of Nose
- Resulting Force is Proportional to the Size of Perturbation (ie. Forces are Controllable)
- Forebody Vortex Control Can Be Accomplished Either Mechanically or Pneumatically

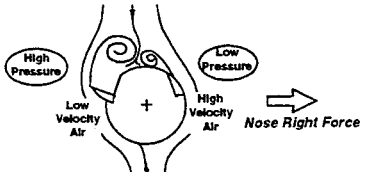

Section A-A
With FVC

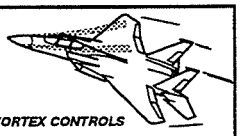

The first phase in the FVC development program for the F-15 was to determine whether FVC would improve flying qualities and could be implemented without a substantial modification to the airframe. The results of a maneuverability analysis showed that FVC can provide a substantial improvement in maneuverability and controllability. A concept layout also demonstrated the feasibility of various mechanical FVC concepts.

During Phase I, the assumption was made that the yawing moments produced by FVC on the F-15 will be similar to those produced by FVC on the HARV aircraft. The goal of Phase II was therefore, to verify the validity of this assumption. A good correlation resulted and proved that the F-15 flow field is conducive to FVC.

FVC can be accomplished through either a pneumatic or a mechanical system. Within these categories, candidate concepts include port blowing, slot blowing, actuated conformal strakes, sliding strakes, rotatable nose cones, or rotatable radomes. The objective of Phase III is to determine which concept is best for the F-15. After the best concept is selected, the next task is to perform a cost benefit study, to determine if FVC makes sense for the F-15.

After passing these critical tests, the next step is to develop and flight test a production FVC system.

F-15 FVC Program Was Designed to Answer Six Important Questions

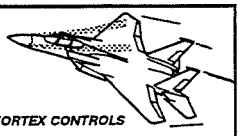

1) *Will FVC Significantly Improve Flying Qualities?..... Yes!*
   - PHASE I: Concept Exploration Study
     - Literature Search, Maneuverability Enhancement Study, and Simulation

2) *Can It Be Done Without A Major Re-build?..... Yes!*
   - PHASE I: Concept Exploration Study
     - Concept Layout

3) *Is The F-15 Forebody Flow Field Conducive to FVC?.....Yes!*
   - PHASE II: Concept Validation Study
     - MDA Low Speed Wind Tunnel Testing

4) *What's The Best FVC Technique for the F-15?..... TBD 1994!*
   - PHASE III: FVC Integration Study
     - Aero Optimization, Trade Study

5) *Is FVC a Good Value for the F-15 Program?.....TBD 1994!*
   - PHASE III: FVC Integration Study
     - Manned Simulation, Cost/Benefit Analysis

6) *How Do We Put It Into Operational Use?..... TBD 1995!*
   - PHASE IV: Flight Test Program
     - Detailed Design and Fabrication, Flight Test

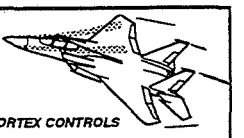

To develop FVC for the F-15, a team was assembled which combines the expertise and resources of highly experienced organizations. At the present time Wright Laboratories is the only organization which has flight tested FVC. Wright Labs also has experience from the STOL Demo and MUSIC programs and are highly knowledgeable of pneumatic FVC technology.

The F-15 System Program Office (SPO) is a critical link for the team, providing insight into the needs of the Air Combat Command (ACC) which is the primary user of F-15's. The F-15 SPO is also an experienced manager of F-15 modifications and is currently managing an F-15 high angle of attack flight test program.

NASA LaRC has gained considerable experience with FVC and high angle of attack technology through the HARV program. NASA LaRC is also an excellent source of high angle of attack testing technology.

MDA brings to the team an unparalleled knowledge of the F-15 system. MDA has experience from the STOL Demo and MUSIC programs, as well as production integration of high angle of attack control systems. MDA also has several years of both pneumatic and mechanical FVC research experience.

Teaming Adds Synergy to FVC Development Program

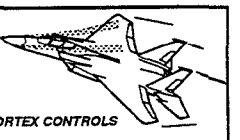

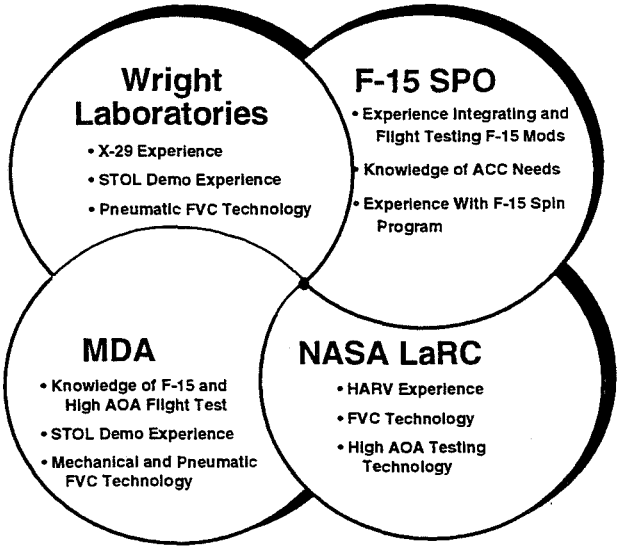

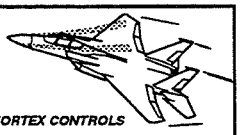

This Page Intentionally Left Blank.

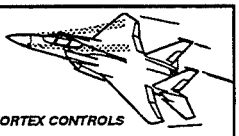

Phase I: Concept Exploration Study

- Results Summary -

Will FVC Significantly Improve Flying Qualities?
Can It Be Done Without A Major Re-build?

- Concept Layout
- VECTOR Maneuverability Analysis

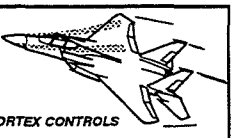

F-15 FOREBODY VORTEX CONTROLS

The High Strake concept offers a relatively simple structural integration challenge. These strakes will mount conformally on the top of the nose barrel with no impact upon radar performance. Actuators and other hardware will mount inside of a ballast bay, and minimal structural redesign is required.

The main drawback to the High Strake concept is the impact upon pilot visibility. In order to achieve the desired aerodynamic performance, the strakes must be made relatively large compared to a strake mounted closer to the tip of the radome. Concerns over blanking of critical visibility sectors are being investigated

High Strakes Offer Relatively Simple Structural Integration

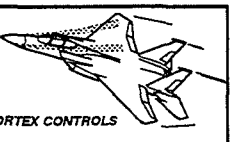

F-15 FOREBODY VORTEX CONTROLS

Pros:

- Structural Attachment on Current Load Path
- Actuators/Systems Inside Ballast Bay
- Same Access to Avionics Suite

Cons:

- Visibility Impact?

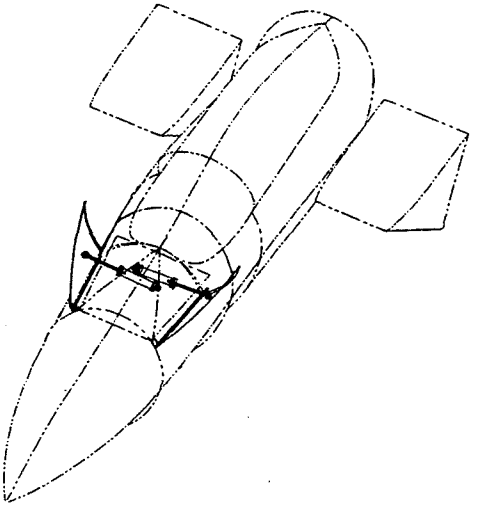

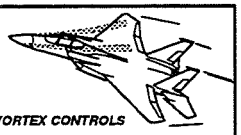

To address the visibility concerns with the high strake concept, several analysis methods are being used. To gain an early look at the visibility impact of the High Strake concept, mock-ups were used to gather pilot comments. Based upon these studies, the strake shape was redesigned to minimize the intrusion of the strake into the pilot's visibility region. Later in the program, flight simulation will be used to help address the visibility concerns.

Visibility Impact Will Be Considered During Strake Testing

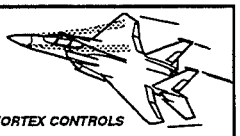

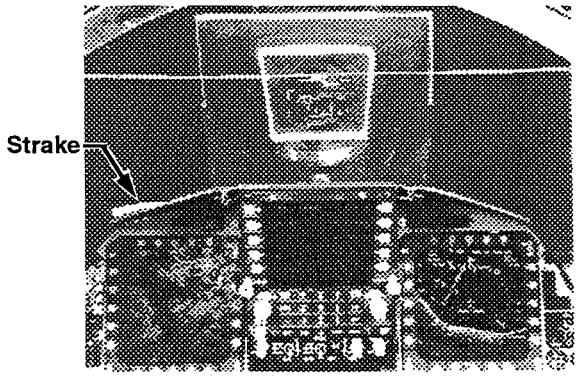

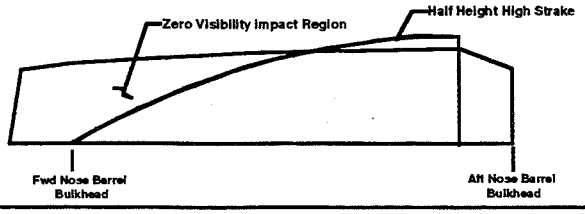

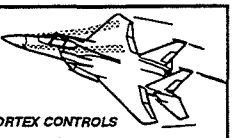

The Rotatable Radome is the second mechanical FVC concept being evaluated. It promises greater aerodynamic performance relative to the High Strake concept and will have a minimal structural impact. A remove and replace installation is expected, with only minor avionics repositioning required.

The greatest concern with this concept is radar performance and system complexity. The inclusion of fixed strakes on the radome is expected to present a considerable radar design challenge. Additionally, the mechanism to actuate the system is expected to be complex and could have a significant impact upon reliability and maintainability.

Rotatable Radome Offers Unique Control Opportunities

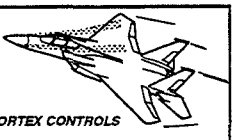

Pros:

- *Strake Can Be Small*
- Improved Low AOA Directional Stability
- Remove and Replace Radome Installation
- Minimal Changes to Airframe Structure and Systems
- Minimal Effect on Avionics Access

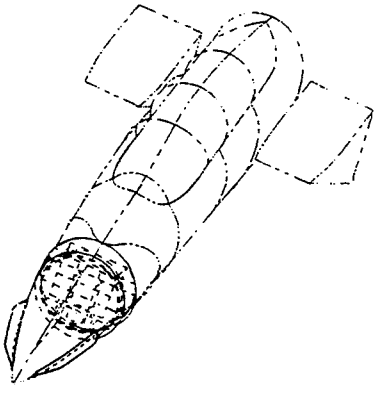

Cons:

- *System Complexity*
- Radar Performance Impact
- Actuation Rates?

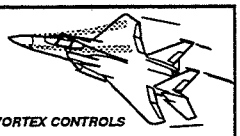

For an early look at performance improvements, the computer program VECTOR was used to determine the maximum achievable dynamics for the F-15 with FVC. VECTOR requires aerodynamic, propulsion, mass and inertia, and actuator data, and returns the maximum achievable aircraft dynamics. In short, the program outputs the capabilities of an aircraft assuming that the aircraft has a "perfect" flight control system.

Program VECTOR Was Used To Gage Maneuverability Improvements

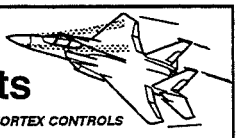

MDA's Program VECTOR Quickly Determines Maximum Achievable Dynamics Across the Flight Envelope

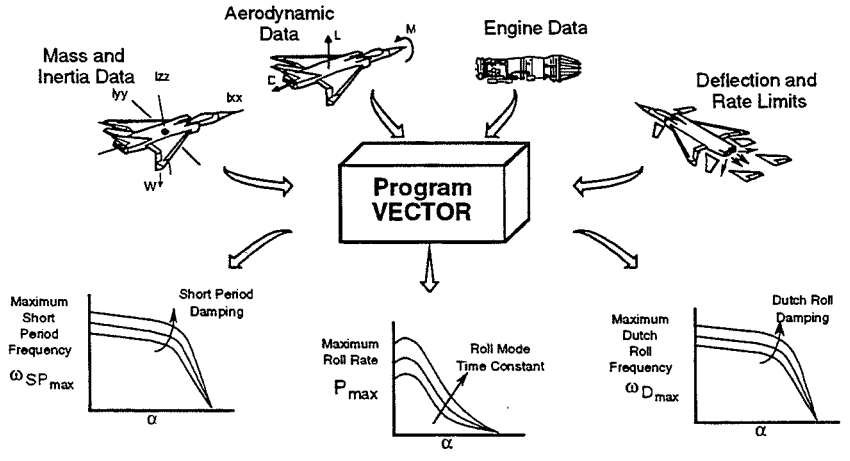

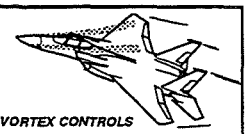

Wind tunnel data for FVC on the F-15 was not available for this early study, requiring the FVC control powers to be estimated. The F-18 HARV FVC database formed the basis of the estimates which was later found to provide an excellent representation of the F-15 FVC characteristics.

Maximum roll rate was found to be significantly improved by FVC. For the baseline aircraft, as with most conventional aircraft, the attainable roll rate drops as angle of attack increases. With FVC, at low angles of attack the roll rate still drops as angle of attack is increased, but as FVC gains effectiveness, the roll rate begins to increase dramatically. The increased yaw control from FVC not only improves roll performance, but will substantially improve departure resistance.

VECTOR Predicts Substantial Roll Rate Improvement At High AOA

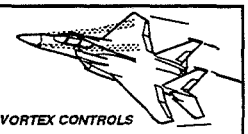

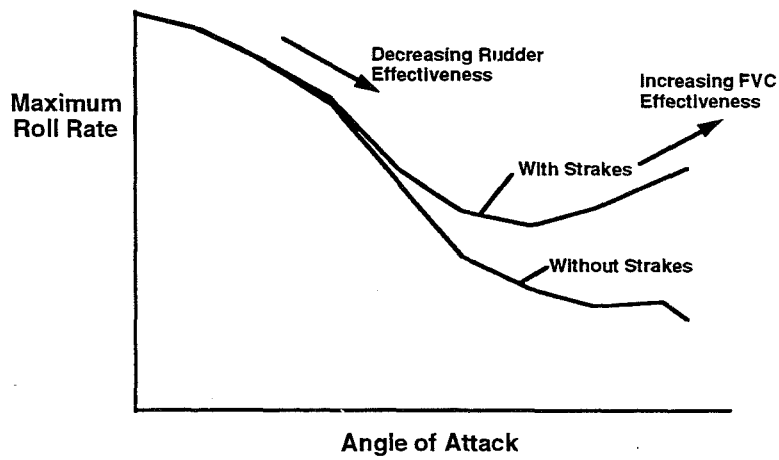

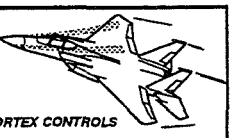

This Page Intentionally Left Blank.

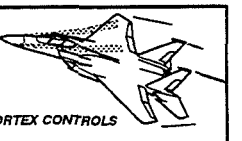

Phase II: Concept Validation Study

- Results Summary -

Is The F-15 Forebody Flow Field Conducive to FVC?

- MDA Low Speed Wind Tunnel Test

Testing was conducted in the MDA Low Speed Wind Tunnel using the 13% F-15 model. Angle of attack range was limited to approximately 35° for this model due to the mounting mechanism. A variety of deflectable strake sizes and positions were evaluated including large strakes to form an upper bound on FVC effectiveness. A curved lead-edge strake shape was used for this initial exploratory test because it provided a generic shape which is less dependent upon local flow characteristics.

The rotatable radome was not evaluated at this time due to the complexity of the required model modifications. The high strake position, shown in the photograph, was found to be the most effective and provided substantial yaw control.

Strake Data Were Acquired in MDA Low Speed Wind Tunnel

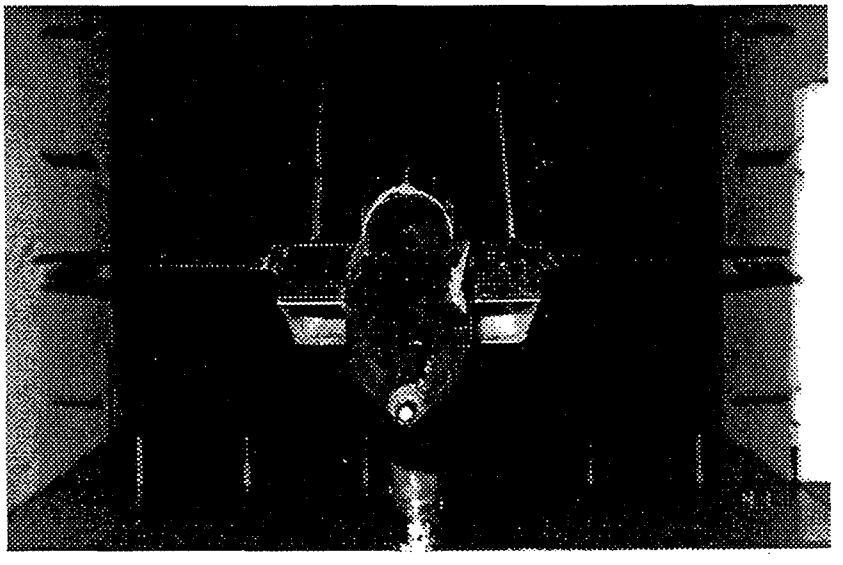

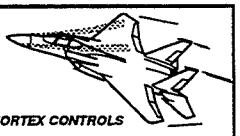

One of the key characteristics of the high strakes is that reduced strake height still provides significant yawing moment control through strake deflection. The full size strake was expected to produce good yawing moments, but in order to minimize visibility impact, it was desired to reduce the strake size.

The data show that the full length, half height strake does result in an yawing moment reduction relative to the full size strake, but the strake still produces a substantial yawing moment. In contrast, the half length, full height strake loses even more yawing moment relative to the full size strake.

Strakes Remain Effective When Height is Reduced

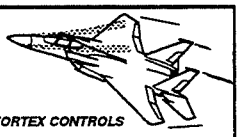

F-15 With High Strakes

MDA Low Speed Wind Tunnel Data

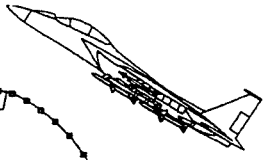

δ = Strake Deflection

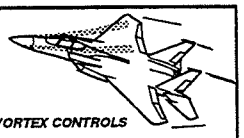

This Page Intentionally Left Blank.

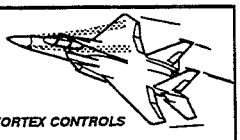

Phase III: Concept Integration Study

- Status and Future Plans -

What's The Best FVC Technique for the F-15?

- **Aero Optimization**
  - Wind Tunnel Testing of Mechanical Devices
- **Manned Simulator Evaluation**

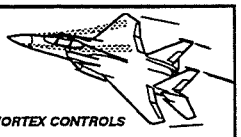

Having proved the desirability and feasibility of FVC on the F-15, the next step was to determine the best FVC concept. Wind tunnel testing was conducted cooperatively with NASA LaRC to develop a database for the mechanical FVC concepts. The strake shape was redesigned for the High Strake concept in order to maximize the strake size, while minimizing the intrusion into the pilots visibility region.

The results showed that both the High Strakes and the Rotatable Radome provide good yaw control.

Mechanical FVC Concepts Were Tested In The NASA 30x60 Ft Tunnel

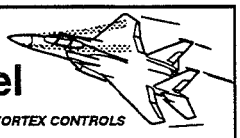

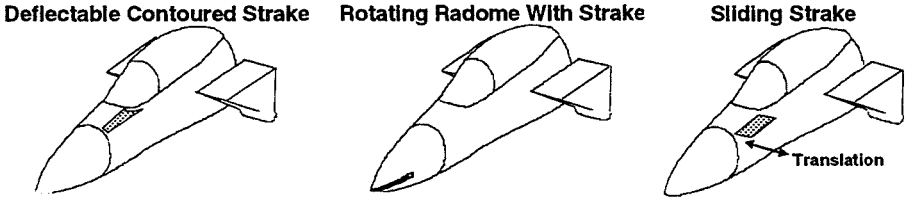

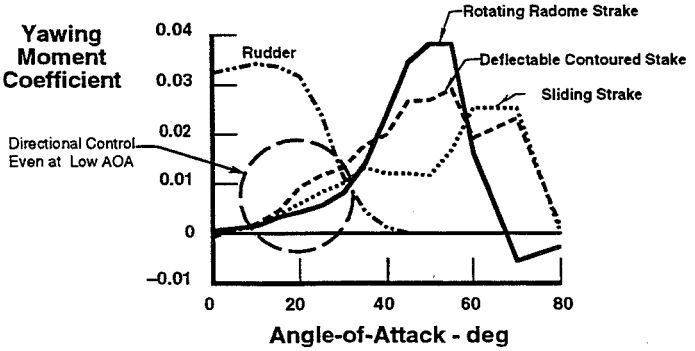

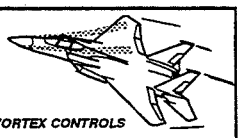

A manned simulation will provide necessary feedback on the desirability of FVC. Both test pilots and operational pilots will be invited for the simulation to provide a diverse perspective. Pilot comments will constitute a major portion of the benefit scale for a cost/benefit analysis.

A vortex control concept will be selected for database development, and an aerodynamic database will be assembled using the NASA LaRC 30x60 Ft Wind Tunnel Data. A limited implementation will be used for the simulation as a cost saving measure. A limited number of configurations and flight conditions will be evaluated in order to simplify control law development and reduce testing time. In addition, no failure modes will be analyzed.

ACC Pilot Manned Sim. Evaluation Will Demonstrate Need For FVC

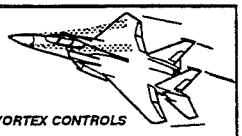

Manned Simulation Will Provide

- An Early Look At Expected Performance
- An Opportunity to Gain Feedback From Air Combat Command (ACC) Pilots
  - New Uses for the Improved Capability
  - Adequacy of Control Power Enhancements
  - Departure Resistance and Spin Recovery Capability

Implementation Plan

- FVC Effectiveness From LaRC 30x60 Ft Wind Tunnel Data
- Mach Effects From HARV Database
- Limited Configurations
- Limited Flight Conditions
- No Failure Modes
- Pilots From ACC . . . Other?

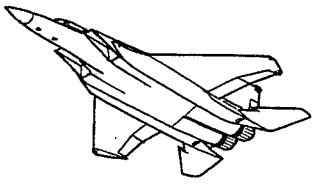

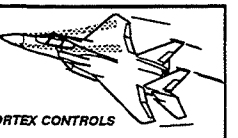

Development of FVC concepts will continue as control laws are developed for a manned simulator evaluation. This will provide the information necessary to conduct trade studies to weigh the benefits of mechanical and pneumatic devices and to conduct a cost/benefit analysis.

The F-15 FVC Program is focused on development of a production FVC system. Flight testing of a near production system will provide an opportunity to further develop tactics to exploit the new flight capability and allow for a smooth transition to production.

Future Plans

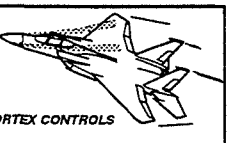

- Complete Aero Optimization for FVC Concepts
- Complete Control Laws and Conduct ACC Pilot Manned Simulator Evaluation
- Pursue:
  - Trade Study to Weigh Benefits of Mechanical and Pneumatic Devices
  - Cost / Benefit Analysis of FVC for F-15
  - Flight Test
  - Production/Retrofit

19951078 45
35 0277

N95-14259

58-02
1610
26

FLIGHT EVALUATION OF PNEUMATIC FOREBODY VORTEX CONTROL IN POST-STALL FLIGHT

DR. LAWRENCE A. WALCHLI

WRIGHT LABORATORY
WRIGHT PATTERSON AFB, OHIO

4TH NASA HIGH ANGLE-OF-ATTACK CONFERENCE

DRYDEN FLIGHT RESEARCH CENTER
JULY 1994

X-29 DESCRIPTION

The high angle-of-attack research vehicle used in this flight test was the X-29A Ship 2. Many of you have seen previous reports on this aircraft's capabilities. This chart should refresh your memories on the technologies on-board. The most notable, of course, is the forward-swept wing. The close-coupled canards were selected to make the aircraft 35 % statically unstable. The digital flight control system employed high alpha control laws which permitted trimmed 1G flight to about 50 degrees and maneuvering flight to about 40 degrees angle of attack.

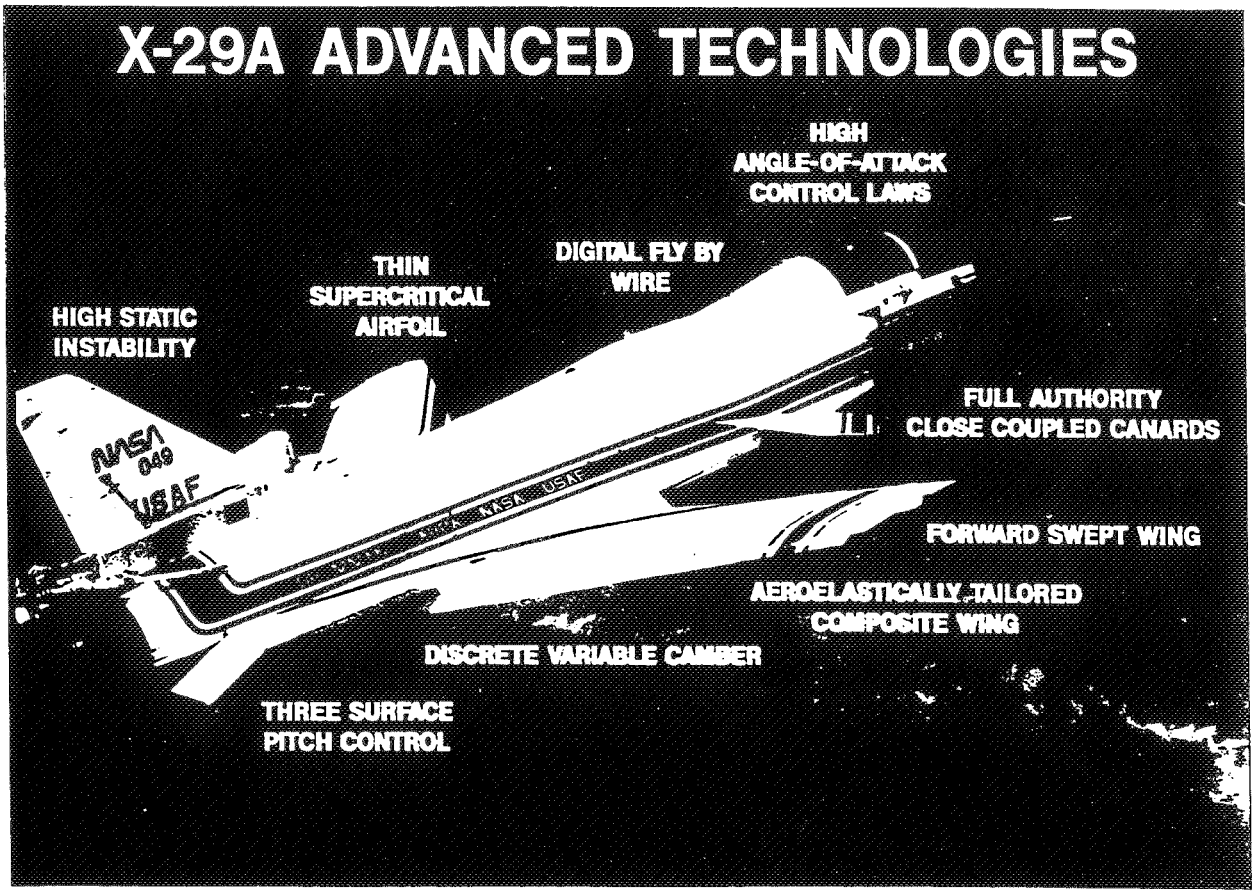

VFC TECHNOLOGY DESCRIPTION

Before we get into the discussion of results of the ground and flight tests, let me say some words about the specific technology upon which I'm reporting. Vortex Flow Control is an aerodynamic concept for producing directional control power at angles of attack where the conventional rudder loses its effectiveness. By using high pressure air jets, located symmetrically on either side of the upper nose section, the vortices shedding off of the nose at high AOA can be moved on command. Blowing on the right side lowers the static pressure there, moving the right vortex closer to the surface. Entrainment of air blows the opposite vortex away from the nose, raising the pressure on the left side. The net result is a nose-right force acting on a long moment arm from the aircraft CG, providing a substantial yawing moment.

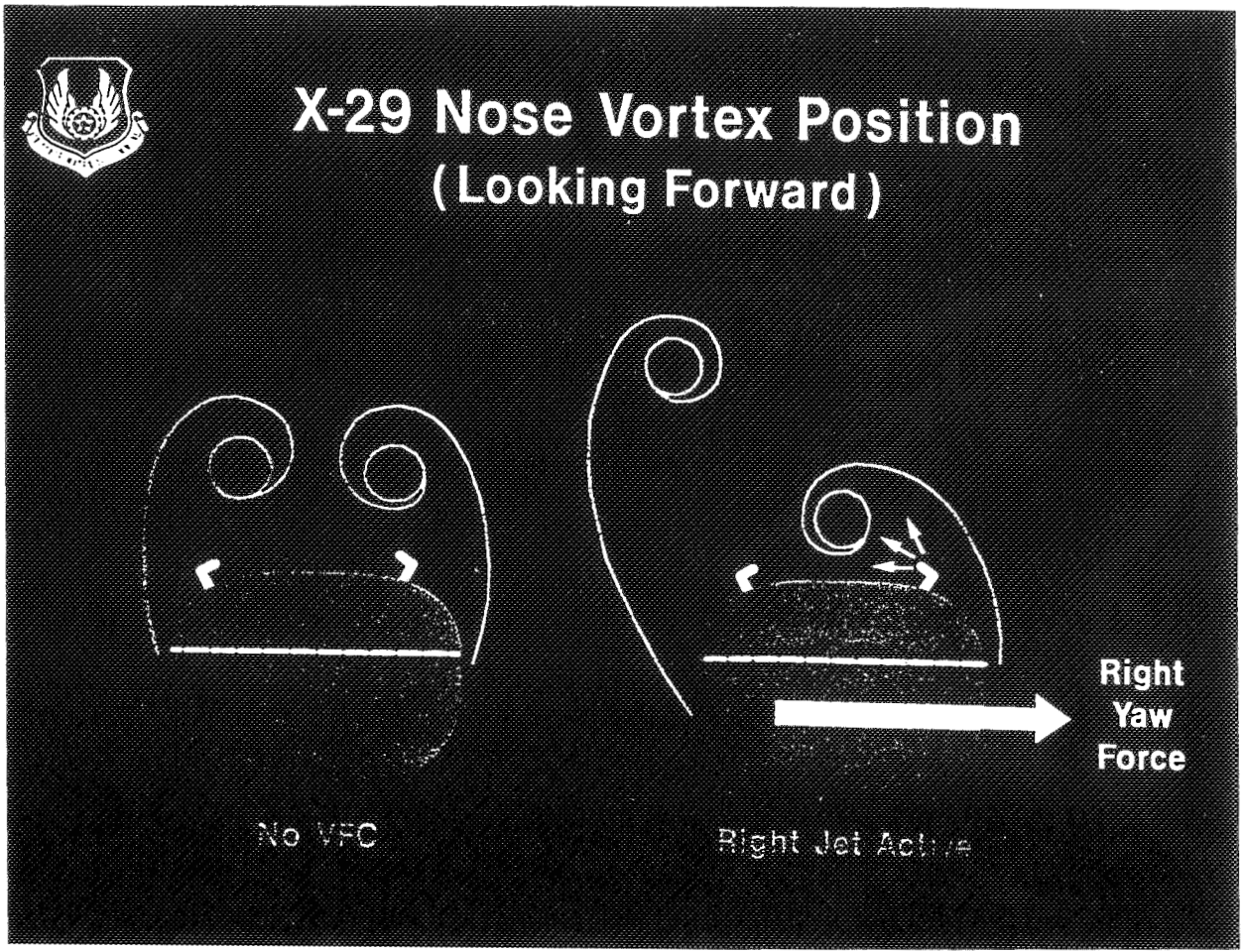

X-29 VFC WIND TUNNEL RESULTS
FOREBODY ONLY

Now some results, starting with our ground tests. The first phase of the program was done in the wind tunnel. We used a 1/8- scale forebody model of the X-29 to perform nozzle optimization studies. Parameters of specific interest included the nozzle size and shape, its location and orientation on the nose, and the blowing coefficient. The data clearly showed that a significant yawing moment could be generated with blowing from AOA of 15 to 55 degrees. Low blowing rates which were of practical interest for flight test produced almost constant effectiveness between 35 and 55 degrees angle of attack.

X-29 VFC WIND TUNNEL RESULTS

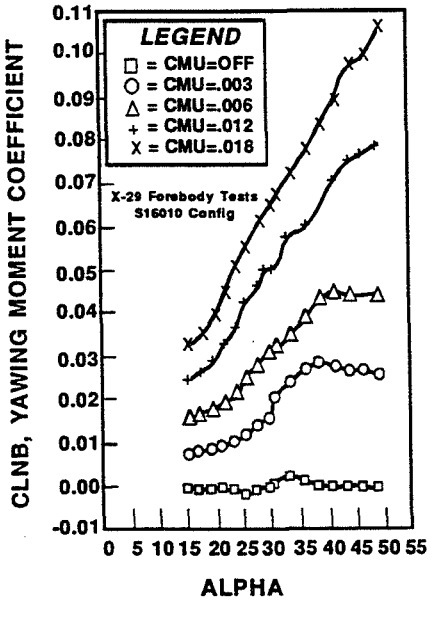

X-29 VFC WIND TUNNEL RESULTS
FULL CONFIGURATION YAWING MOMENT

Buoyed by our success with the forebody model, we tested a 1/8-scale full aircraft model in the Grumman Low Speed wind tunnel. In order to vary the mass flow coefficient, we used two different size nozzles, both of the same basic configuration. This chart shows some synergistic benefit from the full configuration aircraft model. Besides creating side force on the fuselage, the manipulated vortex swept the canopy, providing about 10% more moment than seen in the forebody-only testing. The data shown here have already been transposed to flight test conditions. As you see, we can recover a large portion of the lost rudder power above 30 degrees angle of attack.

X-29 VFC PROGRAM
YAWING MOMENT PREDICTION

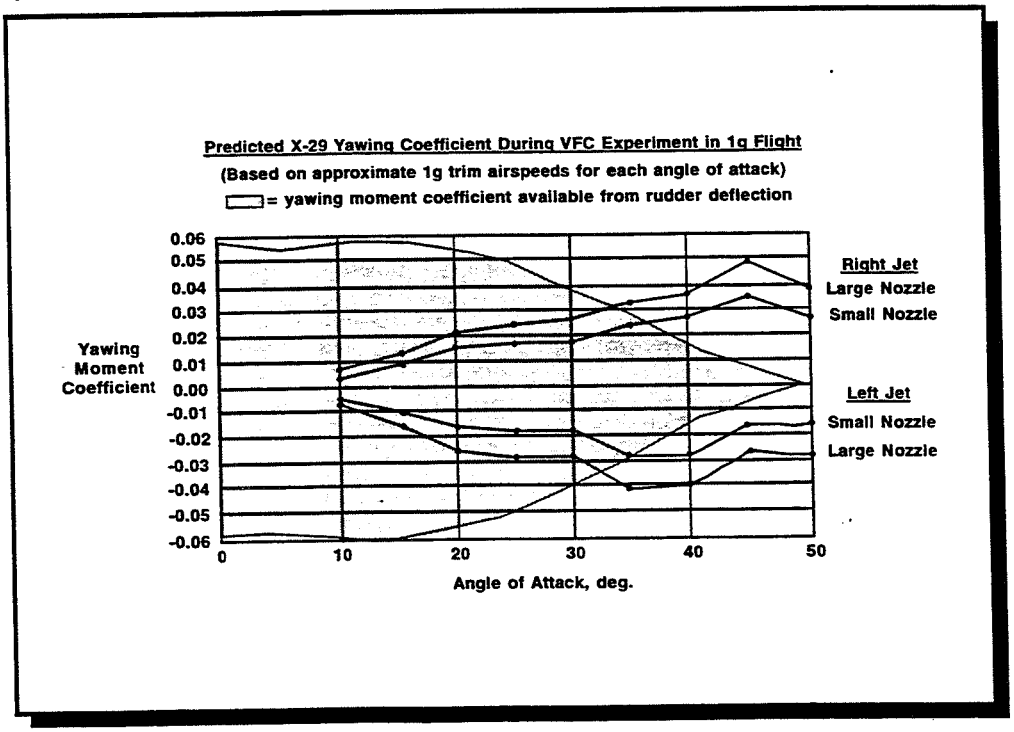

X-29 VFC WIND TUNNEL RESULTS
FULL CONFIGURATION C_n WITH SIDESLIP

To complete the wind tunnel static data picture, we need to look at both the sideslip effect on induced yawing moment and the pitching moment effects caused by the vortex manipulation. This slide shows that the yawing moment is quite well-behaved with sideslip on the model. The data were taken at 35 degrees AOA and appear almost independent of sideslip.

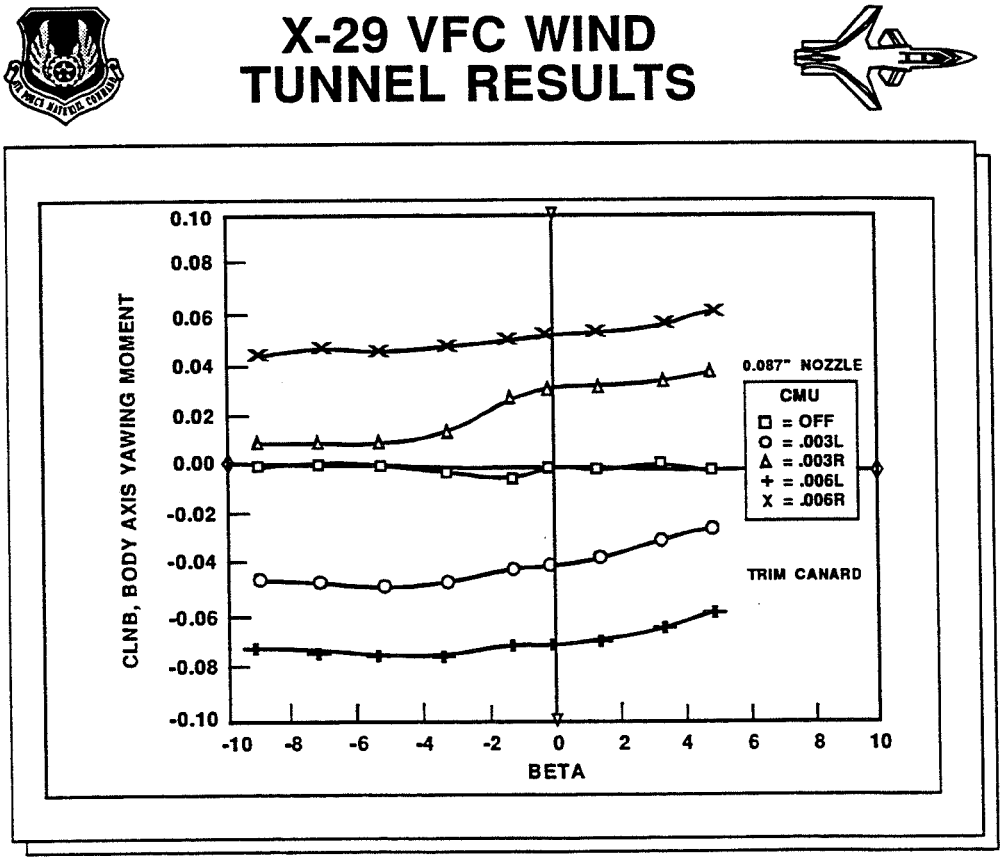

X-29 VFC WIND TUNNEL RESULTS
FULL CONFIGURATION PITCHING MOMENT

Aircraft pitch control power is a critical parameter at very high angle-of-attack conditions and pitching moment increments due to forebody vortex control can aggravate the problem. This slide presents the effects on the pitching moment versus sideslip at 40 degrees angle of attack. A nose-up increment was observed at zero beta on the order of $\Delta C_M = 0.05$. The increments at sideslip depended on whether the upwind or the downwind jet was active. The downwind jet, which is the one responsible for initiating and maintaining the sideslip condition, generated a desirable nose-down pitching moment. The upwind jet, which would return the aircraft to zero beta, generated an undesirable nose-up increment. The observed increments are substantial, but fall within the nose-down authority of the X-29 aircraft up to 50 degrees AOA.

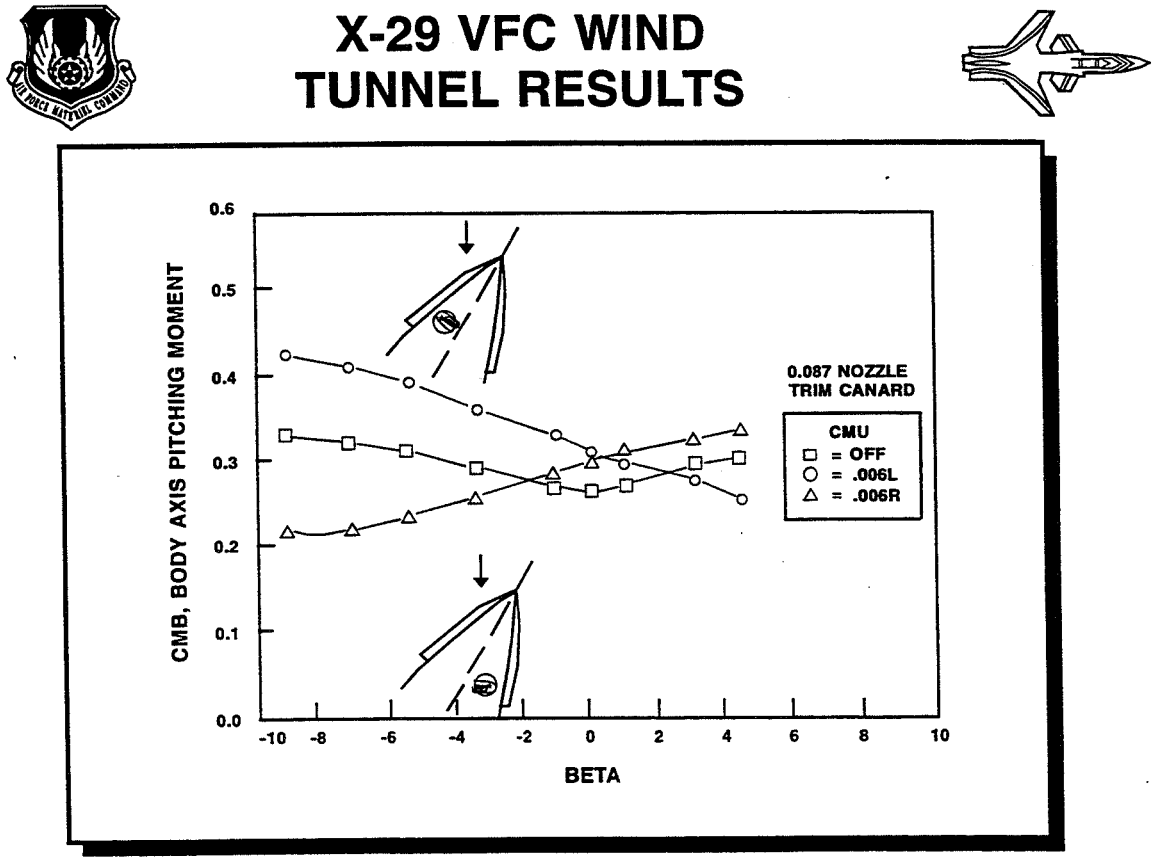

VFC OPTIMIZED NOZZLE DETAILS

These next two slides show you the specific nozzle configuration which produced the results just presented. The important thing to notice on the nozzle detail is the slot and the 10 degree inclination. This concept produced a sheet of air, creating a much larger influence on the vortices than the round jet with which we started.

VFC OPTIMIZED NOZZLE DETAILS

d = NOZZLE INTERNAL DIAMETER, SELECTED FROM SUPPLY PRESSURE AND MASS FLOW REQUIREMENTS.
ALL OTHER DIMENSIONS AS FRACTIONS OF "d".

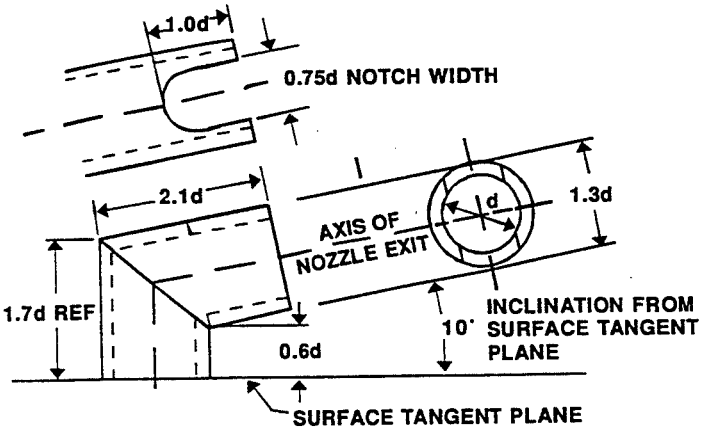

X-29 FOREBODY
NOZZLE CONFIGURATION

The control of the vortices was also sensitive to nozzle location on the forebody. A position too close to the apex of the forebody or the trailing edge of the chines disrupted the formation and shedding of the vortices. Further, it was determined that canting the nozzles in-board sixty degrees helped to pull the active-side vortex further around the fuselage, with the resulting low pressures influencing more of the surface and cross-feeding more external air into the opposite vortex. It should be noted here that our solution is not by any means the only possible combination of nozzle shape, size and location.

X-29 FOREBODY NOZZLE CONFIGURATION

D = FOREBODY MAXIMUM DIAMETER FROM WHICH THE FOREBODY FINENESS RATIO IS DETERMINED.
THE AXIAL LOCATION OF NOZZLES IS SPECIFIED AS A FRACTION OF THIS DIAMETER.

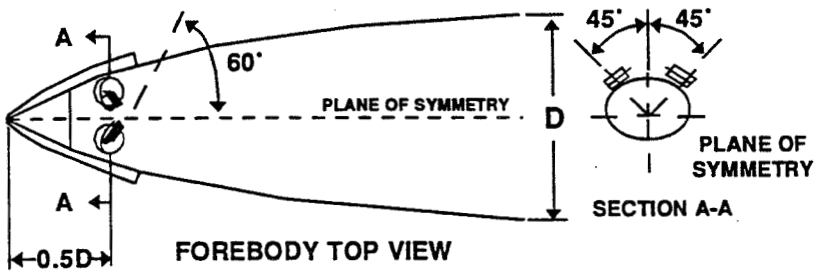

AXIS OF NOZZLE EXIT POINTED 60 DEGREES INWARD TOWARD PLANE OF SYMMETRY.

X-29 VFC SYSTEM
STORED GAS SCHEMATIC

Let's turn our attention now to the VFC flight test program. The mechanization of an on-board blowing system is shown here. The system was designed to support a proof-of-concept experiment and as such had limited capability. Two Kevlar-wrapped, aluminum-lined storage bottles carried up to 13 pounds of 6000 psi gaseous nitrogen (GN_2) aloft. When the system was activated, gas pressure was reduced through two stages of regulation to a nozzle reservoir pressure of 400 psi. Flow was directed by the pilot through the left, right, or both nozzles. Weight flow was calculated from pressure and temperature measurements at two locations -- near the storage tanks and a very precise calculation just upstream of the calibrated nozzles.

X - 29 VFC SYSTEM
STORED GAS SCHEMATIC

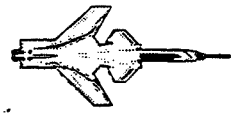

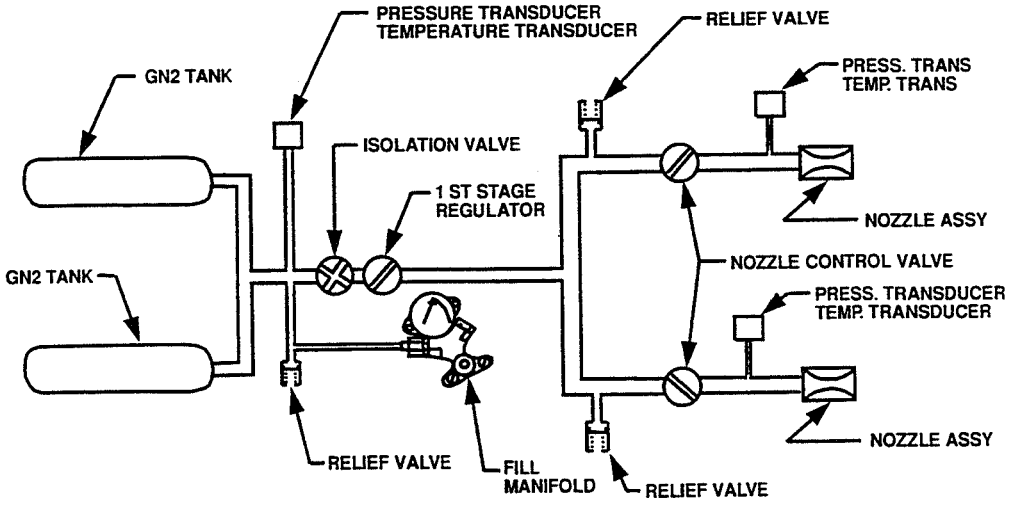

X-29 VFC SYSTEM
STORED GAS INSTALLATION

Location of the system in the X-29 is shown in this slide. The storage bottles were located just forward of the cockpit fire wall along with the first stage of pressure reduction and the fill valve. The air was routed forward along the top of the nose and into the nose cone attachment compartment. At this point, final pressure reduction to 400 psi was accomplished and individual shutoff valves directed the nitrogen to the side of the aircraft commanded by the pilot.

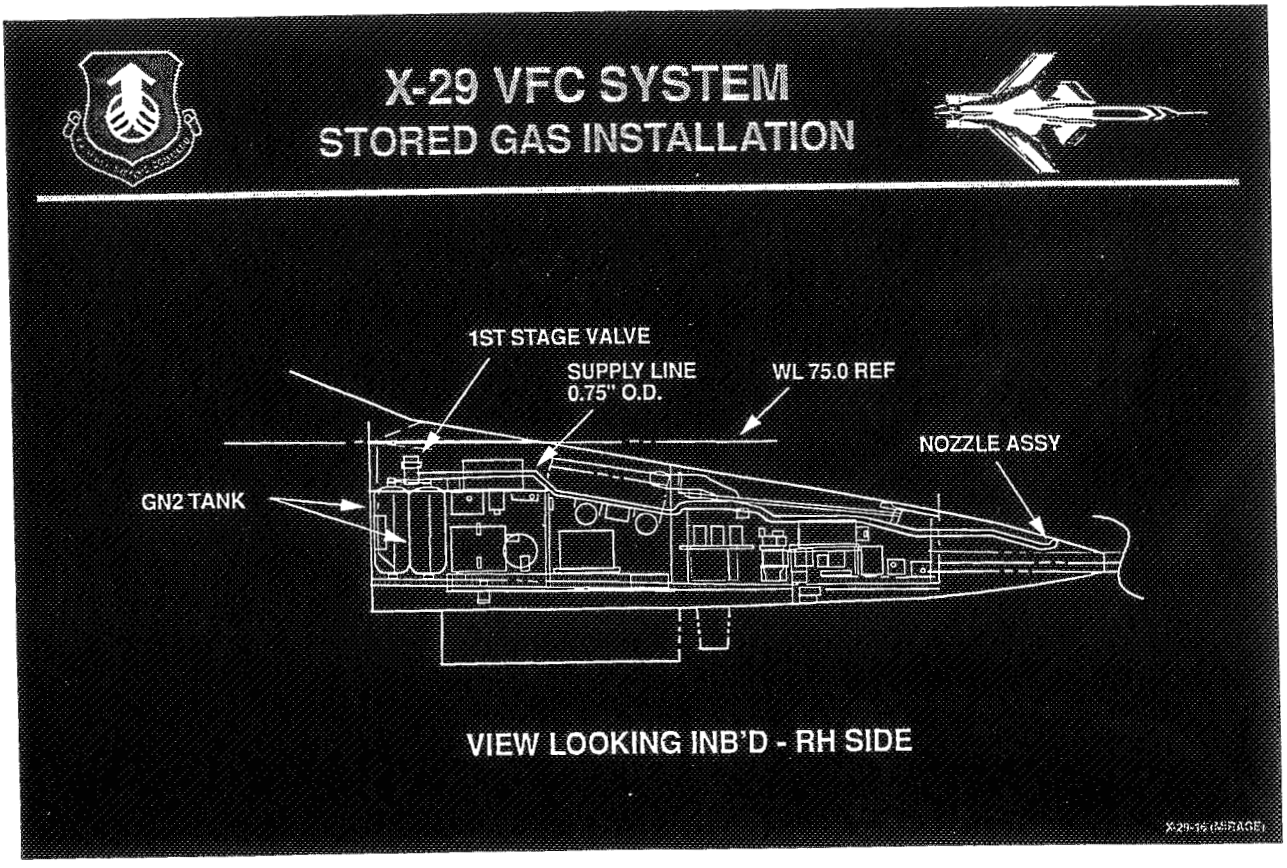

VFC EFFECTIVENESS AT ZERO SIDESLIP

The best measure of the effectiveness of VFC is the control derivative of yawing moment due to blowing, $Cn_{C\mu}$. The chart shows the results obtained from one second pulses of the VFC system during stabilized 1G high alpha test points with less than one degree of sideslip. Three nozzle sizes were tested to cover a range of mass flows (0.202, 0.286, and 0.350 in. dia.). Inertial coupling and engine gyroscopic effects were subtracted from the total flight-measured accelerations to yield the flight values of the aerodynamic coefficients. Measured control surface positions, body-axis rates, and flight conditions were then used to query the aerodynamic database for predicted time histories of the coefficients. An example of the two results is shown here. At angles of attack above 35 degrees, the wing rock and zero sideslip asymmetries of the basic aircraft complicated the analysis of the VFC flight data, resulting in the increased scatter that can be seen at 40 degrees angle of attack.

FLIGHT RESULTS

VFC EFFECTIVENESS AT ZERO SIDESLIP

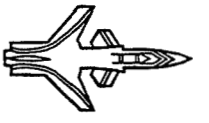

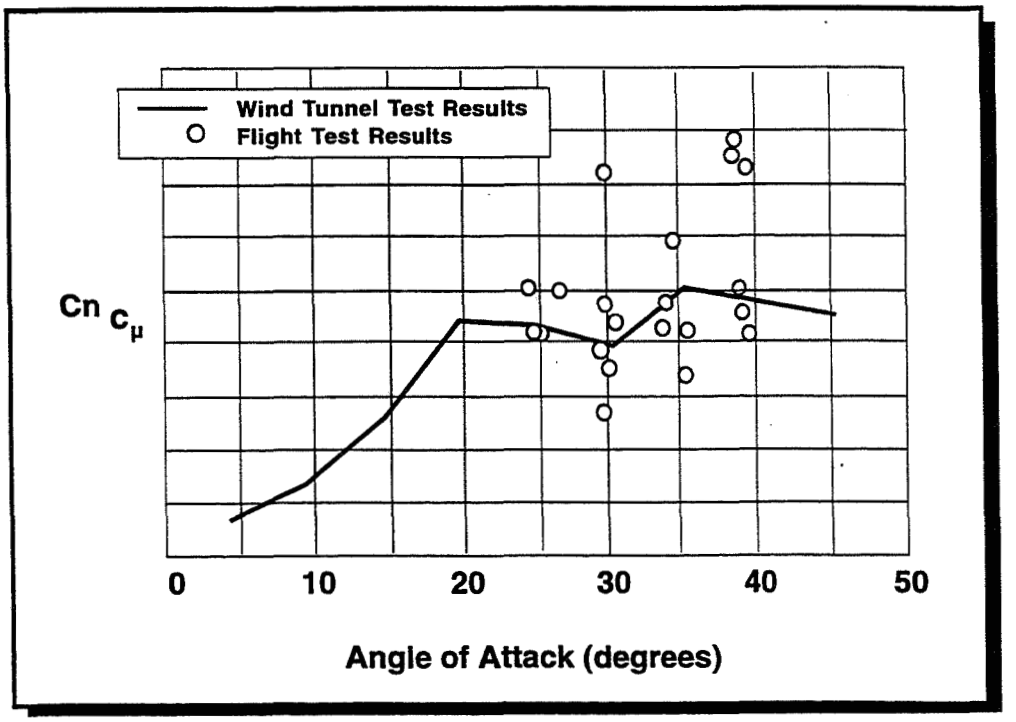

VFC EFFECTIVENESS AT 35 AOA WITH SIDESLIP

This slide shows the VFC effectiveness at 35 AOA due to sideslip. Again, results are from one second pulses. The points on the left resulted from blowing to reduce the pre-established sideslip. Points on the right occurred when blowing was used to increase sideslip. VFC strength does not decrease much when blowing on the same side as the pre-established sideslip; its strength does degrade somewhat when blowing on the opposite side. This suggests that while VFC may be very useful for extended-duration maneuvers, during which VFC causes moderate increasing sideslip, it will not be as effective in reducing a pre-existing sideslip condition. Also shown are the results of two "conventional roll" maneuvers, in which a short VFC pulse was used to oppose the yaw rate generated by a full-stick roll. The data show that aircraft rates do not significantly influence effectiveness.

FLIGHT RESULTS

VFC EFFECTIVENESS AT 35AOA

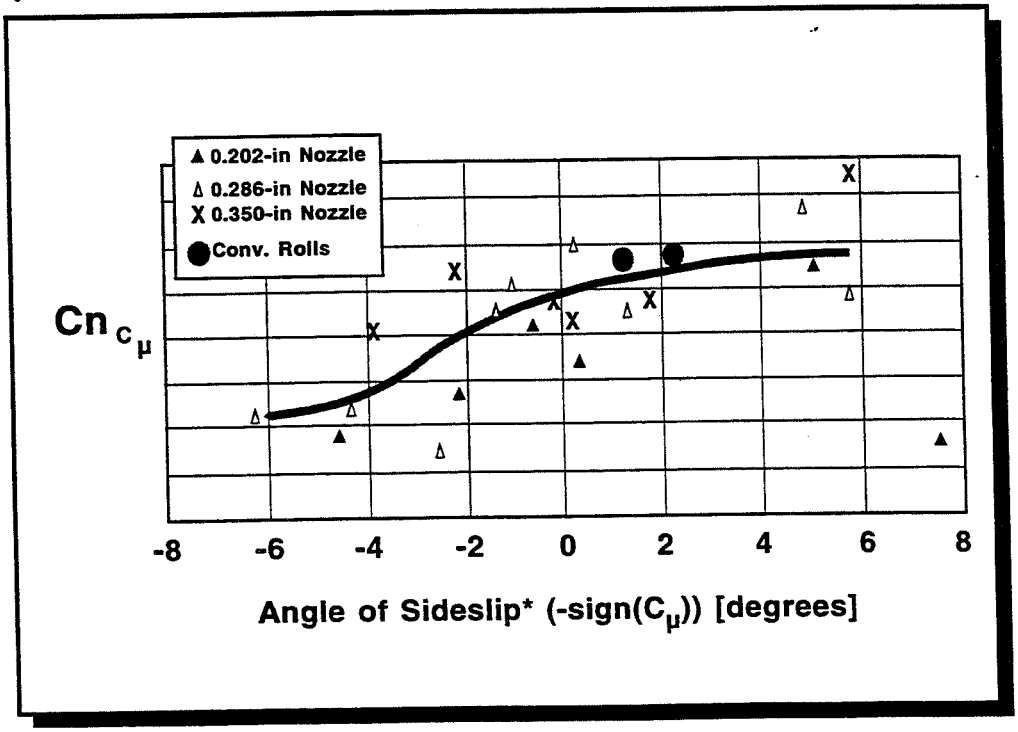

"VFC ROLL" AT 40 AOA

Here are the results of a "VFC-Roll" at 40 degrees AOA. The maneuver consisted of stabilizing the aircraft in 1G flight at the target angle of attack, activating the left VFC nozzle until a target yaw rate was reached, and then switching to the right nozzle in order to stop the VFC-induced rate. The maneuver was flown with the lateral stick and rudder pedals neutral. The purpose of this maneuver, beyond the demonstration of a pure-VFC roll, was to determine the aerodynamic time delay associated with switching from one nozzle to the other. This data is essential for the design of a VFC-based flight control system and can not be obtained from static wind tunnel tests. As can be seen, the time for the full reversal of the yawing moment was less than one half second. Further, the yaw acceleration after the reversal was as strong as the initial acceleration.

FLIGHT RESULTS
"VFC-Roll" at 40AOA

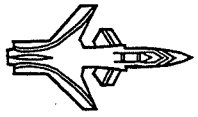

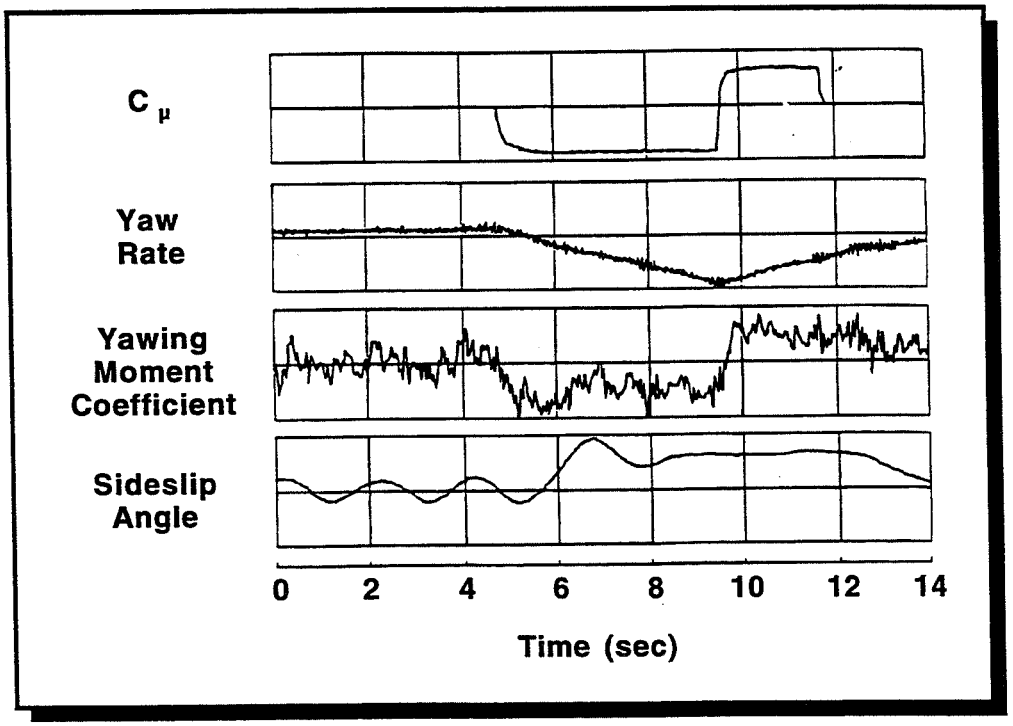

EFFECTS OF VFC ON WING ROCK

One of our program goals was to determine the effects of VFC on wing rock. Wing rock behavior is actually a body rock caused by the oscillatory motion of the forebody vortices. The plot shows the time-history of a 1.5 second VFC pulse at 40 degrees angle of attack. As seen in the sideslip data, this maneuver begins with typical wing rock at 0.5 Hz with a magnitude of ±2 degrees sideslip. The average sideslip angle shifts slightly nose-left, but the frequency and amplitude of the wing rock remain relatively constant. A very careful look at the data reveals a slight reduction in wing-rock amplitude towards the end of the blowing pulse. Our plan to examine wing-rock effects at 40 alpha in the absence of sideslip required short pulses which rendered our results inclusive. By countering the sideslip and roll coupling with aero surfaces at 35 alpha, blowing longer may indeed have eliminated wing rock.

FLIGHT RESULTS

EFFECTS OF VFC ON WING ROCK AT 40AOA

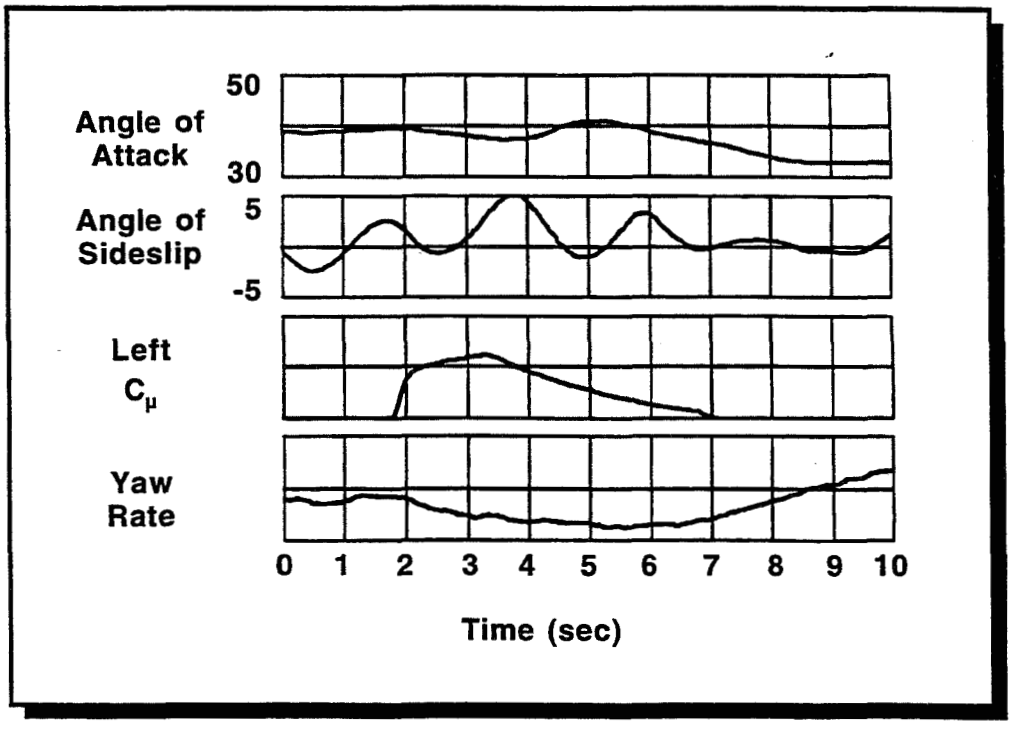

INTEGRATED CONTROLS C_n PREDICTION

How can we use what we've learned to enhance the capability of an advanced weapon system? It seems clear that the best way to include active blowing is to imbed it within the primary control laws. Since forebody blowing serves as a roll coordinator and sideslip regulator, functions satisfied by the rudder at low angles of attack, it behooves the designer to integrate $\gamma Cn_{c\mu}/\gamma t$ (blowing) with $\gamma Cn_{df}/\gamma t$ (rudder) over the entire flight envelope of the aircraft. The combined system would then produce the yaw control power displayed here. The system would be robust enough to coordinate any rolling maneuver within the confines of the aircraft's operational envelope.

INTEGRATED YAWING MOMENT PREDICTION FOR RUDDER AND ACTIVE VFC

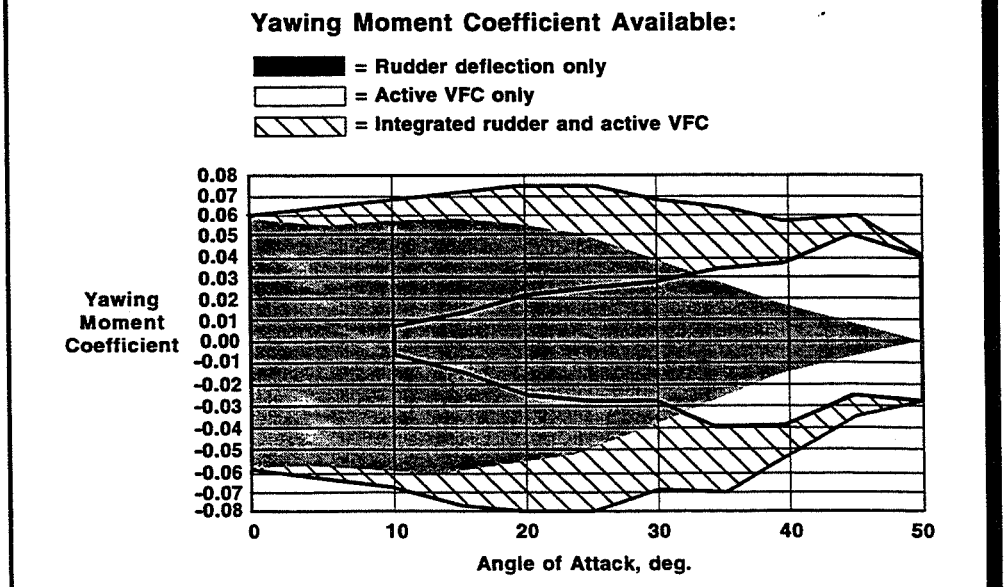

PROPOSED F-15 LATERAL CONTROL
LAWS WITH ACTIVE VFC

An example of this integration is shown in this slide. This is the modified lateral control law for an F-15 aircraft. Note that forebody blowing has been blended with both the horizontal tail and rudder. A six degree of freedom (SDF) solution of the equations of motion using this blended blowing model was performed.

PROPOSED F-15 LATERAL CONTROL LAWS WITH ACTIVE VFC

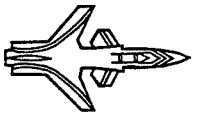

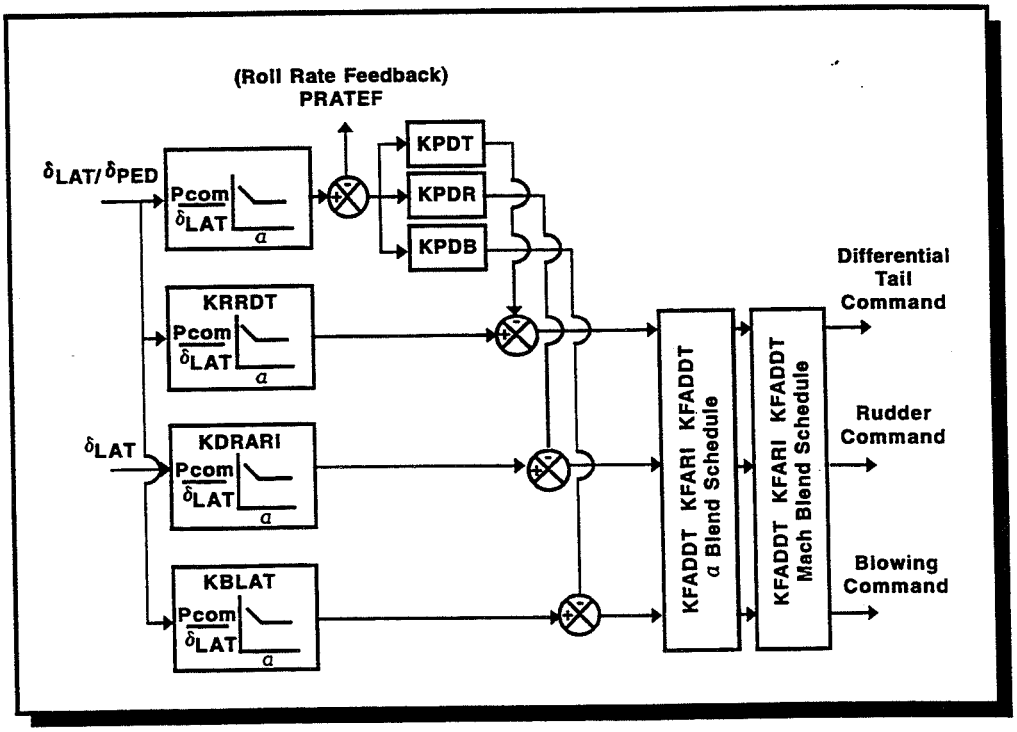

SIMULATED F-15 ROLL
PERFORMANCE WITH ACTIVE VFC

Just a reminder that one of the prime uses of Vortex Flow Control is the coordination of lateral commands. This slide shows the results of the simulation using the integrated control law. The data clearly show a 100 % improvement in stability axis roll rate while at the same time providing excellent coordination. Further, the roll acceleration has tripled over the baseline.

SIMULATED F-15 ROLL PERFORMANCE WITH ACTIVE VFC

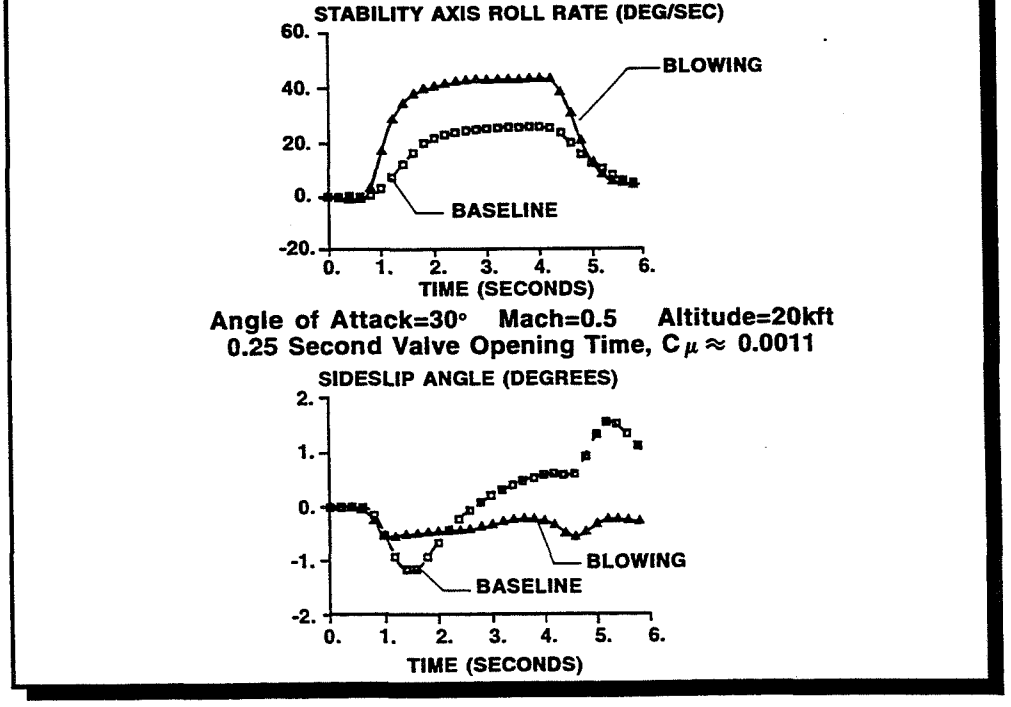

SIMULATED F-15 SPIN RECOVERY WITH ACTIVE VFC

A fully-developed spin was simulated in order to compare baseline and VFC-enhanced control laws. The baseline configuration was used to recover the aircraft. At full recovery, the residual angle of attack was 20 degrees. The task was then repeated using the VFC-enhanced controls. But the task was now arbitrarily redefined to recover the aircraft to a 20 degree alpha condition. The angle of attack chart shows the two solutions give the same overall time to accomplish, about ten seconds. Note on the yaw rate chart that VFC actually ended the spin about five seconds sooner than the baseline control laws. At this point in time, the pilot had to leave his 40 degree angle-of-attack condition and capture the task-selected 20 degrees. So if the task was to simply recover the aircraft, VFC-enhanced controls were significantly superior.

SIMULATED F-15 SPIN RECOVERY WITH ACTIVE VFC

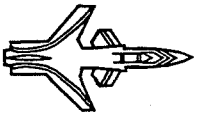

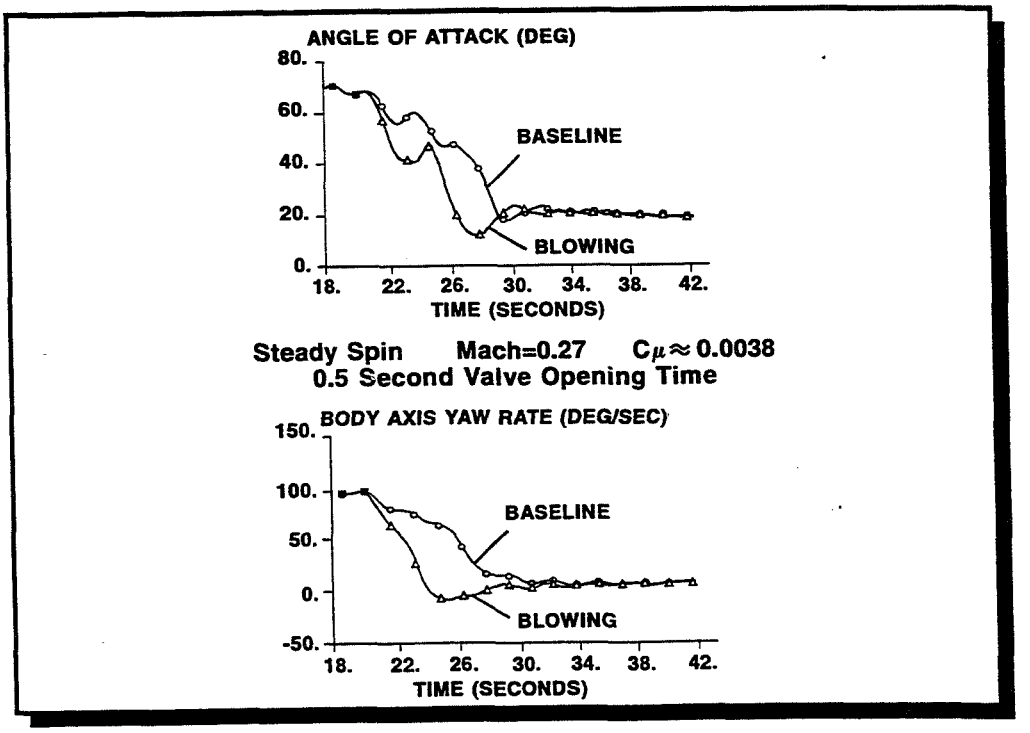

The final portion of my presentation will address a few "lessons learned" on the VFC program. The management of our critical experiment was our first hurdle. The X-29 Technology Demonstration Program had employed up to 200 people. The VFC experiment was a relatively small program which had a relatively small budget and had to be completed in a very short time. The trick was to establish a team with the right mix of technical people who could work effectively and efficiently together. We accomplished this with only ten full time engineers ranging from aerodynamicists to mechanical designers. The entire program from beginning of tunnel testing to the conclusion of flight test reporting was a mere 14 months.

LESSONS LEARNED

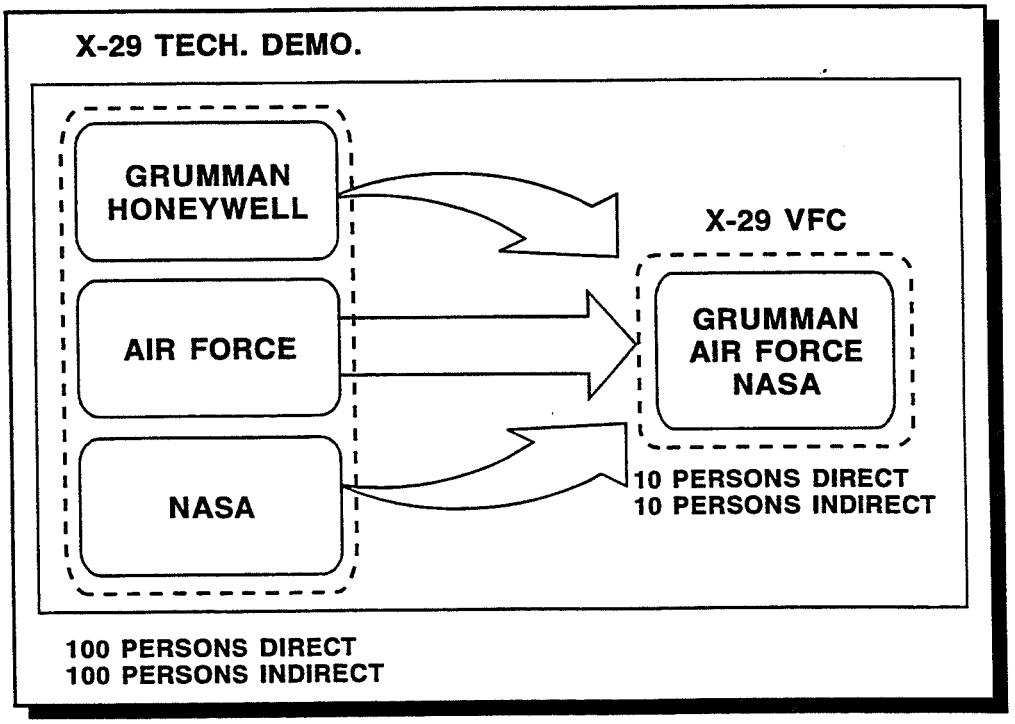

LESSONS LEARNED
TESTBED SELECTION

From a technical point of view, the VFC program needed a testbed with a high AOA, low speed capability, the flight regime where VFC was most effective. The X-29 was directionally stable at angles to almost 45 degrees and had a strong dihedral characteristic to counter the destabilizing effects of the asymmetric blowing. After seven years of test flights throughout the envelope, the aircraft had a large and well-understood data base.

LESSONS LEARNED

X-29

CAPABLE AIRFRAME
EXCELLENT DATABASE
STRONG DIHEDRAL TO COUNTER VFC

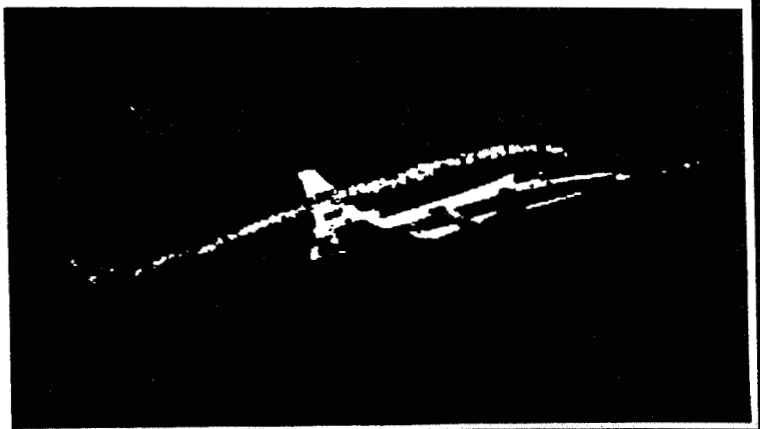

LESSONS LEARNED
SIMULATION FOR RISK REDUCTION

Up front it was considered somewhat of a risk to fly the VFC technology with only static wind tunnel data to predict performance. After much consideration we concluded that our X-29 flight validated simulation was of sufficient fidelity to warrant using the testbed to answer questions on dynamics. So we took our static data base, combined it with the aircraft's dynamics, and used the delta file approach to query the simulator on safety and performance of proposed flight test points. Following each flight, the aircraft model was updated if necessary. By doing this flight-to-flight, we minimized the risk of straying too far from actual aircraft performance.

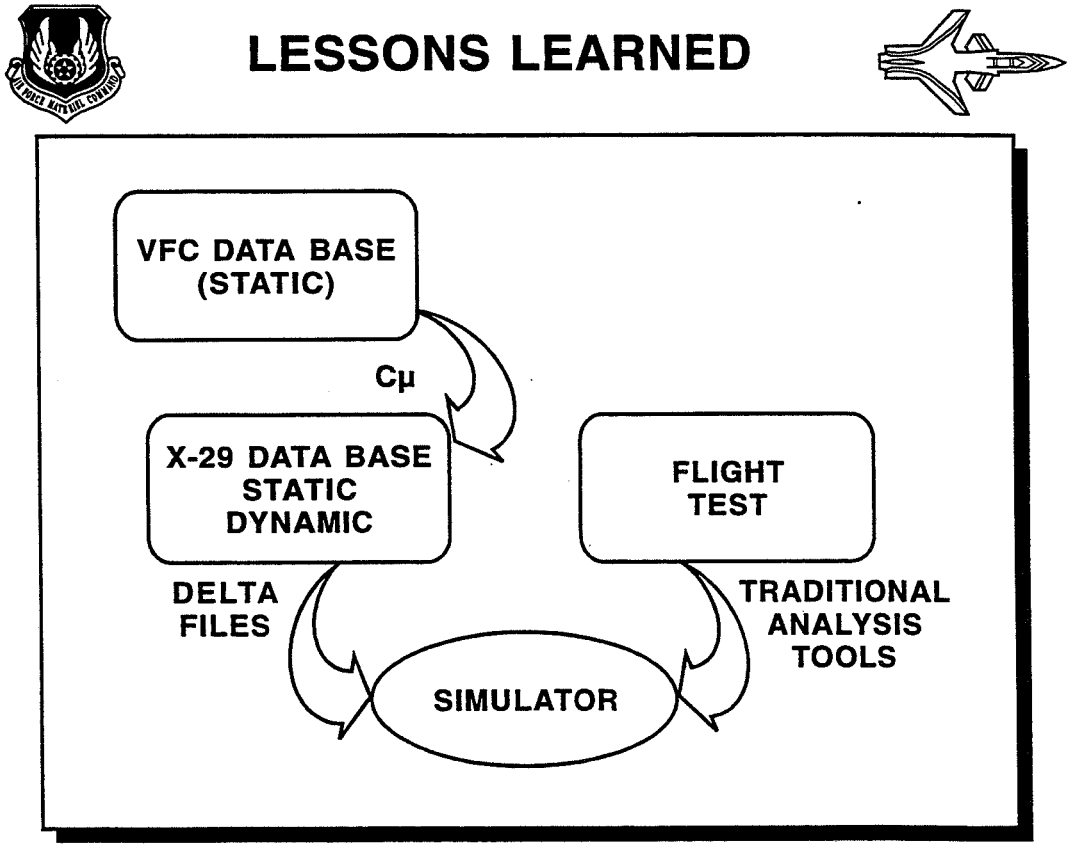

LESSONS LEARNED
BENEFITS OF HIGH PRESSURE SYSTEM

Early in the design phase of the program, we chose the high pressure delivery system as the most effective way to supply the nitrogen needed to power the VFC nozzles. A significant factor in this selection was the ability to store an adequate quantity of gas on board to conduct a meaningful experiment. Based on our results, a high pressure system would be the choice for an operational fully integrated system on an advanced or retrofitted fighter aircraft. High pressure translates to small hardware. Our small nozzles were very effective and caused no aerodynamic perturbations on the baseline characteristics. Further, aircraft modifications were minimized. High pressure in an operational environment does complicate the design process since additional compression devices and heat exchangers would be required, no trivial task!

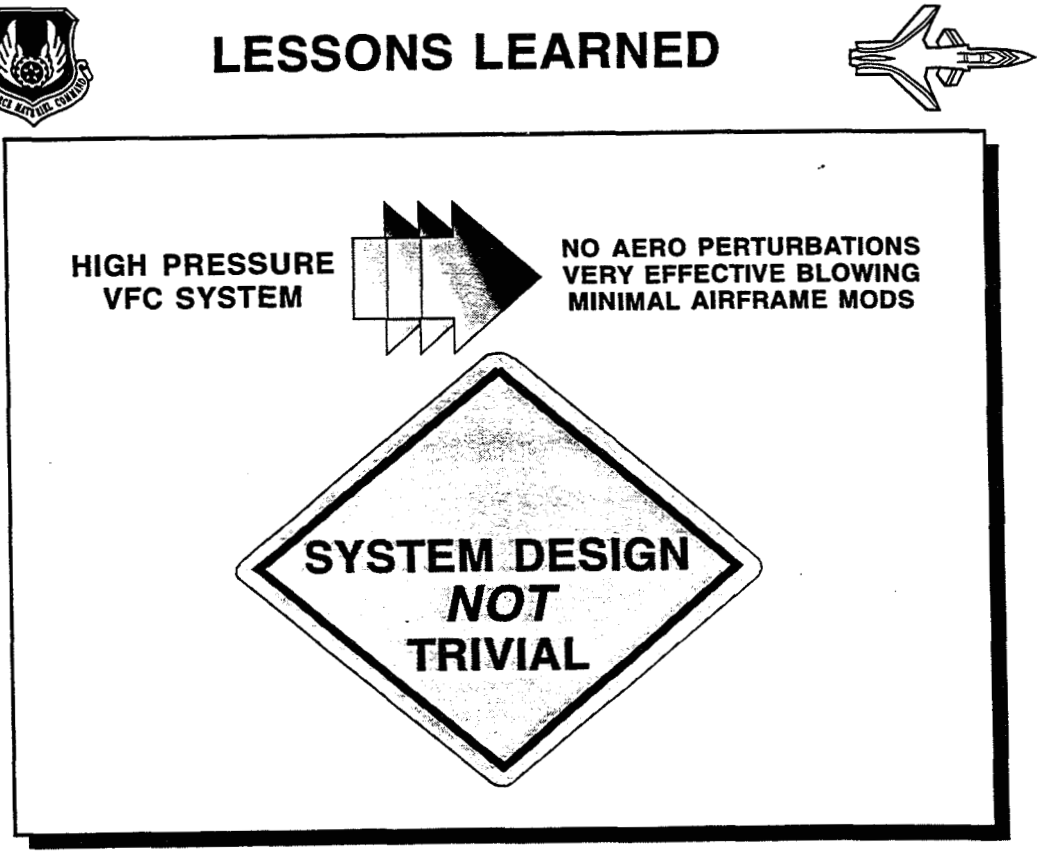

LESSONS LEARNED
ADVANCED WEAPON SYSTEM INTEGRATION

The next step in pursuing the VFC technology as a viable option for incorporation on an operational aircraft is to fully integrate it into the flight control system and vehicle subsystems on a candidate testbed. This step requires three distinct yet interrelated tasks. The on-board gas delivery supply system, probably using engine bleed air, must be developed. Static and dynamic wind tunnel data must be acquired for the candidate testbed configuration. Finally, the testbed itself must be designed, including it's upgraded flight control laws, modified or built, and flight tested throughout its total operating envelope. A well-laid-out program should produce results which lend credence to the hypothesis that VFC is a mature technology ready for application.

RECOMMENDATION

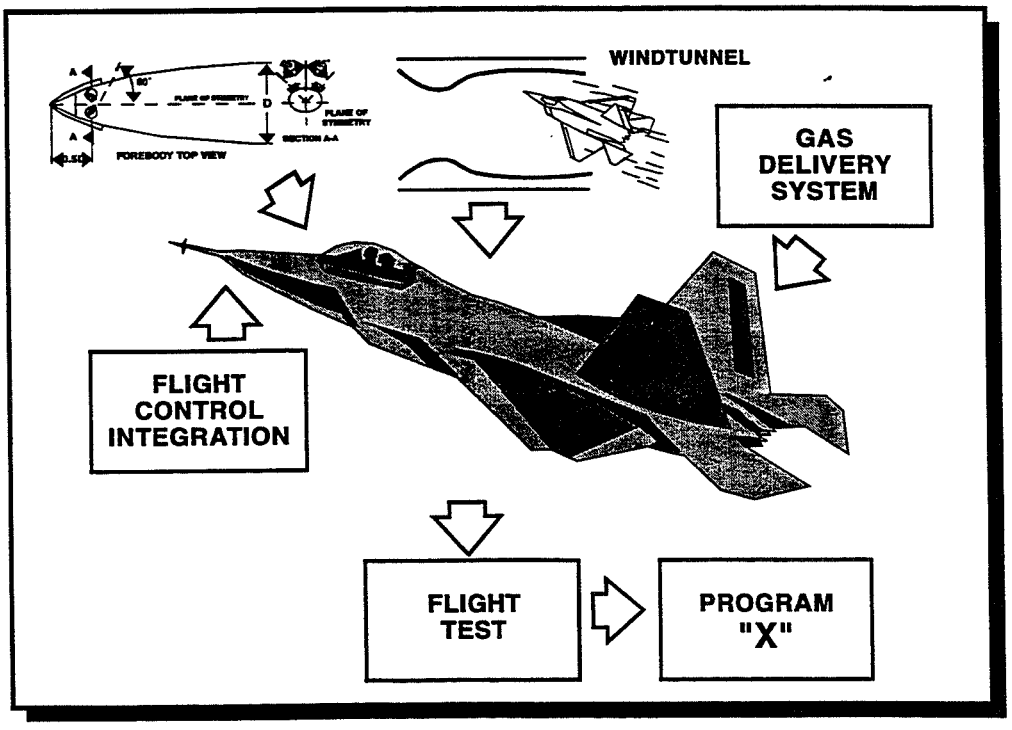

REPORT DOCUMENTATION PAGE

Form Approved
OMB No. 0704-0188

Public reporting burden for this collection of information is estimated to average 1 hour per response, including the time for reviewing instructions, searching existing data sources, gathering and maintaining the data needed, and completing and reviewing the collection of information. Send comments regarding this burden estimate or any other aspect of this collection of information, including suggestions for reducing this burden, to Washington Headquarters Services, Directorate for Information Operations and Reports, 1215 Jefferson Davis Highway, Suite 1204, Arlington, VA 22202-4302, and to the Office of Management and Budget, Paperwork Reduction Project (0704-0188), Washington, DC 20503.

1. AGENCY USE ONLY (Leave blank)	2. REPORT DATE	3. REPORT TYPE AND DATES COVERED
	July 1994	Conference Publication

4. TITLE AND SUBTITLE
Fourth NASA High Alpha Conference

5. FUNDING NUMBERS
WU 505-68-30

6. AUTHOR(S)

7. PERFORMING ORGANIZATION NAME(S) AND ADDRESS(ES)
NASA Dryden Flight Research Center
P.O. Box 273
Edwards, California 93523-0273

8. PERFORMING ORGANIZATION REPORT NUMBER
H-2007

9. SPONSORING/MONOTORING AGENCY NAME(S) AND ADDRESS(ES)
National Aeronautics and Space Administration
Washington, DC 20546-0001

10. SPONSORING/MONITORING AGENCY REPORT NUMBER
NASA CP-10143
Volume 3

11. SUPPLEMENTARY NOTES
This document is a preprint for a conference held at NASA Dryden Flight Research Center, July 12–14, 1994. Conference Chair Donald Gatlin; Technical Chair Victoria Regenie; Administrative Chair Everlyn Cruciani.

12a. DISTRIBUTION/AVAILABILITY STATEMENT
Unclassified—Unlimited
Subject Category 02

12b. DISTRIBUTION CODE

13. ABSTRACT (Maximum 200 words)

The goal of the Fourth High Alpha Conference, held at the NASA Dryden Flight Research Center on July 12–14, 1994, was to focus on the flight validation of high angle-of-attack technologies and provide an in-depth review of the latest high angle-of-attack activities. Areas that were covered include, high angle-of-attack aerodynamics, propulsion and inlet dynamics, thrust vectoring, control laws and handling qualities, tactical utility, and forebody controls.

14. SUBJECT TERMS
Aerodynamics; F-18 HARV; High angle of attack; X-31 aircraft

15. NUMBER OF PAGES
191

16. PRICE CODE
A09

17. SECURITY CLASSIFICATION OF REPORT	18. SECURITY CLASSIFICATION OF THIS PAGE	19. SECURITY CLASSIFICATION OF ABSTRACT	20. LIMITATION OF ABSTRACT
Unclassified	Unclassified	Unclassified	Unlimited